

AD-A258 574



August 1992

THESIS/ ~~DISSERTATION~~

Effects of Material Degradation on Large Space
Structures Dynamic Response

Alan J. Perdiga,

AFIT Student Attending: Pennsylvania State University

AFIT/CI/CIA-92-103

AFIT/CI

Wright-Patterson AFB OH 45433-6583

Approved for Public Release IAW 190-1
Distribution Unlimited
ERNEST A. HAYGOOD, Captain, USAF
Executive Officer

DTIC
ELECTE
DEC 09 1992
S E D

The Pennsylvania State University
The Graduate School

EFFECTS OF MATERIAL DEGRADATION ON
LARGE SPACE STRUCTURES DYNAMIC RESPONSE

A Thesis in
Architectural Engineering

by

Alan J. Perdigao

Submitted in Partial Fulfillment
of the Requirements
for the Degree of

Masters of Science in Architectural Engineering

August 1992


2438

92-31149



I grant The Pennsylvania State University the nonexclusive right to use this work for the University's own purposes and to make single copies of the work available to the public on a not-for-profit basis if copies are not otherwise available.

Accession For	
NTIS	CRA&I
DTIC	TAB
Unannounced	
Justification	
By	
Distribution /	
Availability Codes	
Dist	Avail and / or Special


Alan J. Perdigao

DECLASSIFIED 2.

ABSTRACT

Composite Large Space Structures (LSS) including booms, planar surfaces, antennas, platforms, and space stations are proposed for use in NASA's Space Station "Freedom" and the DOD's Global Protection Against Limited Strikes programs. Because of their low mass and high strength and stiffness, composite repetitive lattice structures are ideal for these space applications. LSS will be required to sustain severe environmental effects - radiation, thermal cycling, atomic oxygen bombardment, collision with micrometeoroids and space debris, and hostile actions - and transient operational loads - docking, slewing, manned activities, control system, and the mobile service center - while maintaining strict mission parameters. Platform pointing is one example of these requirements and necessitates tolerances of less than one-thousandth of a degree. Over time, material and structural degradation will occur due to environmental effects causing a change in the structure's stiffness and dynamic response. Likely, this structural damage will require immediate repair to restore the LSS to full mission capability. This thesis investigates the dynamic response of one LSS - the NASA Dual-Keel Space Station with 5 meter graphite epoxy erectable truss - under one operational load - shuttle docking - and Low Earth Orbit (LEO) environmental conditions, and predicts how the material, structural properties, and dynamic response change over the 20-30 year design life. Results show the effects of material degradation on the station's dynamic response and mission requirements and has applications for NASA and DOD logistics planning for future LSS.

TABLE OF CONTENTS

LIST OF FIGURES	viii
LIST OF TABLES	xiv
ACKNOWLEDGMENTS	xv
Chapter 1. INTRODUCTION	1
1.1. Background	1
1.1.1. Space Policy	1
1.1.1.1. Civilian Space Policy	1
1.1.1.2. Military Space Policy	2
1.1.2. Large Space Structures	4
1.1.2.1. Introduction	4
1.1.2.2. LSS Technology Development	4
1.1.2.3. LSS Applications	5
1.1.2.4. LSS Requirements	7
1.1.2.5. LSS Design Loads	8
1.1.2.6. LSS Structures and Materials	10
1.2 Research Approach	11
1.3 Methodology	12
1.4 Significance of Research	14
1.5 Literature Search	16
Chapter 2. DUAL KEEL SPACE STATION FREEDOM	18
2.1. History	18
2.2. Dual Keel Space Station Baseline Description	20
2.2.1. Configuration	20
2.2.2. Space Station Systems	21
2.2.3. Sub-system Requirements	23
2.2.4. Space Station Disturbances	24

Chapter 3. SPACE STATION DYNAMIC ANALYSIS	25
3.1. Finite Element Model Development	25
3.1.1. Finite Element Model	25
3.1.2. Truss Structure	26
3.1.3. Solar Dynamic Units	26
3.1.4. Photo Voltaic Solar Array	27
3.1.5. Central Station Radiators	27
3.1.6. Photo Voltaic Array Radiators	28
3.1.7. Module Cluster	28
3.1.8. Satellite Servicing and Storage Enclosure ..	29
3.1.9. Alpha Gimbals	30
3.1.10. Miscellaneous Attachments	30
3.2. Solution Technique	31
3.2.1. Governing Equation of Motion	31
3.2.2. Numerical Analysis Technique	32
3.3. Results	33
3.3.1. Rigid Body Response	33
3.3.2. Flexible Body Response	34
3.3.2.1. Transient Analysis	34
3.3.2.2. Left Solar Dynamic Unit - Node 3	35
3.3.2.3. Right Solar Dynamic Unit - Node 159 ..	35
3.3.2.4. Terrestrial Payloads - Node 227	36
3.3.2.5. Stellar Payloads - Node 335	36
3.3.2.6. US Laboratory Module - Node 90	37
Chapter 4. DEGRADATION EFFECTS OF THE LEO ENVIRONMENT ON SPACE STATION COMPOSITE MATERIALS	38
4.1. Space Station Composite Materials	38
4.2. Low Earth Orbit Environmental Effects on Composites	41
4.2.1. Thermal Cycling	41
4.2.2. Solar Radiation	42
4.2.3. Atomic Oxygen Bombardment	42
4.2.4. Micrometeoroid and Space Debris	43
4.2.5. NASA's Long Duration Exposure Experiment ...	45
4.3. Space Station Material Degradation Model	46
4.3.1. Degradation Mechanisms	46
4.3.2. Material Degradation Due to Coating Loss ...	46
4.3.3. Space Station Material Degradation Model ...	47

Chapter 5. EFFECTS OF MATERIAL DEGRADATION ON SPACE STATION DYNAMIC RESPONSE	49
5.1. Approach	49
5.2. Results	50
5.2.1. Rigid Body Response	50
5.2.2. Flexible Body Response	51
5.2.2.1. Transient Analysis	51
5.2.2.2. Left Solar Dynamic Unit - Node 3	51
5.2.2.3. Right Solar Dynamic Unit - Node 159 .	52
5.2.2.4. Terrestrial Payloads - Node 227	52
5.2.2.5. Stellar Payloads - Node 335	53
5.2.2.6. US Laboratory Module - Node 90	53
5.2.2.7. Degraded Cantilever Case	53
Chapter 6. CONCLUSIONS	55
6.1. Research Overview	55
6.2. Conclusions	57
6.2.1. Dual Keel Space Station Structural Design ...	57
6.2.2. Space Station Tube Design	57
6.2.3. Effects of Changes in Modulus of Elasticity on Dynamic Response	59
6.2.4. NASA and Air Force Space Facility Policy ...	60
6.3. Areas for Further Research	62
REFERENCE	57
APPENDIX Space Station Data.....	69

LIST OF FIGURES

1. Dual Keel Space Station Baseline Configuration	79
2. Space Station Orthogonal Tetrahedral Truss Bay	80
3. Space Station Module Cluster	81
4. Space Shuttle Docking Impulse	82
5. Space Station FEM X,Y,Z View	83
6. Space Station FEM -X View	84
7. Space Station FEM -Y View	85
8. Space Station FEM -Z View	86
9. Global Structural Response E=100% at t = 5 sec	87
10. Global Structural Response E=100% at t = 10 sec	88
11. Global Structural Response E=100% at t = 15 sec	89
12. Global Structural response E=100% at t = 25 sec	90
13. Node 80 Response E=100% X,Y,Z Displ./Rot.	91
14. Node 3 Response E=100% X,Y,Z Displ./Rot.	92
15. Node 159 Response E=100% X,Y,Z Displ./Rot.	93
16. Node 227 Response E=100% X,Y,Z Displ./Rot.	94
17. Node 335 Response E=100% X,Y,Z Displ./Rot.	95
18. Node 3 vs. 80 Response E=100% X,Y,Z Displ./Rot.	96
19. Node 159 vs. 80 Response E=100% X,Y,Z Displ./Rot.	97
20. Node 227 vs. 80 Response E=100% X,Y,Z Displ./Rot.	98
21. Node 227 Response E=100% X,Y,Z Lin./Rot. Accel.	99
22. Node 335 vs. 80 Response E=100% X,Y,Z Displ./Rot.	100
23. Node 335 Response E=100% X,Y,Z Lin./Rot. Accel.	101
24. Node 90 Response E=100% X,Y,Z Lin./Rot. Accel.	102

25. Flux Level for Meteor./Space Debris @ 400 Km	103
26. Number of Impacts for 150 SQ M @ 400 Km	104
27. Total Number of Ejecta Generated for 150 SQ M	105
28. Assumed Linear Degradation Model	106
29. Global Structural Response E=78% at t = 5 sec	107
30. Global Structural Response E=78% at t = 10 sec	108
31. Global Structural Response E=78% at t = 20 sec	109
32. Global Structural Response E=78% at t = 35 sec	110
33. Node 80 Response E=78% X,Y,Z Displ./Rot.	111
34. Node 3 Response E=78% X,Y,Z Displ./Rot.	112
35. Node 159 Response E=78% X,Y,Z Displ./Rot.	113
36. Node 227 Response E=78% X,Y,Z Displ./Rot.	114
37. Node 335 Response E=78% X,Y,Z Displ./Rot.	115
38. Node 3 vs. 80 Response E=78% X,Y,Z Displ./Rot.	116
39. Node 159 vs. 80 Response E=78% X,Y,Z Displ./Rot.	117
40. Node 227 vs. 80 Response E=78% X,Y,Z Displ./Rot.	118
41. Node 227 Response E=78% X,Y,Z Lin./Rot. Accel.	119
42. Node 335 vs. 80 Response E=78% X,Y,Z Displ./Rot.	120
43. Node 335 Response E=78% X,Y,Z Lin./Rot. Accel.	121
44. Node 90 Response E=78% X,Y,Z Lin./Rot. Accel.	122
45. Global Structural Response E=56% at t = 10 sec	123
46. Global Structural Response E=56% at t = 20 sec	124
47. Global Structural Response E=56% at t = 30 sec	125
48. Global Structural Response E=56% at t = 45 sec	126
49. Node 80 Response E=56% X,Y,Z Displ./Rot.	127
50. Node 3 Response E=56% X,Y,Z Displ./Rot.	128

51. Node 159 Response E=56% X,Y,Z Displ./Rot.	129
52. Node 227 Response E=56% X,Y,Z Displ./Rot.	130
53. Node 335 Response E=56% X,Y,Z Displ./Rot.	131
54. Node 3 vs. 80 Response E=56% X,Y,Z Displ./Rot.	132
55. Node 159 vs. 80 Response E=56% X,Y,Z Displ./Rot.	133
56. Node 227 vs. 80 Response E=56% X,Y,Z Displ./Rot.	134
57. Node 227 Response E=56% X,Y,Z Lin./Rot. Accel.	135
58. Node 335 vs. 80 Response E=56% X,Y,Z Displ./Rot.	136
59. Node 335 Response E=56% X,Y,Z Lin./Rot. Accel.	137
60. Node 90 Response E=56% X,Y,Z Lin./Rot. Accel.	138
61. Global Structural Response E=34% at t = 10 sec	139
62. Global Structural Response E=34% at t = 20 sec	140
63. Global Structural Response E=34% at t = 35 sec	141
64. Global Structural Response E=34% at t = 55 sec	142
65. Node 80 Response E=34% X,Y,Z Displ./Rot.	143
66. Node 3 Response E=34% X,Y,Z Displ./Rot.	144
67. Node 159 Response E=34% X,Y,Z Displ./Rot.	145
68. Node 227 Response E=34% X,Y,Z Displ./Rot.	146
69. Node 335 Response E=34% X,Y,Z Displ./Rot.	147
70. Node 3 vs. 80 Response E=34% X,Y,Z Displ./Rot.	148
71. Node 159 vs. 80 Response E=34% X,Y,Z Displ./Rot.	149
72. Node 227 vs. 80 Response E=34% X,Y,Z Displ./Rot.	150
73. Node 227 Response E=34% X,Y,Z Lin./Rot. Accel.	151
74. Node 335 vs. 80 Response E=34% X,Y,Z Displ./Rot.	152
75. Node 335 Response E=34% X,Y,Z Lin./Rot. Accel.	153
76. Node 90 Response E=34% X,Y,Z Lin./Rot. Accel.	154

77. Global Structural Response E=12% at t = 10 sec	155
78. Global Structural Response E=12% at t = 25 sec	156
79. Global Structural Response E=12% at t = 45 sec	157
80. Global Structural Response E=12% at t = 60 sec	158
81. Node 80 Response E=12% X,Y,Z Displ./Rot.	159
82. Node 3 Response E=12% X,Y,Z Displ./Rot.	160
83. Node 159 Response E=12% X,Y,Z Displ./Rot.	161
84. Node 227 Response E=12% X,Y,Z Displ./Rot.	162
85. Node 335 Response E=12% X,Y,Z Displ./Rot.	163
86. Node 3 vs. 80 Response E=12% X,Y,Z Displ./Rot.	164
87. Node 159 vs. 80 Response E=12% X,Y,Z Displ./Rot.	165
88. Node 227 vs. 80 Response E=12% X,Y,Z Displ./Rot.	166
89. Node 227 Response E=12% X,Y,Z Lin./Rot. Accel.	167
90. Node 335 vs. 80 Response E=12% X,Y,Z Displ./Rot.	168
91. Node 335 Response E=12% X,Y,Z Lin./Rot. Accel.	169
92. Node 90 Response E=12% X,Y,Z Lin./Rot. Accel.	170
93. Comparative Plots Case 1-5 Node 80 X-Displacement	171
94. Comparative Plots Case 1-5 Node 80 Y-Displacement	172
95. Comparative Plots Case 1-5 Node 80 Z-Displacement	173
96. Comparative Plots Case 1-5 Node 80 X-Rotation	174
97. Comparative Plots Case 1-5 Node 80 Y-Rotation	175
98. Comparative Plots Case 1-5 Node 80 Z-Rotation	176
99. Comparative Plots Case 1-5 Node 3 vs. 80 X-Displ.	177
100. Comparative Plots Case 1-5 Node 3 vs. 80 Y-Displ.	178
101. Comparative Plots Case 1-5 Node 3 vs. 80 Z-Displ.	179
102. Comparative Plots Case 1-5 Node 3 vs. 80 X-Rot.	180

103.	Comparative Plots Case 1-5 Node 3 vs. 80 Y-Rot.	181
104.	Comparative Plots Case 1-5 Node 3 vs. 80 Z-Rot.	182
105.	Comparative Plots Case 1-5 Node 159 vs. 80 X-Displ.	183
106.	Comparative Plots Case 1-5 Node 159 vs. 80 Y-Displ.	184
107.	Comparative Plots Case 1-5 Node 159 vs. 80 Z-Displ.	185
108.	Comparative Plots Case 1-5 Node 159 vs. 80 X-Rot.	186
109.	Comparative Plots Case 1-5 Node 159 vs. 80 Y-Rot.	187
110.	Comparative Plots Case 1-5 Node 159 vs. 80 Z-Rot.	188
111.	Comparative Plots Case 1-5 Node 227 vs. 80 X-Displ.	189
112.	Comparative Plots Case 1-5 Node 227 vs. 80 Y-Displ.	190
113.	Comparative Plots Case 1-5 Node 227 vs. 80 Z-Displ.	191
114.	Comparative Plots Case 1-5 Node 227 vs. 80 X-Rot.	192
115.	Comparative Plots Case 1-5 Node 227 vs. 80 Y-Rot.	193
116.	Comparative Plots Case 1-5 Node 227 vs. 80 Z-Rot.	194
117.	Comparative Plots Case 1-5 Node 227 X-Accel.	195
118.	Comparative Plots Case 1-5 Node 227 Y-Accel.	196
119.	Comparative Plots Case 1-5 Node 227 Z-Accel.	197
120.	Comparative Plots Case 1-5 Node 227 X-Ang.Accel.	198
121.	Comparative Plots Case 1-5 Node 227 Y-Ang.Accel.	199
122.	Comparative Plots Case 1-5 Node 227 Z-Ang.Accel.	200
123.	Comparative Plots Case 1-5 Node 335 vs. 80 X-Displ.	201
124.	Comparative Plots Case 1-5 Node 335 vs. 80 Y-Displ.	202
125.	Comparative Plots Case 1-5 Node 335 vs. 80 Z-Displ.	203
126.	Comparative Plots Case 1-5 Node 335 vs. 80 X-Rot.	204
127.	Comparative Plots Case 1-5 Node 335 vs. 80 Y-Rot.	205
128.	Comparative Plots Case 1-5 Node 335 vs. 80 Z-Rot.	206

129. Comparative Plots Case 1-5 Node 335 X-Accel.	207
130. Comparative Plots Case 1-5 Node 335 Y-Accel.	208
131. Comparative Plots Case 1-5 Node 335 Z-Accel.	209
132. Comparative Plots Case 1-5 Node 335 X-Ang.Accel.	210
133. Comparative Plots Case 1-5 Node 335 Y-Ang.Accel.	211
134. Comparative Plots Case 1-5 Node 335 Z-Ang.Accel.	212
135. Comparative Plots Case 1-5 Node 90 X-Accel.	213
136. Comparative Plots Case 1-5 Node 90 Y-Accel.	214
137. Comparative Plots Case 1-5 Node 90 Z-Accel.	215
138. Comparative Plots Case 1-5 Node 90 X-Ang.Accel.	216
139. Comparative Plots Case 1-5 Node 90 Y-Ang.Accel.	217
140. Comparative Plots Case 1-5 Node 90 Z-Ang.Accel.	218
141. Total Rotation - Node 3 (degrees)	219
142. Total Rotation - Node 159 (degrees)	220
143. Total Rotation - Node 227 (degrees)	221
144. Total Rotation - Node 335 (degrees)	222
145. Max. Linear Acceleration - Node 90 (mm/sec/sec)	223
146. Max. Linear Acceleration - Node 227 (mm/sec/sec)	224
147. Max. Linear Acceleration - Node 335 (mm/sec/sec)	225

LIST OF TABLES

4.1 Space Station Design Requirements	39
4.2 Space Station Truss Structure Orbital Environment Parameters	39
4.3 Space Station Tube Properties	40

ACKNOWLEDGEMENTS

This research topic represents the evolution of traditional terrestrial activities of government, industry, and academia to implement the Nation's long range goals in space. One area, manned space facilities, requires new relationships. Aerospace and architectural/civil engineering communities must work together if our Nation is to be successful in exploiting space to benefit mankind. The foundation was laid at the start of this thesis in 1988 with the American Society of Civil Engineering and the U.S. Air Force Engineering and Services sponsoring the first annual conference titled Engineering, Construction, and Operations in Space. The Air Force also created the Engineering and Services Space Liaison Group (ESSLG) to develop long range goals for the transition of traditional civil engineering roles in space. With the end of the Cold War, the President has directed the National Space Council, chaired by the Vice - President, to pursue an intra - departmental approach to implementing long range national space objectives. The future will no longer see a completely separate civilian and military space effort as was born out of the post Sputnik and Cold War competition. DOD, NASA, and DOE will consolidate their organizational talents and resources to execute programs as the Space Exploration Initiative and Mission to Planet Earth.

Although presently unconventional, this work required the vision and support of several people and organizations. I would like to thank the Air Force Institute of Technology for selecting me for this Masters program and approval of the research topic. I am also indebted to my thesis committee - Dr. Geschwinder, Dr. Sanvido, Dr. Seaburg, and Dr. Jensen - for

assisting me in accomplishing this work. As thesis and graduate advisor, Dr. Geshwinder provided the direction and resources necessary to accomplish this thesis. Within one week of my arrival at Penn. State, he recommended and funded my attendance at the first annual conference - Space 88, Engineering , Construction, and Operations in Space. In retrospect, Dr. Geshwinder's suggestion and investment to an unknown student proved to be the springboard to accomplishing my research goals in space facilities. Over the next two years, I gained further appreciation of his complete dedication and selflessness to me and other students. Dr. Sanvido's enthusiasm, energy, and advice was critical during the frustrating literature search and topic formulation stage. The knowledge and insight gained from my interaction with him, provided the relevance of this work to the overall civil engineering process. Dr. Sanvido constantly reinforced the need to look at the "big picture." Dr. Seaburg, in addition to providing detailed technical comments, ensured that my overall graduate education and research focused on satisfying my long range career goals. Dr. Jensen generously volunteered to participate in this research, even though it was outside of his departmental responsibilities. Without contribution of his expertise in large space structures, structural dynamics, and advanced composites, this thesis could not have been completed.

Outside Penn. State, NASA's Johnson Space Center and Langley Research Center provided much of the data on the design of Space Stations structure, materials, and LEO environmental effects. Specifically I would like to thank Tom Sutter, Steve Tompkins, and Harold Bush from NASA Langley for giving their time and expertise to the work. From the Pentagon, Col. Mike Oakley was helpful for integrating my work within the overall A.F. civil engineering space policy, and provided many contacts to help me with the thesis. Finally, I

would like to thank Col. Mitchell, Program Director for Small ICBM, for encouragement in completing the research.

I would also like to thank my many close friends met while at Penn. State - Jimmy Juwana, Dave Shea, Will Cassidy, and Carol Sue Bernardo. Without their friendship, support, and humor, my graduate experience at Penn. State would have been boring.

Chapter 1

INTRODUCTION

1.1 Background

1.1.1 Space Policy

United States (US) National Security Strategy calls for an evolutionary growth in man's understanding, exploration, settling, and use of space for both civilian and military purposes. On July 20, 1989, President Bush announced:

... The time has come to look beyond brief encounters. We must commit ourselves anew to a sustained program of manned exploration of the solar system and yes, the permanent settlement of space.(1)

Two key elements of the US space strategy are expanding human presence and activity beyond earth orbit and into the solar system and ensuring the freedom of space for exploration and development, for ourselves and all nations.

1.1.1.1 Civilian Space Policy

To expand human presence and activity, the National Space Council under Vice President Quayle has directed the National Aeronautics and Space Administration

(NASA) to build on the successes and expertise developed in the Apollo, Skylab, Space Shuttle and eventually the Space Station Freedom programs, ultimately establishing permanent human settlements on the Moon and putting humans on Mars. This program, referred to as the Space Exploration Initiative (SEI), received continued support by President Bush on January 25, 1992 when he asked the nation to " make a farsighted commitment, one that looks dozens of years and millions of miles beyond the recession and other things that tend to preoccupy us today." (2)

1.1.1.2 Military Space Policy

Under ensuring the freedom of space element, space - the oceans of tomorrow and highways to discovery and commerce - holds the potential for closure and springboards for attack from other nations. Military space policy focuses on assuring access to space and stopping an aggressor before he can use a space system to threaten objects or people in or from space. The Department of Defense (DOD) and the Air Force (AF) have been chartered to ensure US access to space. Current AF space policy states :

1. Space power will be as decisive in future combat as airpower is today.
2. AF must be prepared for the evolution of space power from combat support to the full spectrum of military capabilities.
3. AF will make a solid corporate commitment to integrate space throughout the AF.(3)

Specific roles which the AF is assigned are: space control, force application, force enhancement, and space support. The utility of space was recently proven during Desert Storm. AF Chief of Staff, General McPeak commented "Desert Storm was the first space war ... now we cannot think about the AF without thinking of space." This conclusion was also emphasized by Lt. General Barry, commander of AF Space Systems Division - "Desert Storm brought space out of the closet. Our military, as well as public, gained an appreciation for our dependence on space to accomplish the operational mission." (4)

Unclassified AF space programs such as NAVSTAR Global Positioning System, Defense Satellite Communication System, Defense Meteorological Satellite Program, Defense Satellite Program, National Aerospace Plane, National Launch System, and *Global Protection Against Limited Strikes (GPALS)* all demonstrate the current and future use of space for military applications.

One key element of the planned evolutionary growth of both civilian and military space programs is Large Space Structures (LSS) which provide a key component to the space infrastructure necessary to accomplish man's growth, exploration, settling, and use of space.

1.1.2 Large Space Structures

1.1.2.1 Introduction

With the realization of the Space Shuttle or Space Transportation System (STS) in the late 1970s, on-orbit assembly and deployment of space structures became possible. No longer limited by the transporter's payload volume, scientists and engineers could now conceptualize and design space structures with unlimited dimensions to meet various applications.

1.1.2.2 LSS Technology Development

Initial research into LSS began with NASA, DOD, and the American Institute of Aeronautics and Astronautics (AIAA). Beginning in 1959, the AIAA initiated the annual Structures, Structural Dynamics, and Materials Conference. Articles began to appear in these proceedings in the early 1970's. In 1978, the AIAA initiated specialized conferences on LSS in response to NASA's planning beyond the Shuttle and Skylab programs. NASA's follow-on goal was to develop a permanently manned space station. One of the first specialized conferences held was the AIAA Conference on Large Space Platforms: Future Needs and Capabilities, in September 1978, began the initial conceptual research thrust into LSS. Also in 1978, NASA instituted a similar effort with the first Large Space Systems Technology (LSST) technical review under the LSST

program office. The LSST program office concentrated efforts towards state-of-the-art technology related to large antenna systems design and control; basic technology concerning structures, materials, and analysis; and flight technology experiments.(5) Results of these early research projects and conferences identified future research requirements to mature LSS technology. By the early 1980's, NASA, DOD, and AIAA created major LSS programs focusing on design and analysis techniques, advanced composite materials, structural dynamics and control, and control system and structural interaction. LSS technology has matured so that it can be incorporated into future missions currently under design. To design a LSS, one must understand the application, specific structural requirements, and loads before the structures and materials can be selected.

1.1.2.3 LSS Applications

Typically LSS applications fall into four areas identified by AIAA standards: Earth Services and Communications, Manned Space Facilities, Science and Observation, and Solar and Thermal Energy Systems.

Earth Services and Communication consists of earth satellites or a system of Earth satellites, usually in geostationary orbit, that receive and transmit data and information via one or more radio frequency bands. Services may include communications from earth-to-satellite, satellite-to-earth and satellite-to-satellite. Antennas, reflectors, and

space platforms fall into this area.

Manned Space Facilities are facilities in space with a resident crew that support or perform missions requiring long duration operation, periodic in-space servicing and maintenance, or space-based transportation systems. Space stations, crew and power modules, payloads, and construction bases are examples of space facilities.

Science and Observation LSS support systems as large instruments used either to sense remote objects or phenomena near Earth, on Earth, in the solar system, in deep space, or to make in-situ measurements of the orbital environment. Examples are payloads, radar, telescopes, and mechanical arms that are rotated from spacecraft or space platforms to their targets.

Solar and Thermal Energy Systems are large area structures equipped to collect solar energy and convert it to electrical or heat energy, used either to power space systems, or to produce microwave energy which can be transmitted to Earth for terrestrial purposes. Examples are solar collectors, reflectors, and transmitters.(6)

LSS are planned for use in on-going programs such as Space Station Freedom, SEI, and GPALS.

1.1.2.4 Large Space Structures Requirements

Design of LSS depends on the application's specific mission requirements. Generally, the structure must enclose, protect, support, and provide the desired environment for the attached payloads or subsystems.

Specific structural requirements, such as displacement and acceleration tolerances, define the environment. To meet the environment, strength and dynamic response to applied loads become the primary design considerations to meet the systems support. These requirements range from pointing accuracy for antennas, science and observation instruments, and solar and thermal systems, to acceleration tolerances for lab experiments or payloads on manned space facilities. For example, a one kilometer antenna requires a one millimeter surface tolerance for operation. On a solar powered satellite antenna, pointing accuracy is about 0.0003 degrees; while communication satellites accuracy ranges from 0.03 to 0.05 degrees.(7) Space station solar dynamic units have a maximum rotational requirement of 0.1 degree for operation.(8) For the space station laboratory and some attached payloads, microgravity conditions must be maintained; thus, accelerations are limited to 0.000001 g's.(9) In addition to the system requirements, the expected loads must be known before the structure can be designed.

1.1.2.5 LSS Design Loads

Space structures are designed for all significant loads experienced during operation. These loads vary in magnitude and are divided into four general mission phases: prelaunch, launch, interorbit boost, space erection, and space operation.(10)

Prelaunch loads occur from material fabrication, handling, ground transportation, and qualification testing. Because of microgravity conditions in space, structures could conceivably perform adequately in space but fail when exposed to prelaunch loads imposed in one-"g" conditions on Earth.

Launch loads occur from energy transmitted by launch vehicle accelerations through interfaces and acoustic noise. These loads occur for thirty minutes or less, and reach their maximum values at final burnout (maximum acceleration). LSS that are erectable will experience these loads as individual members - packed and undeployed. For the STS launch vehicle, these loads range from 5 to 6 g's during launch and from 3 to 8 g's in an abortive launch and landing (depending upon the axis).(11) For designing structural strength requirements, launch loads typically govern, leading to space structures being referred to as "launch structures".

Inter-orbit boost loads occur once the LSS is constructed and deployed. To maintain a desired orbit decay due to atmospheric drag (station keeping) or to achieve

a higher energy orbit, the spacecraft must be re-boosted via on board thrusters. For the space station, station keeping is required every 1-2 months and consists of four 75 lb. thrusters firing for six minutes.(12)

Space erection and construction can cause large loads on the structure until it reaches final configuration. An illustration is the space station assembled from the STS. During erection, the structure will be attached and reattached to the STS. NASA investigations have shown that struts can easily be broken during construction and even damage some subsystems such as the photovoltaic system.(13)

Once operational, the LSS will experience a multitude of internal and external loads while maintaining mission requirements. For manned platforms such as the space station, internal loads include: crew motion, fluid transfer, rotating machinery, payload slewing, mobile service system (equipment and payload transfer device), reboost, and control system torques. Externally applied loads are due to station operations and the orbital space environment. Under external operations, the station will have the shuttle or orbital maneuvering vehicle docking with the station. The orbiting structure will also experience aerodynamic drag, solar pressure drag, gravity gradient, solar thermal, and electrostatic/electromagnetic body forces.(14)

Because of microgravity in space, most operational loads are insignificant to the strength of the structure and the main operational requirement of the structure is

restricting the LSS dynamic response to meet mission requirements. This is a function of the stiffness of the configuration and materials.

Space structures and materials must be strong enough to support the prior loads, and limit the structure's dynamic response to meet the mission requirements.

1.1.2.6 LSS Structures and Materials

In space, structures and materials must be lightweight, possess high strength and stiffness, be dimensionally stable, and long life. Because of these requirements, LSS typically use repetitive lattice structures due to their simplicity, low mass, high stiffness, and packing efficiency; and employ advanced composite materials due to their high specific strength and stiffness, low coefficient of thermal expansion, and ability to withstand the harsh space environment over extended design lives.(15)

The low Earth orbit space environment is harsh and hostile for any material, especially composites. Consequently, these effects must be considered in the design and performance of the structure and materials over their design lives. Major degradation effects from the space environment on composite materials include: thermal and mechanical cycling, ultra-violet radiation, atomic oxygen bombardment, micrometeoroid/space debris collision, and physical aging. Over time, these effects degrade the materials, changing their mechanical properties which govern the structure's

dynamic response.

1.2 Research Approach

Composite Large Space Structures are proposed for use in NASA's Space Station "Freedom," the Global Protection Against Limited Strikes, and other space programs. Once deployed, these structures will be required to sustain severe environmental effects - radiation, temperature, atomic oxygen bombardment, collision with meteoroid and man-made debris, and hostile actions - and transient operational loads - docking, slewing, construction and other manned activities, and control system thrusters - while maintaining strict mission parameters. Over time, material and structural degradation will occur due to environmental effects causing a change in the structure's stiffness and dynamic response. Likely, this structural damage will require immediate repair to restore the LSS to full mission capability.

This thesis investigates the dynamic response of one LSS - NASA's Dual-Keel Space Station "Freedom" - under one applied operational load - an aborted shuttle docking - and then evaluates the changes on the dynamic response due to material degradation effects of the space environment on LSS materials. The dynamic response will be evaluated at five subsystem locations and compared to their associated deflection and acceleration requirements. These five subsystems locations are: two station solar dynamic units positioned at the ends of the horizontal boom; terrestrial pointing payloads

at the center of the lower keel boom; stellar pointing payloads at the center of the upper keel boom; and the space station laboratory module located in the station's central modal cluster (see Figure 1). Analysis will be repeated using a linear material degradation model representing the effects of the LEO space environment on material properties over the station's 20-30-year design life. Results will show the affects of material degradation on the station's dynamic response and subsystem displacement and acceleration requirements.

1.3 Methodology

The research was conducted as follows:

- a. Provide a brief history of space station, it's configuration, structure and materials, and subsystems;
- b. Develop a finite element model (FEM) of the station;
- c. Perform a dynamic analysis of the space station FEM under an applied aborted docking impulse using ADINA - A Finite Element Program for Automatic Dynamic Incremental Nonlinear Analysis - software and evaluate the station's response relative to the station's geometric center at five locations:

1. Solar Dynamic Unit on boom's left end;
 2. Solar Dynamic Unit on boom's right end;
 3. Terrestrial pointing payloads at the center of the lower keel boom;
 4. Stellar pointing payloads at the center of the upper keel boom;
 5. Space station laboratory module located in the central module cluster;
- and compare against these payload, subsystem, and laboratory experiment requirements.

d. Investigate the effects of the LEO space environment on space station materials over a 30 year design life and develop a material degradation model that approximates these effects.

e. Apply the degradation model to the space station FEM and re-perform the dynamic analysis with the aborted shuttle docking load, and investigate the response at the five locations relative to payload, subsystem, and laboratory requirements.

f. Present results and conclusions from analysis.

g. Identify areas for further research.

1.4 Significance of Research

US space policy calls for an evolutionary growth into the use of space for civilian and military objectives. The author, as a member of the USAF Engineering and Services Space Planning and Requirements Integration Team (ESSPRIT) formerly the Engineering and Services Space Liaison Group, is directed to research and develop long range plans to normalize traditional terrestrial civil engineering activities into space. One of the five basic space roles of USAF Engineering and Services (E&S) is to develop capabilities to construct, operate, maintain and repair facilities in space.(16) NASA's Space Station Freedom represents the first true space facility and serves as a model for analysis for potential future military space facilities. With terrestrial facilities E&S establishes a Reoccurring Work Plan (RWP) to maintain building subsystems over their design lives to meet functional requirements. This will also be the case for space facilities. This paper investigates the maintenance requirements for the structural subsystem of space facilities over their anticipated design life and operational environment in Low Earth Orbit (LEO).

The need for on-orbit maintenance was proven during the SKYLAB program:

Initial planning for SKYLAB envisioned only a limited degree of inflight maintenance. As with previous spaceflight programs, dependence was to be placed on components of very high reliability and the use of redundant

systems, was necessary. As the program evolved, however, the Skylab systems became increasingly complex. In addition, the manned periods were lengthened, and plans were developed to have astronauts perform more and more tasks. It became obvious that even with high reliability systems, failures could occur. And if they did, they could jeopardize mission completion. Gradually, a concept was developed which called for considerable maintenance to be performed by the flight crew.(17)

With a cost of \$30 billion for Space Station "Freedom," the stakes are much higher than with Skylab. Freedom will serve as the initial infrastructure for future space industrialization, colonization, and exploration. As with Skylab and the Hubble Space telescope, design errors and failures will delay future programs such as lunar colonies and manned exploration of Mars. Current allocation for Extravehicular Activity (EVA) and Intravehicular Activity (IVA) maintenance time is limited to 1170 hours annually for all station systems; which equates to 3.2 hours per day.(18)

To date, no literature has been found which relates the effects of material degradation on the response of an operational LSS, such as space station, compared to mission requirements. This thesis attempts to investigate this question and assist NASA and AF civil engineers in forecasting resource requirements for LSS maintenance.

1.5 Literature Search

Current literature and research focuses on "smart" structures. Structures become "smart" when, like the human body, they can "feel" or evaluate their present strength and identify injury or damage through sensors (nerves) such as fiber optic filaments. Smart structures can also increase strength and stiffness mechanically as needed for various load inputs based on serviceability criteria. NASA is investigating the use of smart large space structures under the Control of Flexible Structures (COFS) program. This program uses embedded sensors, actuators, and active/passive dampening, to permit precision positioning, pointing, tracking and vibration suppression for LSS. One application for smart LSS is the monitoring of structural properties over the design life, sensing changes, and identifying required repair locations. Preliminary investigations into potential algorithms for non-destructive sensing/inspection of degradation in stiffness and dynamic response were reported in References (19-23). These methods involved sensing changes of the structures natural frequency, modes, and deflections to point out damage locations. Results show difficulty identifying damage in individual members, and appears to require further research. Although these investigators have concentrated on damage sensing, only two papers found considered the effects of degradation on the structures dynamic response.

Chen studied the change in stiffness of a simple mast beam by assuming a percent damage/degradation in materials, then compared the resulting frequencies and mode

shapes to the undamaged case. Results proved that low levels of degradation had significant effects on dynamic response.(24) Kalyanasundarem's work probed a load induced degradation model with a range of 10% reduction and concluded that even at small levels, degradation significantly affects the modal response of LSS.(25) To date, no literature found relates environmental induced degradation on the structure's dynamic response and the system's mission requirements.

Chapter 2

DUAL KEEL SPACE STATION FREEDOM

2.1 History

With the success of the Skylab program and an operational Space Transportation System, NASA began plans in the late 1970s for their next major goal - to construct a permanently manned space station in Low Earth Orbit (LEO). In May, 1982, NASA established the Space Station Task Force to consolidate and direct space station activities, and identify mission requirements. Based on the task force results, a manned space station will serve the following missions:

- A laboratory in space for the conduct of science and the development of new technologies;
- A permanent observatory to look down upon the Earth and out at the universe;
- A transportation node where payloads and vehicles are stationed, assembled, processed, and propelled to their destinations;
- A servicing facility where these payloads are maintained and if necessary, repaired;
- An assembly facility where, due to ample time on-orbit and the presence of appropriate equipment, large structures are put together and checked out;

- A manufacturing facility where human intelligence and the servicing capability of the station combine to enhance commercial opportunities in space; and
- A storage depot where payloads and parts are kept on-orbit for subsequent deployment.(26)

Support for the station's concept and mission was emphasized in 1984 during then President Reagan's State-of-the-Union Address to Congress and the public:

... America has always been greatest when we dared to be great. We can reach for that greatness again. We can follow our dreams to the distant stars, living and working in space for peaceful, economic, and scientific gain. Tonight, I am directing NASA to develop a permanently manned space station and to do it in a decade.(27)

Space station support continued into the present Bush administration through statements at the 20th anniversary of the Apollo lunar landing; "the station is a first step for sustained manned exploration." (28)

Fiscal pressures have caused the original Initial Operating Capability (IOC) of 1994 to slip to 1999. The House Committee on Science, Space, and Technology in 1992 requested an independent review of space station concept for possible downsizing and redesign to lower costs.

Although the final configuration may change between now and deployment, this research focusses on the Dual Keel space station baseline.

2.2 Dual Keel Space Station Baseline Description

2.2.1 Configuration

Various space station configurations were investigated to meet mission goals in 1984 by the Systems Engineering and Integration "skunk-works" of the space station program office at Johnson Space Center. Although many science-fiction inspired shapes were considered, transportation, growth flexibility, maximum payload area, and stiffness considerations led to an investigation of revolutionary shapes. The main configuration criteria established by NASA included: capability of evolutionary growth in all three directions and accommodating unanticipated alterations; allow for a variety of shuttle compatible, customer friendly payloads with minimum interference to growth and space station operations; provide a stiff and stable framework to minimize control-structure interaction, simplify the pointing systems of stellar, solar, and Earth observation instruments, and accommodate microgravity experiments. In August, 1984, the skunk-works published the Space Station Reference Configuration Description, yielding four primary candidate gravity gradient stabilized truss structures, known as power towers: the deployable single-fold truss with 9-ft. bays; a deployable double-fold; an erectable truss with 15 ft. bays; and the deployable double-fold delta shaped keel using a

tetrahedral truss with 10 ft. members. (29) The following year, NASA's Langley Research Center conducted a trade study evaluating the use of either deployable or erectable trusses for space station. The study evaluated specific trusses against the following requirements:

- stiffness, mass, and cost;
- customer accommodations (payloads, growth, and spacecraft construction);
- space station operations (payload movement, maintenance, and services);
- space construction (EVA time, reliability, safety, and construction experience).(30)

Although earlier studies perceived the deployable truss as the most advantageous, the evaluation concluded the 15 ft. erectable truss is superior. In January, 1986, NASA selected the 5 meter (15 ft.) erectable truss as the baseline for space station and changed the configuration from a power-tower to a new dual keel design. The Dual Keel Baseline configuration is shown in Figure 1.

2.2.2 Space Station Systems

As described earlier, the station is a multi-purpose, multi-mission, facility and support a crew of eight. The station will operate at an altitude of 250 nautical miles, in a low inclination - 28.5 degree - elliptical orbit. The stations velocity averages around

18,000 miles-per-hour. The station will orbit in a Earth-fixed attitude with the upper and lower keels pointed towards Earth. The primary structure is 476 ft. along the horizontal axis and 361 ft. along the vertical axis with an overall mass of 570,000 lbm. The structure is assembled from 5 meter (16.4 ft.) orthogonal tetrahedral trusses with 2 inch diameter graphite epoxy tubes and a wall thickness of 0.06 inches (see Figure 2). Attached to the center of the structure is the interconnected module cluster, containing the US laboratory and habitat modules, the European Space Agency (ESA) lab module, and the Japanese Experiment Module (JEM)(see Figure 3). These four aluminum modules have varying diameters and lengths, but on average, have an inside diameter of 174 inches and 0.115 inch thickness. These modules, along with their interconnecting airlocks, tunnels, and shuttle docking ports, constitute fifty percent of the station's mass. On both ends of the horizontal boom are the solar dynamic units (SDU), consisting of parabolic solar collectors and thermal radiators. Adjacent to the both SDUs are the photovoltaic (PV) solar arrays. These arrays are 80 feet in length, 15 feet wide, and 1.3 inches thick. Collectively, both the SDUs and PV arrays produce the station 75 kW power requirements, with 50 kW allocated to users and 25 kW for station keeping. The station's two thermal control radiators are also located on the horizontal boom. They consist of a 30 ft. support boom and radiators which are 50 ft. long, 8.75 feet wide, and 1.3 inches thick aluminum box. The attitude control system consists of a control-moment-gyro located at the center of the horizontal boom, and attitude control thrusters on the corners of the upper and lower keels. The upper keel boom supports several solar and stellar pointing payloads, while the lower keel boom supports Earth pointing

payloads. Two satellite and orbital maneuvering vehicle (OMV) servicing and storage enclosures are located inside the upper and lower keels. The mobile service center traverses the entire truss structure to place and relocate payloads. Utility trays run along the base of the entire truss framework and provide power and thermal control to all systems.

2.2.3 Subsystem Requirements

Under the space station specification, the station and structure must limit the deflections and accelerations to allow proper functioning of payloads, experiments, and subsystems. This research will focus on three subsystems. In the US laboratory module, microgravity research requires accelerations below 0.00001 times the Earth's gravity. For the solar dynamic units, rotation of the *parabolic collectors must be less than 0.1 degrees* from the solar vector for performance. Attached stellar, solar, and terrestrial payloads located on the station's upper and lower booms must meet certain pointing requirements. Although none have been defined yet, it is assumed that they will be in the range of the SDU's requirement of 0.1 degree maximum rotation. The structure must meet these requirements under a series of operational and non-operational disturbances.

2.2.4 Space Station Disturbances

Disturbances to the station cause dynamic responses by the structure potentially exceeding system requirements if the structure is not stiff enough. Operational disturbances consist of crew motion, machinery, payload slewing, MSC operations, control system torques, solar array rotation, and mass changes due to payload relocation. Non-operational disturbances include reboost, assembly, and space shuttle/OMV docking. This paper applies an aborted shuttle docking impulse as shown in Figure 4. An aborted shuttle dock is defined as a 500 lb. force, for 1 second, on the modules airlock, with the shuttle not attaching.

Chapter 3

SPACE STATION DYNAMIC ANALYSIS

3.1.1 Finite Element Model

To determine the station's dynamic response located at the solar dynamic units, payloads, and laboratory module under an aborted shuttle dock, a detailed finite element model has been created using ADINA software, NASA specifications, and earlier dynamic analysis performed (31-48). The model is shown in Figures 5-8. The global X,Y,Z coordinate system is located at the models geometric center, node 80. The positive Y-axis extends from the center of the horizontal boom in the left or port direction, with the negative Y-axis right or starboard of the center boom. Positive Z-axis is below the geometric center, towards the lower keel, and negative Z-axis is up towards the upper keel, again from the geometric center. Negative X-axis extends from the rear or aft of node 80. Units of measure selected are meter, kilogram, newton, radians, and seconds. The station's dimensions are 22.5 meters (73.8 ft.) in the X-axis, 150 meters (492 ft.) in the Y-axis, and 110 meters (361 ft.) in the Z-axis.

The total model consists of 448 nodes and 1417 beam elements with 2,688 degrees-of-freedom. Station's total mass is 1,214 million kilograms. For analysis, the station is assumed to be at rest and gravity is zero. Damping is assumed to be 0.5%

critical. Material properties are assumed to be isotropic and linear elastic with displacements small. Material properties are defined by the modulus of elasticity and Poisson's ratio.

3.1.2 Truss Structure

The stations primary truss structure consists of 5 meter truss bays as shown in figure 2, and 50.8 mm (2 inch) outside diameter graphite/epoxy tubes with wall thickness of 1.824 mm (0.072 inches) and are modelled as two node beam elements representing the tube properties. The tube modulus of elasticity is 276 giga-newtons per square meter (40 MSI) and a lineal density of 0.21 Kg/M. Truss joints are assumed to be rigid, behave linearly, and have a mass of 2.26 Kg/node. For the baseline erectable structure, research has shown to validate the modeling of the station elements with beam elements and rigid joints.(49) Truss members effective stiffness is reduced to 248.3 giga-newtons per square meter to account for the presence of joints.(50-65)

3.1.3 Solar Dynamic Units

Solar Dynamic Units (SDU) are located on both ends of the horizontal booms (nodes 3,159) and are modelled as two node rigid beams, 9.92 meters long, with concentrated masses of 2,833 Kg at nodes 3 and 159, and 3,531 Kg at nodes 2 and 160, representing the solar collector/converters and reflectors/radiators, respectively. Support

attachments of the SDU to the truss structure are modelled as rigid beams. Pointing accuracy criteria require the rotation of nodes 3 and 159 not exceed 0.1 degree rotation from the solar vector for proper operation. Total rotation is defined by the Pythagorean theorem which states the resultant is the square root of the sum of the squares of Y and Z rotations.(66)

3.1.4 Photo Voltaic Solar Arrays

Two solar arrays are located along the horizontal beam adjacent to the SDUs and consist of a central deployable mast to which two blankets covered on one side by solar cells are attached. The mast is 24.4 meters long and the blankets are 4.57 meters wide. These photovoltaic (PV) arrays are modelled as two node beam elements with equivalent stiffness and density, located at nodes 20-21, 28-29, 137-138, and 143-144. PV attachment supports to the main truss are modelled as rigid beams.

3.1.5 Central Station Radiators

The two central station radiators are located along the horizontal boom between and parallel to the PV arrays and verticle booms of the upper and lower keels. The radiators contain a 9.15 meter support boom made of aluminum tubes ($E=69$ giga-newtons/square meter) with an outside diameter of 0.61 meters and a inside diameter of 0.607. The lineal density is 5,510 Kg/cubic meter. The radiators extend beyond the

support and are 15.24 meters long, with the cross-sectional properties of a 2.67 meter by 0.033 meter aluminum box with a thickness of 0.0012 meters. The radiators density is 521,670 Kg/cubic meter. Both support boom and radiator are modelled as two node beam elements and are located at nodes 42-44, 45-47, 119, 123-124, and 120-122. Radiator attachment supports are modelled as rigid beams.

3.1.6 Photo Voltaic Array Radiators

PV radiators are located within the same truss bay as the PV arrays, but extend perpendicular to them. PV radiators are modelled identically to the central radiators, except they possess no support booms. Nodes that connect the PV radiators are 26-27 and 145-146.

3.1.7 Module Cluster

The module cluster - consisting of the US laboratory and habitation modules, the Japanese Experiment Module (JEM), the European Space Agency (ESA) logistics module, and connecting airlocks and tunnels - is attached to the top truss face in the center bays of the horizontal boom and aft (negative X-direction) support extension. All modules are modelled as two node beam elements with cross sectional properties of a 4.419 meter outside diameter and 4.416 meter inside diameter aluminum cylinder. Densities and lengths vary with module. The four airlocks located at nodes 77-79, 90-

92, 413-415, and 426-428, have lengths of 3.2 meters and density of 37.462 Kg/cubic meter. The two tunnels, linking the four major modules, are located between nodes 78 and 91, and 414 and 427. Tunnels density is 37.462 Kg/ cubic meter and is 10 meters long. The US habitation module located between nodes 72, 77, and 415, has a length of 13.258 meters and a density of 51.191 giga-Kg/ cubic meter. The US laboratory module located between nodes 85, 90, and 428, is 13.258 meters long and has a density of 112,730 Kg/cubic meter. The ESA logistics module is 13.258 meters in length, with a density of 65,640 Kg/ cubic meter, and is located between nodes 411-413. Between nodes 424-426 is the JEM, which is 15.09 meters in length and has a density of 62,100 Kg/ cubic meter. The module cluster is attached to the primary structure using rigid beams. For analysis, the shuttle docks at the airlock node 92. Microgravity research is conducted in the US laboratory module - node 90.

3.1.8 Satellite Servicing and Storage Enclosures

One satellite service enclosure (SSE) is located at the intersection of the lower keels right verticle booms intersection with the main horizontal boom. The SSE is modelled as a box truss structure by adding two nodes and five members to the corner structure. Nodes that make up the SSE are 86-87, 98-99, 227-228, and 446-447. The lower left corner is node 446 as shown in Figure 6. A mass of 6,889 kg is placed at each of these nodes to approximate the SSE's total mass of 55,115 Kg. Members are modeled as two-node beam elements and do not contribute to the primary structures stiffness.

3.1.9 Alpha Gimbals

Alpha gimbals are located on both sides of the horizontal boom between the PV arrays and the central radiators. Their function is to rotate the PV arrays and SDUs to track the solar vector. These gimbals are assumed to be locked and possess the same stiffness and mass of a five meter bay.

3.1.10 Miscellaneous Attachments

Miscellaneous attachments such as the attitude reaction control system (RCS), mobile service center (MSC), payloads, utility trays, and control-moment-gyros are modelled as attached masses. The CMG is identified by node 106. The RCS trusters are located in the four corners, exterior face, at nodes 206, 248, 313, and 357, with an attached mass of 476.2 Kg each. The MSC is modelled by four nodes - 56, 59, 60, 63 - with 6,889 Kg/node. Node 63 is located at the intersection of the upper keel transverse boom and the horizontal boom as shown in Figure 6. Four stellar and terrestrial payloads totalling 194,006 Kg mass, are represented by concentrated masses at nodes 227, 330, 335, and 340. For analysis of the dynamic effects on these payloads, nodes 335 on the center of the upper keel and node 227 on the lower keel will be reference points.

3.2 Solution Technique

3.2.1 Governing Equations of Motion

To determine the structure's dynamic response and time-history analysis of the Dual Keel space station finite element model at the specified locations and loading function, the coupled, second order, ordinary differential equations of motion must be solved.

$$[M]\{\ddot{D}\} + [C]\{\dot{D}\} + [K]\{D\} = \{R_{ext}\} \quad (1)$$

Where $[M]$, $[C]$, and $[K]$ are the models mass, dampening, and stiffness matrices, respectively. The accelerations, velocity, and displacement vectors are $\{\ddot{D}\}$, $\{\dot{D}\}$, and $\{D\}$. Externally applied loads are represented by $\{R_{ext}\}$.(67)

This analysis uses ADINA software to analyze the complete FEM.(68) Equivalent beams were not used due to the desire to investigate the behavior of individual members. The station's structural geometry, material properties (modulus of elasticity, Poisson's ratio, length, area, and moment of inertia), masses, and shuttle impulse docking load were input to generate and assemble element and structure mass, damping, and stiffness matrices, and loading vector. Masses are considered lumped and damping is 0.5% critical.

3.2.2 Numerical Analysis Technique

The equations of motion are solved using Newmarks implicit, average acceleration (trapezoidal rule), direct integration method. This method was selected over other methods (i.e., modal) due to the size of the model, computer capacity, expediency, and accuracy. Direct integration uses an approximation to replace the time derivatives $\{\ddot{D}\}$ and $\{\dot{D}\}$ in equation (1) by differences in the displacement $\{D\}$ at various instants of time. Where:

$$\{D\}_{n+1} = \{D\}_n + \Delta t \{\dot{D}\}_n + 0.5 \Delta t [(1-2b)\{\ddot{D}\}_n + 2b\{\ddot{D}\}_{n+1}] \quad (2)$$

and

$$\{\dot{D}\}_{n+1} = \{\dot{D}\}_n + \Delta t [(1-g)\{\ddot{D}\}_n + g\{\ddot{D}\}_{n+1}] ; \quad (3)$$

with b and g selected as 0.25 and 0.5 respectively. For $b = 0.25$ provides maximum high frequency dissipation, and $g = 0.50$ produces no algorithmic dampening. These values also result in unconditional stability. Initial conditions placed the model at rest.(69)

Time steps selected were small initially, (0.005 milli-seconds) due to the impulsive loading and unfamiliarity with the structure's response. Later this increment was increased outside the impulsive load due to the structure's long period of vibration. The method initially forms and factors an effective stiffness matrix, along with an

effective load vector, and solves for the displacement $\{ D \}_{n+1}$. The velocity $\{ \dot{D} \}_{n+1}$ and acceleration $\{ \ddot{D} \}_{n+1}$ are updated and the analysis is continued for the next time step. The time history results of the structure and nodes are plotted using ADINA-PLOT.

3.3 Results

3.3.1 Rigid Body Response

The finite element model's rigid body response to a 2,225 Newton, 1 second docking impulse applied in the negative X- direction at node 92 is shown at four time intervals - 5,10,15, and 25 seconds - in Figures 9-12. Rigid body displacements and rotations at node 80 are shown in Figure 13. Node 80 is the models geometric center and approximates the center of gravity. Further description of the model's rigid body response is shown in Figures 13-17, at four model edge points - node 3 on the left end of the horizontal boom; node 159 on the right end of the horizontal boom; node 335 at the center of the upper keel boom; and node 227 located at the center of the lower keel boom.

The structure's rigid body response can be characterized primarily by rigid body displacement in the negative X-direction, and secondarily by displacements in the negative Z-direction with rotations about the positive Y-axis and negative Z-axis.

Viewing the response at node 80 over a 25 second interval in Figure 13, maximum X-displacement is -20 mm; Z-displacement is -1 mm; Y-rotation and Z-rotation is +0.25 and -0.09 milliradians, respectively. This response is expected due to the location and direction of the docking impulse at node 92. Node 92 lies -5 meters in the Y-axis (right); -5 meters in the Z-axis (above); and +6.5 meters in the X-axis (fore) from node 80. Because node 92 is located at the fore airlock in the module cluster, along with the high stiffness and mass of the cluster relative to the remaining structure, intuitively the eccentric impulse would result in a torque and rotation about the positive Y and negative Z axes, and a displacement in the negative Z-direction of node 80. Also, the negative X-displacement is expected due to the impulse in the X-direction. To isolate and evaluate the model's flexible body response, the five subsystem responses are evaluated relative to node 80.

3.3.2 Flexible Body Response

3.3.2.1 Transient Analysis

Analysis is conducted to evaluate the maximum transient response of the subsystems relative to their operational/mission requirements under an aborted shuttle docking impulse. Response of nodes is relative to the station's geometric center, node 80. The time interval is taken to be 25 seconds based upon review of the model's period over longer time intervals.

3.3.2.2 Left Solar Dynamic Unit - Node 3

The relative response of node 3 is dominated by displacement in the positive X-direction as shown in Figure 18. The nodal response cycles through in a displaced state also in the positive X-direction due to the station's rotation about the Z-axis. The maximum X-displacement is 7.5 mm. The Y and Z displacements are 0.375 mm and 2 mm respectively. Major rotations are about the Y and Z axis; both are 0.13 milliradians. The X-axis rotation is 0.05 milliradians.

The transient response is evaluated against the SDU's pointing requirement of 0.1 degree rotation from the solar vector. The total rotation (θ_T) is defined as the $\text{SQRT}(\theta_y^2 + \theta_z^2)$ which equates to 0.011 degrees.

3.3.2.3 Right Solar Dynamic Unit - Node 159

Response of the right SDU is similar to the left SDU as shown in Figure 19. However the Z-axis rotation causes a displacement in the negative X-direction. X, Y, and Z displacements are 6 mm, 0.35 mm, and 1 mm, and rotations about the X, Y, and Z axis are 0.03, 0.15, and 0.12 milliradians. Total rotation is found to be 0.011 degrees.

3.3.2.4 Terrestrial Payloads - Node 227

Both displacements and accelerations are evaluated for payloads attached to the lower keel boom. X-displacements are coupled with a rigid body rotation about the positive Y-axis as shown in Figure 20. Maximum displacements are 12.5 mm, 1.5 mm, and 0.21 mm for the X, Y, and Z directions. Rotations about the X, Y, and Z axis are 0.0175, 0.14, and 0.06 milliradians respectively.

Against the payload pointing requirement of 0.1 degrees, the total rotation is 0.009 degrees.

Terrestrial pointed payloads acceleration response is shown in Figure 21. Maximum linear accelerations in the X, Y, and Z directions are 0.002, 0.0009, and 0.009 m/sec/sec respectively - exceeding a 0.00001 g or 0.000098 m/sec/sec acceleration requirement.

3.3.2.5 Stellar Payloads - Node 335

As with payloads on the lower keel boom, stellar pointing payloads response is evaluated and shown in Figures 22-23. Rigid body rotation about the positive Y-axis causes the X-displacements to cycle in the negative (see Figure 22). Displacements and rotations about the X, Y, and Z axes are 10 mm, 0.8 mm, 0.18 mm, and 0.025, 0.15,

and 0.055 milliradians. The total rotation is 0.01 degrees. Accelerations in the X, Y, and Z directions are 0.002, 0.001, and 0.00175 m/sec/sec, exceeding the 0.00001 g or 0.000098 m/sec/sec requirement.

3.3.2.6 US Laboratory Module - Node 90

For microgravity experiments located in the laboratory module, accelerations must also be limited to 0.00001 g or 0.098 mm/sec/sec. Figure 24 shows the acceleration responses in the X, Y, and Z directions to be 30, 40, and 60 mm/sec/sec also exceeding requirements by 600 percent.

Chapter 4

DEGRADATION EFFECTS OF THE LEO ENVIRONMENT ON SPACE STATION COMPOSITE MATERIALS

4.1 Space Station Composite Materials

In space, structural materials must be lightweight, have high strength and stiffness, be dimensionally stable, and sustain long life. Due to high transportation costs (\$2,500/lb to LEO), materials properties must be evaluated against their density. Advanced composite materials are ideal for space applications because they are twenty-five times as strong as steel for the same weight. High strength and stiffness is required by materials to prevent member buckling during severe loads such as shuttle docking, while possessing sufficient stiffness to prevent the structure's natural frequencies from interacting with the spacecraft's control system. Composite's high strength and dimensional stability allow precision pointing of payloads and antenna while experiencing operational and environmental loads. Materials must also retain their properties over the mission design life with little or no maintenance while exposed to the harsh space environment. For space station, the design life is thirty years.

For space station, the design requirements and environmental parameters are listed below in Tables 4.1 and 4.2. (70)

TABLE 4.1 Space Station Design Requirements

- Maximum axial load of +/- 1200 lbs.
- Axial Coefficient of Thermal Expansion (CTE) of
0.0 +/- 0.00000005 per degree Fahrenheit
- Nominal diameter of 2 inches
- Low outgassing
- Joints must allow easy tube replacement on orbit
- 30 year design life

TABLE 4.2 Space Station Truss Structure

Orbital Environmental Parameters

- Solar Radiation (UV) 1353 Watts/M/M
- Atomic Oxygen (long term influence) 10^{23} atoms/cm
- Electron radiation dose (30 years) 10^{17} rads
- Maximum thermal cycling +/- 150 degree Far., 175,000 , 90 minute cycles

Based on these criteria, NASA selected graphite/epoxy tubes for use in the station's 5 meter truss structure. The tubes are two inches in diameter, with a composite thickness of 1.52 mm. ARMCO Pitch P-75 fibers with an epoxy fiber resin FR - 8703 are the specific material types. The fiber volume is 60% and the lay-up used is

(O_2 , +/-20, O_2)s. To improve the life and durability, a 0.152 mm aluminum coating of 7075-T73 type is placed on the interior and exterior tube walls. Properties are listed below in Table 4.3.

TABLE 4.3 Space Station Tube Properties

- Modulus of Elasticity (E) Longitudinal 36 Msi
- Modulus of Elasticity (E) Transverse 1 Msi
- Coefficient of Thermal Expansion (CTE) -0.9 u in/in
- Euler Buckling Load (L=8 ft.) 8800 lbs.
- Density 0.3 lbs./Lin. Ft.

To understand the design and environmental effects on tube materials over their design life, the LEO environment is discussed along with the impact. Major environmental effects on composites driving space station material design are: thermal cycling, solar radiation, solar radiation, atomic oxygen bombardment, and micrometeoroid/space debris impact.

4.2 Low Earth Orbit Environmental Effects on Composites

4.2.1 Thermal Cycling

Spacecraft, such as the space station, orbiting the Earth in LEO will experience extreme thermal cycling ranging from -300 °F to + 220 °F during the 90 minute orbital period. Over thirty years, this equates to 175,000 thermal cycles, and can degrade both the mechanical properties and dimensional stability of composites so that mission requirements are no longer met. Key composite properties which define the materials sensitivity to changes in solar radiation and temperature are the materials solar absorption / solar emittance - which affects the heat absorbed and radiated - and the CTE - which characterizes the amount of deformation a material will exhibit under temperature changes. For bare graphite epoxy tubes, their solar absorption/emittance are both 0.85, resulting in the tubes actual temperature ranges to be -150 °F to +175 °F in LEO. The CTE of bare graphite epoxy tubes is -1.1 in./in. in the longitudinal direction. Laboratory analysis into the effects of LEO thermal cycling on graphite epoxy tubes showed that matrix microcracks developed and caused a 35% decrease of torsional stiffness. The longitudinal and flexural stiffness were unchanged due to the fiber's resilience to thermal effects (matrix materials shrink ten times more than fibers). The CTE of the tubes showed a 1300% change due to thermal cycling. To minimize thermal distortions, the aluminum coating tailors the tube CTE from -1.1 to -0.9 in./in. When the tubes are attached to the aluminum joints, the CTE of the structure is near zero. When the coated

tubes and joints were tested for thermal cycling, no microcracks were produced, or significant changes in mechanical properties ($< 10\%$). The tests concluded that thermal cycling had no significant effects on the material properties.(71)

4.2.2 Solar Radiation

With the absence of a full Earth atmosphere, solar radiation in LEO is twice as intense when compared to the Earth's surface. Composites are highly susceptible to degradation from solar radiation, especially ultra-violet (UV) radiation. UV photons specifically damage composite matrix materials through embrittlement. To protect the composite, the added aluminum coating has been shown to reduce the effects of composite UV degradation on mechanical properties as tensile strength below significant levels. However, a 2% reduction in the solar absorption/emmittance was observed along with yellowing of the aluminum surface when exposed to simulated LEO radiation.(72)

4.2.3 Atomic Oxygen Bombardment

Almost 80% of the atmospheric density in LEO is atomic oxygen, and represents a major threat to the life of composite materials. Atomic oxygen is a highly reactive oxidizer. Results from recent shuttle experiments demonstrated composites vulnerability to atomic oxygen erosion. The effects of atomic oxygen erosion depend on the efficiency of the process - what fraction of the oxygen atoms striking the spacecraft actually react

with the surface - and carry away atoms of the spacecraft materials.(73) For spacecraft in LEO travelling at speeds of 7.5 Km/sec, the atomic oxygen flux is 150,000 million atoms/cm/cm/sec. Shuttle flight experiments showed composite material losses of 1-5 microns over a 5-7 day mission. If this is extrapolated to the station's 30 year life, a 3.4 mm loss in graphite epoxy tube thickness could occur. Considering that the thickness of the station's tube is only 1.52 mm, these materials would erode away in less than 15 years. The use of an aluminum coating - which is inert to atomic oxygen - provides the necessary protection to composites over the thirty-year design life.(74-77)

4.3.4 Micrometeoroid and Space Debris

LEO also possesses orbiting solid particles consisting of micrometeoroids and space debris which can puncture and fracture spacecraft materials. Meteoroids are particles left over from the formation of the Universe or from products of collisions between natural space bodies in the solar system. These particles are smaller than a grain of sand, with densities of about 1 gm/cm³, and travel at speeds of 30 Km/sec. Space debris consists of objects left over from spaceflight activities beginning in 1957 and include spent stages, separation hardware, inoperative satellites, and collision/explosive products. Debris product densities range from 2.7 - 8 gm/cm³, and travel at speeds of 10 KM/sec. The USAF tracks over 5,000 of these debris objects larger than 2 cm in size with radar; but the quantity, size, and location of smaller micrometeoroid and space debris objects are unknown.(78)

For the space station, manned modules possess protection against debris collision; however, protection of the truss tubes is not considered to be necessary by NASA.(79)

The effects of collision between micrometeoroid/space debris with the space station structural tubes is a function of the particle size. NASA research has shown that local damage from particle collisions is 10-20 times the particle diameter. The depth of penetration is roughly three times the diameter.(80)

Particle sizes, quantity, growth, and probability of impacting spacecraft surfaces is estimated by models simulating the explosion and impact processes. (81-86) One such model by Seebaugh, uses existing data from NASA researchers Cour-Palais, Su, and Kessler. The two model parameters are fluxes of meteoroids and space debris fragments at orbital altitudes of interest, and the number of ejecta particles generated by a hypervelocity impact on a spacecraft surface. Figure 17 shows the flux levels of micrometeoroid and space debris at a LEO altitude (400 Km). Figure 18 shows the potential impacts on a 150 sq. meter surface, and Figure 19 shows the number of ejecta particles generated per orbit for the same cross section and orbit from the current baseline, to the 1990s, and beyond 2010. Results showed that by 2010, each 5 meter aluminum coated space station tube would be penetrated by 10 micrometeoroid/space debris particles impacts per year.

Again, present knowledge of the quantity and size of space debris and micrometeoroids is limited and approximate. One NASA experiment recently flown - Long Duration Exposure Facility (LDEF) - studied the quantity and size of particles in LEO along with the effects of impacts and other environmental effects on space station materials.

4.2.5 NASA's Long Duration Exposure Facility

In April, 1984, NASA launched LDEF from the Shuttle to study the LEO environment and its effect on space station materials, systems, and organisms. 100 different materials were exposed to the LEO environment to evaluate effects on mechanical, electrical, and optical properties. Preliminary results, found following LDEF's return in Jan. 1990, reinforced earlier mentioned laboratory research into the effects of the LEO environment on materials. NASA concluded "surface effects are dominated by atomic oxygen erosion and micrometeoroid/space debris impacts." A final LDEF report is due to be published in January, 1993.(87)

4.3 Space Station Material Degradation Model

4.3.1 Degradation Mechanisms

Most of the earlier mentioned LEO environmental effects can be mitigated by proper selection and tailoring of composite materials and coatings. However, coupling of individual effects can be significant and reduce the material life expectancy and require some periodic inspection, maintenance, and repair. Research and laboratory experiments have investigated the combined effects of thermal cycling, radiation, and atomic oxygen bombardment on the baseline graphite epoxy tubes with aluminum coating. Results conclude that the design appears to have produced space station tubes that will maintain their strength, stiffness, and dimensional stability over the thirty year design life. But one potential mechanism has been ignored or concluded insignificant - the combined effects of micrometeoroid/space debris or handling errors penetrating or scratching the aluminum coating, exposing the graphite epoxy to atomic oxygen erosion. Some research found may lead NASA to re-evaluate the assumption.

4.3.2 Material Degradation Due to Coating Loss

In Long-Life Assurance For Space Station: Is It An Issue, the threat to long life space station tubes due to penetration of coatings and atomic oxygen bombardment was highlighted.

... Smaller tube penetrations are likely to be too widespread and too small for local corrective action. Replacement of a significant number of tubes for this widespread damage will place further demands on space station resources. Research is needed to evaluate the combined effects of all tube damage modes on tube stiffness and strength in order to allow redesign. (88)

LDEF also confirmed this potential mechanism by concluding:

... composites used in LEO such as space station, will require protection from atomic oxygen and penetrating impacts. Coatings such as aluminum may provide the solution; however, complete characterization of the coating/composite material system is needed to provide confidence that its functional integrity will be maintained. Another approach to reduce the structures sensitivity to the penetration and atomic oxygen erosion phenomena is to use thicker structures." (89)

4.3.3 Space Station Material Degradation Model

In the absence of LDEF results until next year, a linear degradation model of the tubes longitudinal modulus of elasticity is assumed to evaluate the sensitivity of penetration/erosion effects on the space station's dynamic response and mission requirements. The model, shown in Figure 20, represents a 3% degradation per year.

Results quantify the sensitivity of the structure's dynamic response to variations in the modulus of elasticity or stiffness.

Although a structures stiffness is a function of the material properties of the matrix and fiber, (modulus, Poisson's ratio, ply orientation, and thickness) and the structures geometry (length, area, moment of inertia, and shear areas for beam elements), the model chooses the longitudinal modulus of elasticity as the variable to reflect degradation. This is reasonable because intuitively any degradation or damage from impacts, holes, or atomic oxygen erosion would cause loss of laminate plies, reducing the laminates overall modulus of elasticity. Although the behavior would be non-linear as with composite laminate fracture behavior, this simplistic model chooses a linear reduction of the longitudinal modulus of elasticity to reflect degradation and changes in the structures stiffness.

Chapter 5

EFFECTS OF MATERIAL DEGRADATION ON SPACE STATION DYNAMIC RESPONSE

5.1 Approach

Dynamic analysis is re-performed applying a linear degradation model to the existing space station FEM by reducing (degrading) the primary truss structure's stiffness (modulus of elasticity) from 0 to 88% in increments of 22% . ($E=100\%$, 78% , 56% , 34% , and 12% of the original modulus of 248.3 Giga-Newtons/m/m). The aborted shuttle impulse is reapplied. Subsystem locations and requirements are re-evaluated for each case as in Chapter 3. Results of specific degraded cases and response is not discussed, but are treated as cases for comparison and evaluation of the combined effects of all five cases. Detailed output data in the same format of Chapter 3 is located for case 1 - 100%E - in Figures 9 to 24; for case 2 - 78%E - in Figures 29 to 44; for case 3 - 56%E - in Figures 45-60; for case 4 - 34%E - in Figures 61-76; and for case 5 - 12%E - in Figures 77-92.

Summary plots are presented as a curved trend line representing the "best fit" using a least squares method. The curve passes a smooth fit through the graphing

area. The plot doesn't connect the data points, but does give a feel for the fluctuation of the data. In some cases the actual relationship should appear linear for lower levels of degradation and as a curve at high levels as the response approaches infinity. For simplicity the output is graphed as a curve to show the overall trend of response as degradation is increased.

5.2 Results

5.2.1 Rigid Body Response

Material degradation had no effects on the rigid body response of the space station FEM model and applied docking impulse. As in section 3.3.1, the rigid body response for cases 1-5 at node 80 is dominated by rigid body displacements in the negative X-direction and secondarily by displacements in the negative Z-direction with rotations about the positive Y-axis and negative Z-axis as shown in comparison plots of node 80 in Figures 93-98. To isolate and evaluate the model's flexible body response, the five subsystem responses, under degraded conditions, are evaluated relative to node 80.

5.2.2 Flexible Body Response

5.2.2.1 Transient Analysis

To analyze the effects of material degradation for cases 1-5, increasing time intervals are used ranging from 25 to 70 seconds; due to the expected increase in the period of vibration at subsystem nodes. Intuitively, softening the structure should correspond to an increase in displacements / rotations and a decrease in accelerations. Each subsystem is discussed as in Chapter 3, along with the degradation effects on mission requirements.

5.2.2.2 Left Solar Dynamic Unit - Node 3

Under degraded conditions, node 3 remains governed by displacement in the positive X-direction as shown in Figures 99-104. The period of the X-displacement nearly tripled from case 1 to 5, and the displacement magnitude also tripled from 7.5 mm to 20 mm. Total rotation doubled from 11 to 24 milli-degrees, but remained below the 100 milli-degree requirement for SDU operations as plotted in Figure 141. The relationship between degradation and total rotation is non-linear.

5.2.2.3 Right Solar Dynamic Unit - Node 159

Response of the right SDU is similar to the left as shown in comparative plots, Figures 105-110. The X-displacement period tripled, with maximum X-displacement also tripling from 6 to 20 mm. The total rotation was tripled also, from 11 to 32 milli-degrees; still below the SDU requirement. The relationship between degradation and rotation was also non-linear (see Figure 142).

5.2.2.4 Terrestrial Payloads - Node 227

For terrestrial pointing payloads on the station's lower keel, positive X-displacements dominate as shown in Figures 111-116. The response period tripled and the X-displacement more than doubled from 12.5 to 28 mm under case 5. Total rotation almost doubled from 11 to 17 milli-degrees, well below the 100 milli-degree requirement (see Figure 143) Linear and angular acceleration decreased as expected from reduced stiffness from 2 to 1.1 mm/sec/sec; well above the 0.1 mm/sec/sec microgravity requirement (see Figures 117-122, and 146). Figure 146, as well as Figures 145 and 147, represent the maximum acceleration in the X-direction. This direction represents the axis with maximum acceleration, due to the applied shuttle dock load in the negative X-direction.

5.2.2.5 Stellar Payloads - Node 335

Negative X-displacements characterize the response of payloads on the upper keel. The period of response nearly tripled, with X-displacements doubling from 9.5 to 21 mm. Total rotation doubled non-linearly from 10 to 22 milli-degrees, but remained below the 100 milli-degree requirement. Maximum linear accelerations were roughly halved from 2.2 to 1.1 mm/sec/sec and exceeded microgravity conditions (see Figures 123-134, 144, and 147).

5.2.2.6 U.S. Laboratory Module - Node 90

Linear accelerations at node 90 remained constant at approximately 30 mm/sec/sec; exceeding the 0.1 mm/sec/sec requirements as shown in Figures 135-140, and 145. This is expected because of the docking impulse at module node 92, and the constant stiffness of the modules during analysis.

5.2.2.7 Degraded Cantilever Case

An additional case was evaluated to investigate the effects of changing the stiffness of the stations cantilever arms only. Results showed that at high levels of degradation, both uniform and selected degradation produced roughly the same displacements and rotation. Thus this additional case was excluded from further

discussion.

Chapter 6

CONCLUSIONS

6.1 Research Review

The Air Force Engineering and Services Space Planning and Requirements Integration Team (ESSPRIT) has been chartered to develop long range plans and policy for normalizing traditional terrestrial civil engineering functions into space. One key element of the Air Force Engineering and Services Space Support Policy is to "... develop capabilities to design, construct, operate, maintain, and repair facilities in space." The author, as a member of this team, investigated the effects of material degradation on large space structures (LSS) dynamic response and subsystem requirements, using Space Station "Freedom" as an example. The goal was to investigate requirements for development of a Reoccurring Work Plan for the maintenance and repair of the structural subsystem of a space facility. The sub-elements of the research were:

- a. Develop a Finite Element Model (FEM) of NASA's Dual Keel Space Station;

- b. Perform a dynamic analysis of the model under an assumed worst case load - an aborted shuttle dock - and evaluate the structures response relative to subsystem displacement and acceleration requirements;
- c. Investigate potential degradation effects of the LEO environment on Space Station structural materials;
- d. Using a simplistic degradation model, evaluate the effects of changes in the materials longitudinal modulus of elasticity on the stations dynamic response and subsystem requirements over the 30 year design life;
- e. Estimate design changes or maintenance and repair requirements for the structure over the expected design life.

From this research, several conclusions were reached concerning the design, maintenance, and repair of LSS.

6.2 Conclusions

6.2.1 Dual Keel Space Station Structural Design

The Space Station design configuration, using five meter orthogonal truss bays and graphite-epoxy truss tubes coated with aluminum, provides a stiff and stable platform for subsystem and payload pointing requirements. Results of the dynamic analysis, with an aborted shuttle dock, showed that solar dynamic units, terrestrial pointing and stellar pointing payloads experienced only a 0.01 degree maximum total rotation; one tenth of their 0.1 degree total rotation pointing requirements. The acceleration requirements of the U.S. Laboratory Module were six hundred times greater than allowed; while upper and lower keel payloads were twenty times greater. The acceleration results confirm earlier NASA studies; which also concluded the need for shock isolation systems for microgravity payloads and processing activities.

6.2.2 Space Station Tube Design

The design of the Space Station tubes to meet the NASA specification of long-life - retaining required material properties over the thirty year design life when exposed to the LEO environment without maintenance - possesses program risk. Future NASA and DOD LSS design and maintenance concepts must include the effects of micrometeoroid/space debris impacts penetrating coatings and allowing

atomic oxygen erosion. Although laboratory results from NASA have concluded the design of aluminum coated, graphite-epoxy tubes will meet requirements when exposed to LEO radiation, thermal cycling, and atomic oxygen bombardment, the effects of micrometeoroid/space debris penetration of the aluminum coating and subsequent atomic oxygen erosion have not been included in the design or logistics planning. This can be explained by the overall uncertainty of the micrometeoroid/space debris problem. Review of Johnson Space Center and contractor models, which predict the current and future quantities and probable impacts of micrometeoroid/space debris impact with spacecraft, are shown to vary widely. NASA models show a small probability of impact; whereas Seebaugh's model estimated ten penetrating impacts per year per member by 2010. Other researchers have recently confirmed this observation.

Cruse, in Long-Life Assurance For Space Station: Is It An Issue, highlighted the logistics consequences of the current Space Station design:

... Smaller tube penetrations are likely to be too widespread and too small for local corrective action. Replacement of a significant number of tubes for this widespread damage will place further demands on Space Station resources. Research is needed to evaluate the combined effects of all tube damage modes on tube stiffness and strength in order to allow redesign. (90)

In April, 1991, Whitaker, upon preliminary review of returned LDEF experiments, reached the same conclusion:

... composites used in the LEO environment such as Space Station, will require protection from atomic oxygen and penetrating impacts. Coatings such as aluminum may provide the solution; however, complete characterization of the coating/composite material system is needed to provide confidence that its functional integrity will be maintained. Another approach to reduce the structures sensitivity to penetration and atomic oxygen erosion phenomena, is to use thicker structures. (91)

To investigate the structures sensitivity to degradation from this phenomena, an assumed three percent per year reduction in the tubes longitudinal modulus of elasticity was investigated and compared against subsystem requirements.

6.2.3 Effects of Changes in Modulus of Elasticity on Dynamic Response

Analysis of the stations dynamic response with the modulus of elasticity ranging from 100% to 12% of the original modulus, concluded that the design is relatively insensitive to large variations. Although the maximum total rotation of the solar dynamic units and payloads tripled from the 100% case, no subsystem exceeded the 0.1 degree total rotation pointing requirement. However, if high levels of

degradation result in complete strut loss, functional integrity could be lost.

6.2.4 NASA and Air Force Space Facility Policy

Our Nation's future is in space; both for civilian and military applications. By the end of the decade, the U.S. will operate a permanently manned outpost in LEO with Space Station "Freedom." From this first space facility will evolve additional Earth-orbiting facilities, and the eventual exploration and settlement of the Moon and Mars. In this decade, DOD will also make a similar size investment with the deployment of GPALS. The combined investment and space operations will undoubtedly yield additional civilian and military applications in space. As these new applications evolve, especially for manned presence, additional space facilities will be required. To execute these potential future missions, our traditional functions and organizations, as A.F. Engineering and Services, must evolve.

Space Station, dissimilar to Skylab, represents our Nation's first true space facility. Unlike the Space Transportation System (STS), which returns to Earth following a seven day mission, Space Station will remain in orbit for thirty years. If an item fails on-orbit, it will require repair on-orbit. NASA organizationally has little experience for operating and maintaining deployed systems, especially logistics support. The Augustine Committee Report highlighted this concern:

... Space projects tend to be very unforgiving of any form of neglect or human failing - particularly with respect to the engineering discipline. Spacecraft incorporating flaws are not readily "recalled" to the factory for modification. It is in this category of problem that has evoked much criticism directed at NASA in recent years, although new technology there are growing opportunities for systems that are self-healing.(92)

DOD is not exempt from this criticism; however possesses substantial experience in providing logistics support to personnel and systems deployed and operated at remote sites throughout the world. The cross flow of knowledge and experience within organizations can contribute to our Nation's overall goals in space.

For the Air Force, the time is now to begin planning for the year 2010. A.F. Space Command and ESSPRIT have developed the Engineering and Services Space Master Plan, however little resources have been dedicated towards the tasks identified. If civil engineering activities are to be normalized in space, near-term activities should be focused on the design, construction, and operational planning of both space launch infrastructure and orbiting space facilities. Hopefully this research provides one building block to normalize civil engineering activities in space.

6.3 Areas for Future Research

Future studies for the maintenance and repair of LSS should focus on the following:

- a. Characterize the size, quantity, and location of micrometeoroid/space debris in LEO;
- b. Investigate new materials and coatings to either protect or withstand the impact of micrometeoroid/space debris;
- c. Evaluate the effects of coating penetration and resulting change in material properties;
- d. Develop plans for inspection and repair of structural damage, including the use of selected "smart" members;
- e. Determine effects of lost members on subsystem requirement and maintenance;
- f. Perform additional on-orbit test and evaluation of composite tubes exposed to the LEO environment, and evaluate actual degradation.

REFERENCES

1. Stewart, R.W., and D. Jehl. " Bush Seeks Big Budget Hike for Space Program." Los Angeles Times, January 25,1992, 1,12.
2. Bush, George. National Security Strategy of the United States. 1991-1992.
Washington, D.C. : Brassey's Inc, 1991.
3. HQAFSPACECOM Engineering and Services Space Plans Office and New Mexico Engineering Research Institute. Air Force Civil Engineering and Services Space Master Plan. Colorado Springs, CO.: HQAFSPACECOM/CEP, September, 1991.
4. Spense, Laura. "Launch Pad For Ideas." Leading Edge, February, 1992, 12-15.
5. NASA. Large Space Systems Technology. 1978 - Proceedings of the First Annual Technological Review. Nov. 1978. Washington, D.C.:GPO, 1978.
6. AIAA Subcommittee on Terminology, Symbols, and Units of the AIAA Committee on Standards for Large Space Structures. AIAA Astronautical Standard - AAS - 0001 - 81. Washington, D.C.:AIAA,1981.

7. Foster, N.. "A Study of Large Space Structures." Washington, D.C. : GPO,1985.
8. Dorsey, J.T., et al. "Dynamic Characteristics of Two 300 KW Dual Keel Space Station Concepts." Washington, D.C.:GPO,1986.
9. Priest, Claude C.. "Overview of Space Station." Proc. of the NASA Conference, Measurement and Characterization of the Acceleration Environment on Board the Space Station. August 11-14,1986. GPO:Washington, D.C.,1986.
10. Foster, N.. " A Study of Large Space Structures." Washington, D.C.: AIAA, 1981.
11. Agrawal, Brij. Design of Geosynchronous Spacecraft. Englewood Cliffs, New Jersey:Prentice Hall Inc.,1986.
12. Dorsey, J.T., et al. "Dynamic Characteristics of Two 300 KW Dual Keel Space Station Concepts." Washington, D.C.:GPO,1986.
13. Dursch, H. and C. Hendricks. "Development of Composite Tube Protective Coatings." NASA CR-172164. Washington, D.C.:GPO,1983.
14. Foster, N.. "A Study of Large Space Structures." Washington, D.C.: GPO, 1985.

15. Tenney, D.R.. "Durability of Spacecraft Materials." Proc. of the NASA/AIAA Advanced Materials Technology Seminar. November 16-17, 1982. Washington, D.C.: GPO, 1982.
16. HQUSAFSPACECOM Engineering and Services Space Plans Office and The New Mexico Engineering Research Institute. Air Force Civil Engineering and Services Space Master Plan. Colorado Springs, CO.: HQUSAFSPACECOM/CEP, Sept., 1991.
17. NASA. Skylab-Our First Space Station. Washington, D.C.: GPO, 1972.
18. Cruse, T.A., et al. "Long Life Assurance for Space Station: Is it an Issue?" Proc. of the AIAA SDM Issues of the International Space Station. April 21-22, 1988. AIAA: New York, N.Y., 1988.
19. Herdee, J.E. and V.C. Matzen. "System Identification: A Question of Uniqueness Revisited." Proc. of the 4th VPI/AIAA Symposium on the Dynamics and Control of Large Structures. June 6-8, 1983. Edited by L. Meirovitch.
20. Smith, S.W. and S.L. Hendricks. "Evaluation of Two Identification Methods For Damage Detection in LSS." Proc. of the 4th VPI/AIAA Symposium on the Dynamics

and Control of LSS. June 6-8, 1983. Edited by L. Meirovitch.

21. Ohkami, Y., et al. "Dynamic Simulation of Space Structures Subject to Configuration Change." Proc. of the 4th VPI/AIAA Symposium on the Dynamics and Control of LSS. June 6-8, 1983. Edited by L. Meirovitch.

22. Vander Velde, W.E.. "Detection of Component Failure in Flexible Spacecraft Control Systems." Proc. of the 4th VPI/AIAA Symposium on the Dynamics and Control of LSS. June 6-8, 1983. Edited by L. Meirovitch.

23. Matyka, Paul. " A Program for the Development of Fault Tolerant LSS." Proc. of the NASA Conference - Structural Dynamics and Control of LSS. Jan. 21-22, 1982. GPO: Washington, D.C., 1982.

24. Chen, J.C. and J.A. Garba. "System Identification for LSS Damage Assessment." Proc. of the NASA Workshop on Structural Dynamics and the Control Interaction of Flexible Structures. Apr. 22-24, 1986. GPO: Washington, D.C., 1986.

25. Kalyanasundaram, S., et al. "Effects of Degradation on Material Properties on the Dynamic Response of LSS." AFOSR Contract Report F49670-83-C0067. 1985. GPO: Washington, D.C., 1985.

26. Marshall, W.R.. " Role of Space Station - The How of Space Industrialization." Proc. of the 2nd NASA Symposium on Space Industrialization. Feb. 13-15, 1984. Washington, D.C.:GPO, 1984.
27. President Ronald Reagan, State of the Union Address, 25 Jan. 1984.
28. President George Bush, National Space Policy Speech, July 20, 1989.
29. Mikulas, M.M.. "Deployable-Erectable Trade Study for Space Station Truss Structures." NASA. Washington, D.C. :GPO, 1986.
30. Mikulas, M.M.. "Construction and Utilization of a Space Station Assembled from 5 - Meter Erectable Struts." NASA. Washington, D.C.,GPO,1986.
31. Ayers, J.K. and Tae Lim. " Dynamic Characteristics of a Space Station Freedom Mars Evolution Reference Configuration." Proc. of the AIAA 28th Aerospace Sciences Meeting. Jan. 8-11,1990. Washington, D.C.: AIAA,1990.
32. Belvin, W.K.. " Modeling of Joints for the Dynamic Analysis of Truss Structures." NASA TP-2661. GPO: Washington,D.C.,1986.

33. Sesak, J.R., M.J. Gronet, and G.M. Marinas. "Passive Dampening Augmentation for Flexible Structures." Proc. of the First NASA/DOD CSI Technology Conference. Nov. 18-21, 1986. GPO: Washington, D.C., 1986.
34. Folkman, S.L. and F.J. Redd. "Measurement and Modeling of Joint Dampening in Space Structures." Proc. of the AIAA SDM Issues of the International Space Station. April 21-22, 1988. AIAA: New York, N.Y., 1988.
35. Engles, R.C.. "A General Method for the Dynamic Analysis of Structures Overview." Proc. of NASA Workshop on Structural Dynamics and Control Interaction of Flexible Structures. Apr. 22-24, 1986. GPO: Washington, D.C., 1986.
36. ASCE Task Committee. "Identification of LSS: A State of Practice Report." Proc. of NASA Workshop on Structural Dynamics and Control Interaction of Flexible Structures. Apr. 22-24, 1986. GPO: Washington, D.C., 1986.
37. Meirovitch, L.. "A Computational Approach to the Control of Large Order Structures." Proc. of the NASA Workshop. Modeling. Analysis. and Optimization Issues for LSS. May, 1982. Washington, D.C.: GPO, 1982.
38. Stahle, C.V.. "Analysis and Testing of LSS." Proc. of the NASA Workshop. Modeling. Analysis. and Optimization Issues for LSS. May, 1982. Washington,

D.C.:GPO,1982.

39. Chen, J. and J. Garba. "Verification for LSS." Proc. From the NASA Conference - Large Space Antenna Technology. Dec. 4-6, 1984. GPO: Washington,D.C.,1984.

40. Young, J.W., et al. "Control/Structures Interaction Study of Two 300 KW Dual Keel Space Station Concepts." GPO: Washington, D.C., 1986.

41. NASA. "Space Station Reference Configuration." GPO: Washington, D.C., 1984.

42. Dorsey, J.T.. "Dynamic Characteristics of Power Tower Space Stations With 15-Ft. Truss Bays." GPO: Washington,D.C.,1986.

43. Dorsey, J.T.. "Dynamic Characteristics of a Space Station Solar Wing Array." GPO: Washington, D.C.,1986.

44. Moore, C.J., et al. "Space Station Structures and Dynamic Test Program." GPO:Washington, D.C.,1986.

45. Housner, J.M.. " Structural Dynamics Model and Response of the Deployable Reference Space Station." GPO: Washington,D.C.,1986.

46. Ayers, J.K.. "Structural Dynamics and Attitude Control Study of Early Manned Capability Space Station Configurations." GPO:Washington, D.C.,1978.
47. Cooper, P.A., et al.. "Multidisciplinary Capability for Analysis of the Dynamics and Control of Flexible Space Structures." Proc. of the First NASA/DOD CSI Technology Conference. Nov. 18-21, 1986. GPO:Washington, D.C.,1986.
48. Sutter, T.R., et al.. "Dynamics and Control of a Reference Space Station Configuration." Proc. of the AIAA SDM Issues of the International Space Station. April 21-22, 1988. AIAA:New York,N.Y.,1988.
49. Folkman, Steve. "Measurement and Modeling of Joint Dampening in Space Structures." Proc. of the AIAA SDM Issues of the International Space Station. April 21-22, 1988. AIAA: New York, N.Y., 1988.
50. Tenney, D.R.. "Durability of Spacecraft Materials." Proc. of the NASA/AIAA Advanced Technology Seminar. Nov. 16-17, 1982. Washington, D.C.:GPO, 1982.
51. Bush, H.G., et al. "Some Design Considerations for Large Space Structures." Proc. of the ASME/AIAA 18th Structures, Structural Dynamics and Materials Conference. Mar. 21-23, 1977. AIAA:New York, N.Y.,1977.

52. Hedgepeth, J.M.. "Preliminary Design Requirements for LSS." Proc. of the 2nd AIAA Conference on Large Space Platforms. Feb. 2-4,1981. AIAA:New York,N.Y.,1981.
53. Bush, H.G., et al. "A Concept for a Mobile Remote Manipulator." NASA. Washington, D.C.:GPO,1984.
54. NASA. Benefit/Cost Study for LSS." NASA CR-144936. Washington, D.C.:GPO.1986.
55. NASA Space Station Program Office. Engineering and Configurations of Space Stations and Platforms. Park Ridge, N.J.: Noyes Publications, 1985.
56. Bluck, R.M. and R.R. Johnson. "Fabrication of Slender Struts for Deployable Antennas." NASA CR-172164. Washington, D.C.:GPO,1983.
57. Johnson, R.R., and M.H. Kual. "Development and Properties of Aluminum-Clad Graphite/Epoxy Tubes for Space Structures." Proc. of the AIAA SDM Issues of the International Space Station. April 21-22, 1988. AIAA:New York,N.Y.,1988.
58. Blankenship, C.P. and J.C. Yu. "Structures and Materials Technology for Space Station." Proc. of the AIAA SDM Issues of the International Space Station. April 21-

22,1988. AIAA:New York, N.Y., 1988.

59. Tenney, D.R., S.S. Tompkins, and G.F. Sykes. "NASA Space Station Materials Research." Proc. of the NASA Conference on Large Antenna Systems Technology. Dec. 4-6, 1984. GPO:Washington, D.C., 1984.

60. Ararwal, B.D., and L.J. Broutman. Analysis and Performance of Fiber Composites. New York, N.Y.: John Wiley and Sons, 1980.

61. Wu, Edward M. "Strength Theories of Composites: Status and Issues." Proc. of the NASA/GWU Workshop on Failure Analysis and Mechanisms of Fibrous Composite Structures. March 23-25,1982. GPO:Washington, D.C., 1983.

62. Hahn, H.T.. "Failure Mechanisms." Proc. of the NASA/GWU Workshop on Failure Analysis and Mechanisms of Fibrous Composite Structures. March 23-25, 1982. GPO:Washington, D.C., 1983.

63. Tsai, S.W.. Composite Design. New York, N.Y.:Think Composites, 1987.

64. Halpin, J.C.. Primer on Composite Materials. New York, N.Y.:McGraw Hill, 1985.

65. Jones, S.. Mechanics of Composite Materials. New York, N.Y.:McGraw Hill, 1985.
66. Young, J.W., et al. "Control/Structures Interaction Study of Two 300 KW Dual Keel Space Station Concepts." GPO: Washington, D.C.,1986.
67. Cook, Robert D., et al. Concepts and Applications of Finite Element Analysis. New York, N.Y.: John Wiley and Sons, 1989.
68. ADINA R and D Inc.. Automatic Dynamic Incremental Nonlinear Analysis. Watertown, MA.: ADINA R and D Inc., 1989.
69. Cook, Robert D., et al. Concepts and Applications of Finite Element Analysis. New York, N.Y.: John Wiley and Sons, 1989.
70. Tompkins, S.S., et al. "Response of Composite Materials to Space Station Orbit Environment." Proc. of the AIAA SDM Issues of the International Space Station. April 21-22,1988. AIAA:New York, N.Y.,1988.
71. Tenney, D.R., et al. "NASA Space Materials Research." Proc. From NASA Conference - Large Space Antenna Technology . Dec. 4-6, 1984. GPO:Washington, D.C.,1984.

72. Dursch, H. and C. Hendricks. "Development of Composite Tube Protective Coatings." NASA CR-172164. Washington, D.C.: GPO, 1983.

73. Dursch, H. and C. Hendricks. "Development of Composite Tube Protective Coatings." NASA CR-172164. Washington, D.C.: GPO, 1983.

74. Tenney, D.R.. "Durability of Spacecraft Materials." Proc. of the NASA/AIAA Advanced Materials Technology Seminar. Nov. 16-17, 1982. Washington, D.C.: GPO, 1982.

75. Cruse, T.A., et al. "Long Life Assurance for Space Station: Is it an Issue?" Proc. of the AIAA SDM Issues of the International Space Station. Apr. 21-22, 1988. AIAA: New York, N.Y., 1988.

76. Tenney, D.R., et al. "NASA Space Materials Research." Proc. from the NASA Conference - Large Space Antenna Technology. Dec. 4-6, 1984. GPO: Washington, D.C., 1984.

77. Woodcock, Gordon, R.. Space Stations and Space Platforms. Malabar, Fla.: Orbit Book Co., 1986.

78. Woodcock, Gordon, R.. Space Stations and Space Platforms. Malabar, Fla.:Orbit Book Co.,1986.
79. Cruse, T.A., et al. "Long Life Assurance for Space Station: Is it an Issue?" Proc. of the AIAA SDM Issues of the International Space Station. Apr. 21-22, 1988.
AIAA: New York, N.Y., 1988.
80. Tenney, D.R.. "Durability of Spacecraft Materials." Proc. of the NASA/AIAA Advanced Materials Technology Seminar.Nov. 16-17, 1982. Washington, D.C.: GPO, 1982.
81. NASA Space Station Program Office. Engineering and Configurations of Space Stations and Platforms. Park Ridge, N.J.: Noyes Publications, 1985.
82. Woodcock, Gordon, R.. Space Stations and Space Platforms. Malabar, Fla.: Orbit Book Co.,1986.
83. Rantanen, R.O.. "Spacecraft Environments: Design Considerations." Proc. of Space 88. ASCE:New York,N.Y., 1988.
84. Tenneyson, R.C.. "Composite Materials in a Simulated Space Environment." AFOSR-78-3694-A Contract Report. GPO:Washington,D.C.,1980.

85. Seebaugh, W.R.. "Effects of Meteoroids and Space Debris on the Particulate Environment for Space Station." Proc. of the NASA Workshop, A Study of Space Station Contamination Effects. Oct. 29-30, 1987. GPO: Washington, D.C., 1987.
86. Thompson, D.F., and H.W. Babel. "Material Applications on the Space Station, Key Issues and The Approach to Their Solution." Proc. from the 34th International SAMPE Symposium. May 8-11, 1989. SAMPE: New York, N.Y., 1989.
87. ASM International. "LDEF Mission Update: Composites in Space." Advanced Materials and Processes. April, 1991.
88. Cruse, T.A., et al. "Long Life Assurance for Space Station: Is it an Issue?" Proc. of the AIAA SDM Issues of the International Space Station. April 21-22, 1988. AIAA: New York, N.Y., 1988.
89. Whitaker, A.F.. "Coatings Could Protect Composites from Hostile Space Environment." Advanced Materials and Processes. April, 1991.
90. Cruse, T.A., et al. "Long Life Assurance for Space Station: Is it an Issue?" Proc. of the AIAA SDM Issues of the International Space Station. April 21-22, 1988. AIAA: New York, N.Y., 1988.

91. Whitaker, A.F.. "Coatings Could Protect Composites from Hostile Space Environment." Advanced Materials and Processes. April, 1991.

92. NASA. Report of the Advisory Committee on the Future of the U.S. Space Program. Draft Copy. GPO: Washington, D.C., 1990.

APPENDIX
SPACE STATION DATA

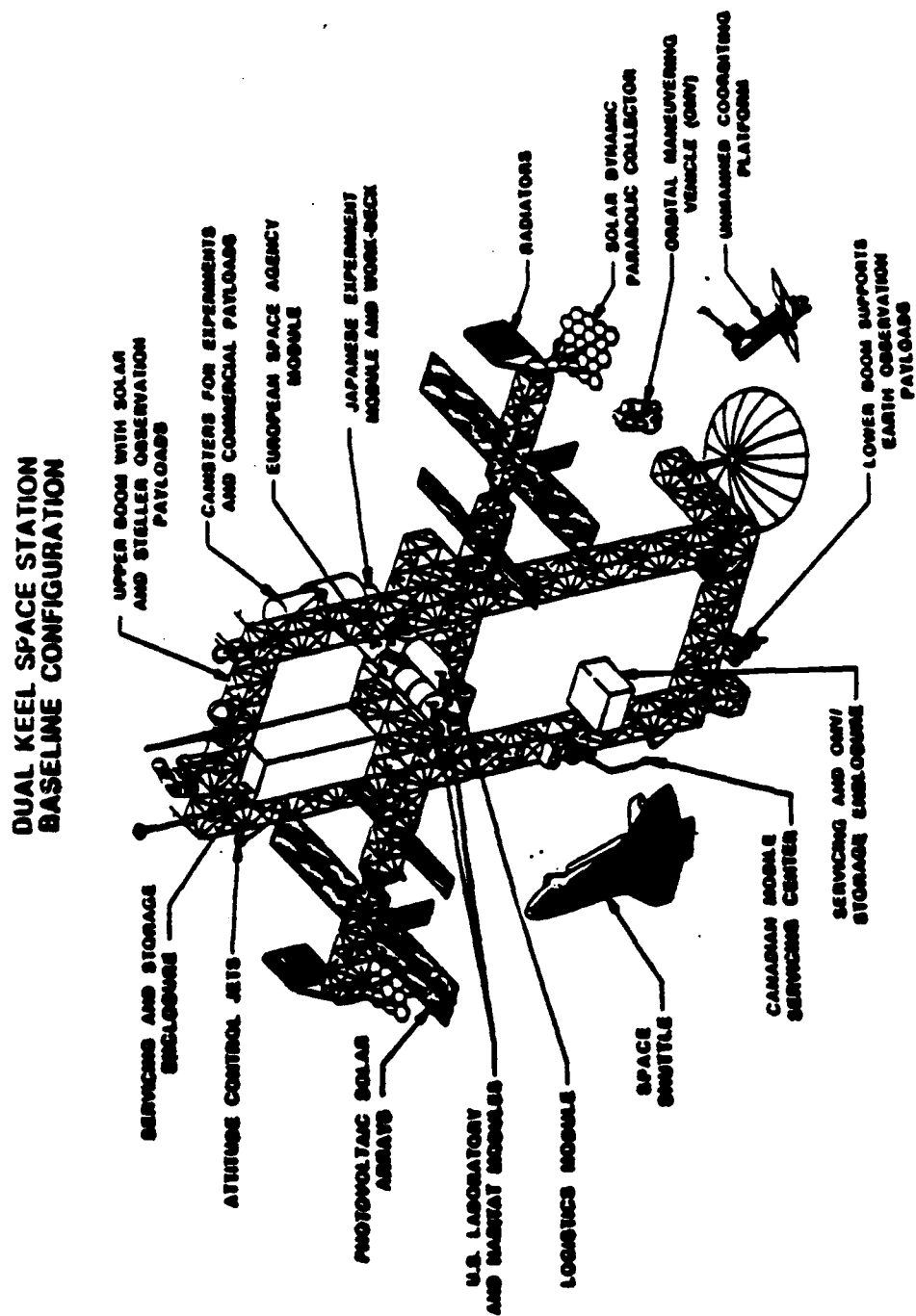


Figure 1 Dual Keel Space Station Baseline Configuration (9)

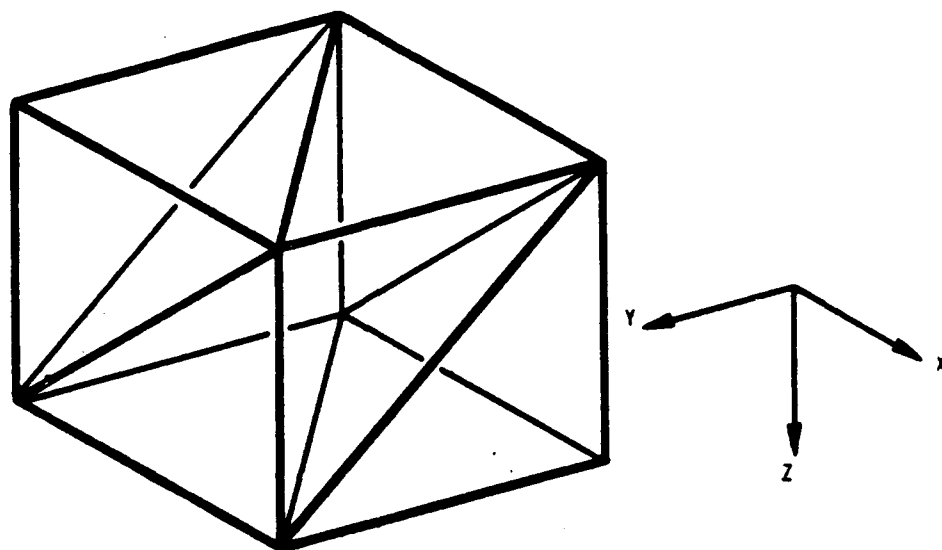


Figure 2 Space Station Orthogonal Tetrahedral Truss Bay (8)

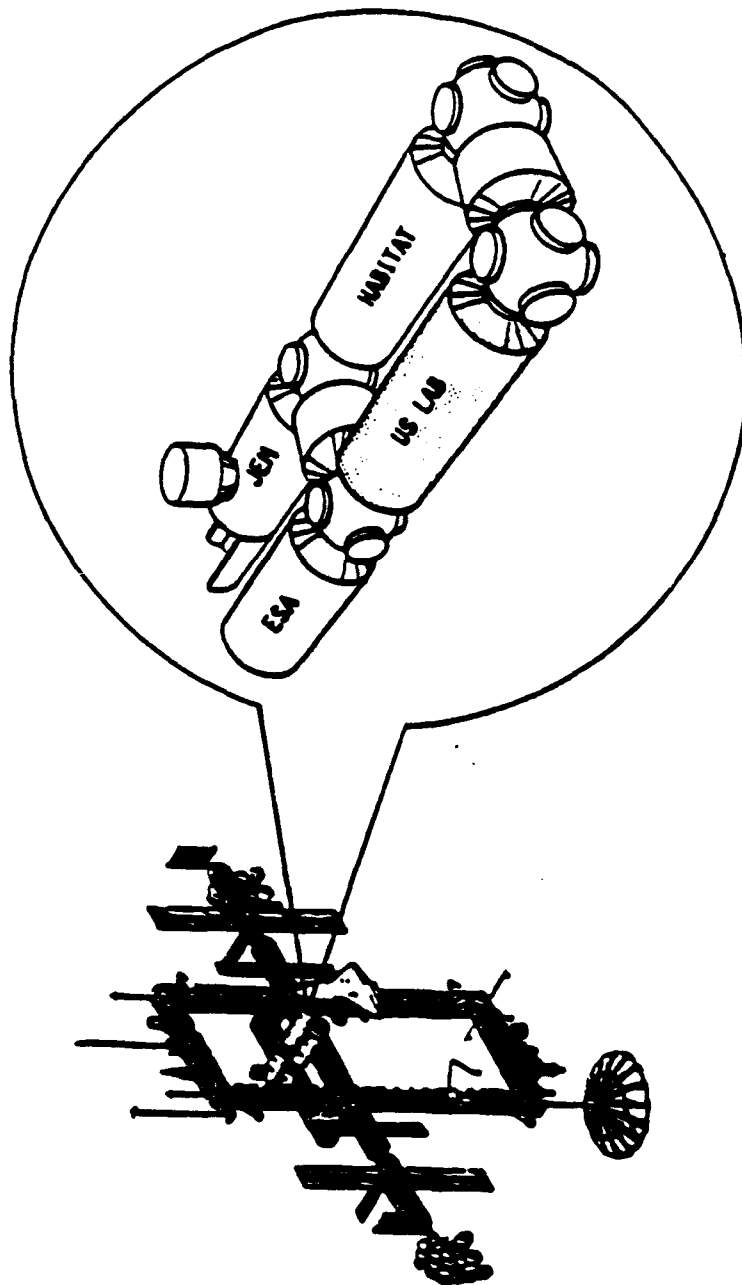


Figure 3 Space Station Module Cluster (9)

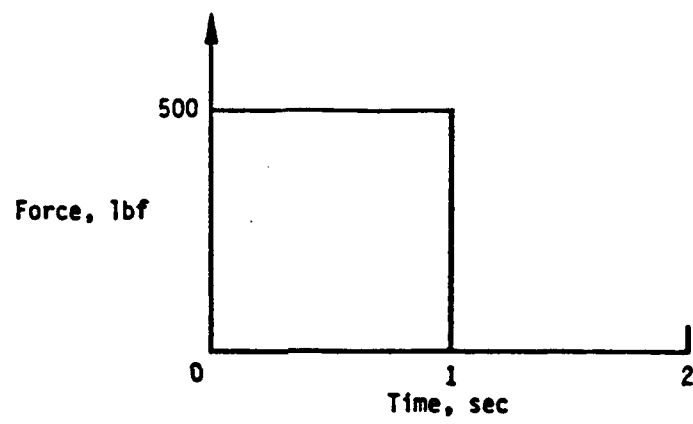


Figure 4 Space Shuttle Docking Impulse (8)

ADINA-PLOT VERSION 4.0 3. 29 APRIL 1992
SPACE STATION MODEL 1

ADINA ORIGINAL
6 527

XVMIN -54 80
XVMAX 51 27
YVMIN -60 22
YVMAX 50 01

GEOMETRY CHECK - VIEW 1

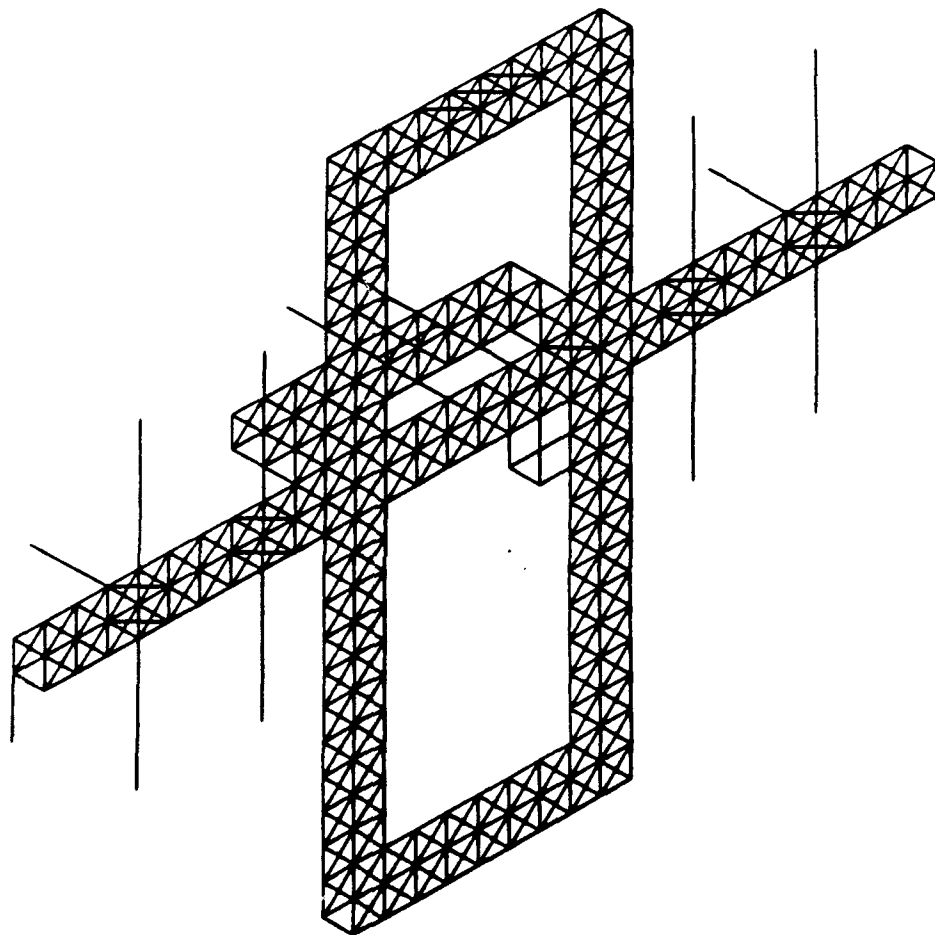


Figure 5 Space Station FEM X,Y,Z View

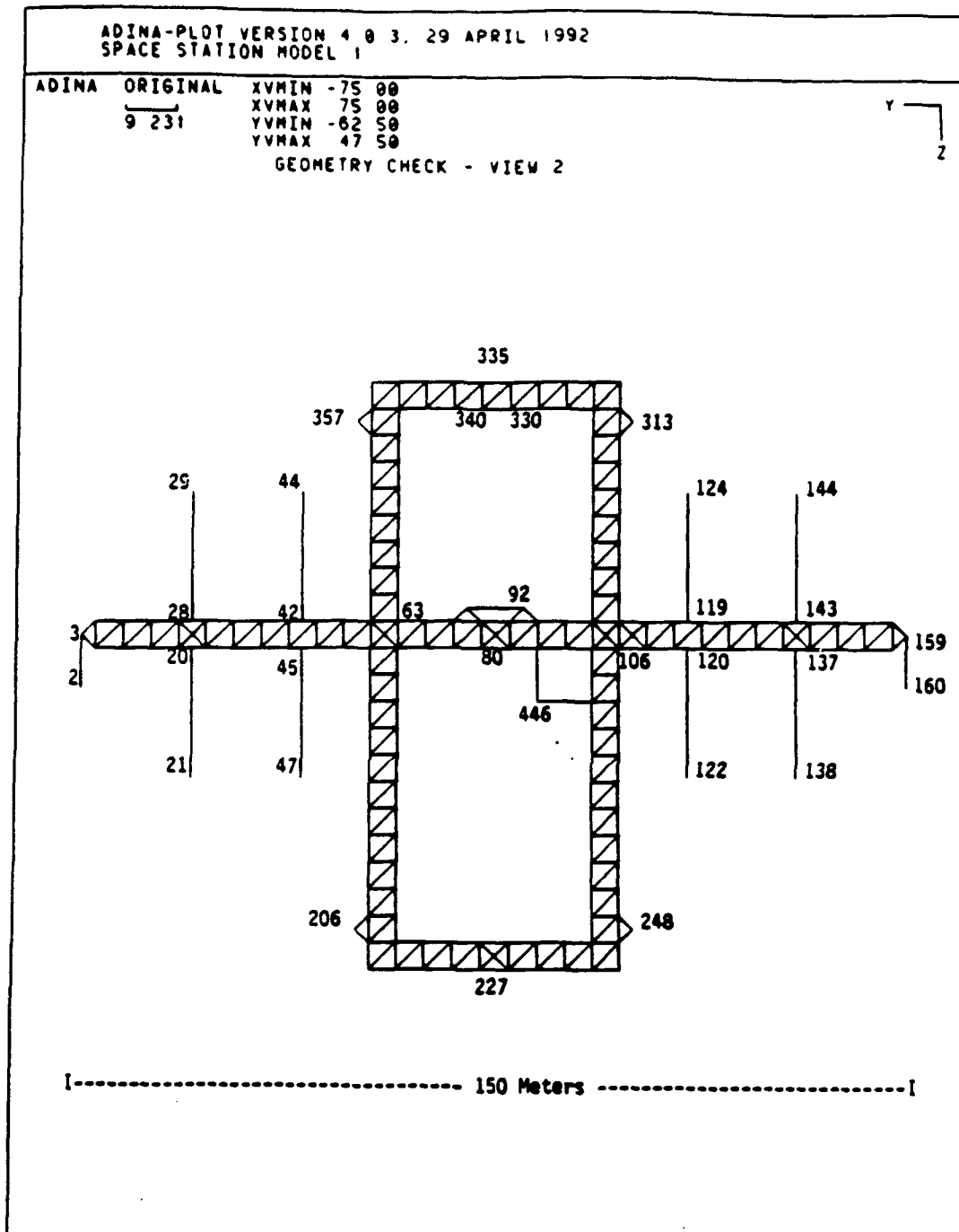


Figure 6 Space Station FEM -X View

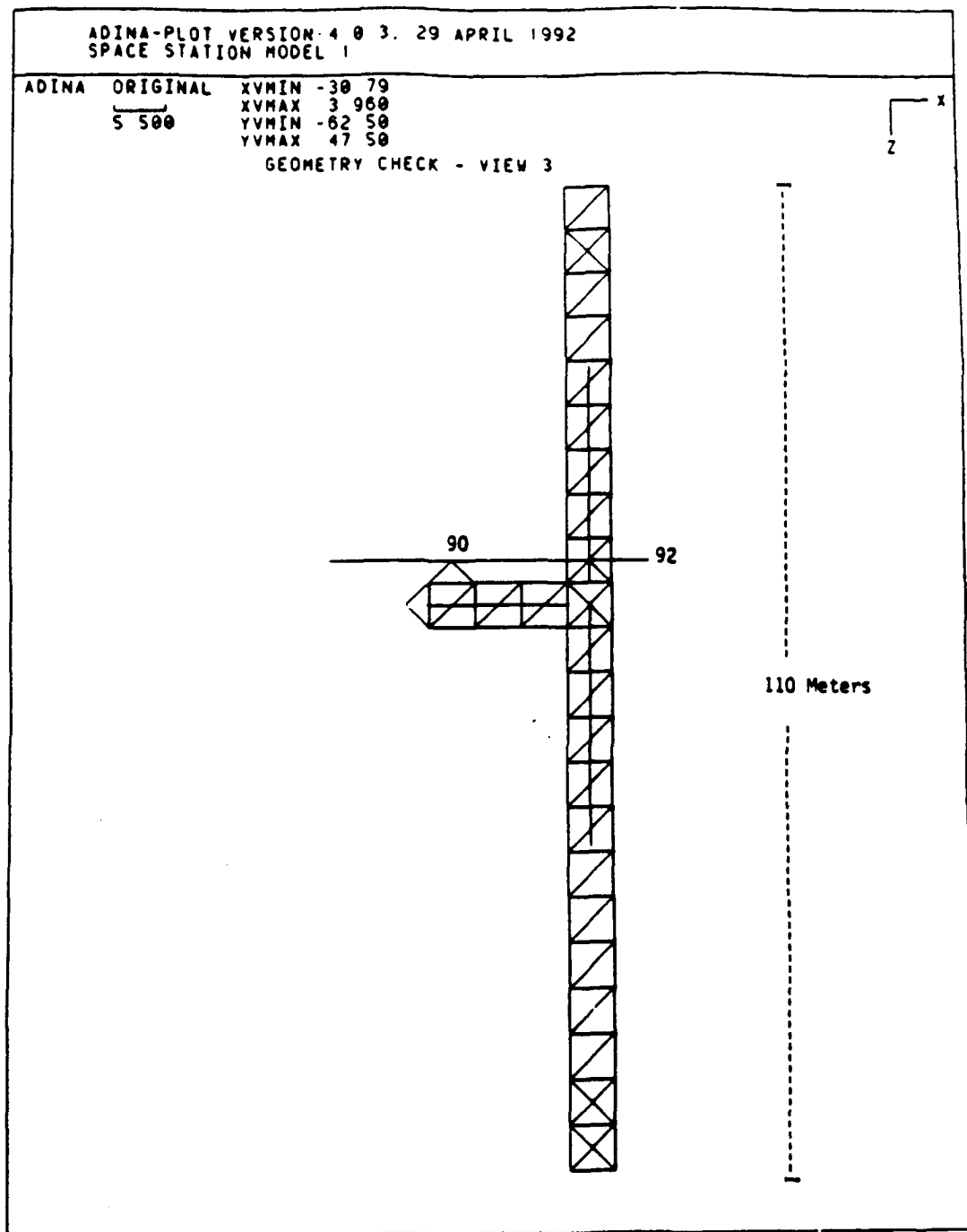


Figure 7 Space Station FEM -Y View

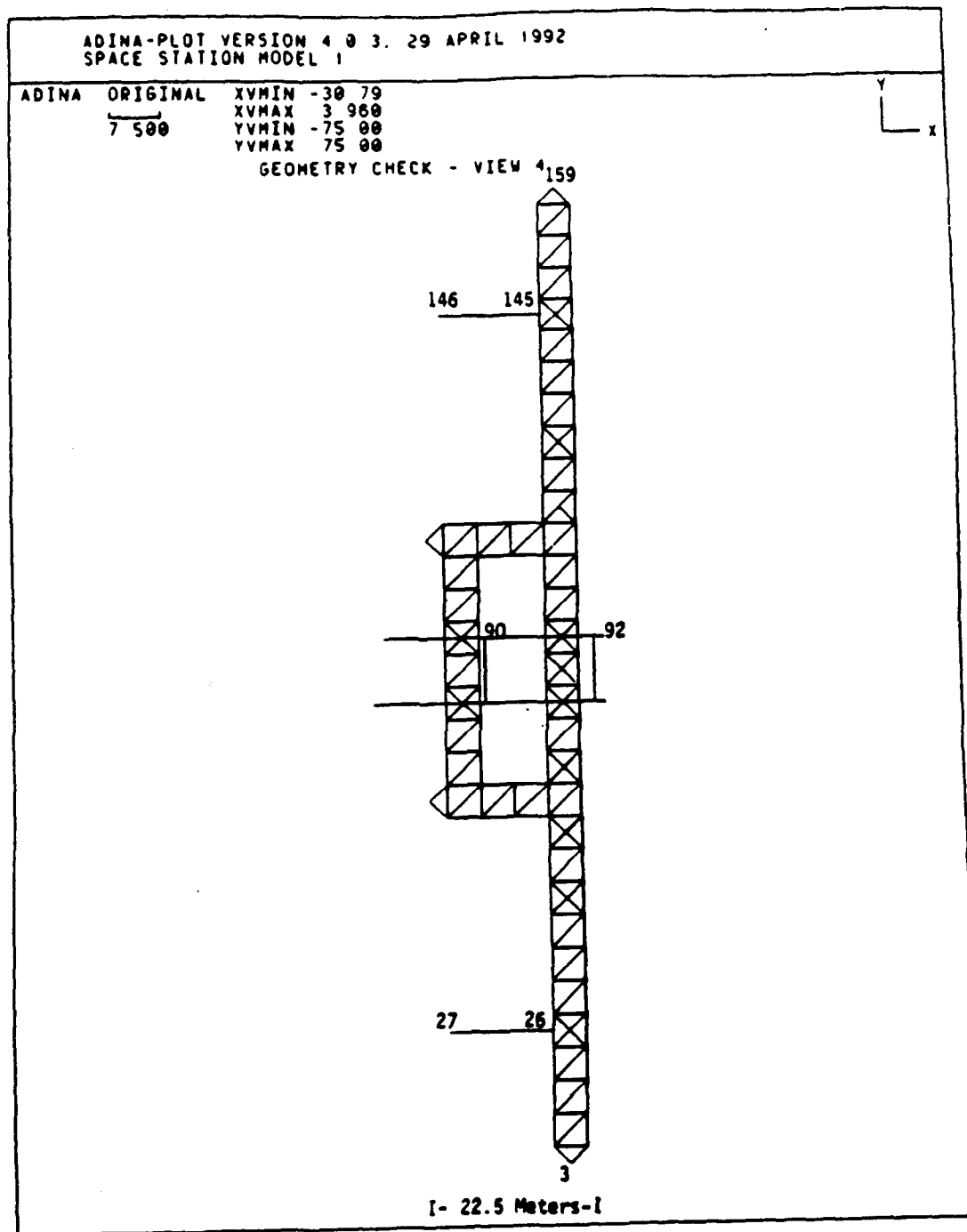


Figure 8 Space Station FEM -Z View

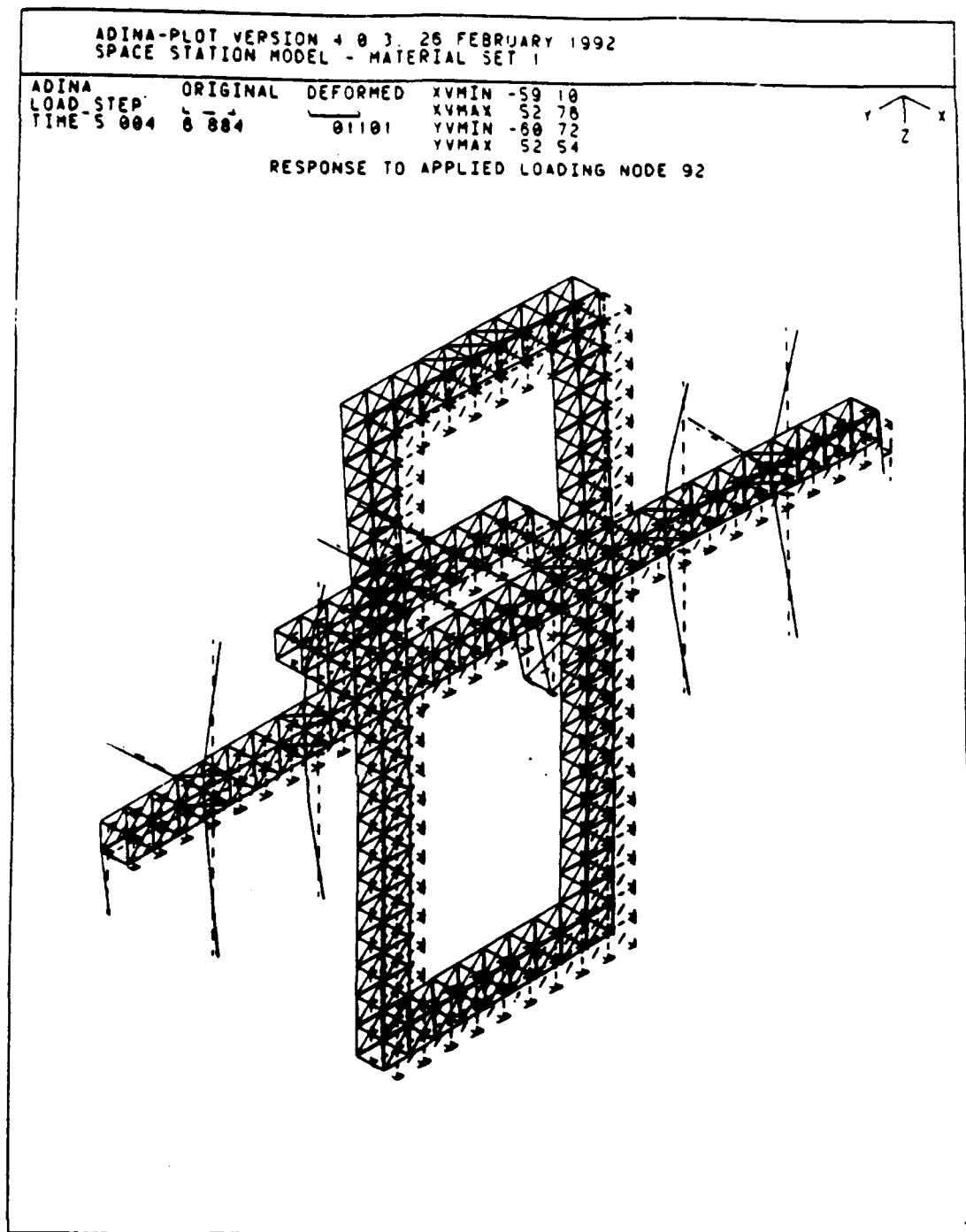


Figure 9 Global Structural Response E=100% at t = 5 sec

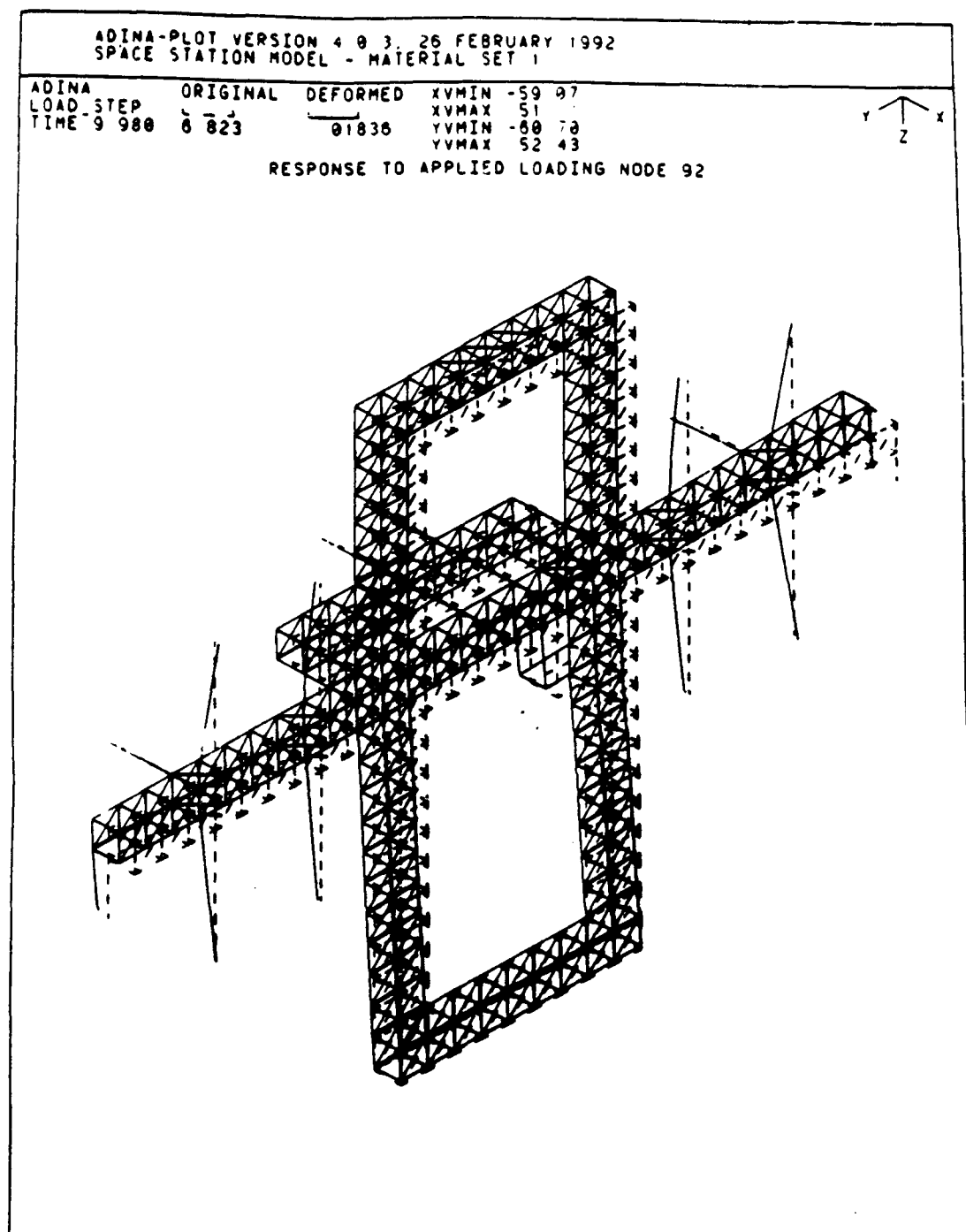


Figure 10 Global Structural Response E=100% at t = 10 sec

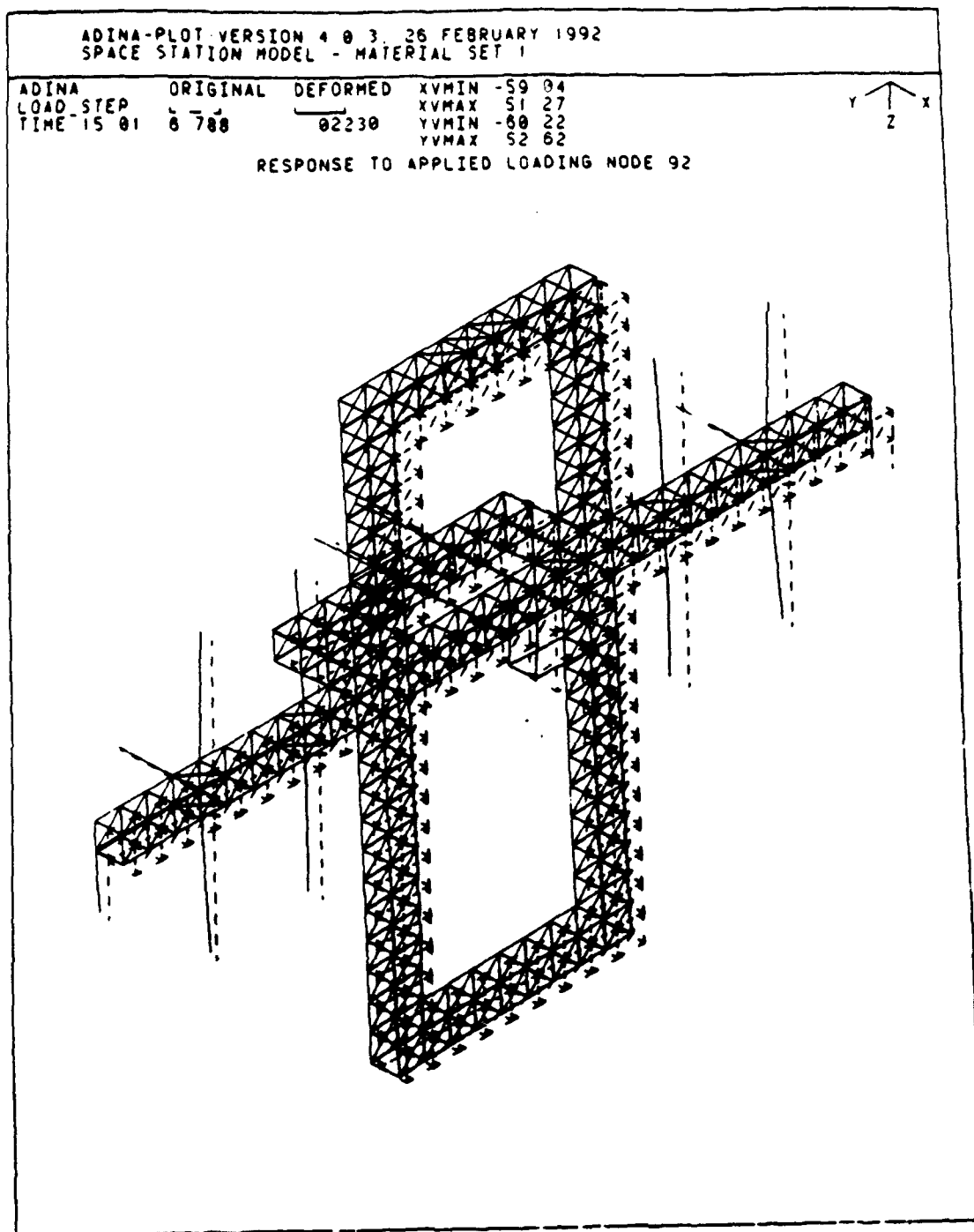


Figure 11 Global Structural Response E=100% at t = 15 sec

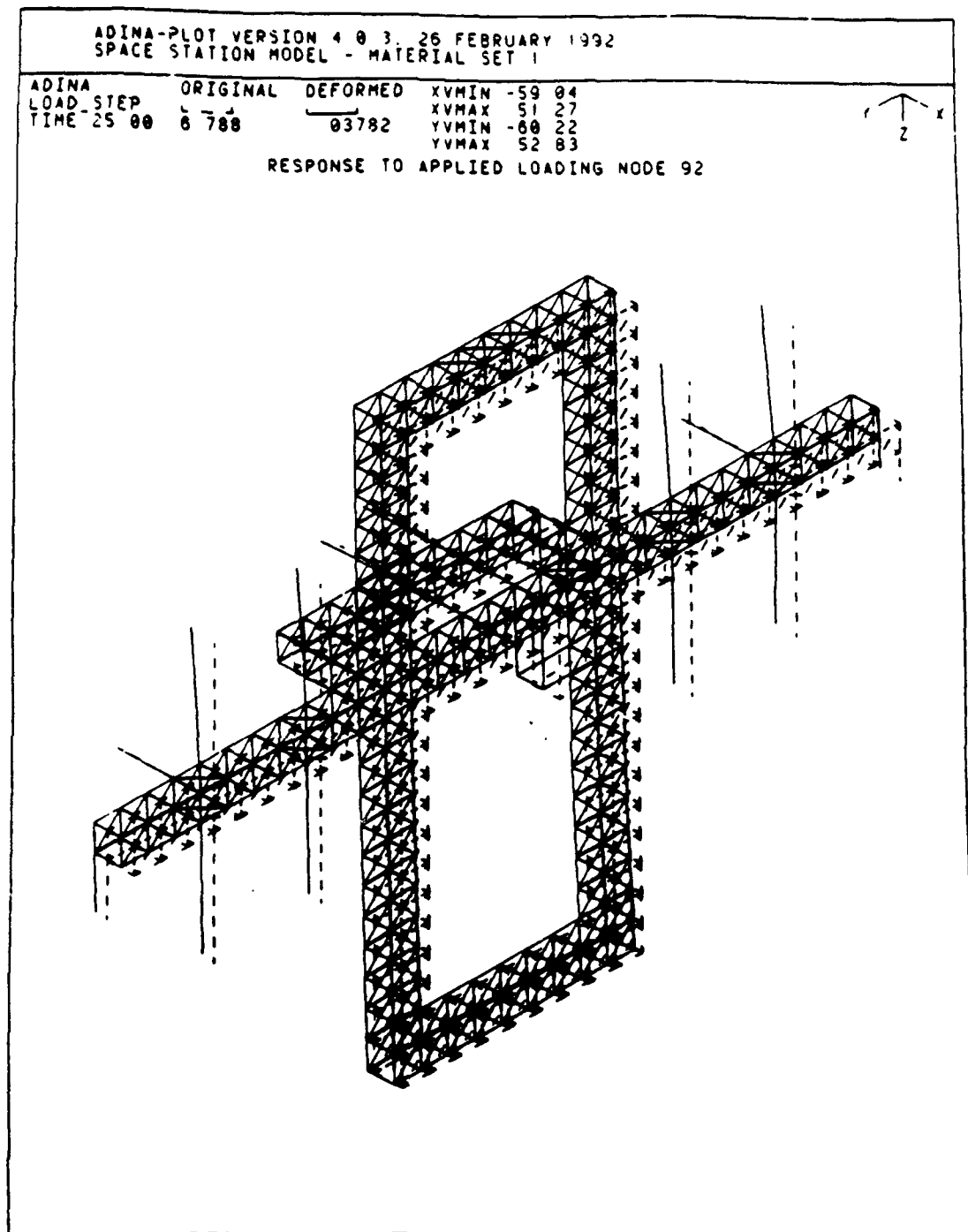


Figure 12 Global Structural Response E=100% t = 25 sec

ADINA-PLOT VERSION 4.0.3, 19 FEBRUARY 1992
SPACE STATION MODEL - MATERIAL SET 1

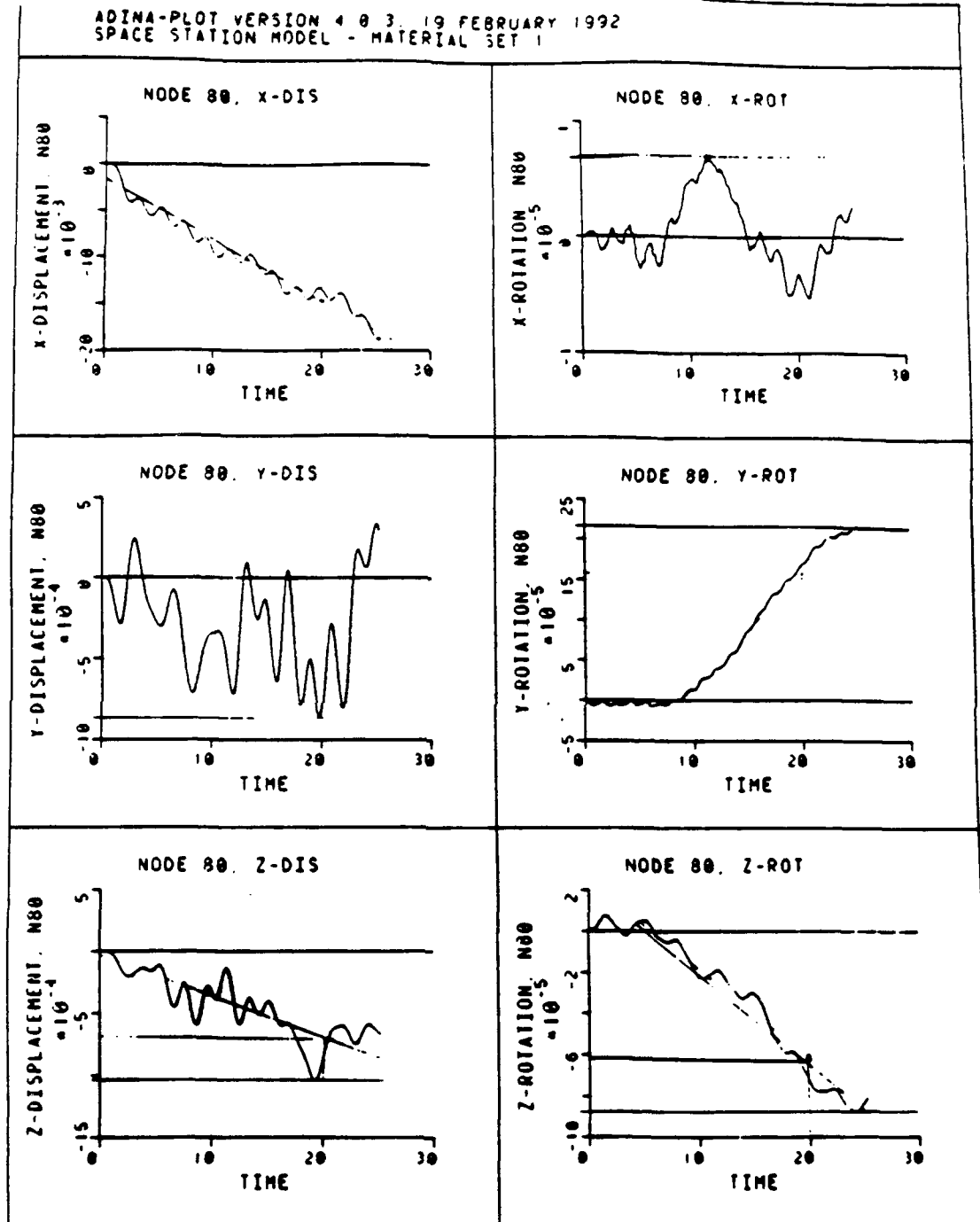


Figure 13 Node 80 Response E=100% X,Y,Z Displ./Rot.

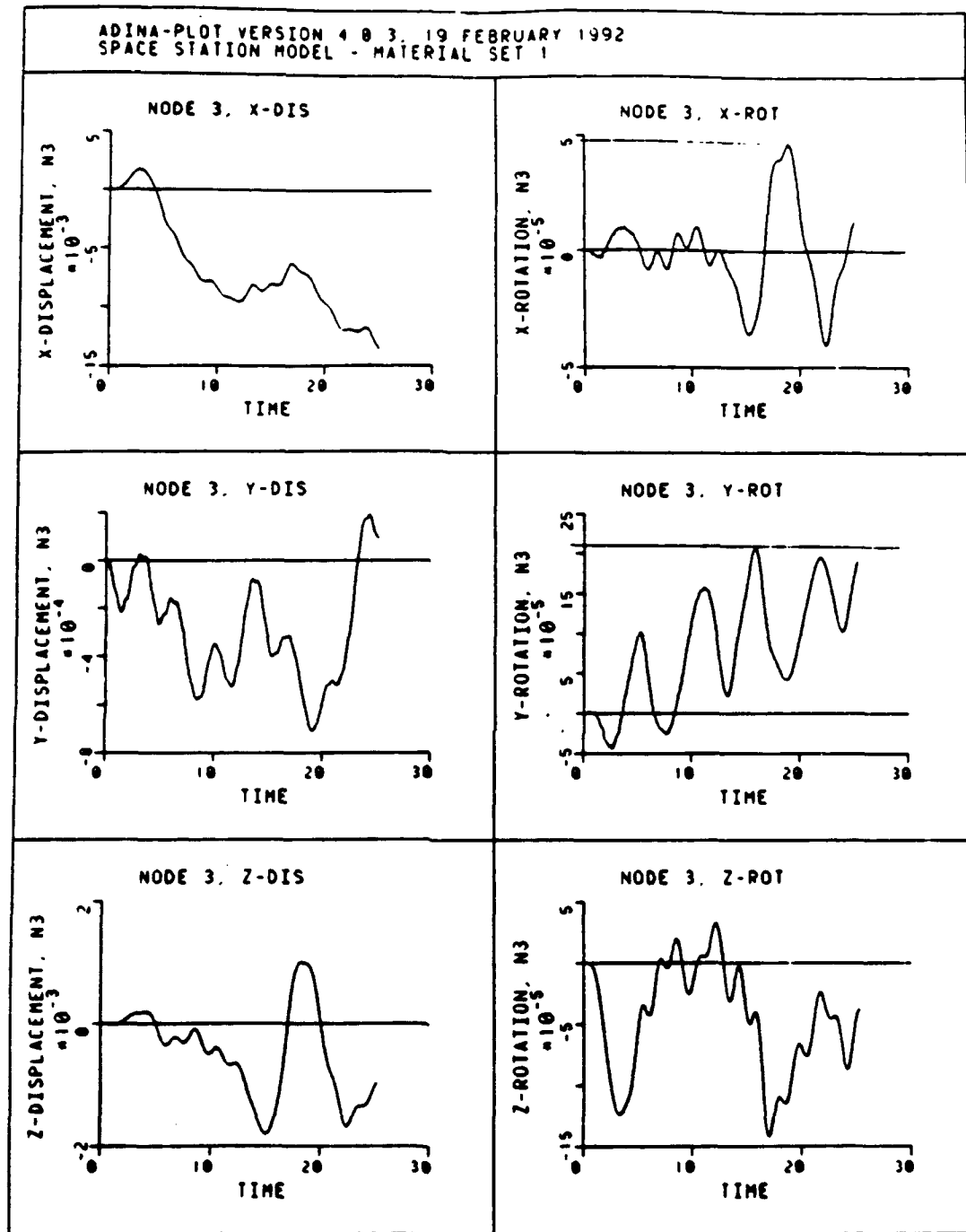


Figure 14 Node 3 Response E=100% X,Y,Z Displ./Rot.

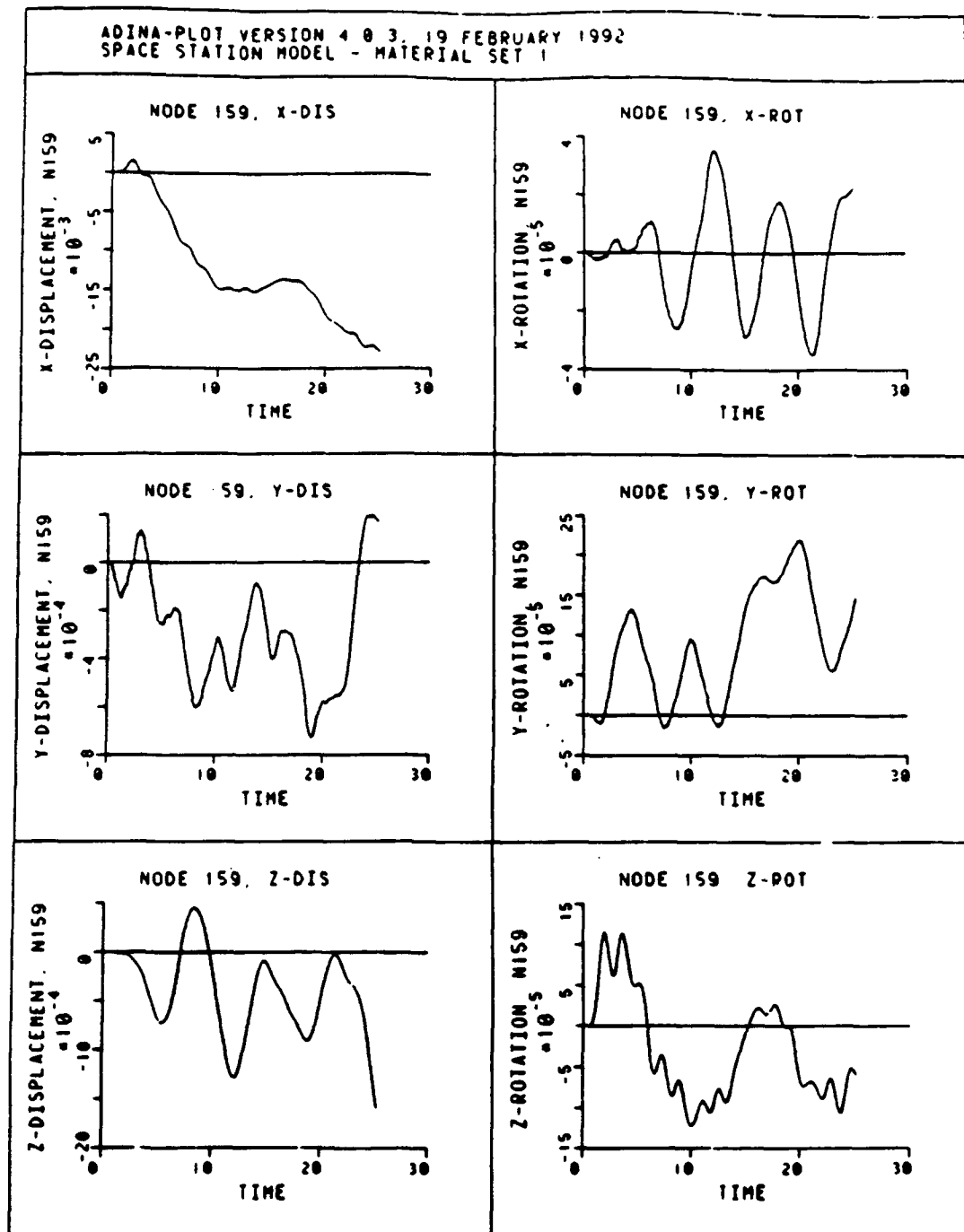


Figure 15 Node 159 Response E=100% X,Y,Z Displ./Rot.

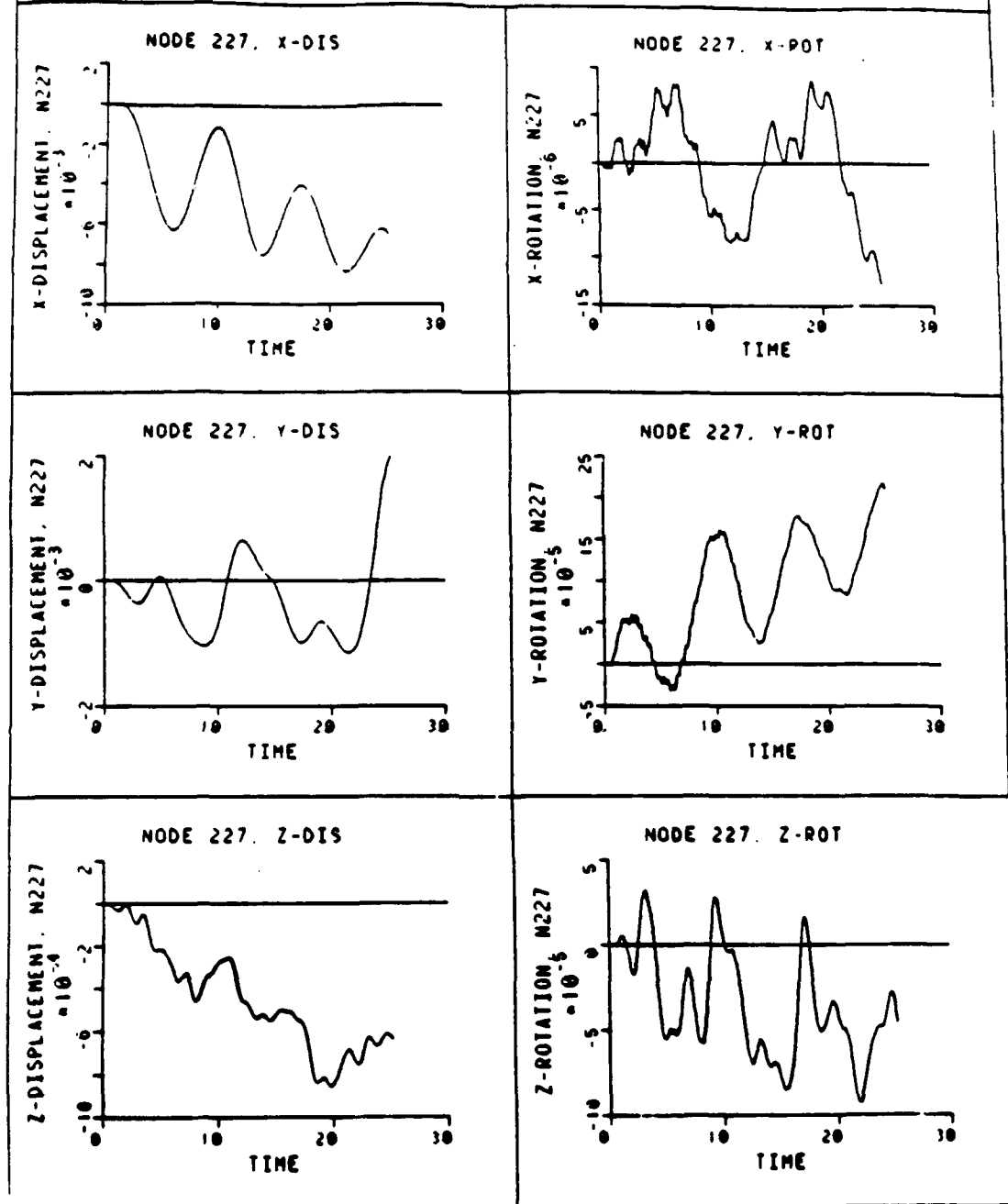


Figure 16 Node 227 Response E=100% X,Y,Z Displ./Rot.

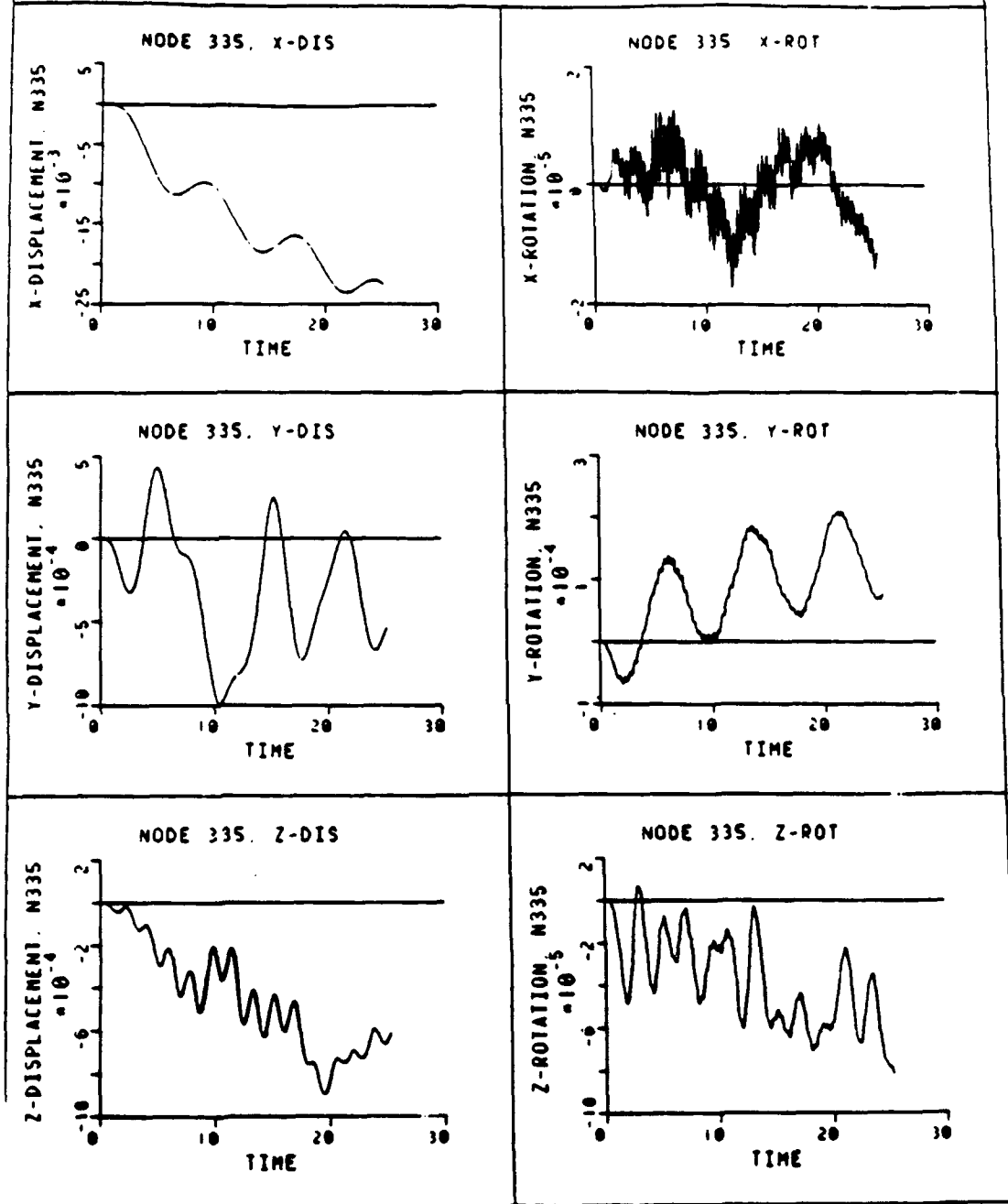


Figure 17 Node 335 Response E=100% X,Y,Z Displ./Rot.

ADINA-PLOT VERSION 4.0.3, 19 FEBRUARY 1992
SPACE STATION MODEL - MATERIAL SET 1

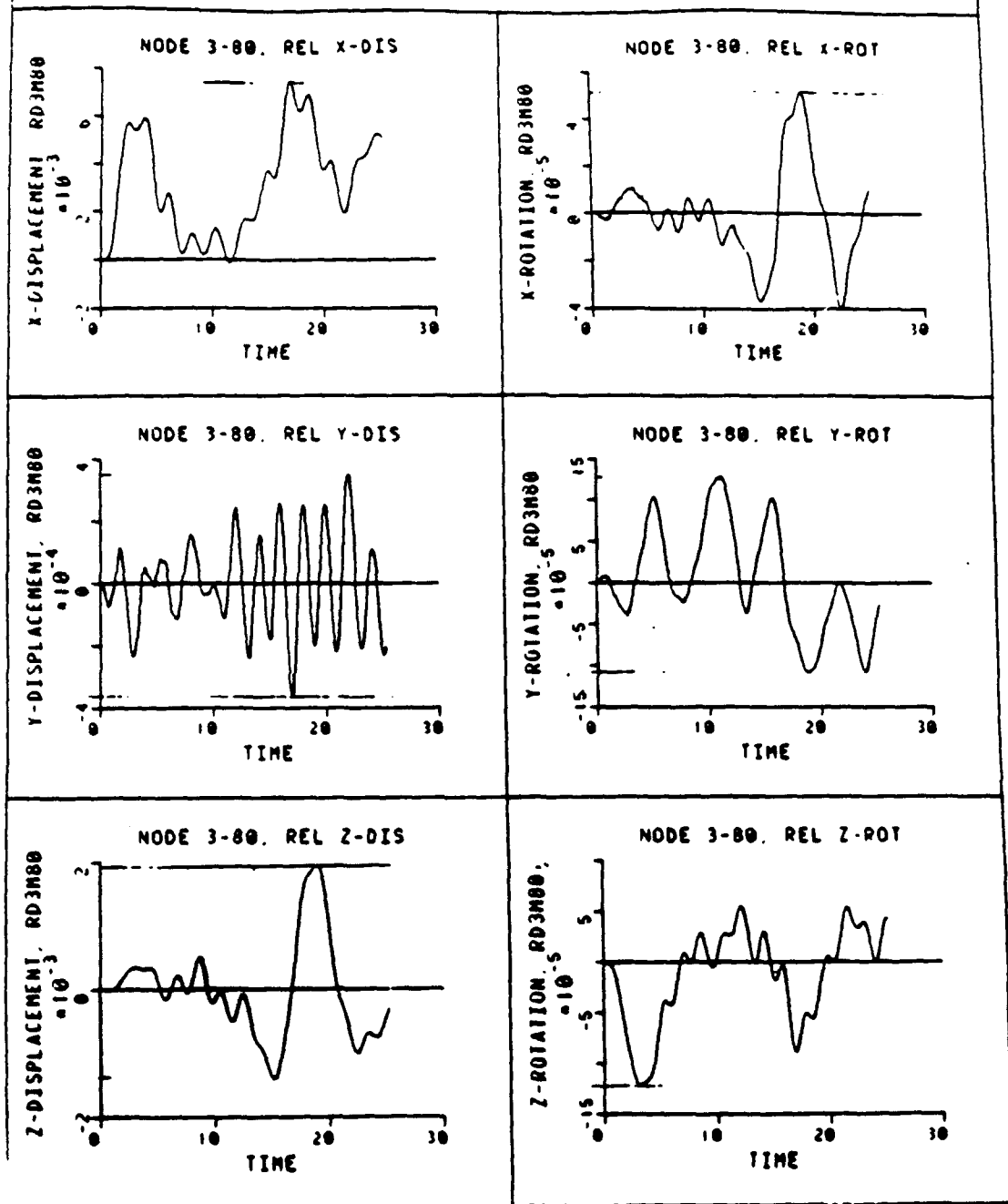


Figure 18 Node 3 vs. 80 Response E=100% X,Y,Z Displ./Rot.

ADINA-PLOT VERSION 4.0.3, 19 FEBRUARY 1992
SPACE STATION MODEL - MATERIAL SET 1

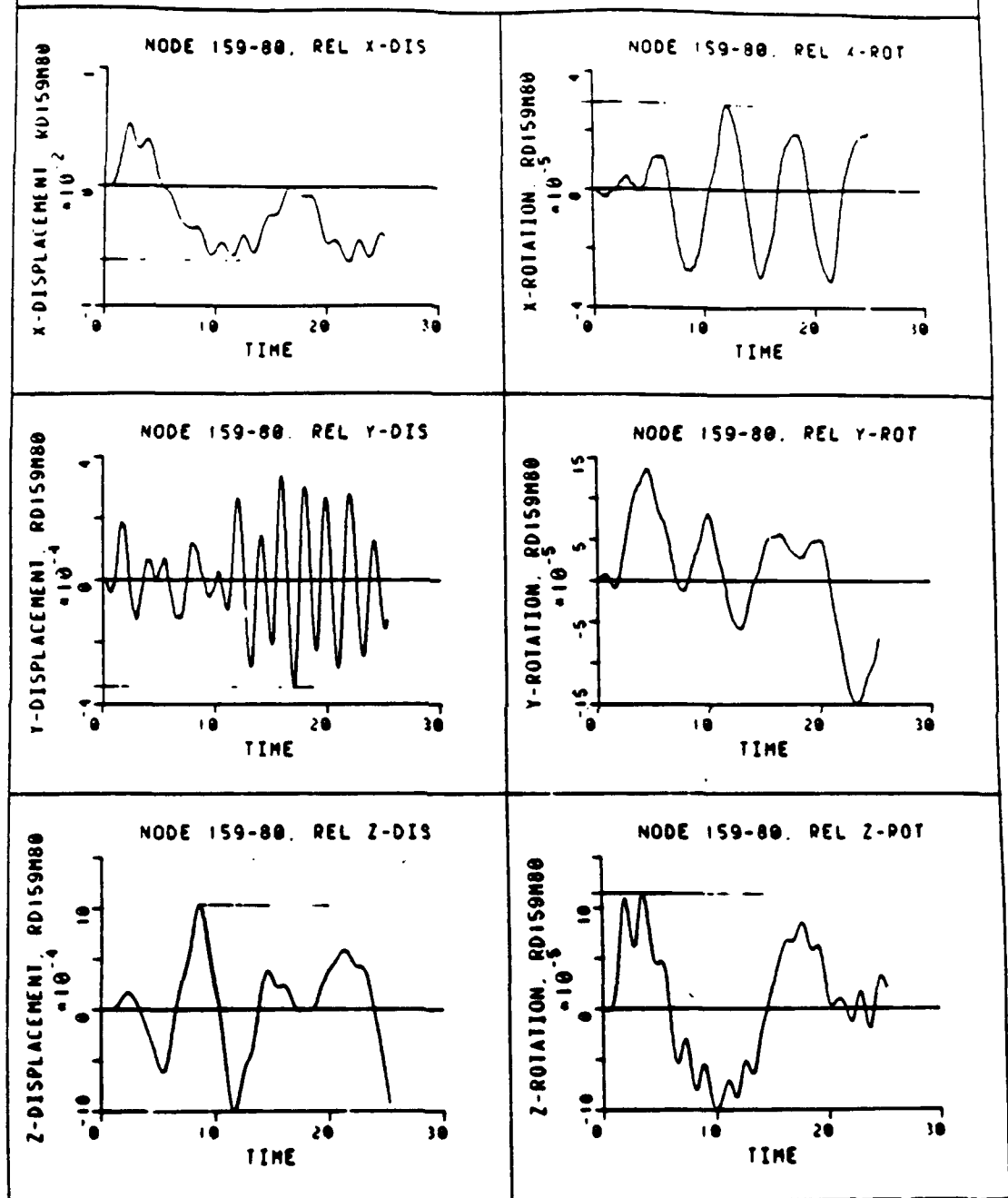


Figure 19 Node 159 vs. 80 Response E=100% X,Y,Z Displ./Rot.

ADINA-PLT VERSION 4.0.3, 19 FEBRUARY 1992
SPACE STATION MODEL - MATERIAL SET 1

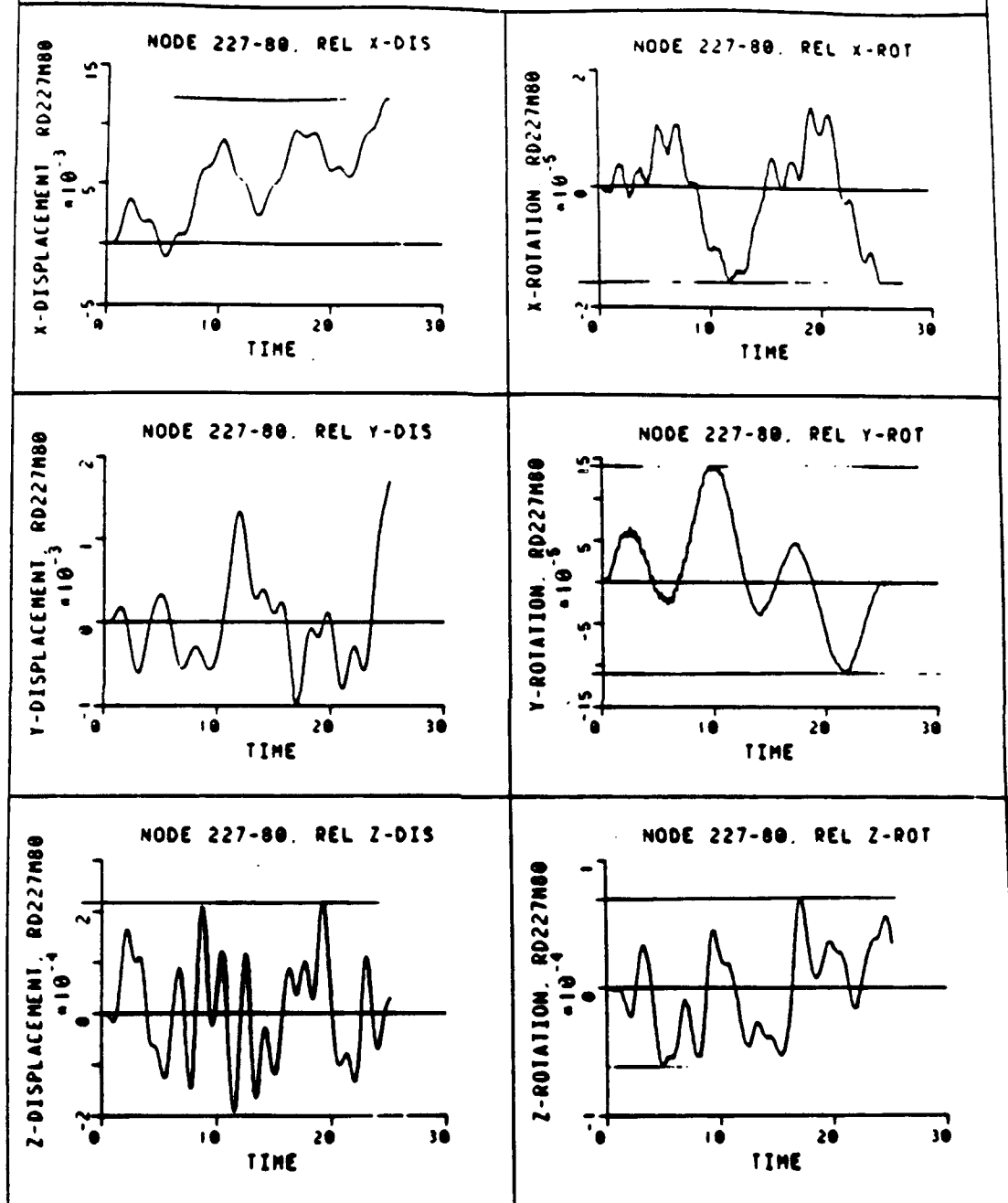


Figure 20 Node 227 vs. 80 Response E=100% X,Y,Z Displ./Rot.

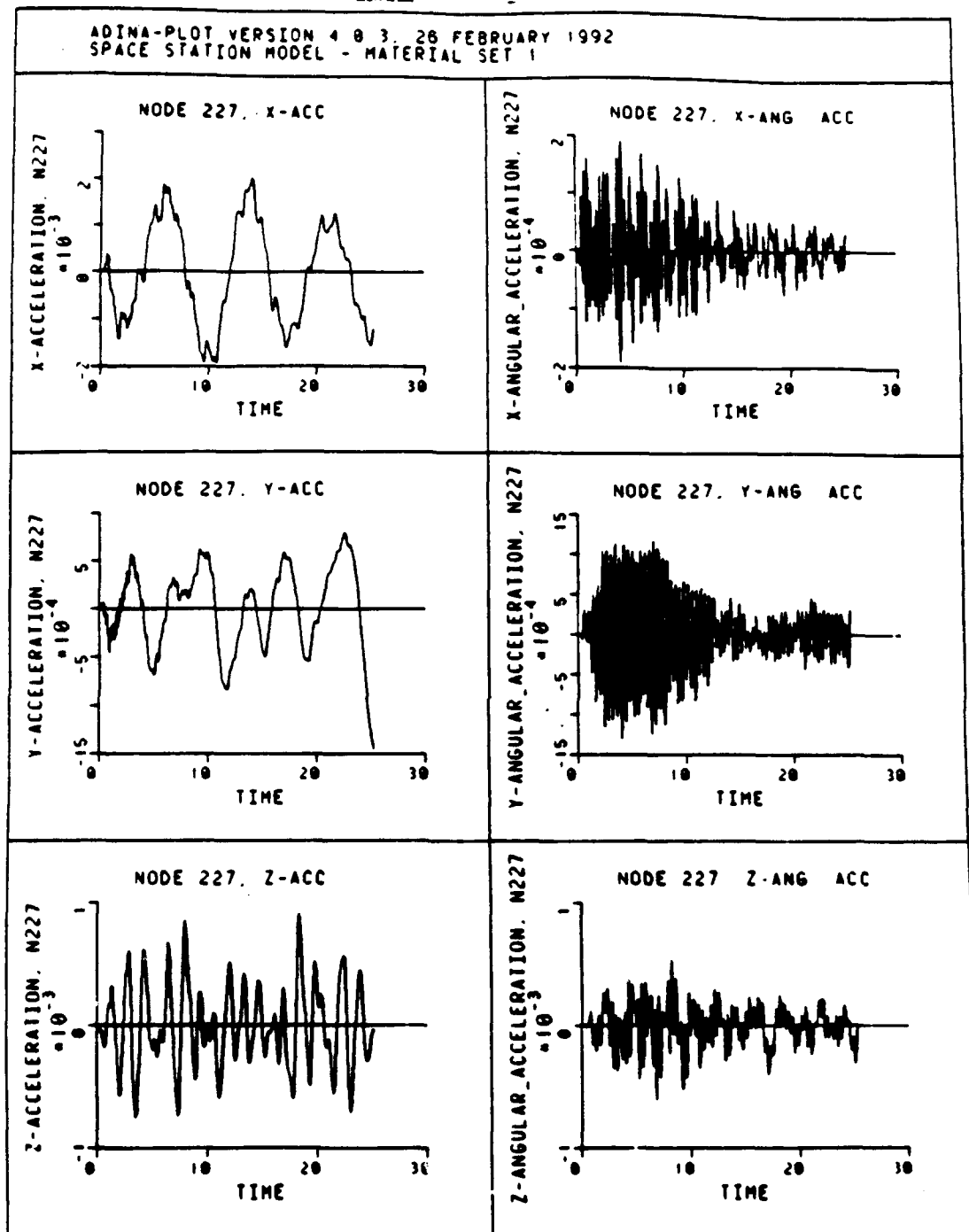


Figure 21 Node 227 E=100% Response X,Y,Z Lin./Rot. Accel.

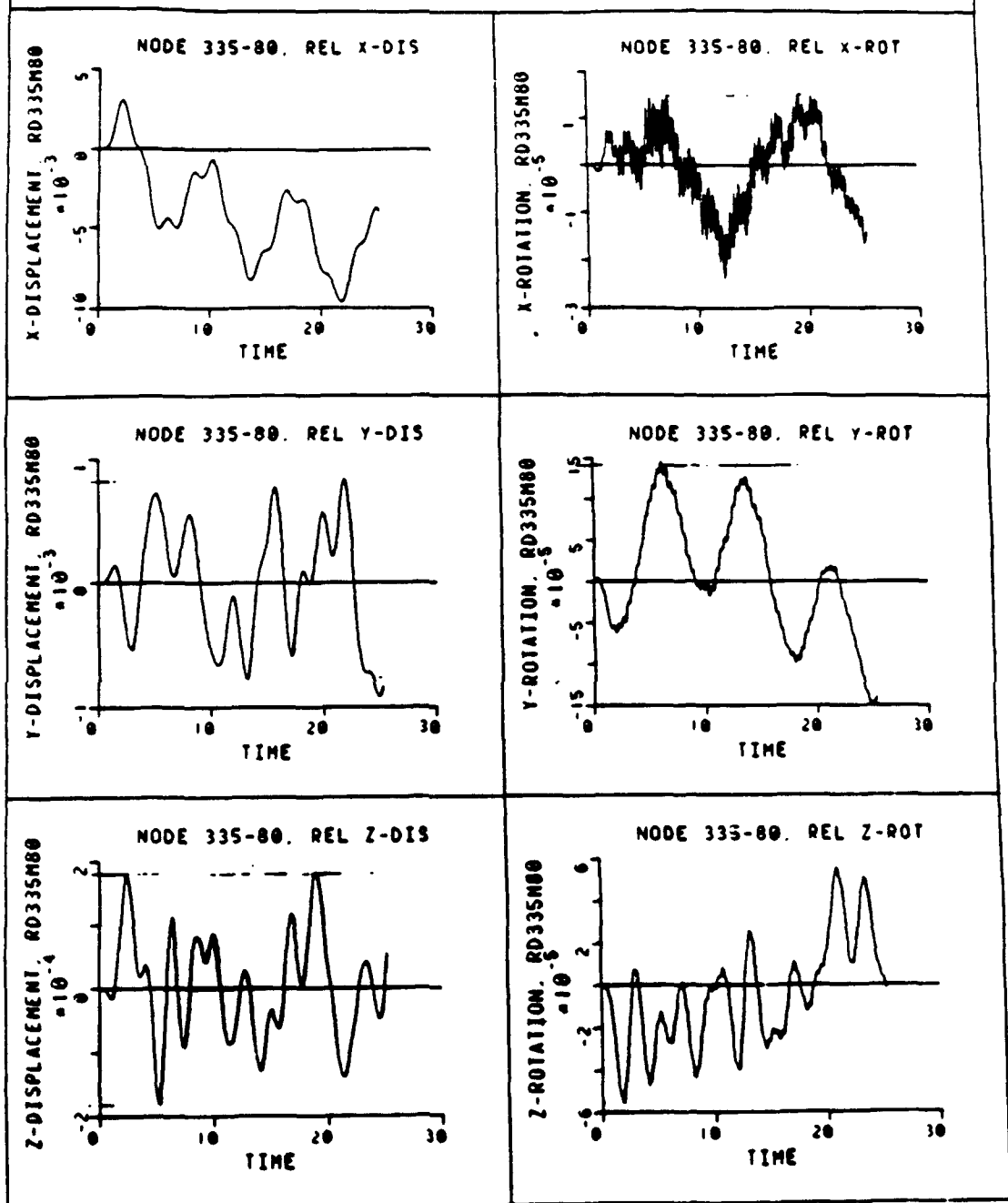


Figure 22 Node 335 vs.80 Response E=100% X,Y,Z Displ./Rot.

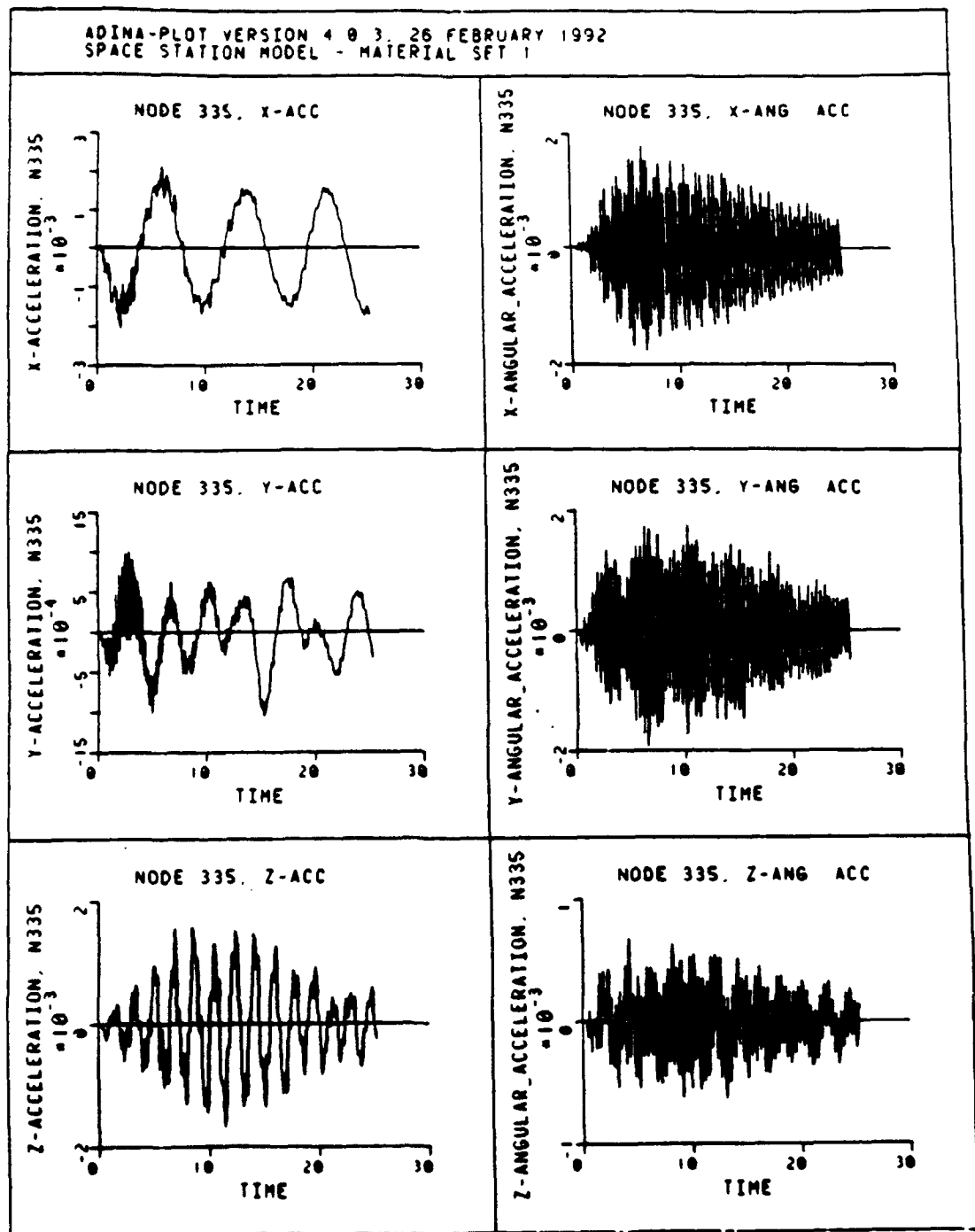


Figure 23 Node 335 Response E=100% X,Y,Z Lin./Rot. Accel.

ADINA-PLOT VERSION 4.0.3, 19 FEBRUARY 1992
SPACE STATION MODEL - MATERIAL SET 1

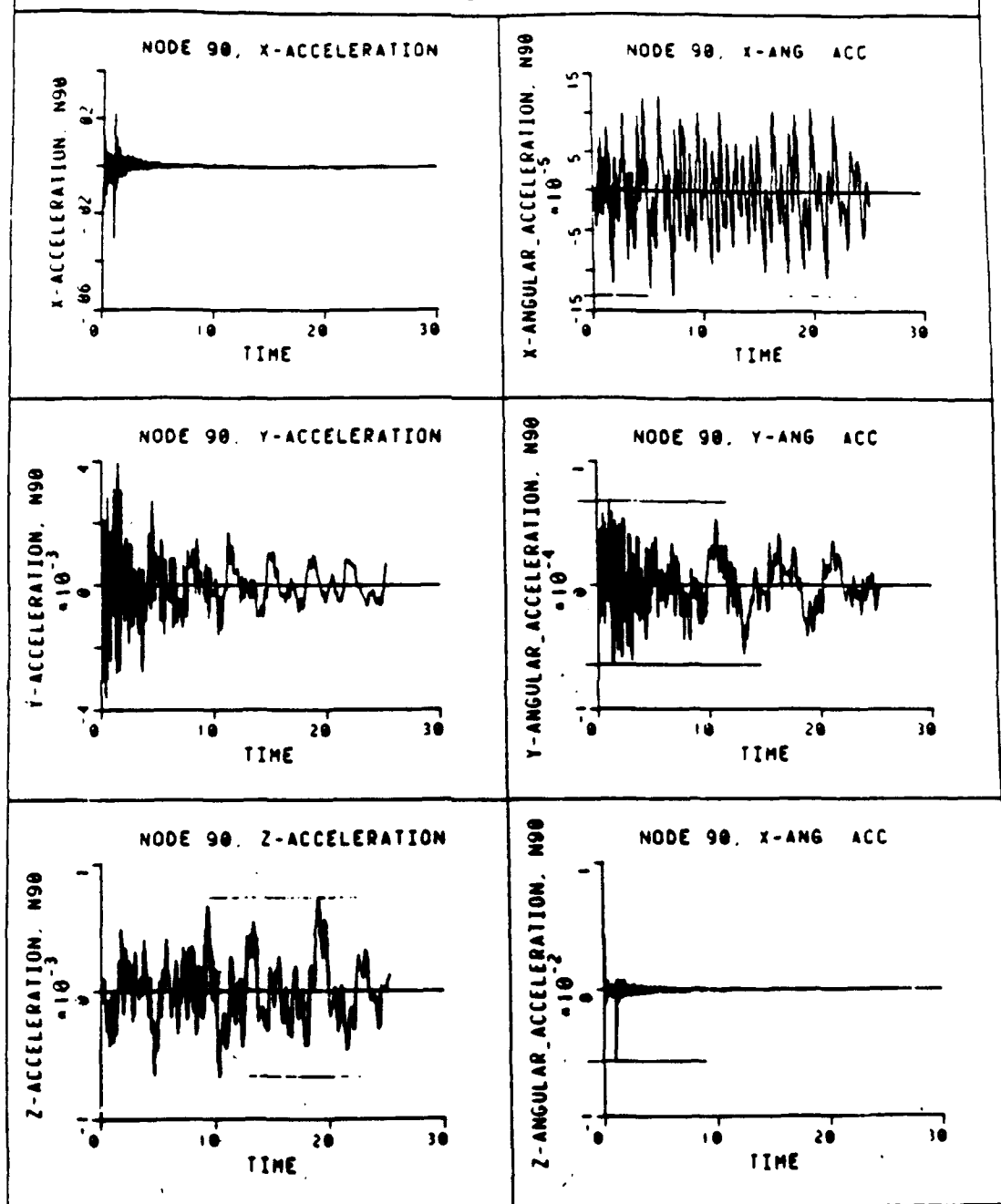


Figure 24 Node 90 Response E=100% X,Y,Z Lin./Rot. Accel.

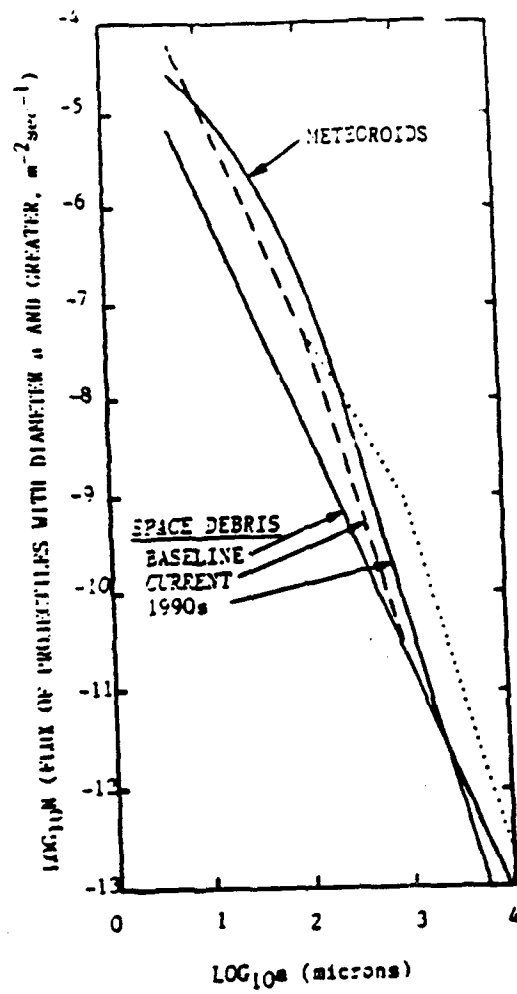


Figure 25 Flux Level for Meteor./Space Debris @ 400Km (85)

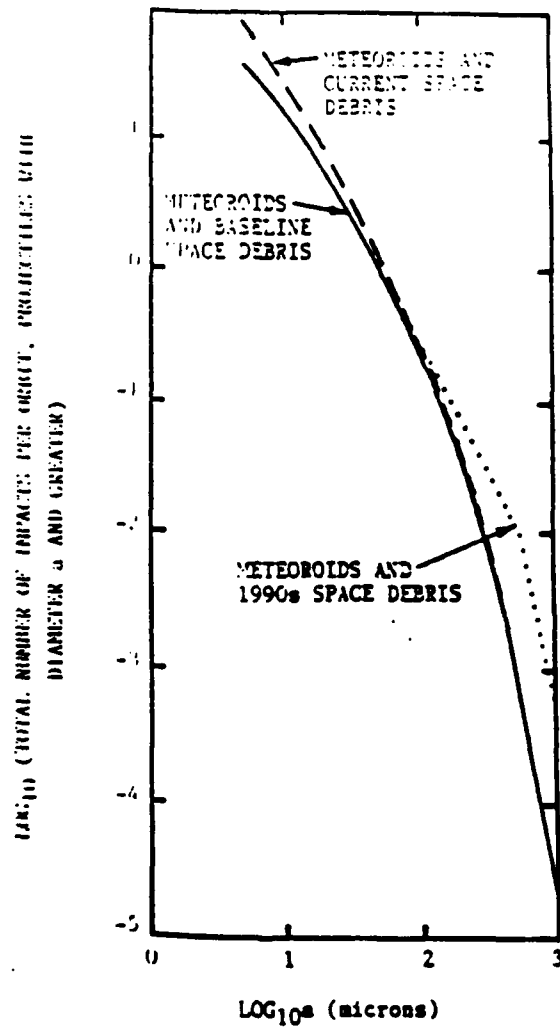


Figure 26 Number of Impacts for 150 SQ M @ 400Km (85)

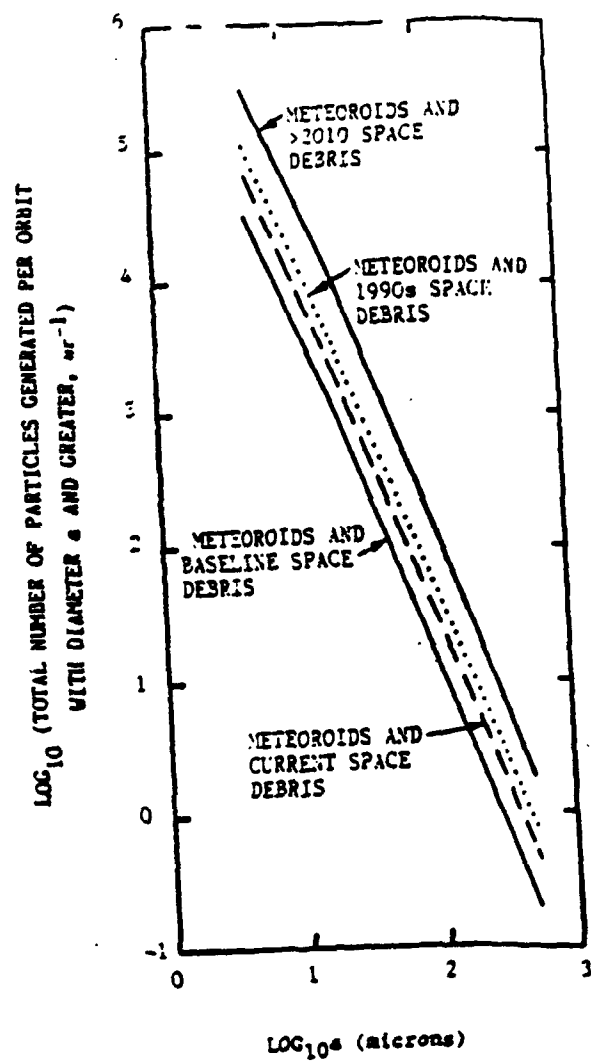


Figure 27 Total Number of Ejecta Generated for 150 SQ M (85)

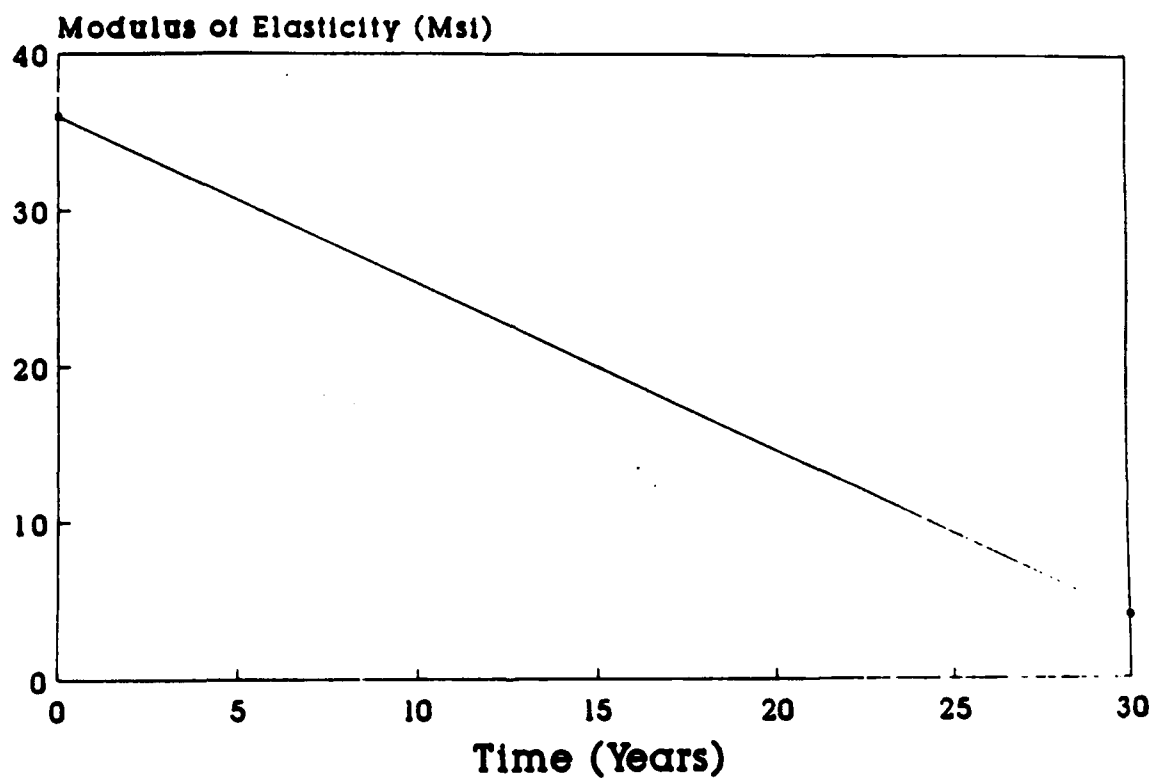


Figure 28 Assumed Linear Degradation Model

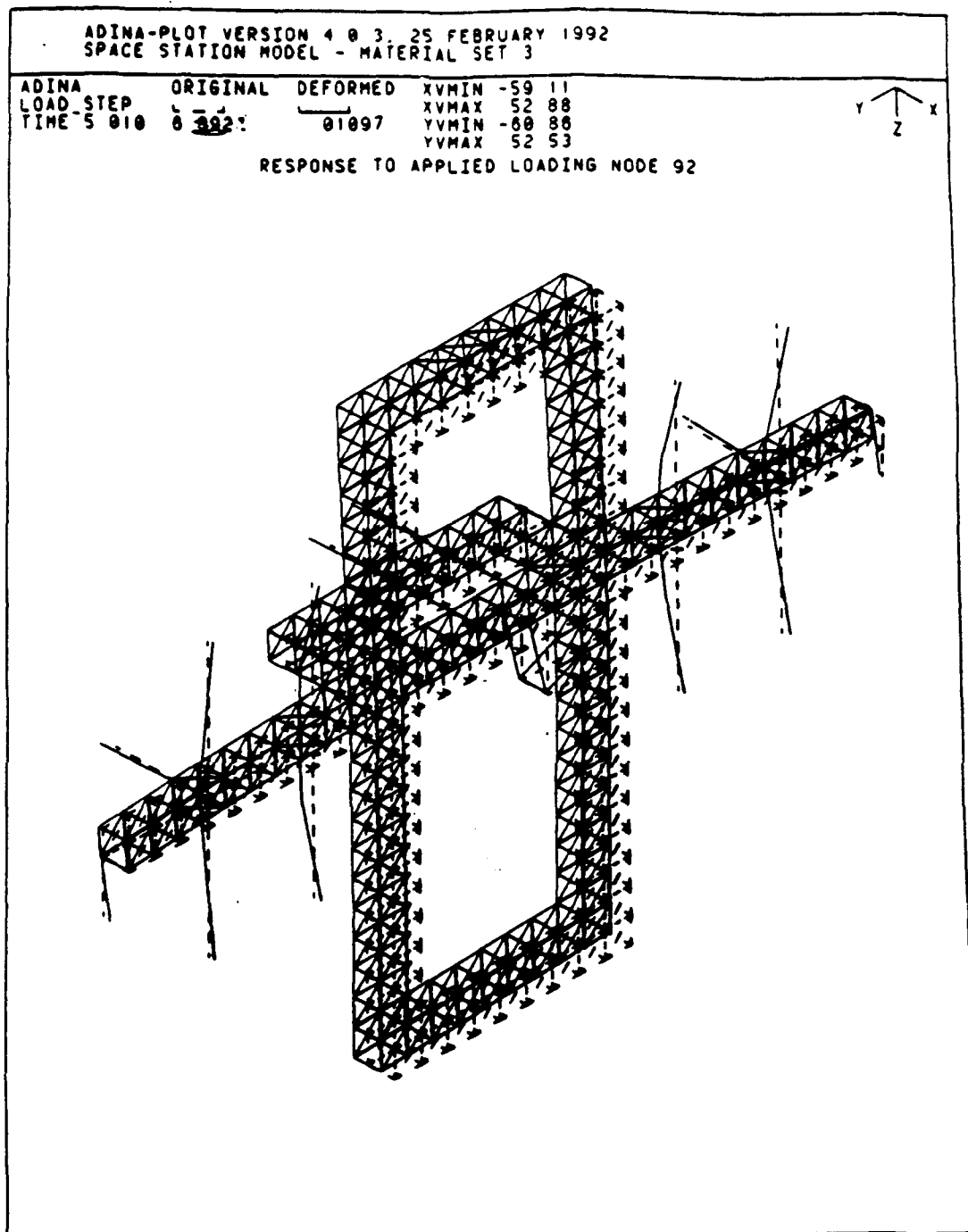


Figure 29 Global Structural Response E=78% at $t = 5$ sec

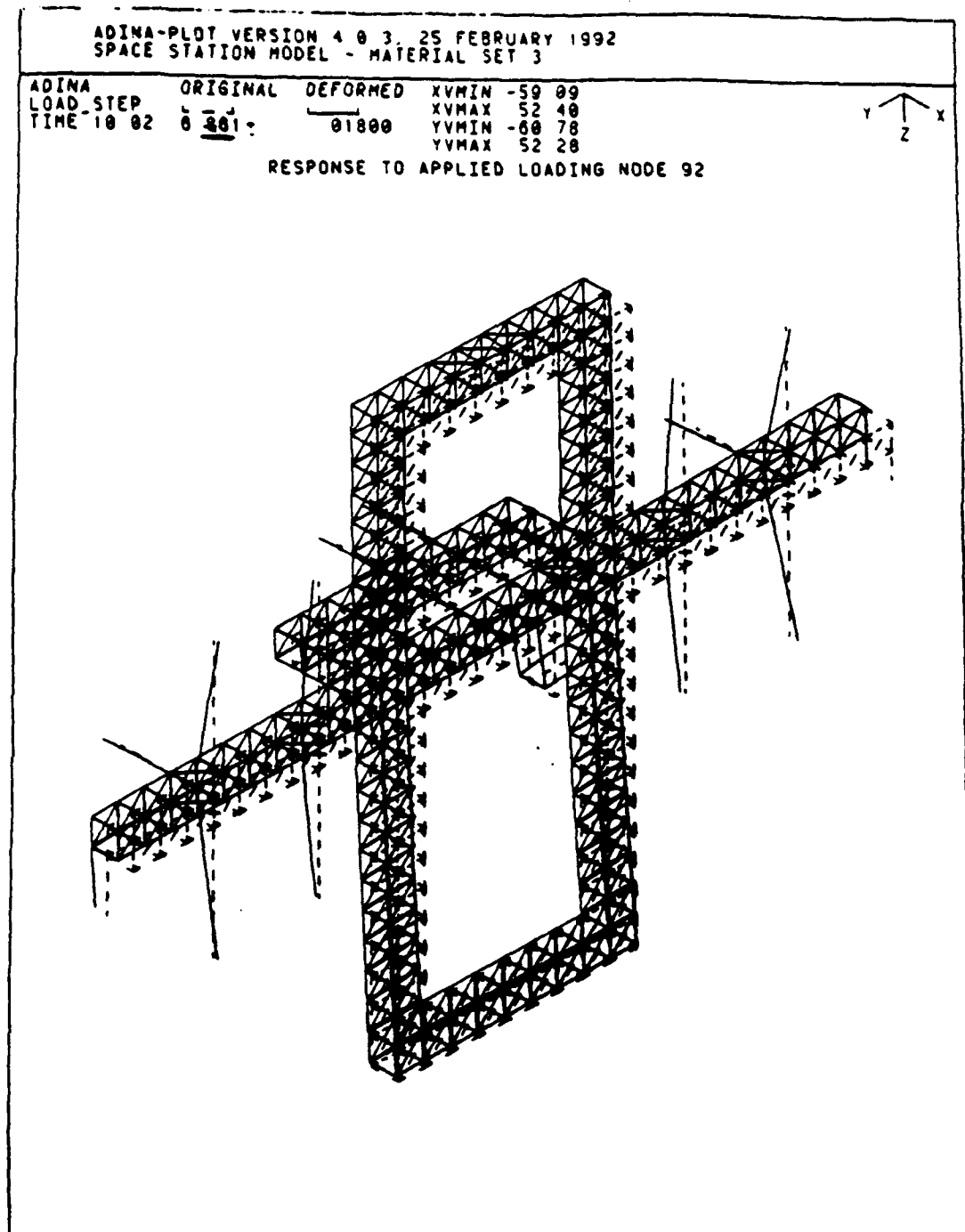


Figure 30 Global Structural Response $E=78\%$ at $t = 10$ sec

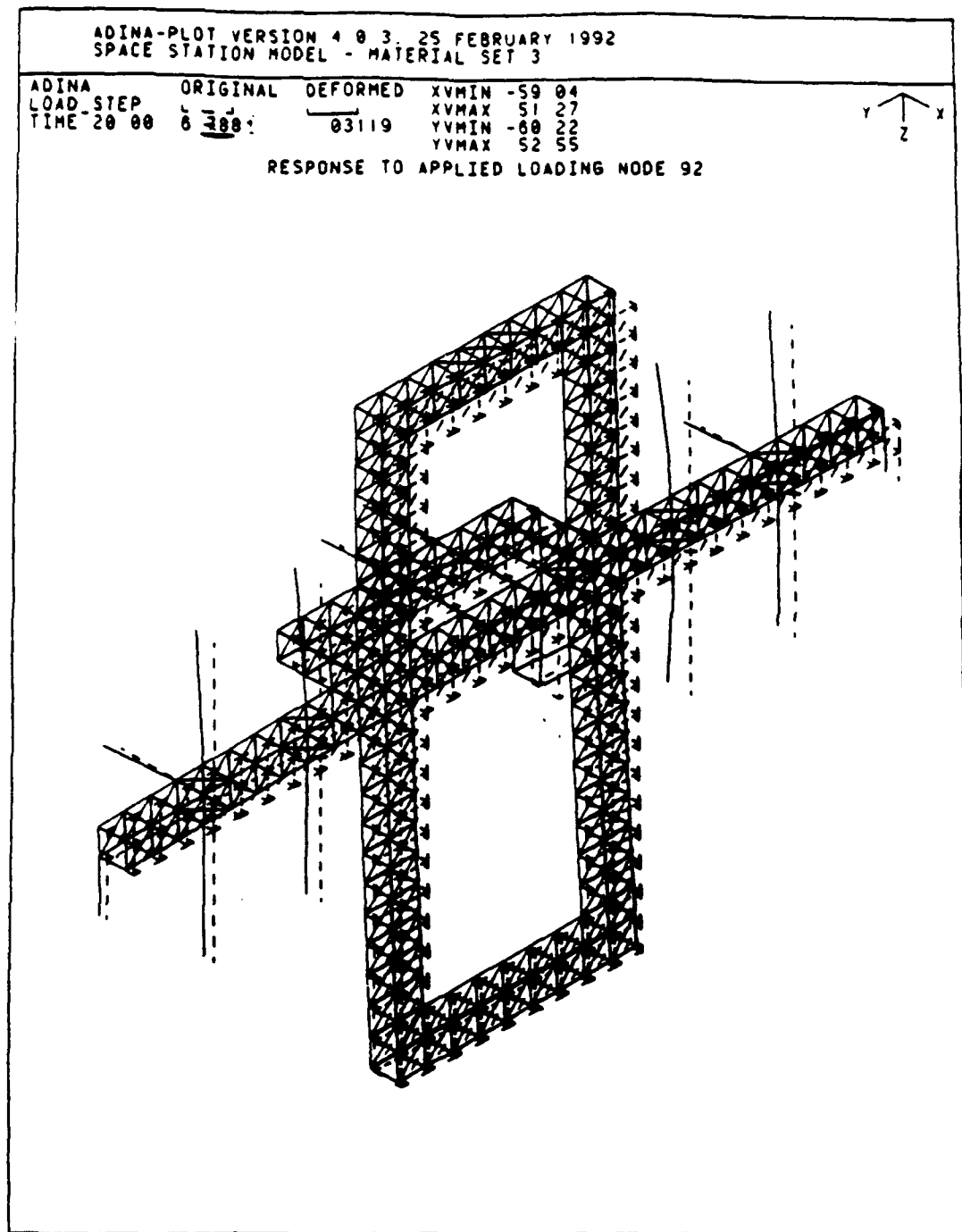


Figure 31 Global Structural Response E=78% at t = 20 sec

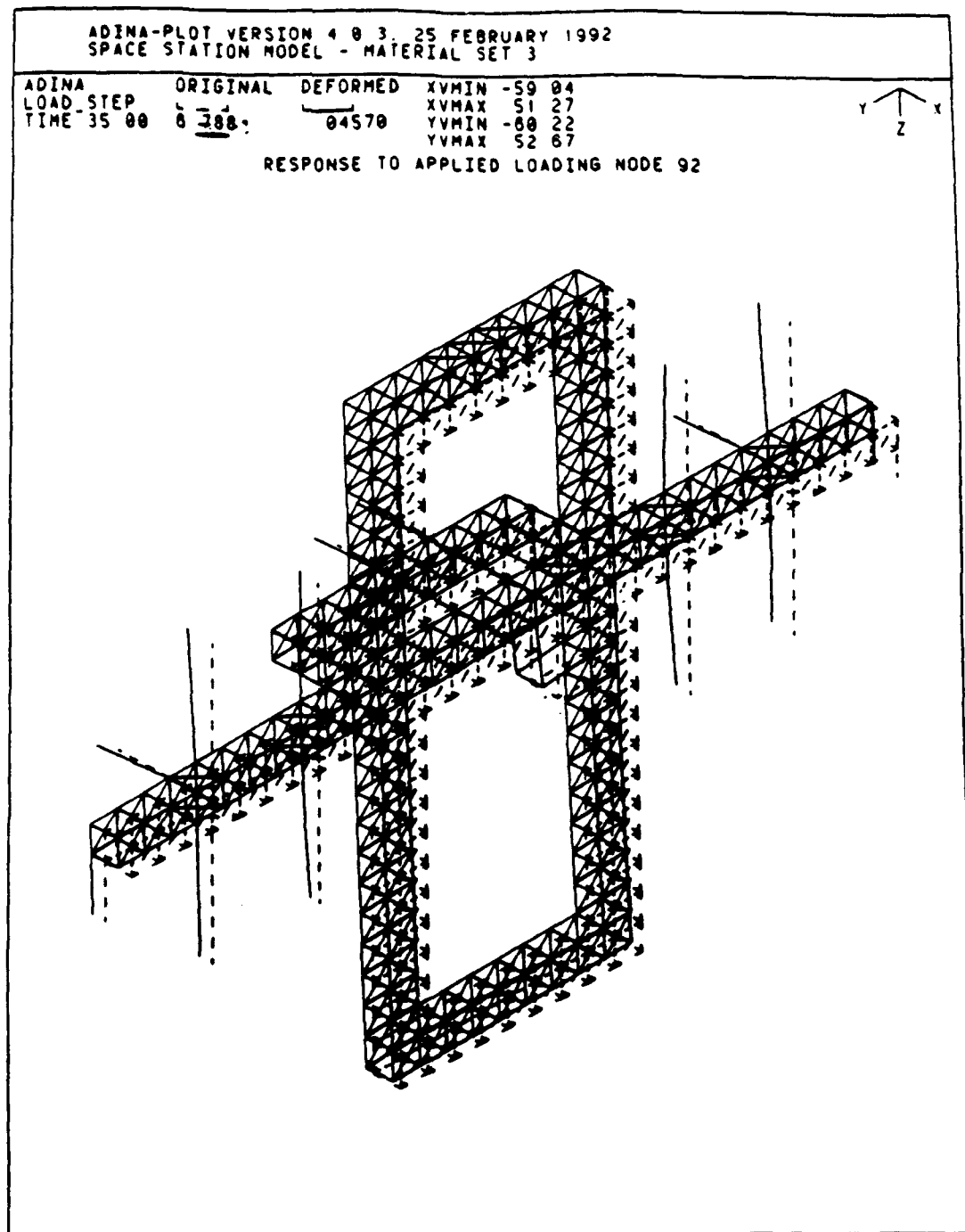


Figure 32 Global Structural Response E=78% at t = 35 sec

ADINA-PLOT VERSION 4.0.3, 24 FEBRUARY 1992
SPACE STATION MODEL - MATERIAL SET 3

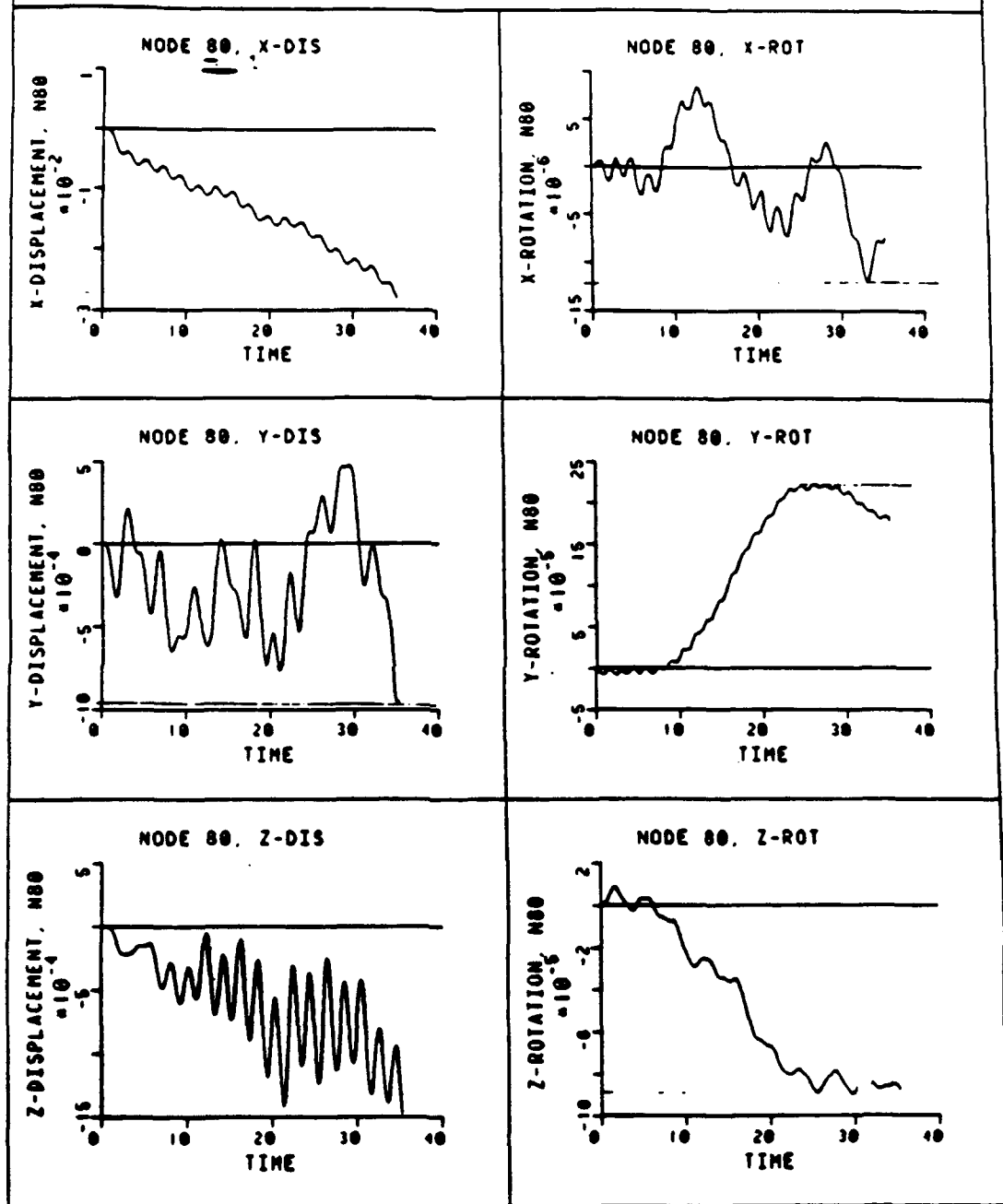


Figure 33 Node 80 Response E=78% X,Y,Z Displ./Rot.

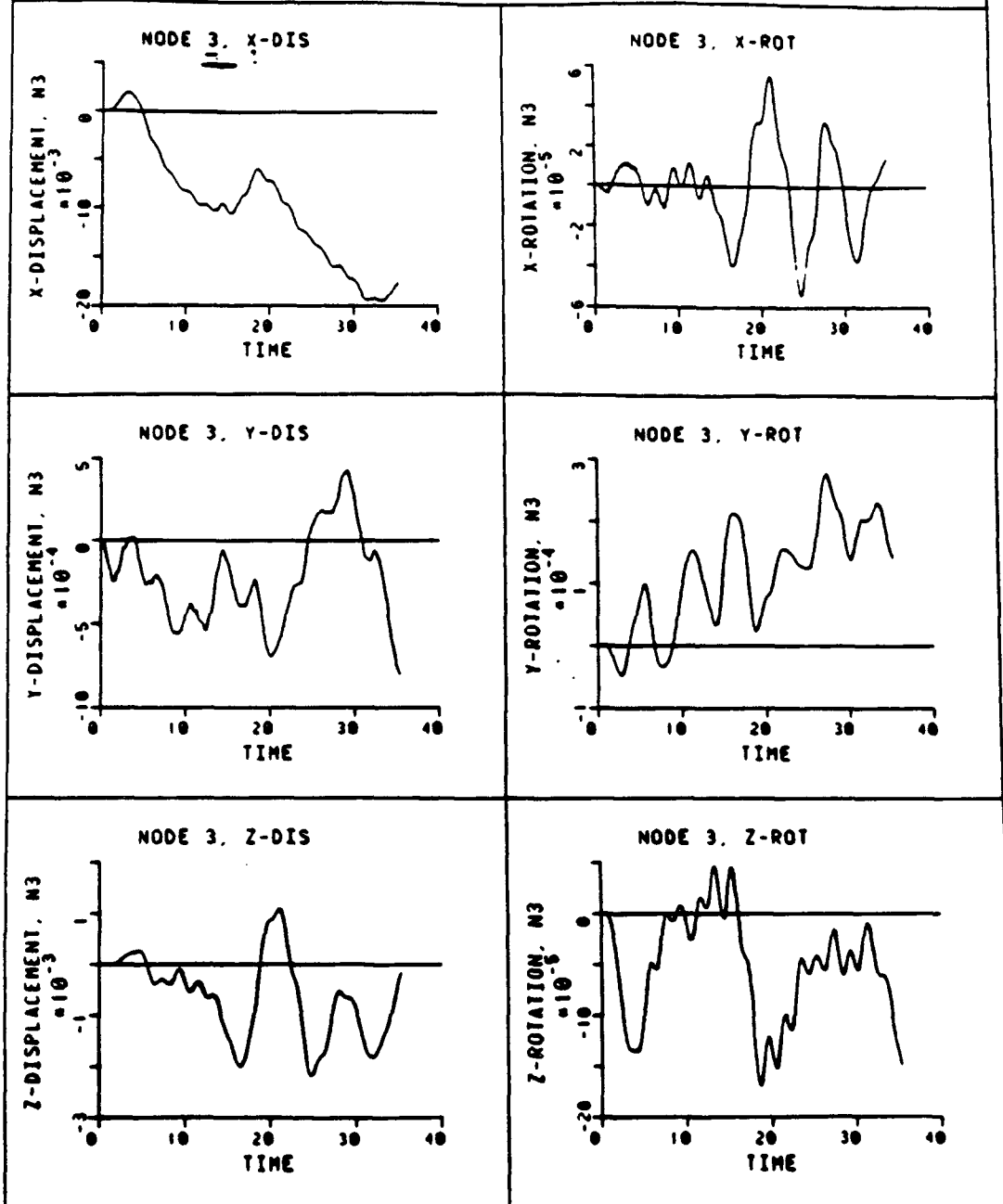


Figure 34 Node 3 Response E=78% X,Y,Z Displ./Rot.

ADINA-PLOT VERSION 4.0 3. 24 FEBRUARY 1992
SPACE STATION MODEL - MATERIAL SET 3

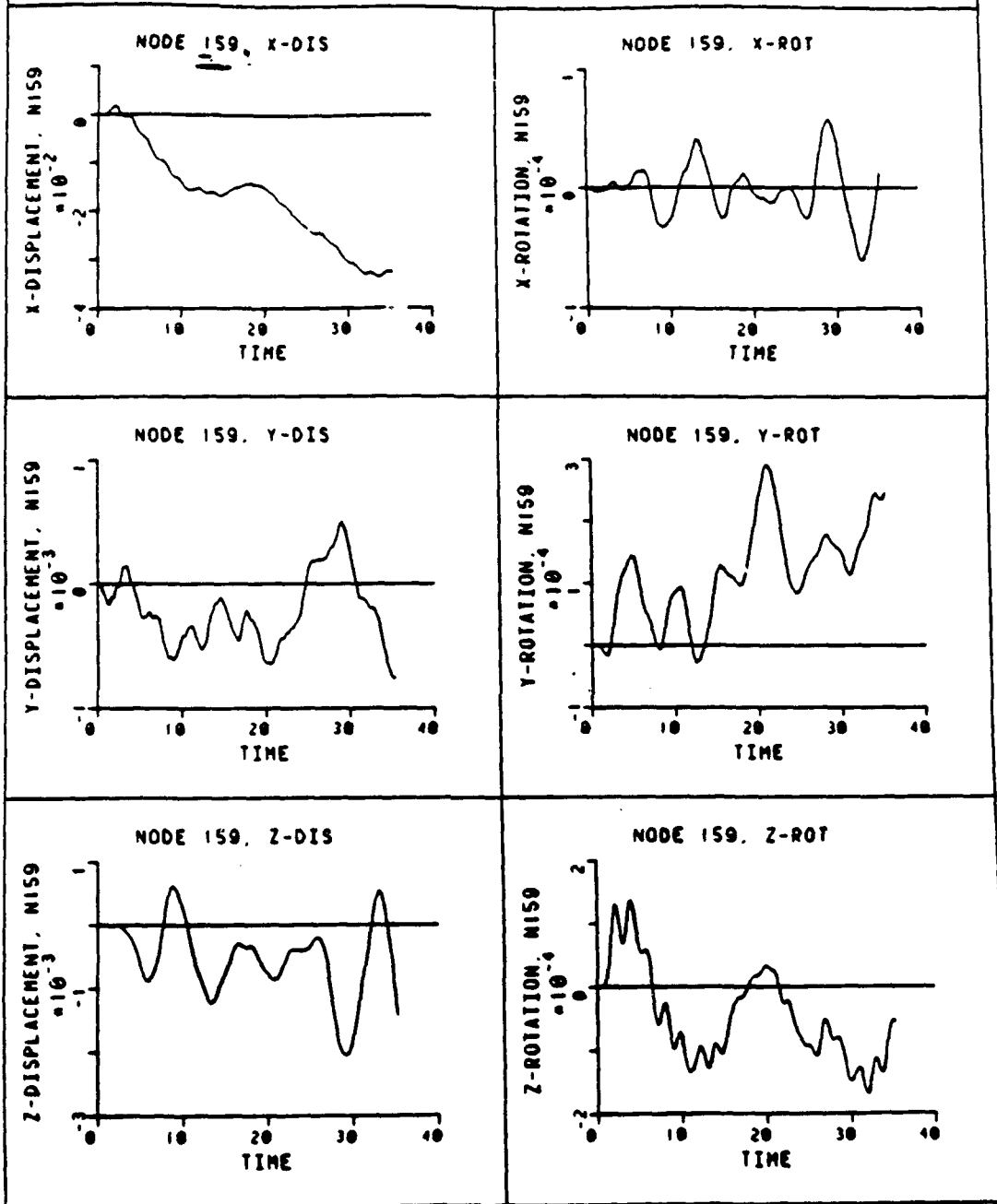


Figure 35 Node 159 Response E=78% X,Y,Z Displ./Rot.

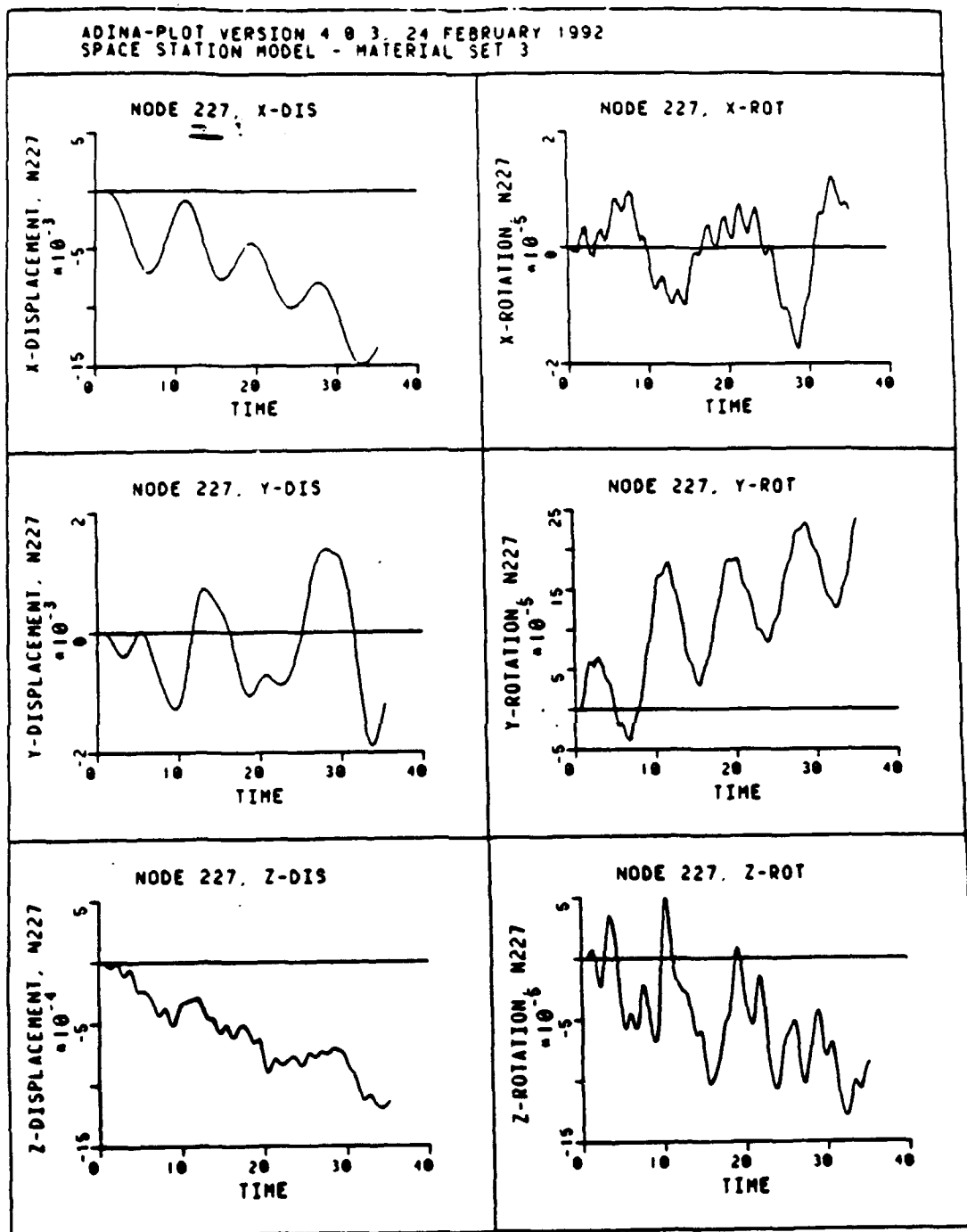


Figure 36 Node 227 Response E=78% X,Y,Z Displ./Rot.

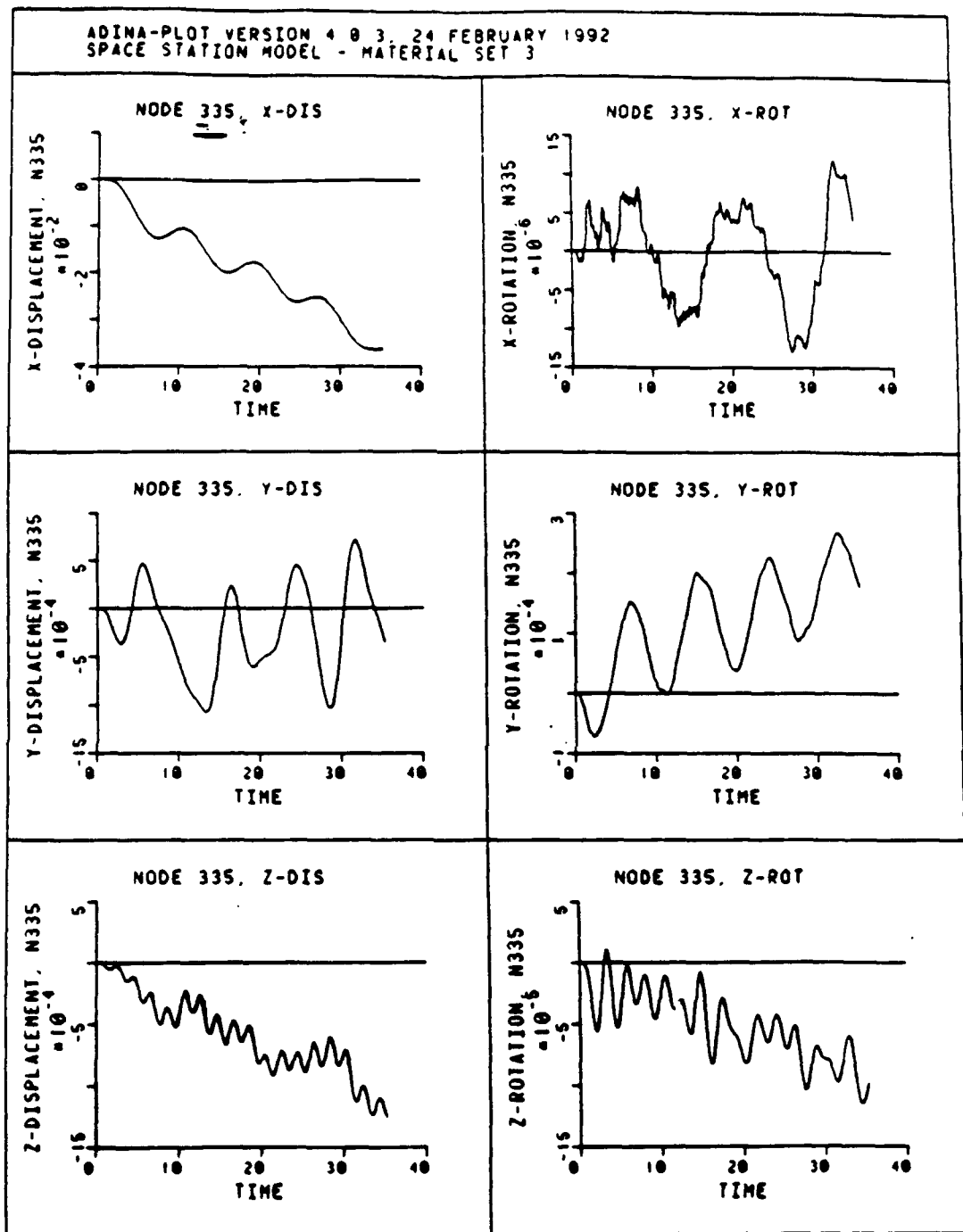


Figure 37 Node 335 Response E=78% X,Y,Z Displ./Rot.

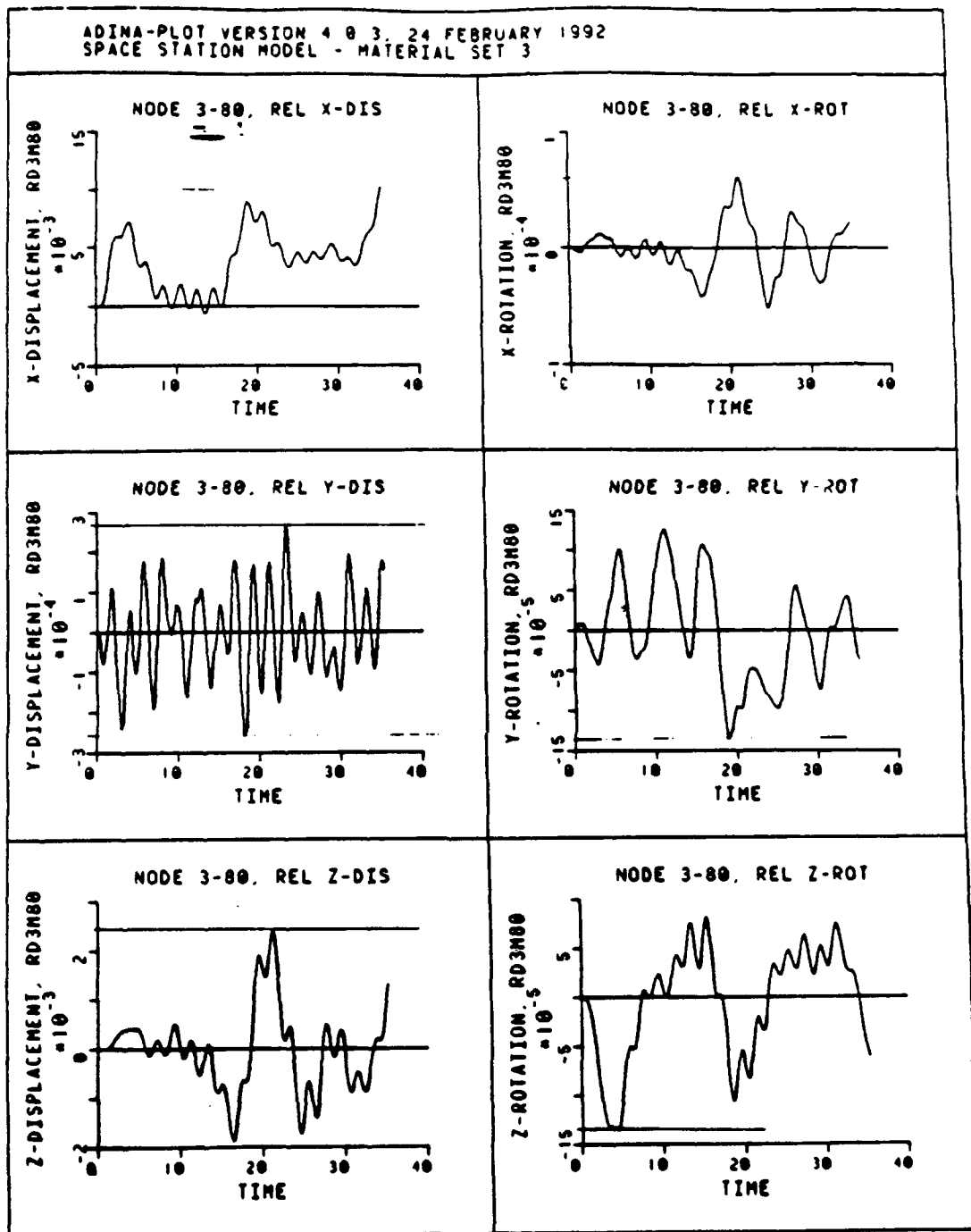


Figure 38 Node 3 vs. 80 Response E=78% X,Y,Z Displ./Rot.

ADINA-PLOT VERSION 4.0.3, 24 FEBRUARY 1992
SPACE STATION MODEL - MATERIAL SET 3

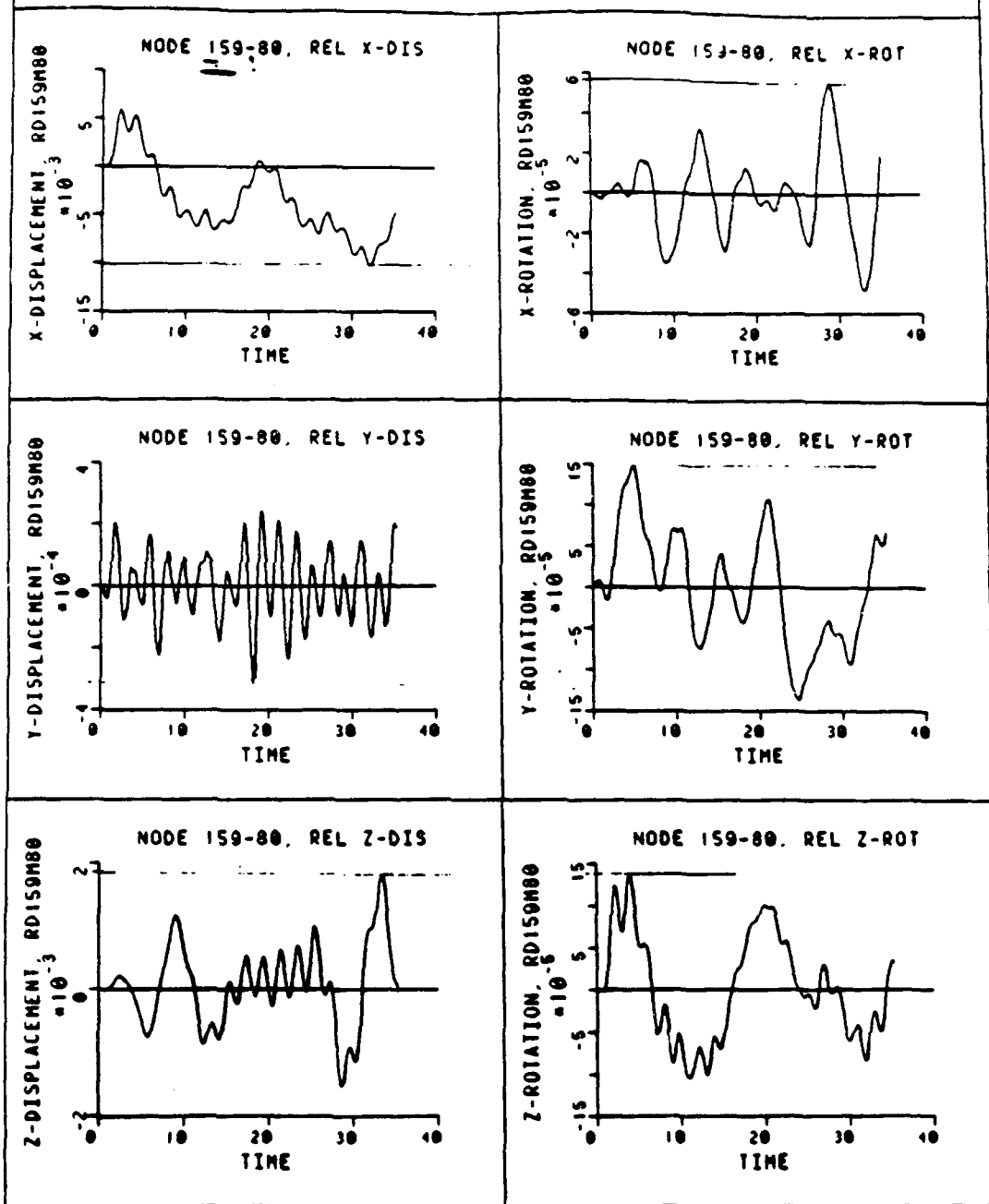


Figure 39 Node 159 vs. 80 Response E=78% X,Y,Z Displ./Rot.

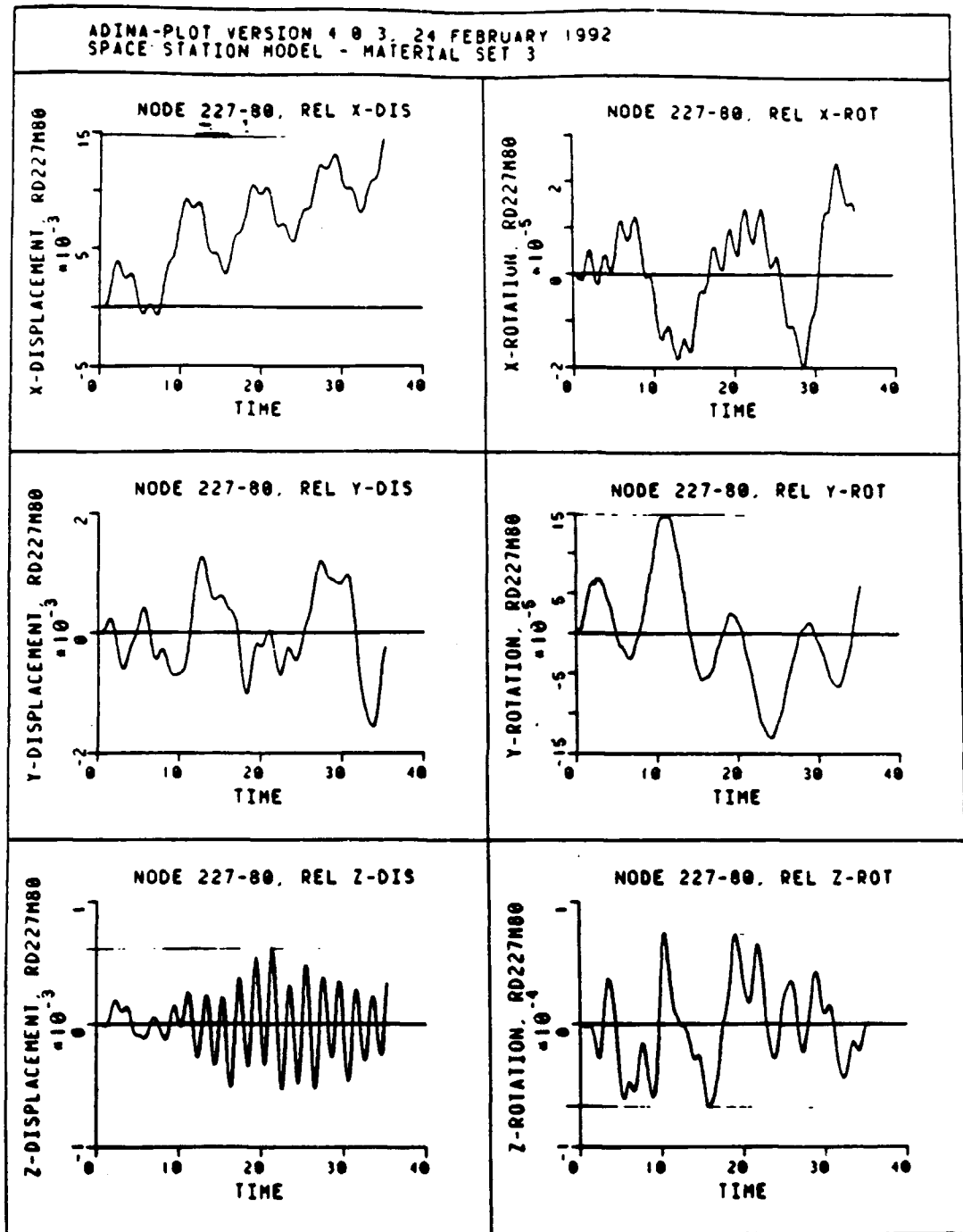


Figure 40 Node 227 vs. 80 Response E=78% X,Y,Z Displ./Rot.

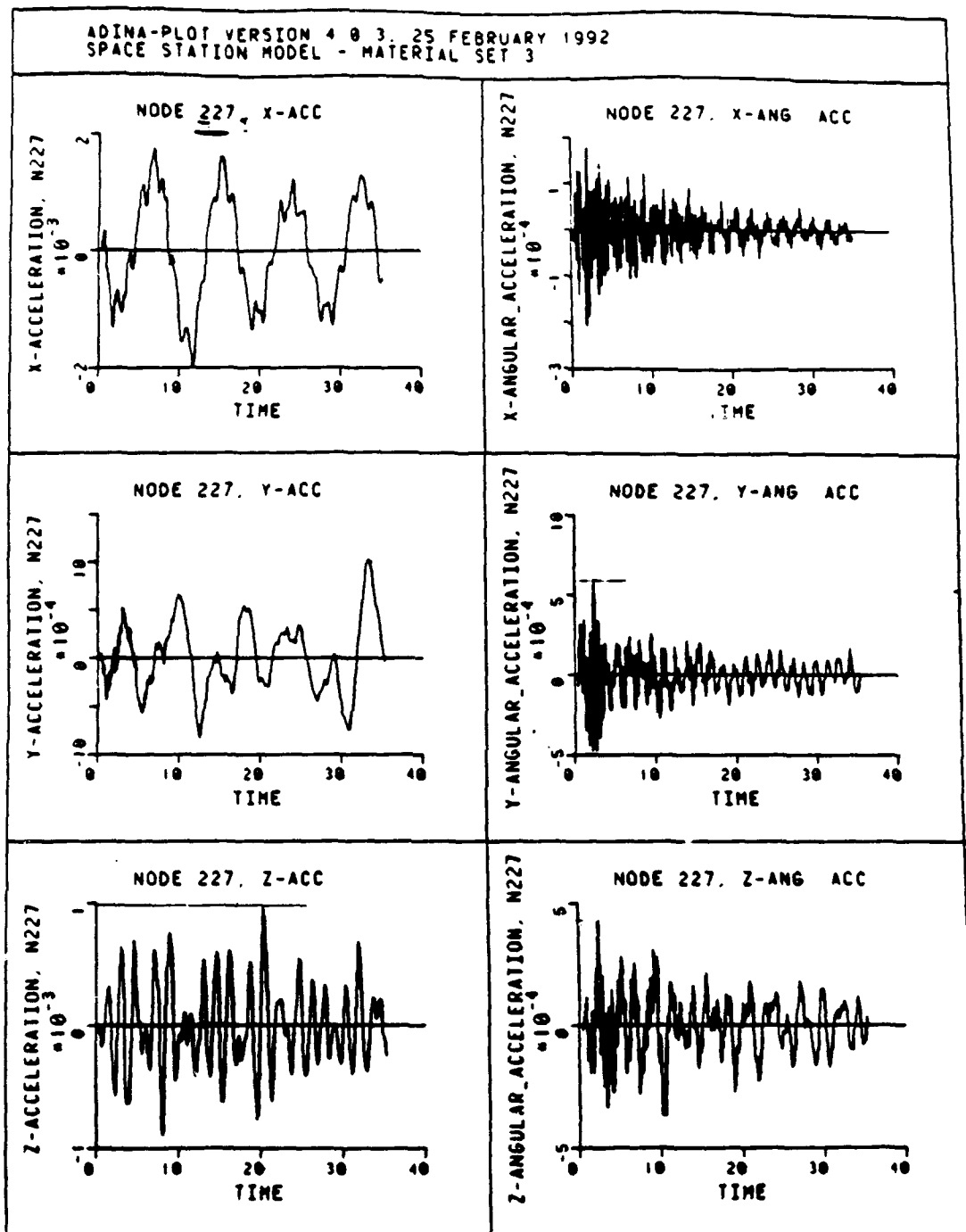


Figure 41 Node 227 Response E=78% X,Y,Z Lin./Rot. Accel.

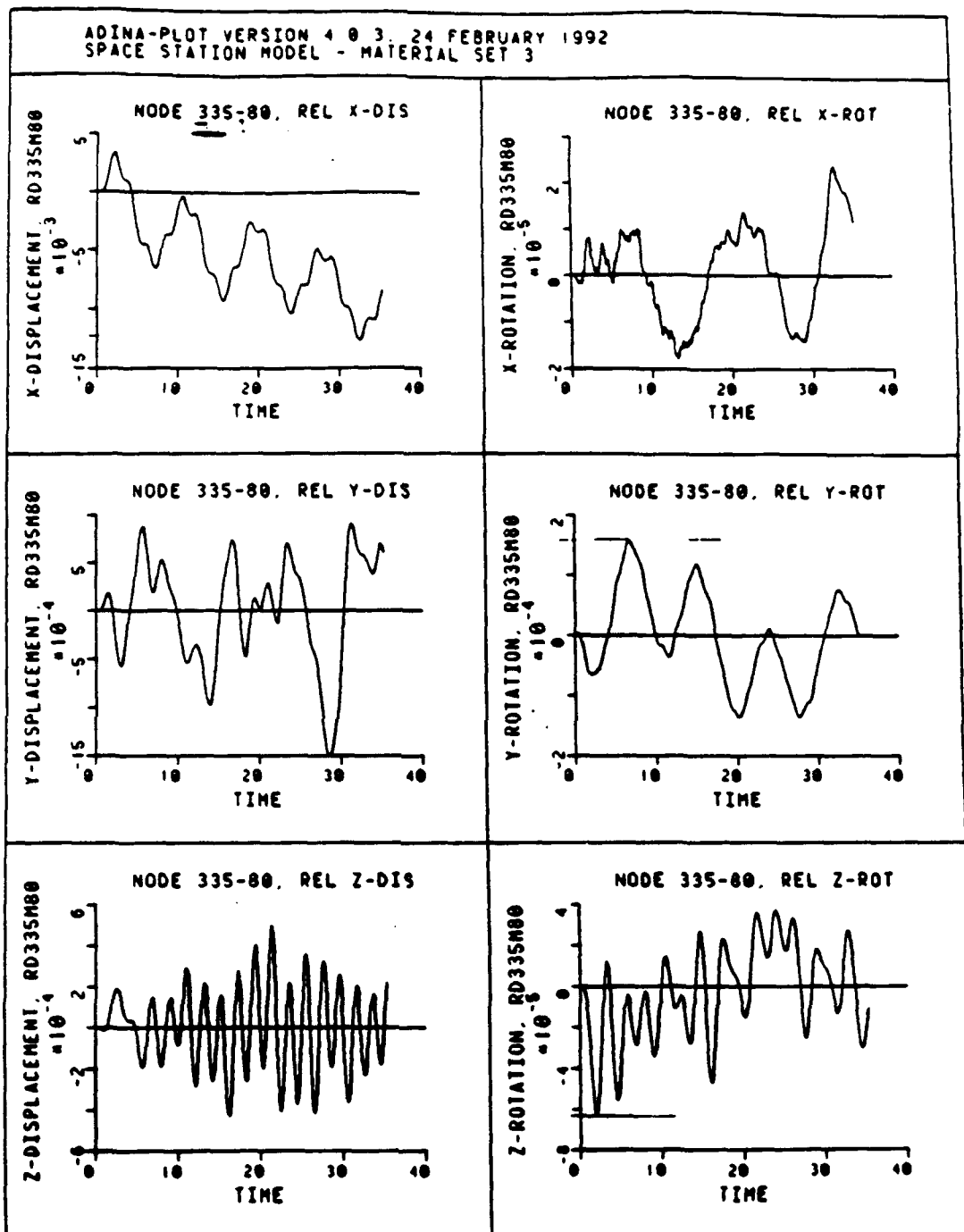


Figure 42 Node 335 vs. 80 Response E=78% X,Y,Z Displ./Rot.

ADINA-PLOT VERSION 4.0.3, 25 FEBRUARY 1992
SPACE STATION MODEL - MATERIAL SET 3

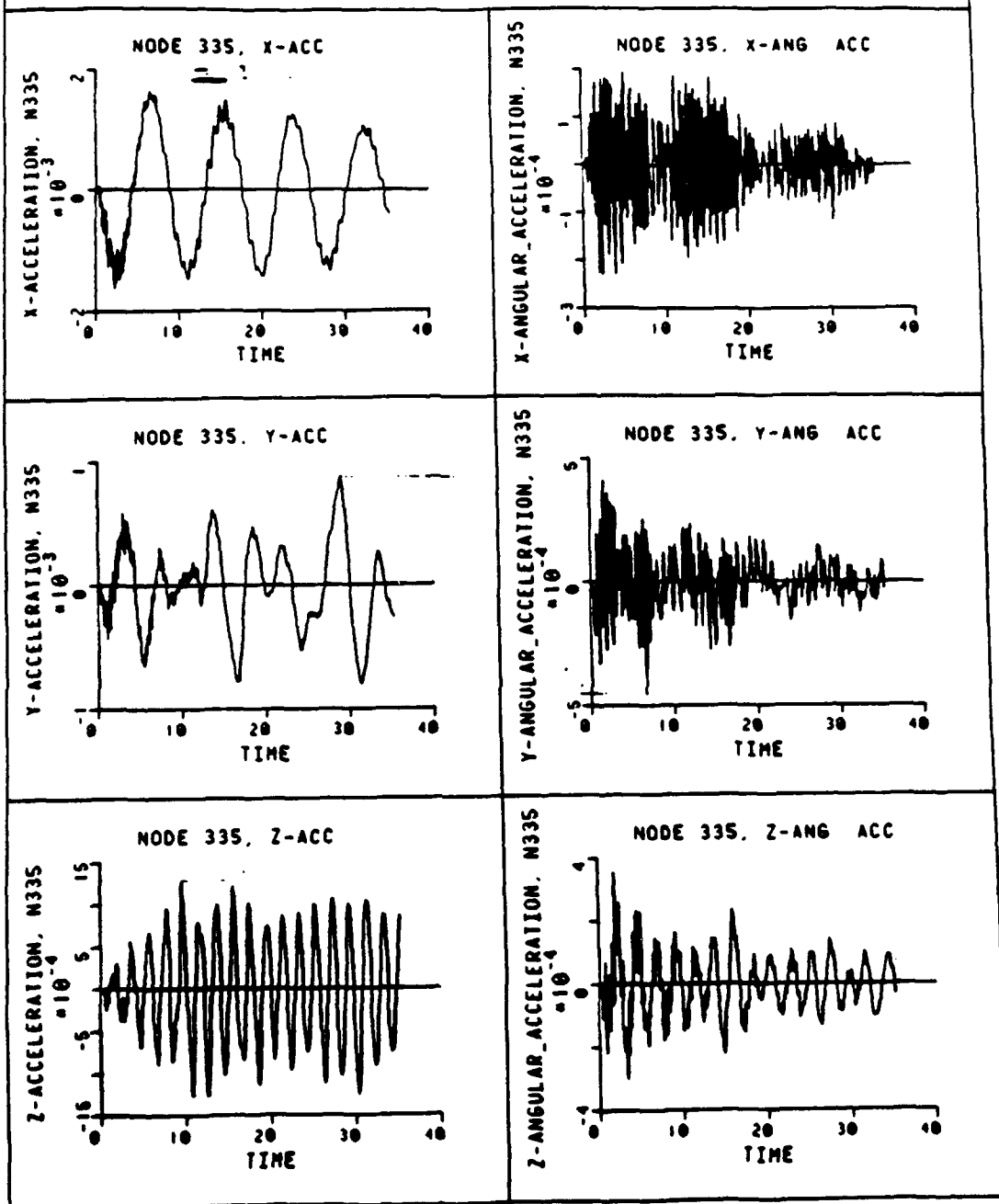


Figure 43 Node 335 Response E=78% X,Y,Z Lin./Rot. Accel.

ADINA-PLOT VERSION 4.0 3. 24 FEBRUARY 1992
SPACE STATION MODEL - MATERIAL SET 3

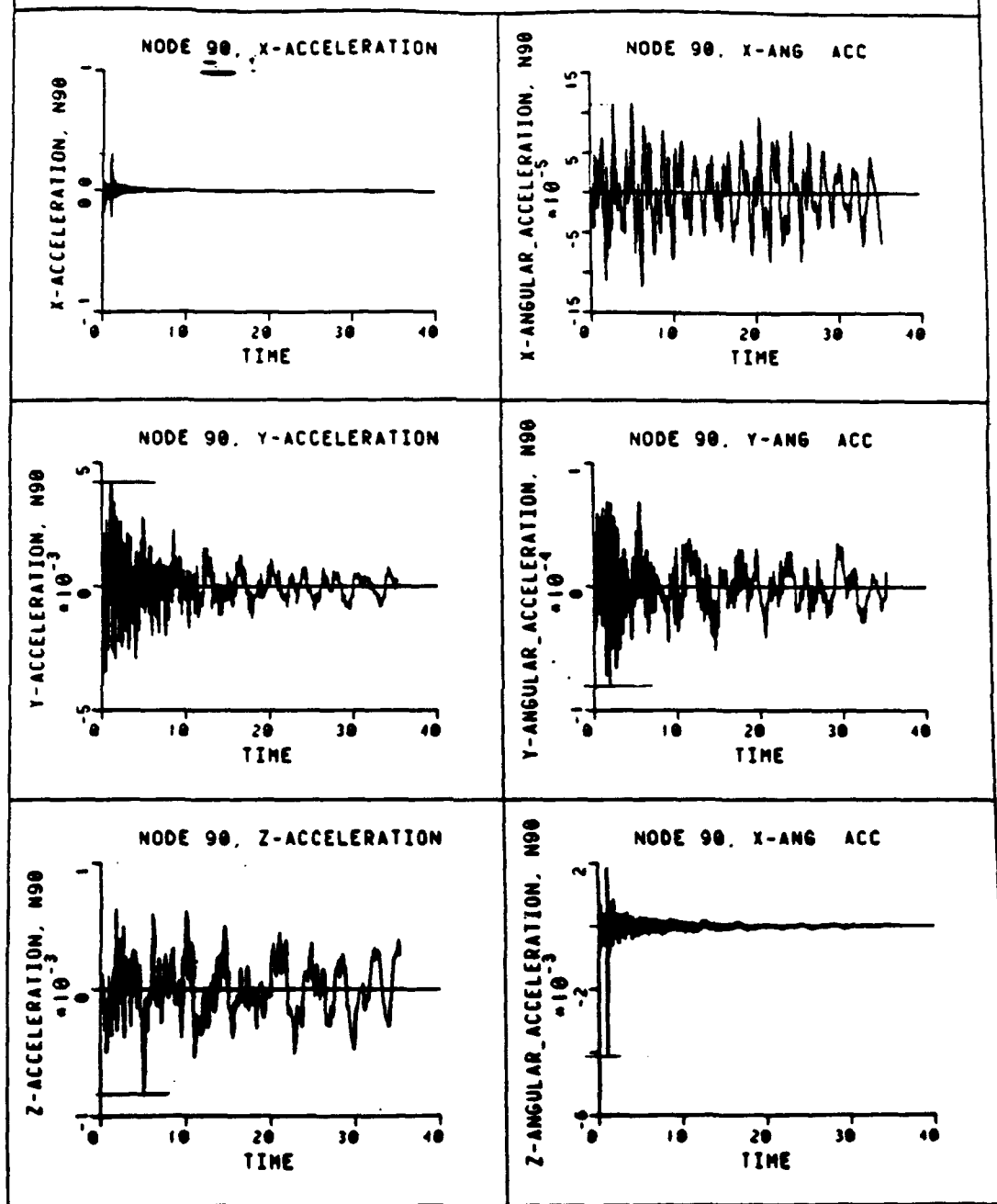


Figure 44 Node 90 Response E=78% X,Y,Z Lin./Rot. Accel.

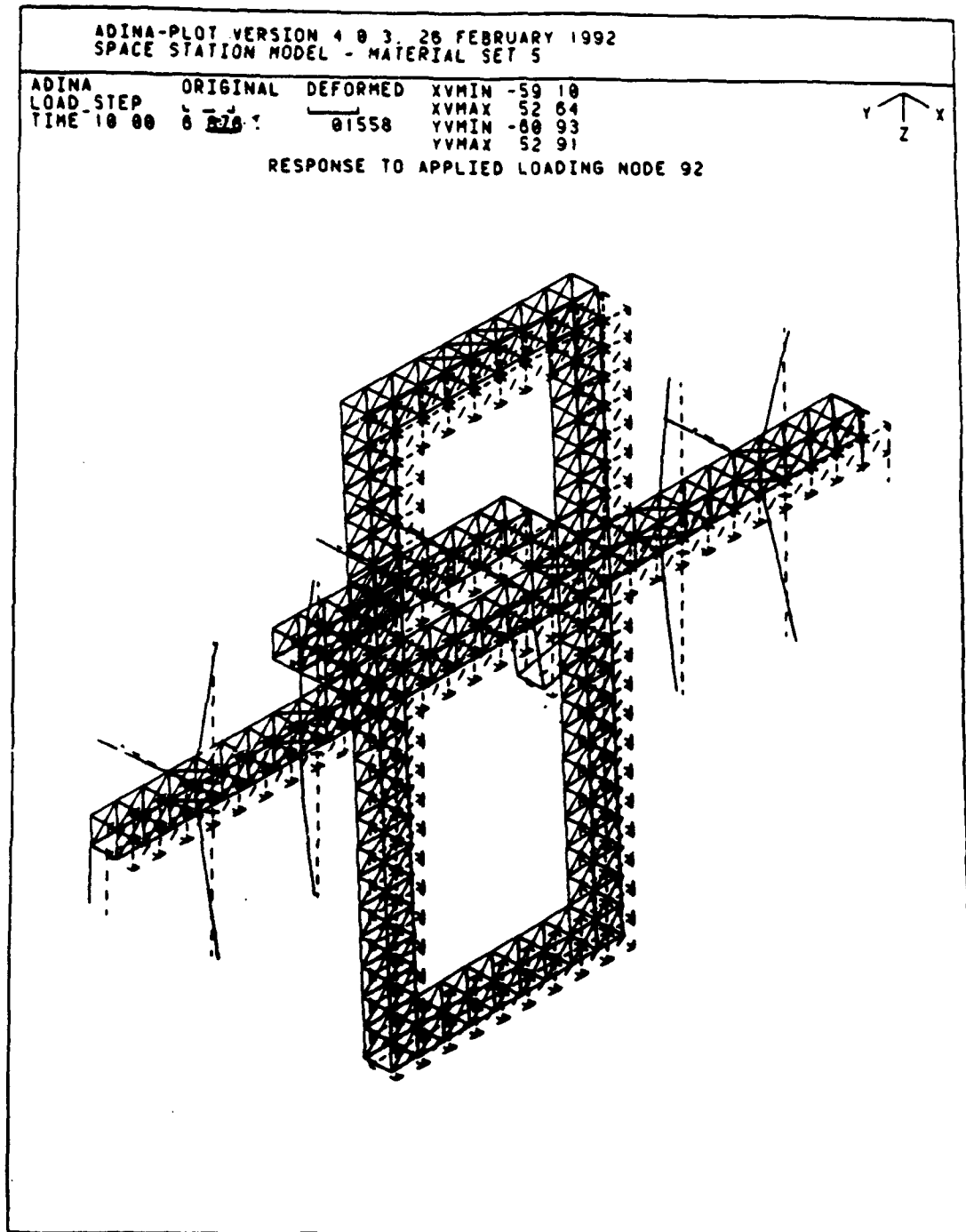


Figure 45 Global Structural Response E=56% at $t = 10$ sec

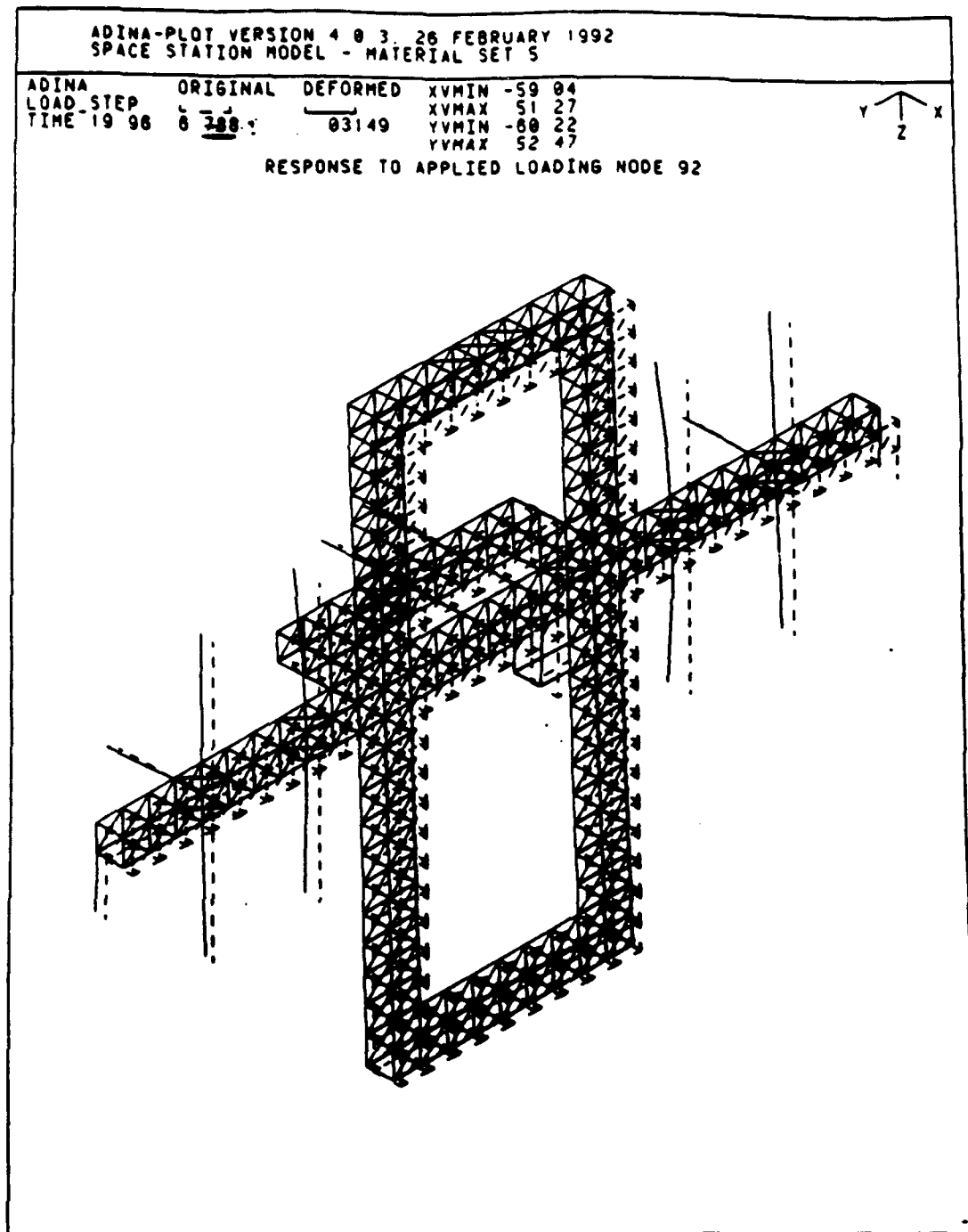


Figure 46 Global Structural Response E=56% at t = 20 sec

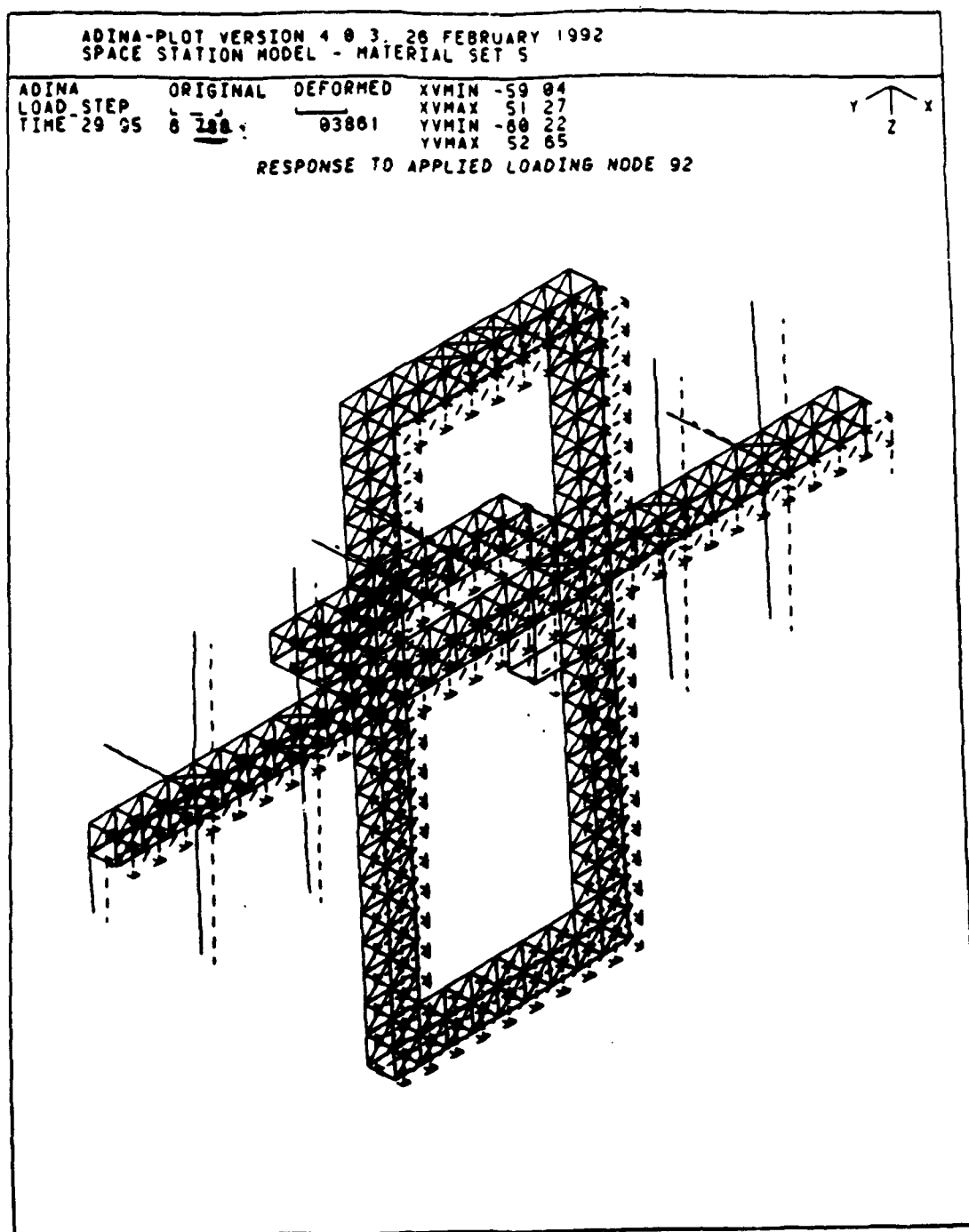


Figure 47 Global Structural Response E=56% at t = 30 sec

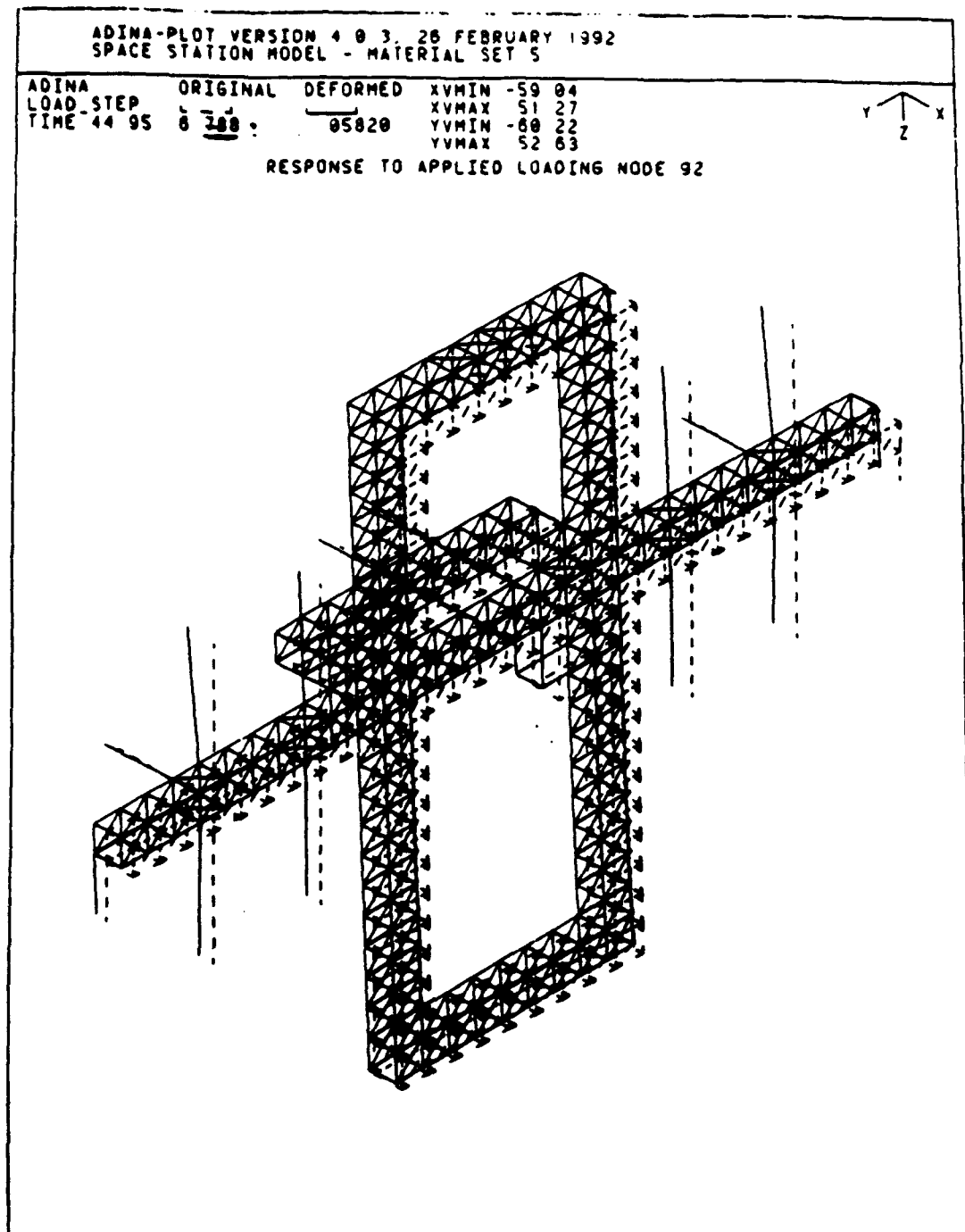


Figure 48 Global Structural Response $E=56\%$ at $t = 45$ sec.

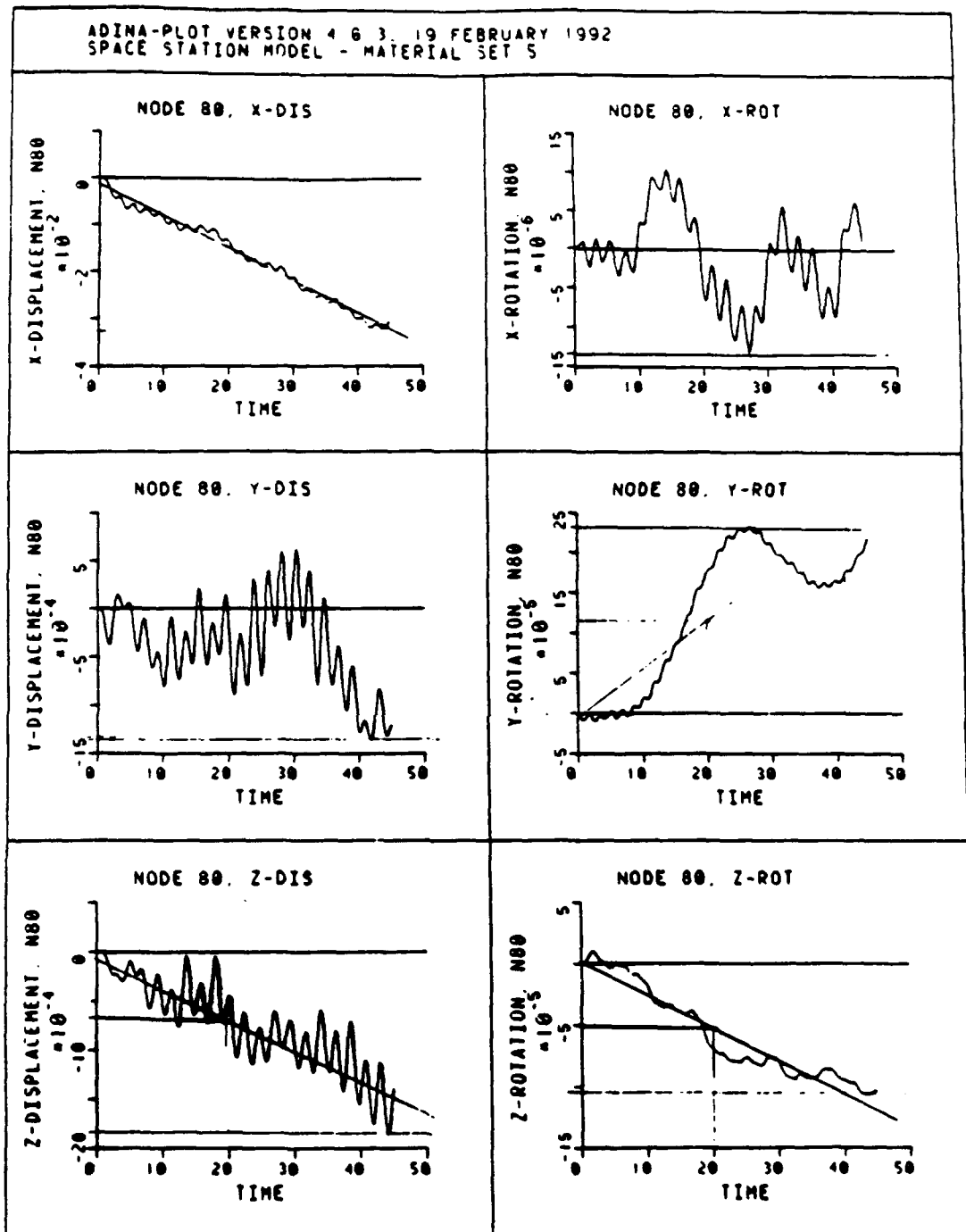


Figure 49 Node 80 Response E=56% X,Y,Z Displ./Rot.

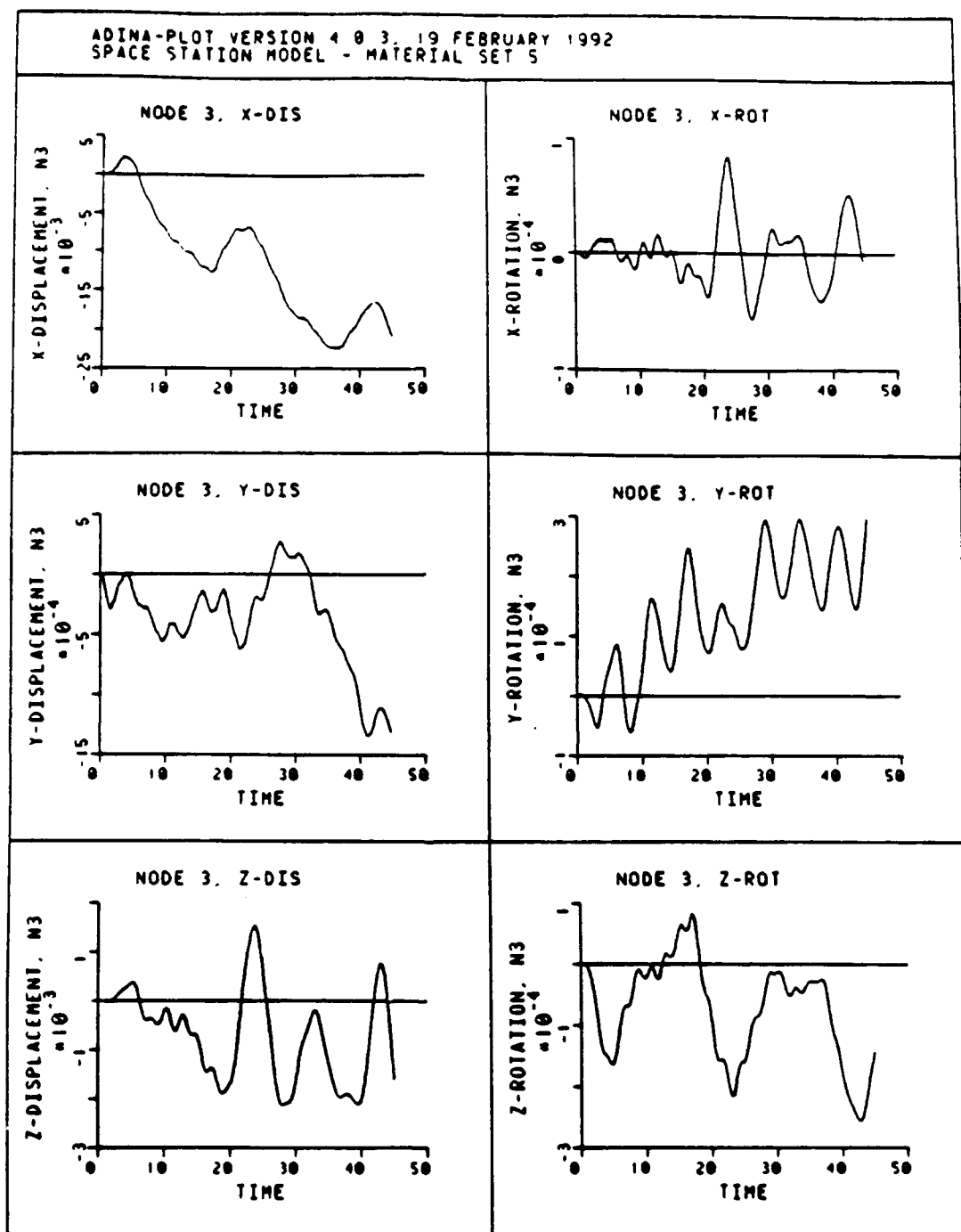


Figure 50 Node 3 Response E=56% X,Y,Z Displ./Rot.

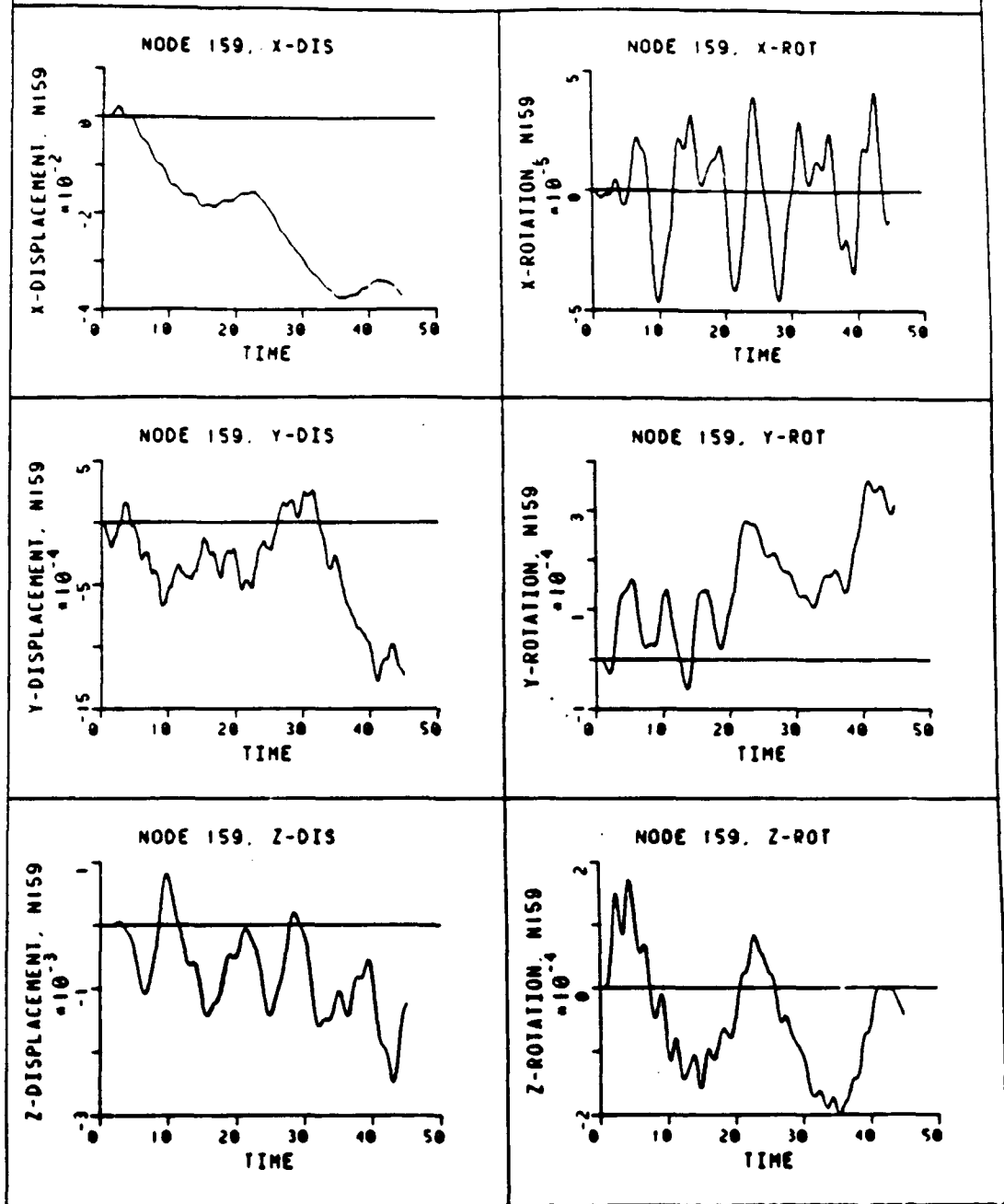


Figure 51 Node 159 Response E=56% X,Y,Z Displ./Rot.

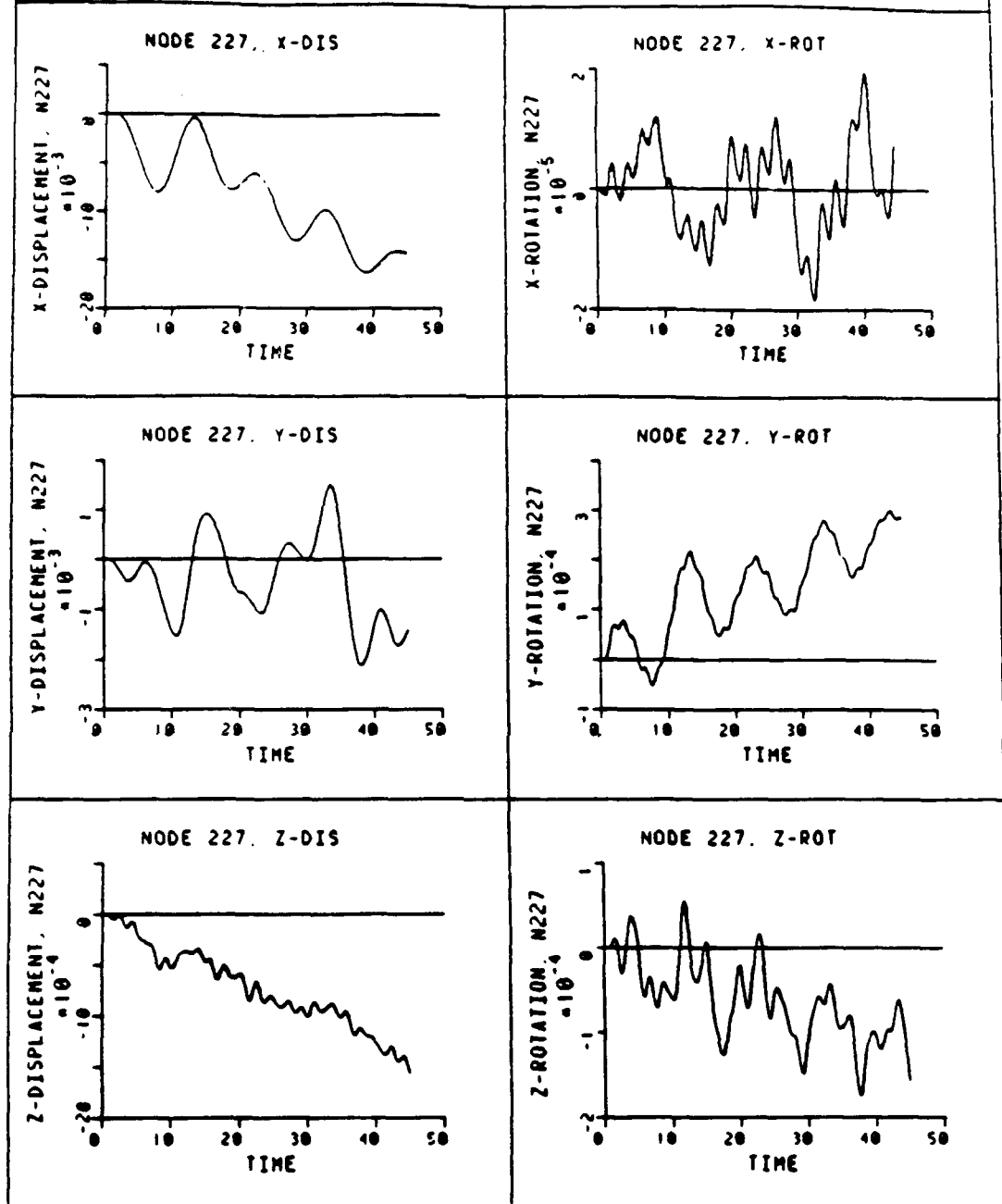


Figure 52 Node 227 Response E=56% X,Y,Z Displ./Rot.

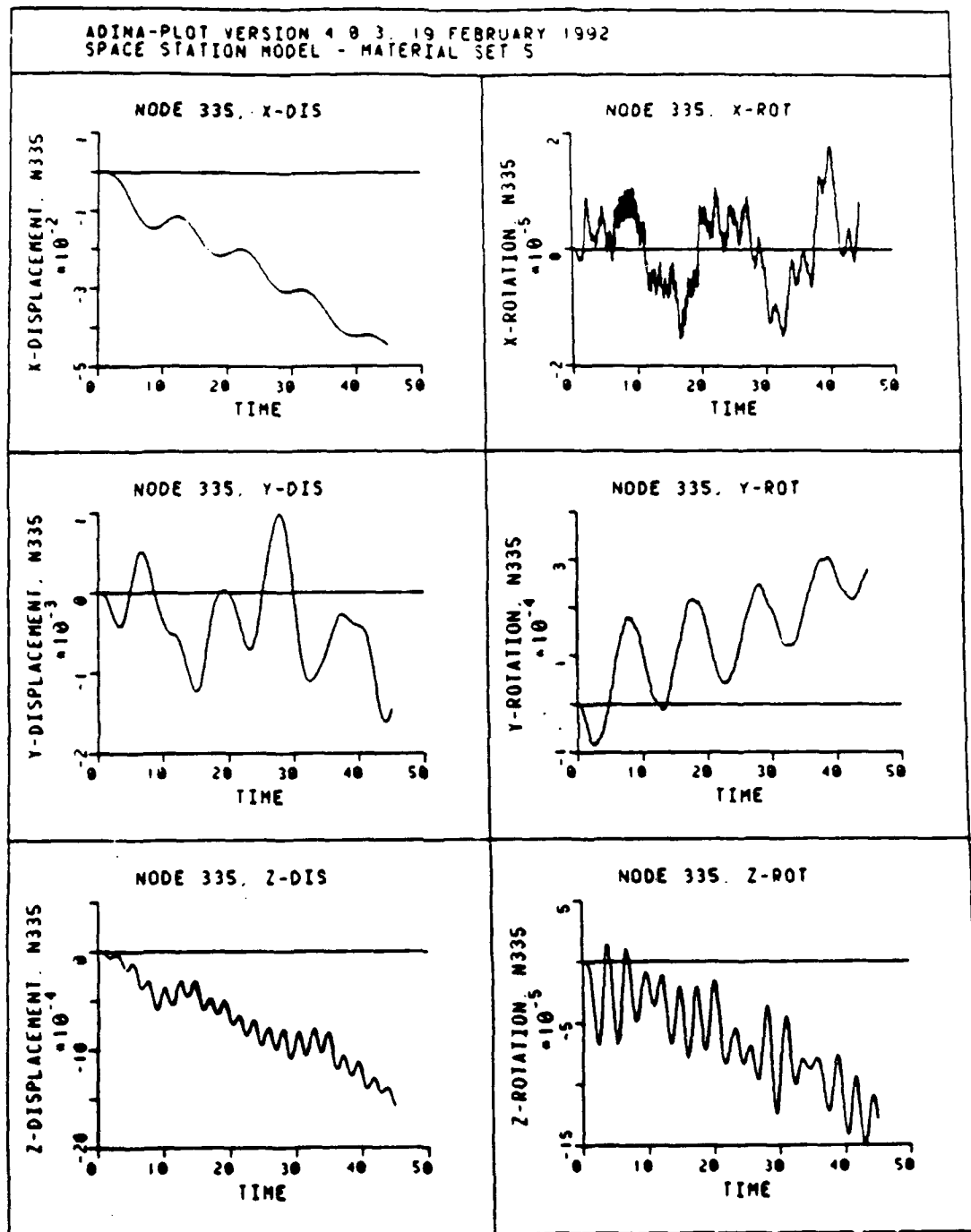


Figure 53 Node 335 Response E=56% X,Y,Z Displ./Rot.

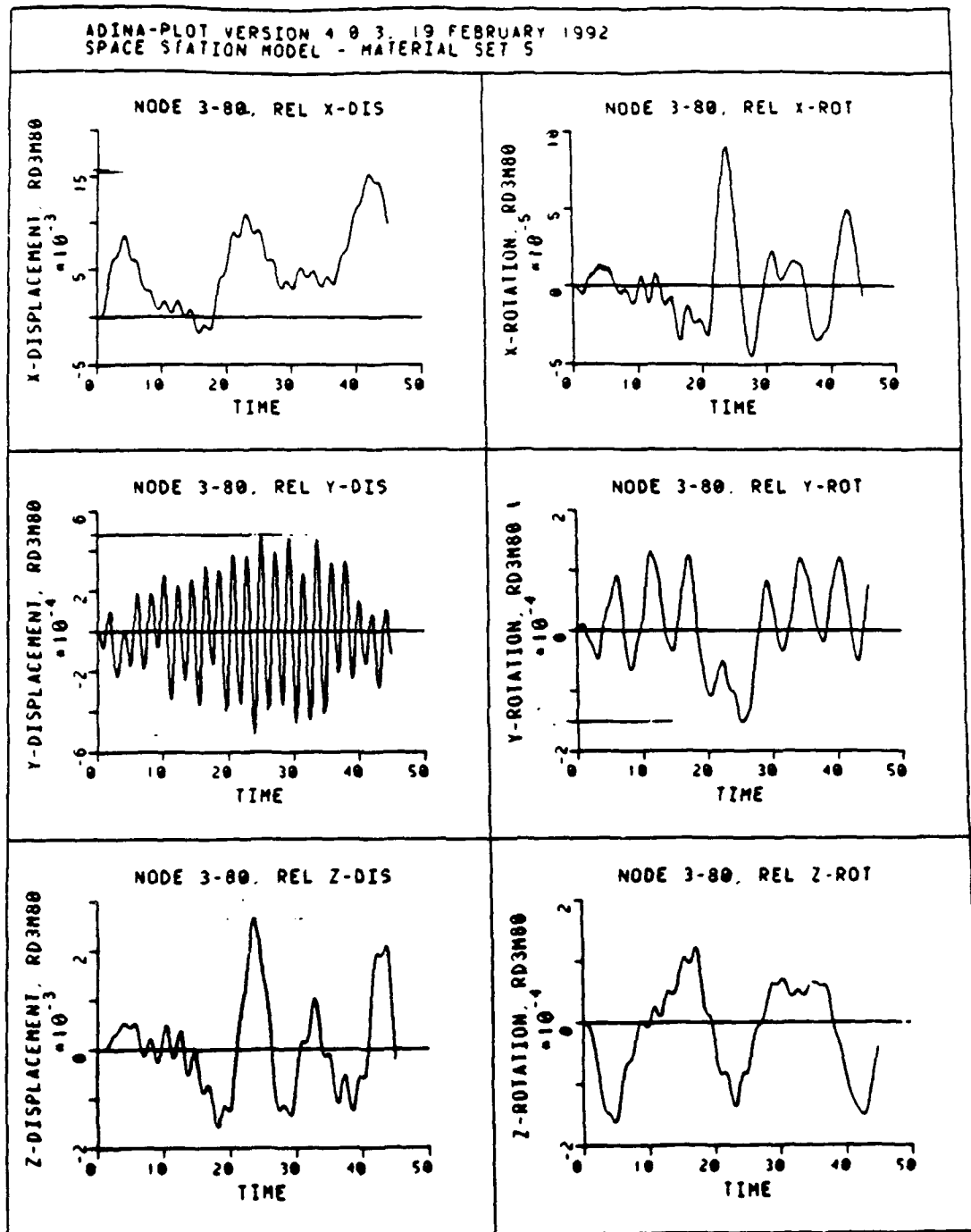


Figure 54 Node 3 vs. 80 Response E=56% X,Y,Z Displ./Rot.

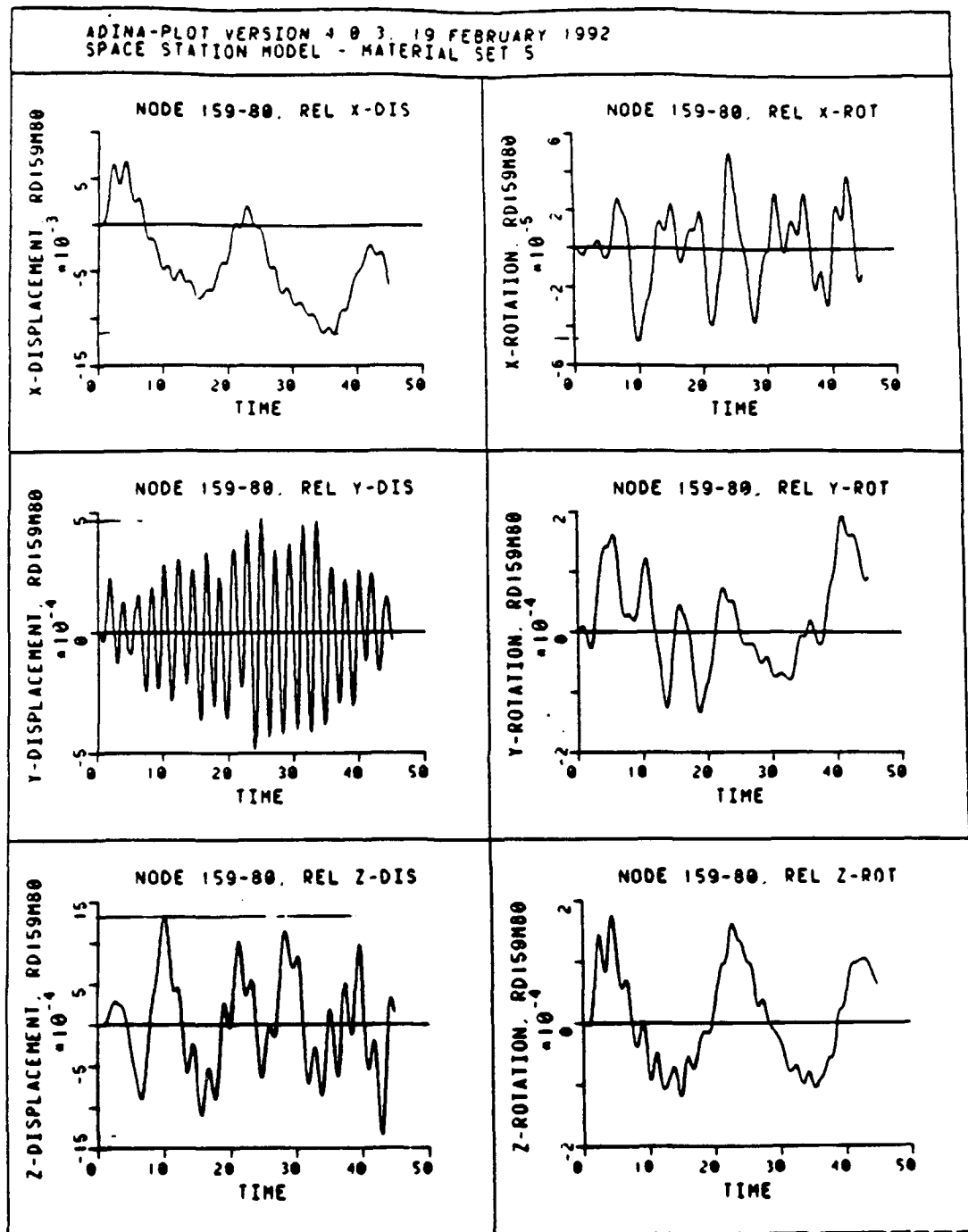


Figure 55 Node 159 vs. 80 Response E=56% X,Y,Z Displ./Rot.

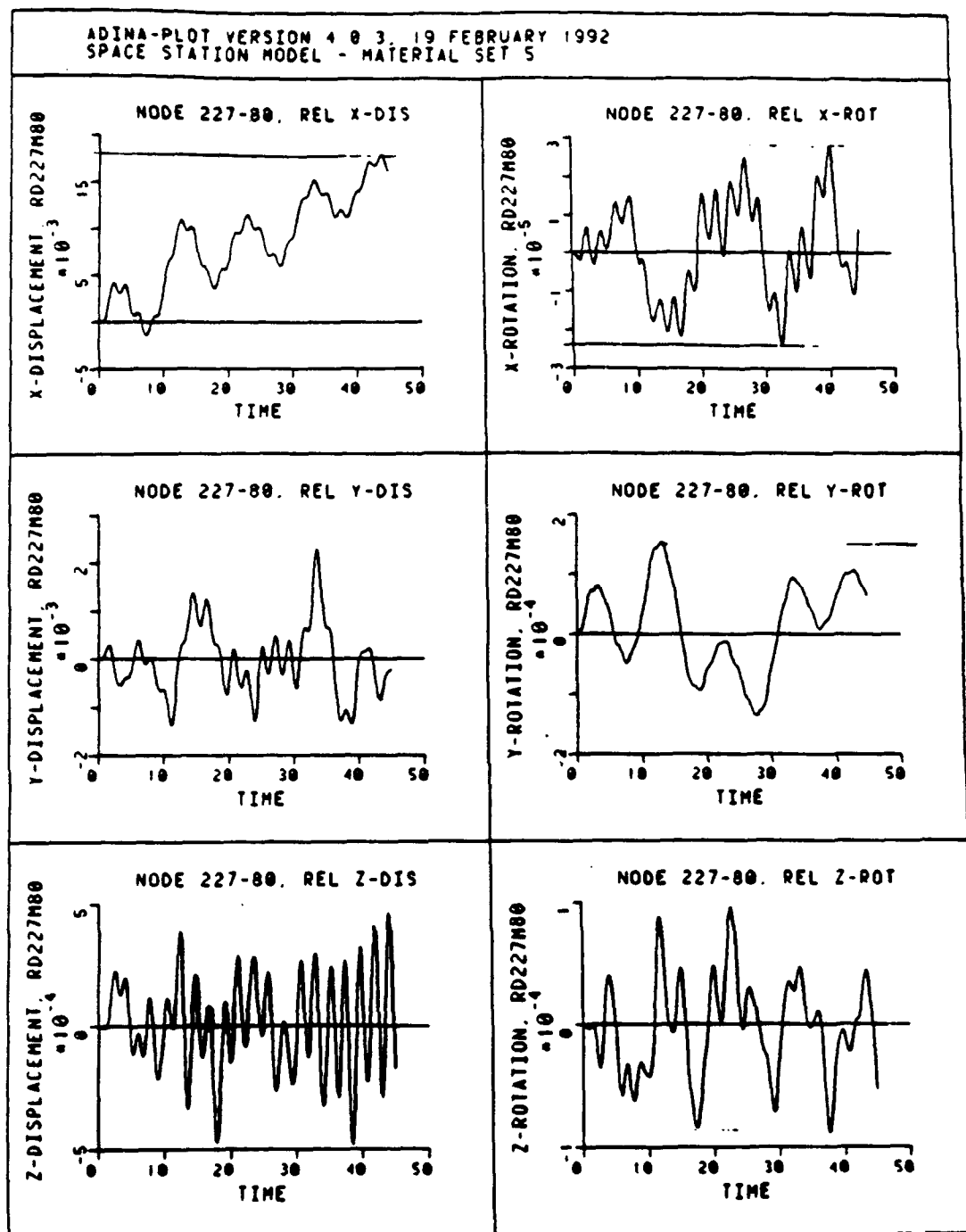


Figure 56 Node 227 vs. 80 Response E=56% X,Y,Z Displ./Rot.

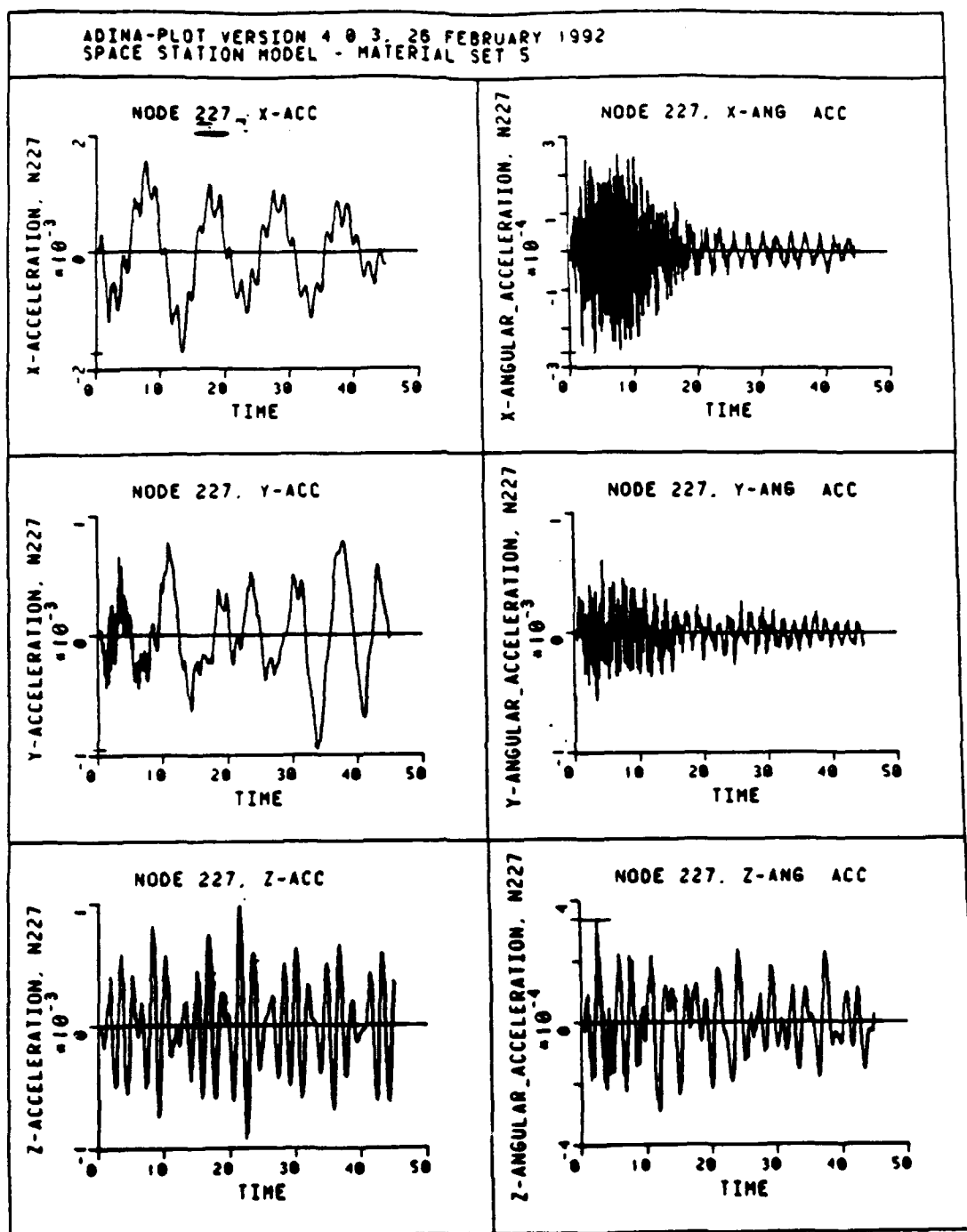


Figure 57 Node 227 Response E=56% X,Y,Z Lin./Rot. Accel.

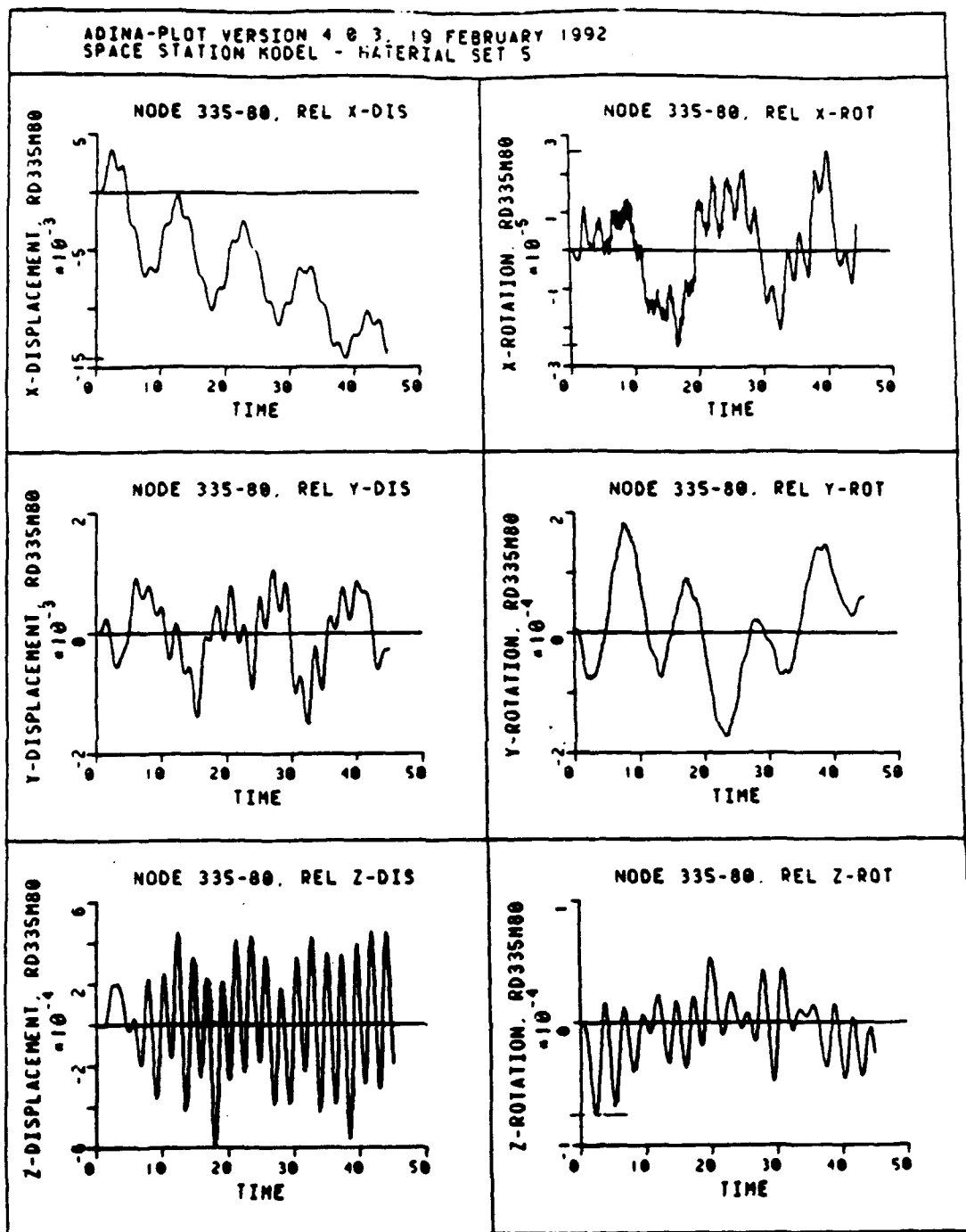


Figure 58 Node 335 vs. 80 Response E=56% X,Y,Z Displ./Rot.

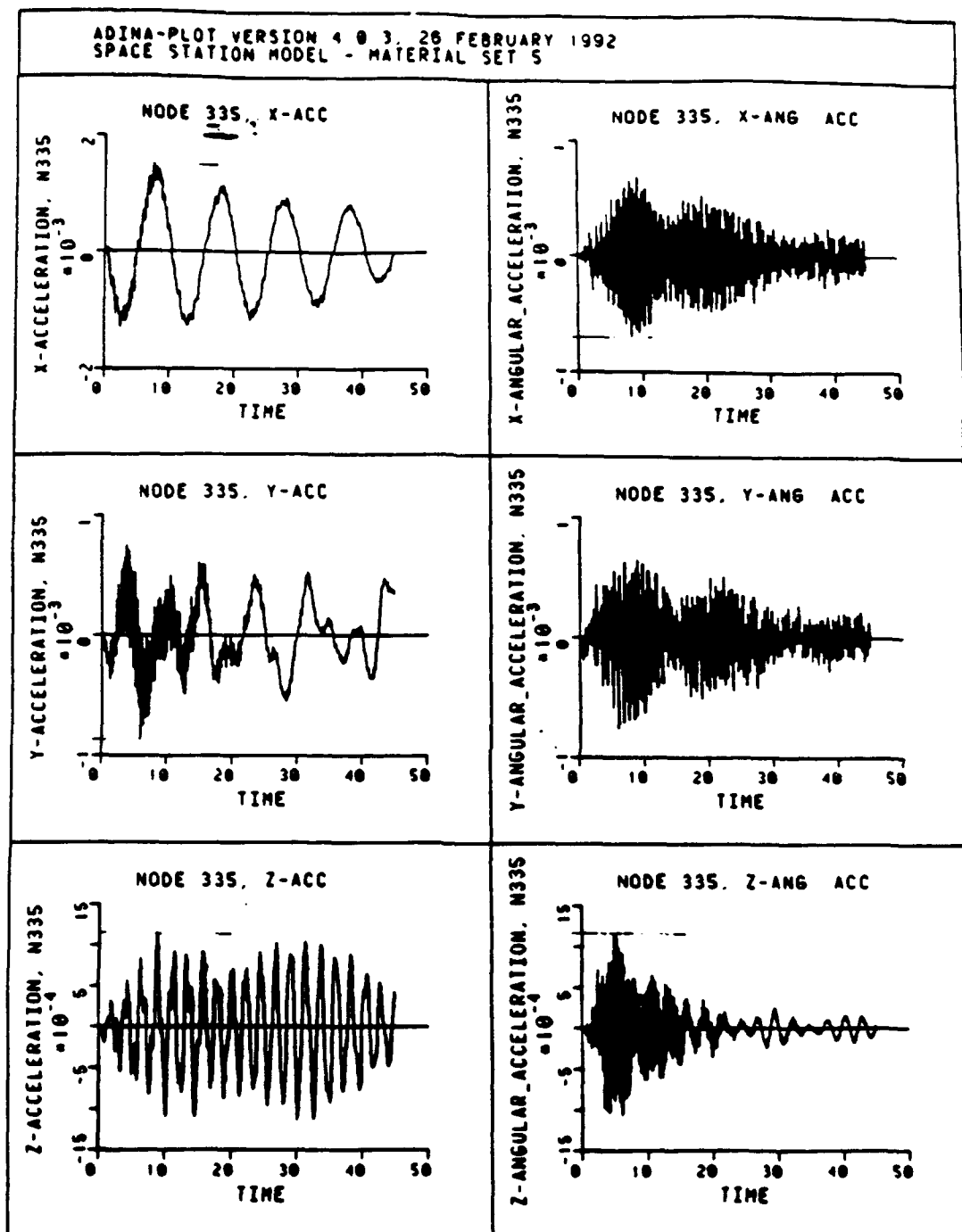


Figure 59 Node 335 Response E=56% X,Y,Z Lin./Rot. Accel.

ADINA-PLOT VERSION 4.0.3, 19 FEBRUARY 1992
SPACE STATION MODEL - MATERIAL SET 5

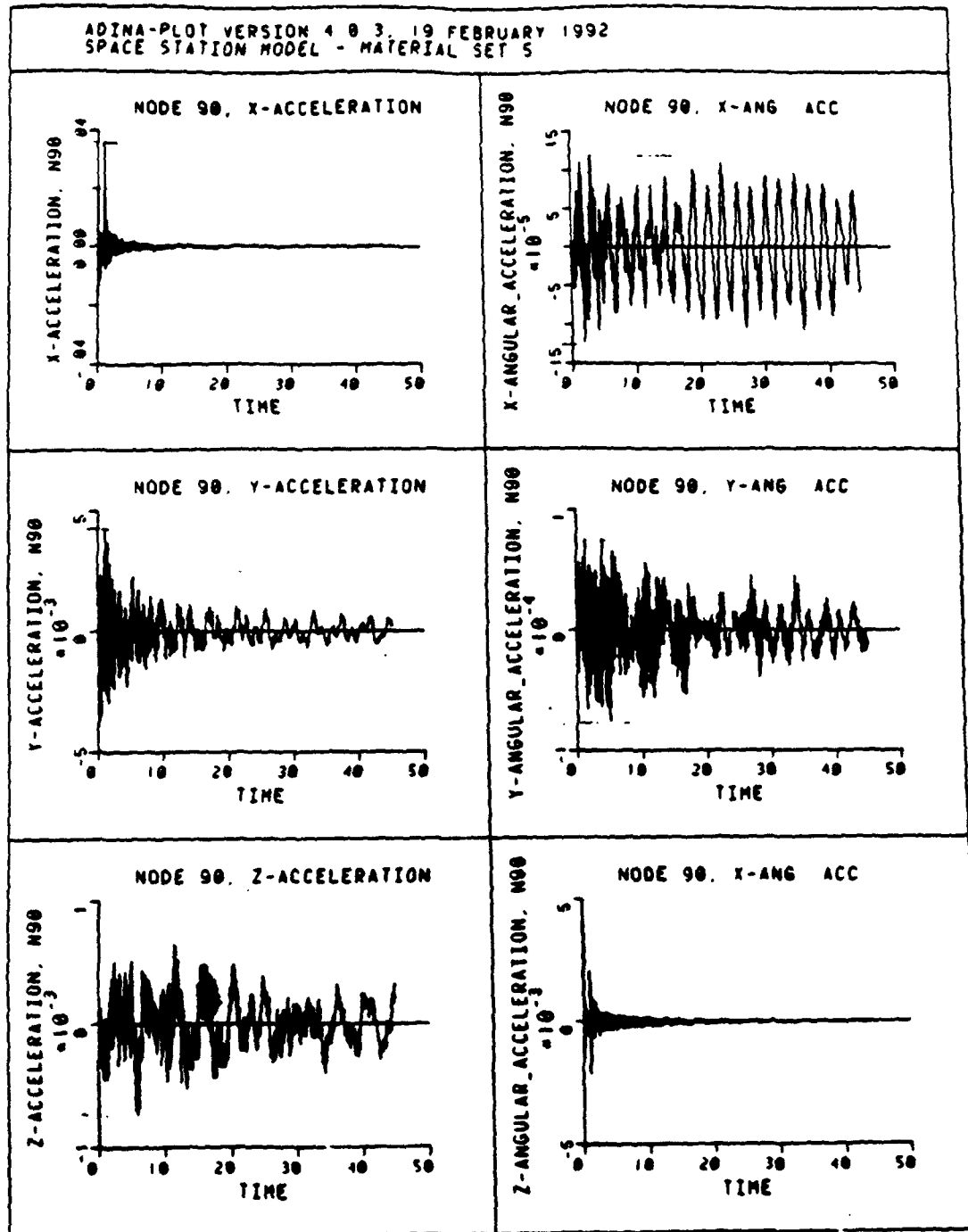


Figure 60 Node 90 Response E=56% X,Y,Z Lin./Rot. Accel.

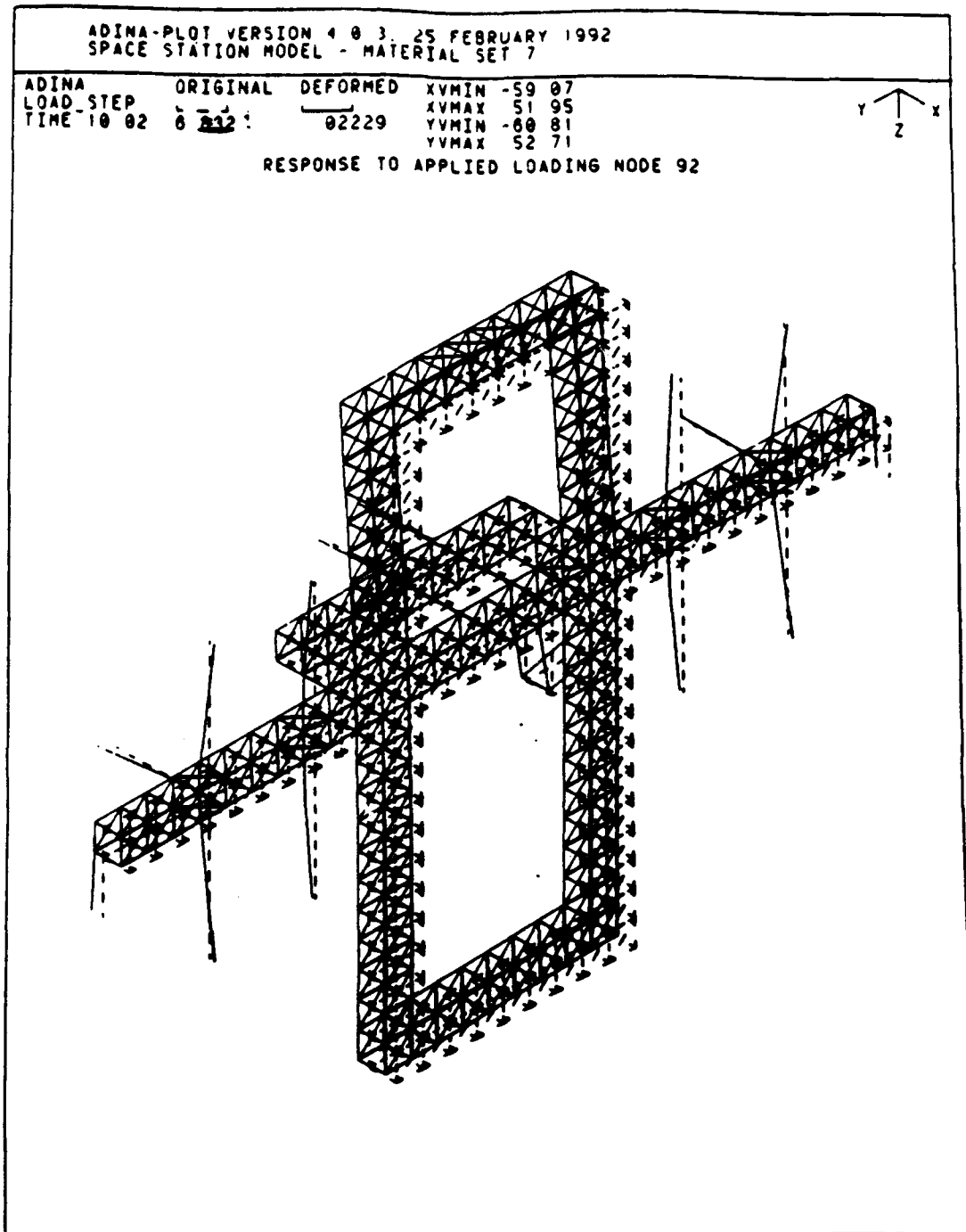


Figure 61 Global Structural Response E=34% at t = 10 sec.

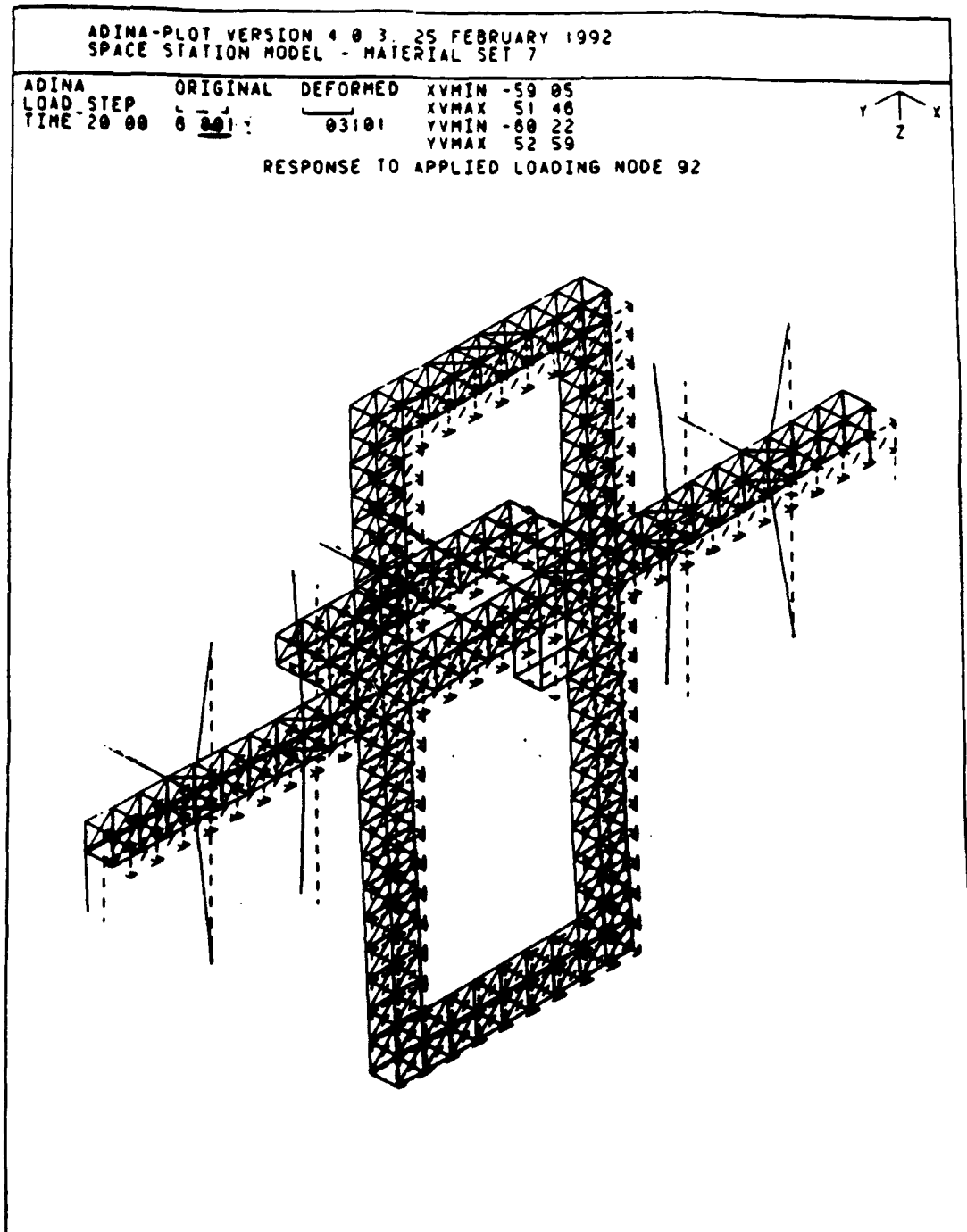


Figure 62 Global Structural Response $E=34\%$ at $t = 20$ sec.

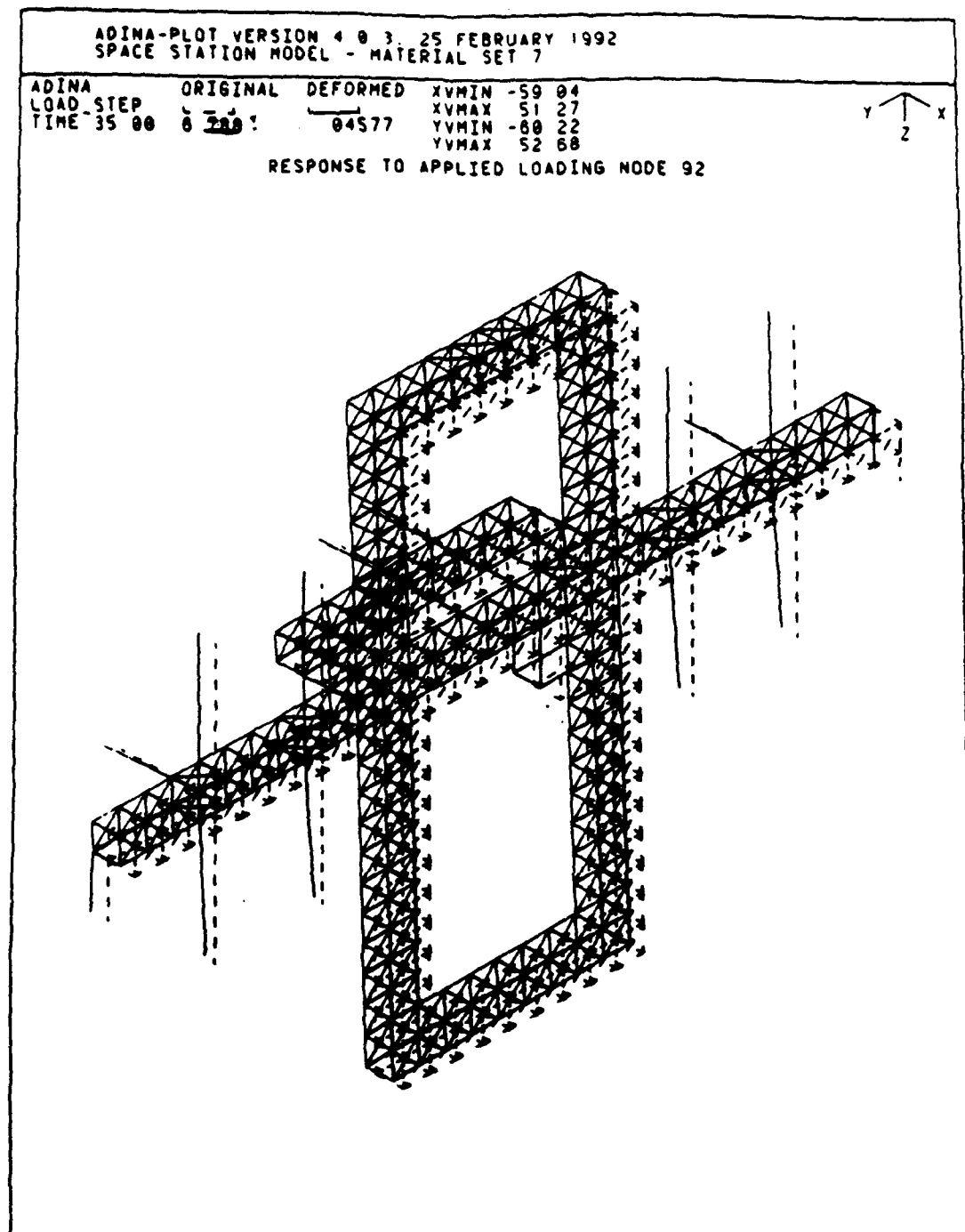


Figure 63 Global Structural Response $E=34\%$ at $t = 35$ sec.

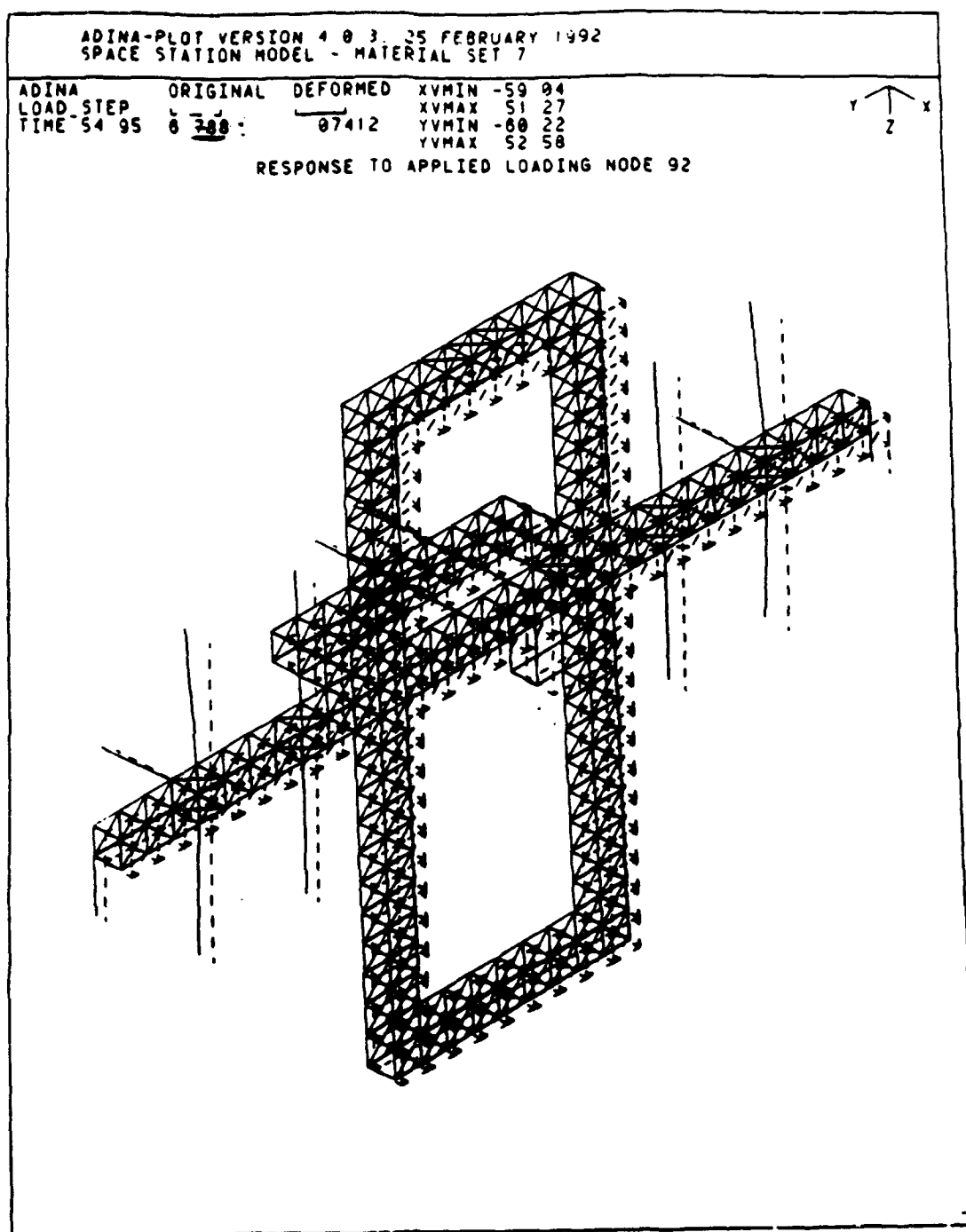


Figure 64 Global Structural Response $E=34\%$ at $t = 55$ sec.

ADINA-PLOT VERSION 4.0.3, 25 FEBRUARY 1992
SPACE STATION MODEL - MATERIAL SET 7

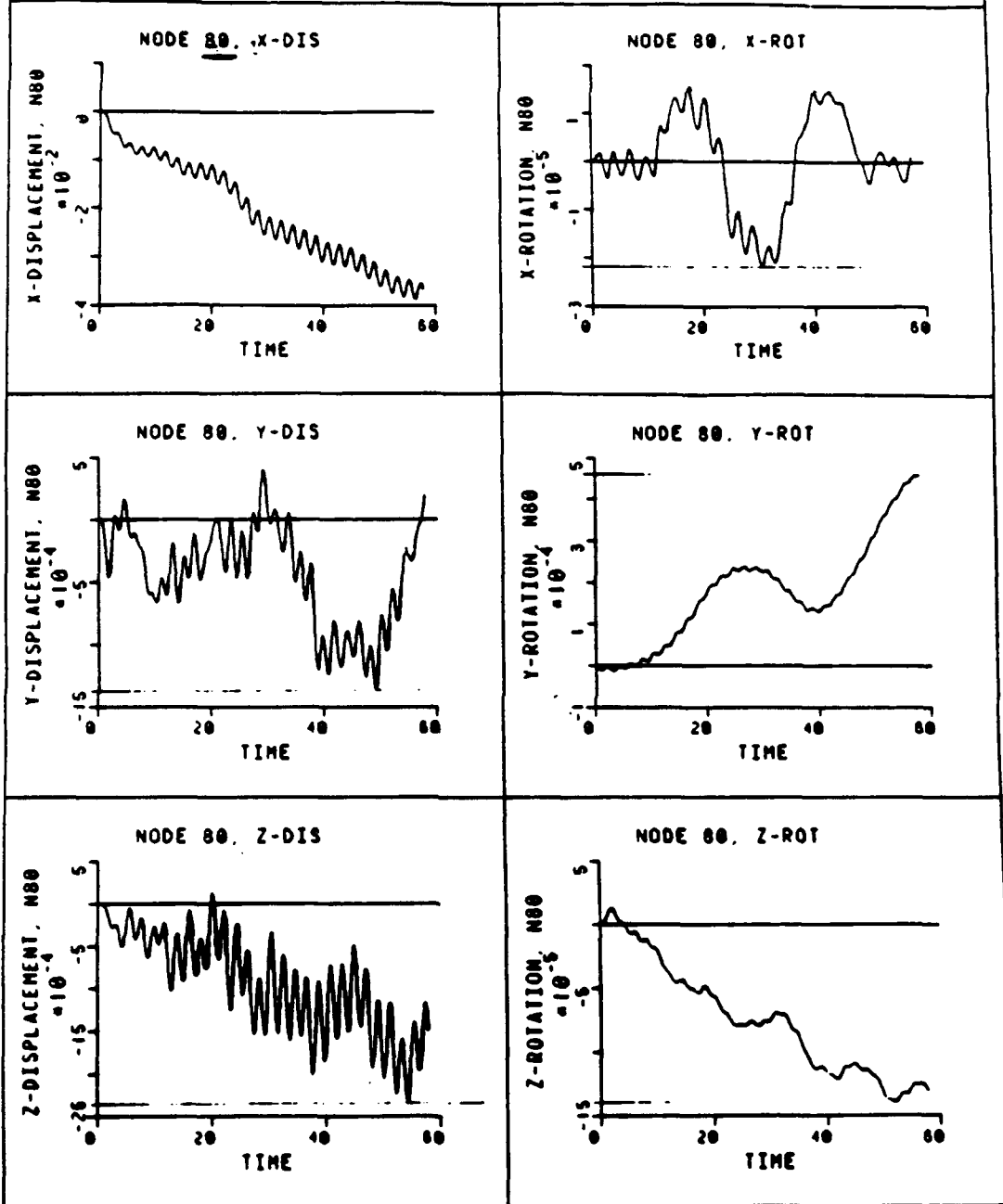


Figure 65 Node 80 Response E=34% X,Y,Z Displ./Rot.

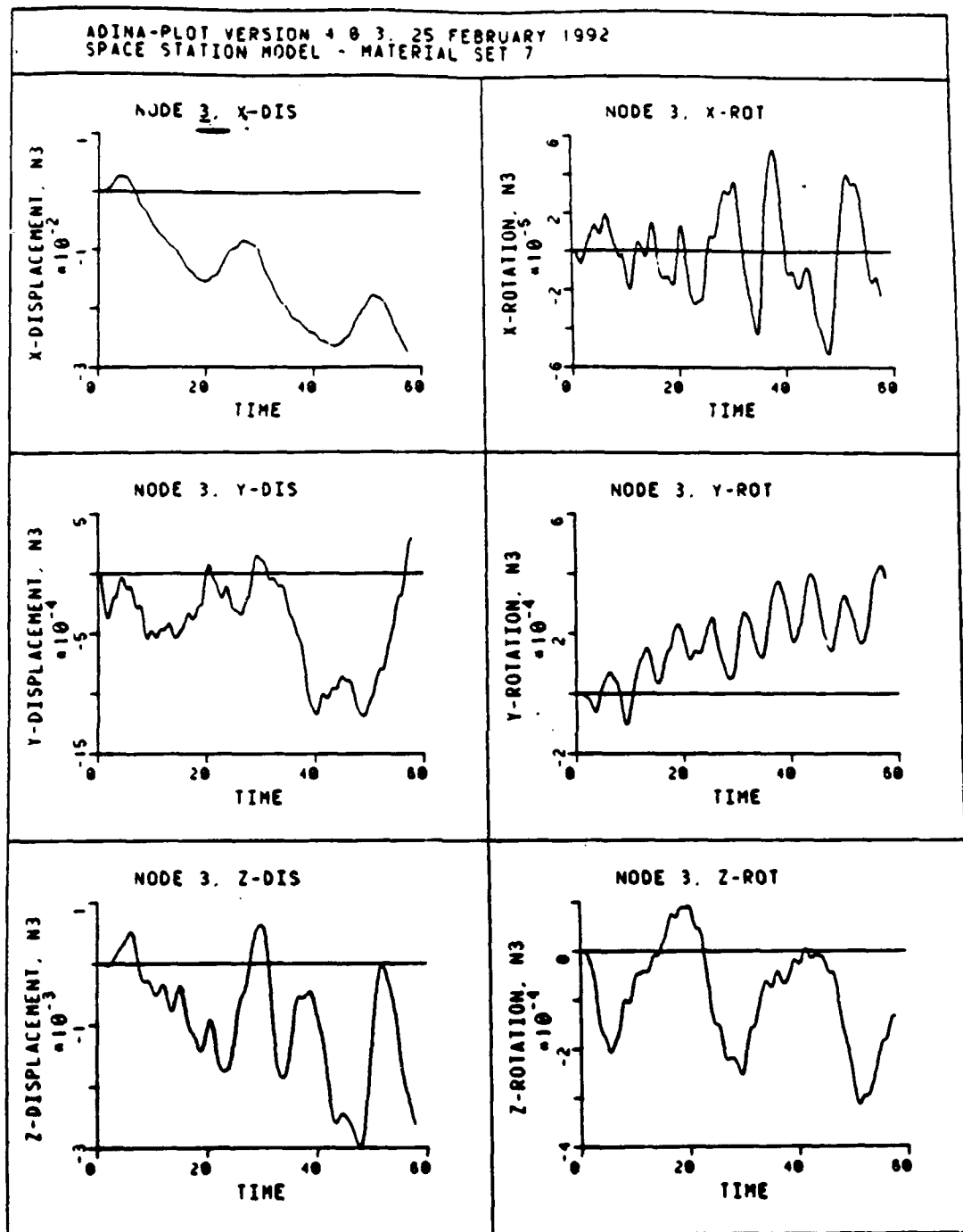


Figure 66 Node 3 Response E=34% X,Y,Z Displ./Rot.

ADINA-PLOT VERSION 4.0.3, 25 FEBRUARY 1992
SPACE STATION MODEL - MATERIAL SET 7

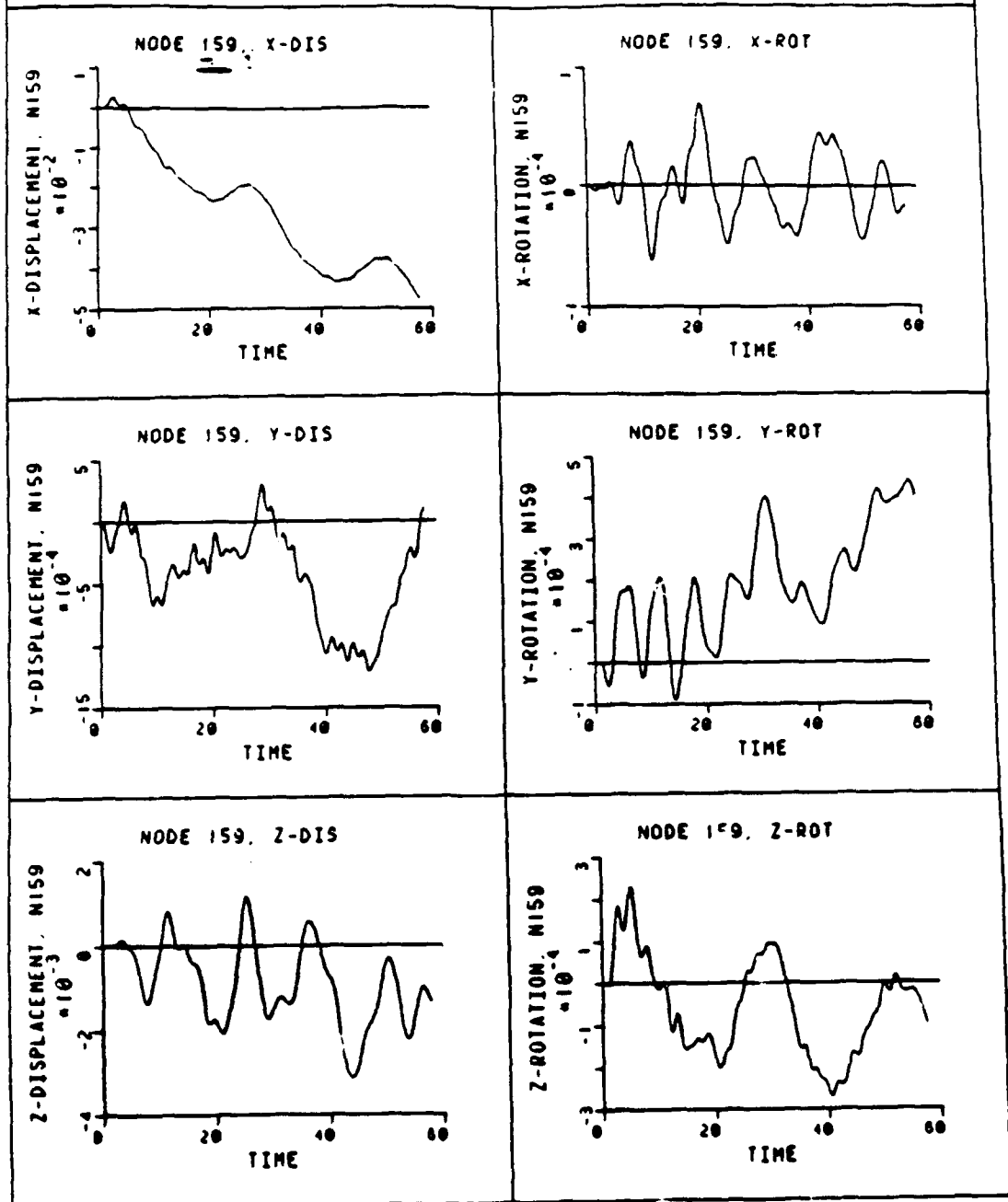


Figure 67 Node 159 Response E=34% X,Y,Z Displ./Rot.

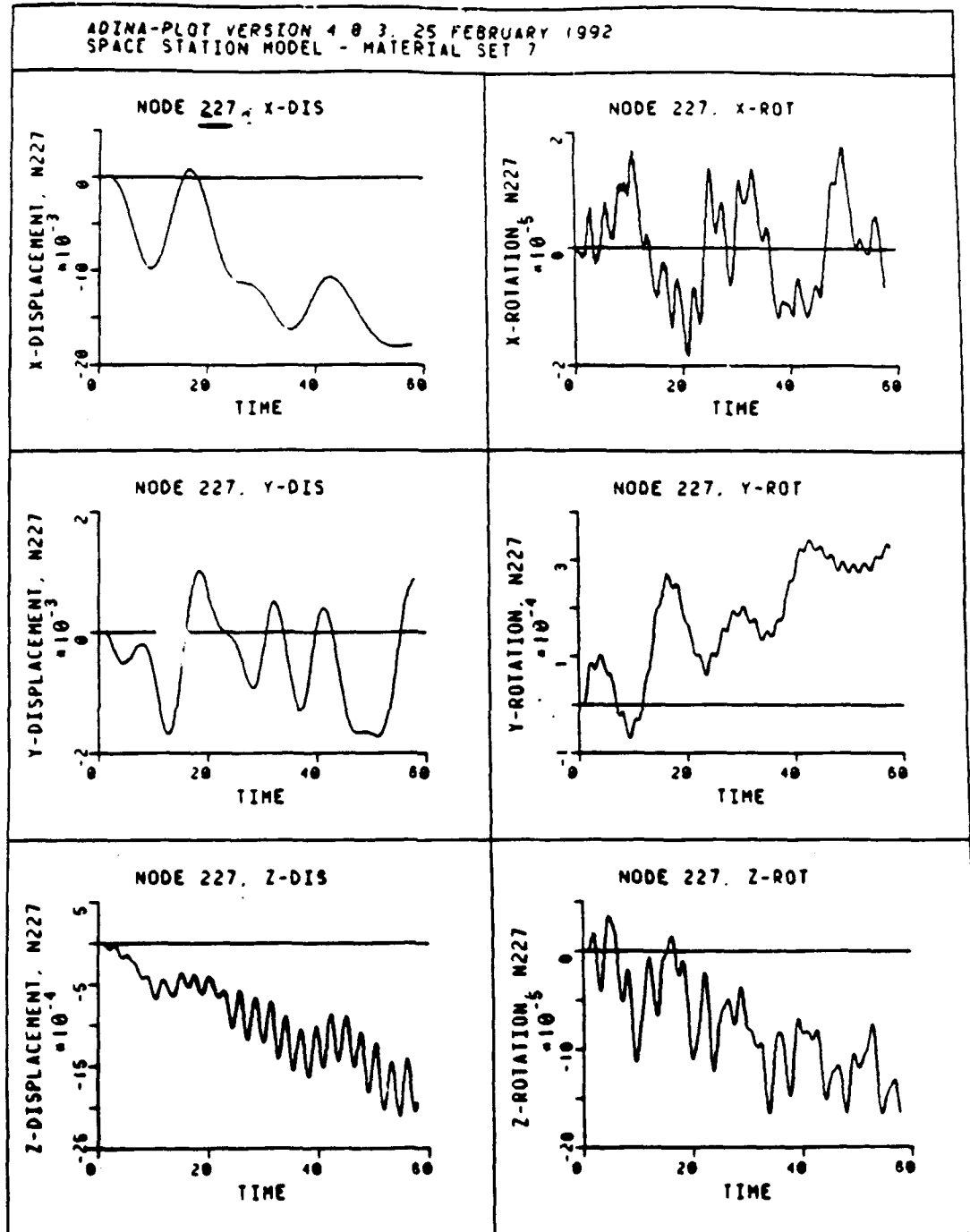


Figure 68 Node 227 Response E=34% X,Y,Z Displ./Rot.

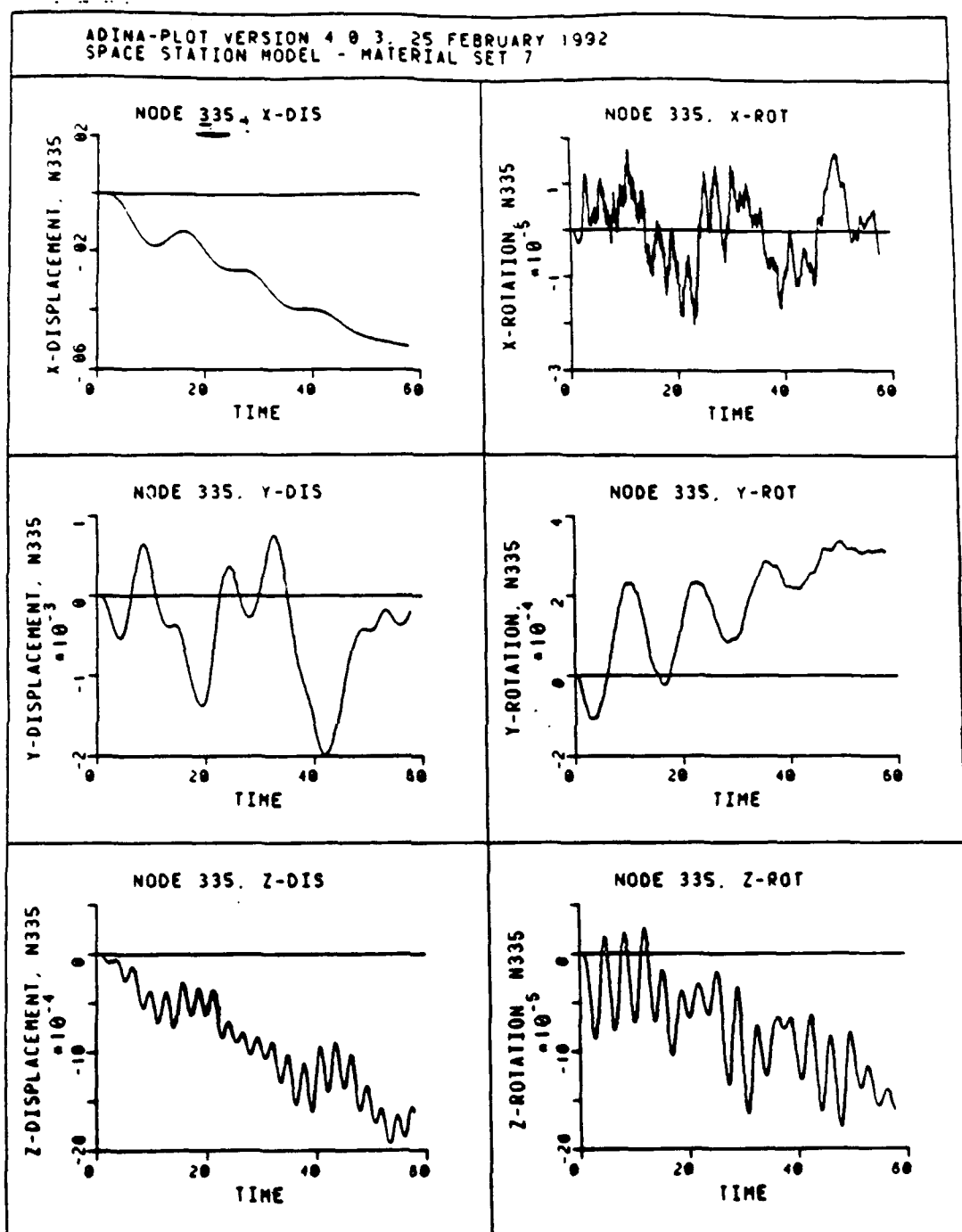


Figure 69 Node 335 Response E=34% X,Y,Z Displ./Rot.

ADINA-PLOT VERSION 4.0.3, 25 FEBRUARY 1992
SPACE STATION MODEL - MATERIAL SET 7

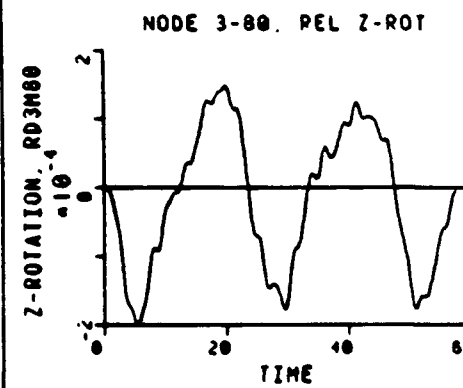
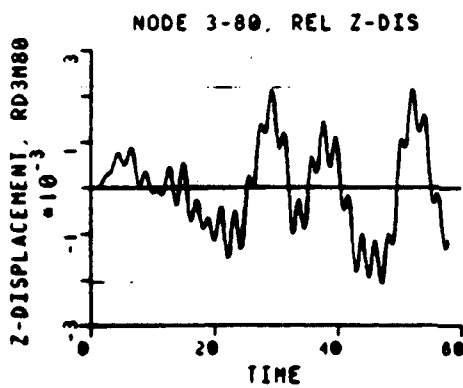
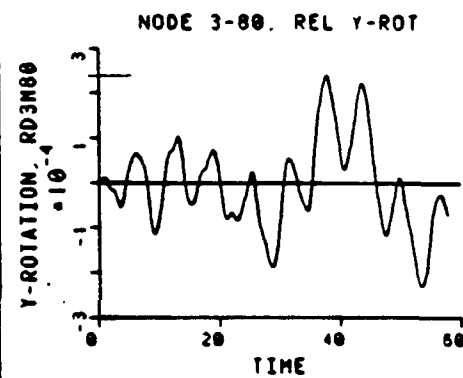
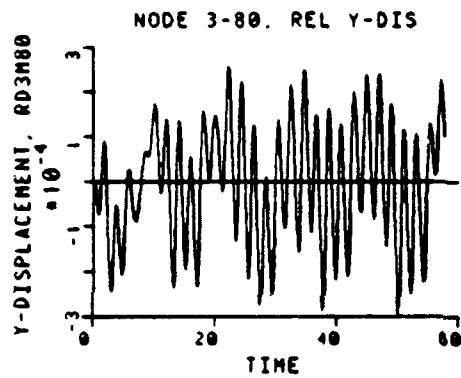
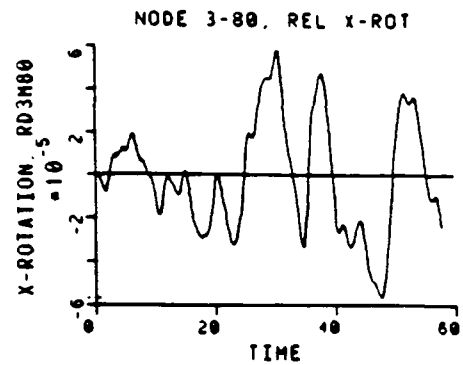
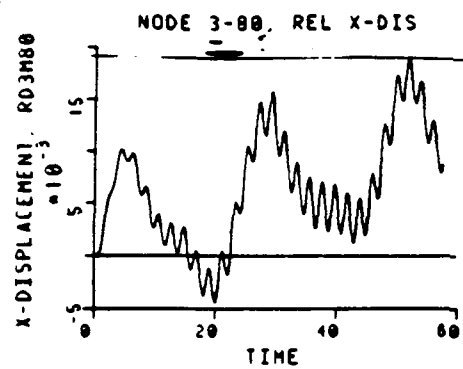


Figure 70 Node 3 vs. 80 Response E=34% X,Y,Z Displ./Rot.

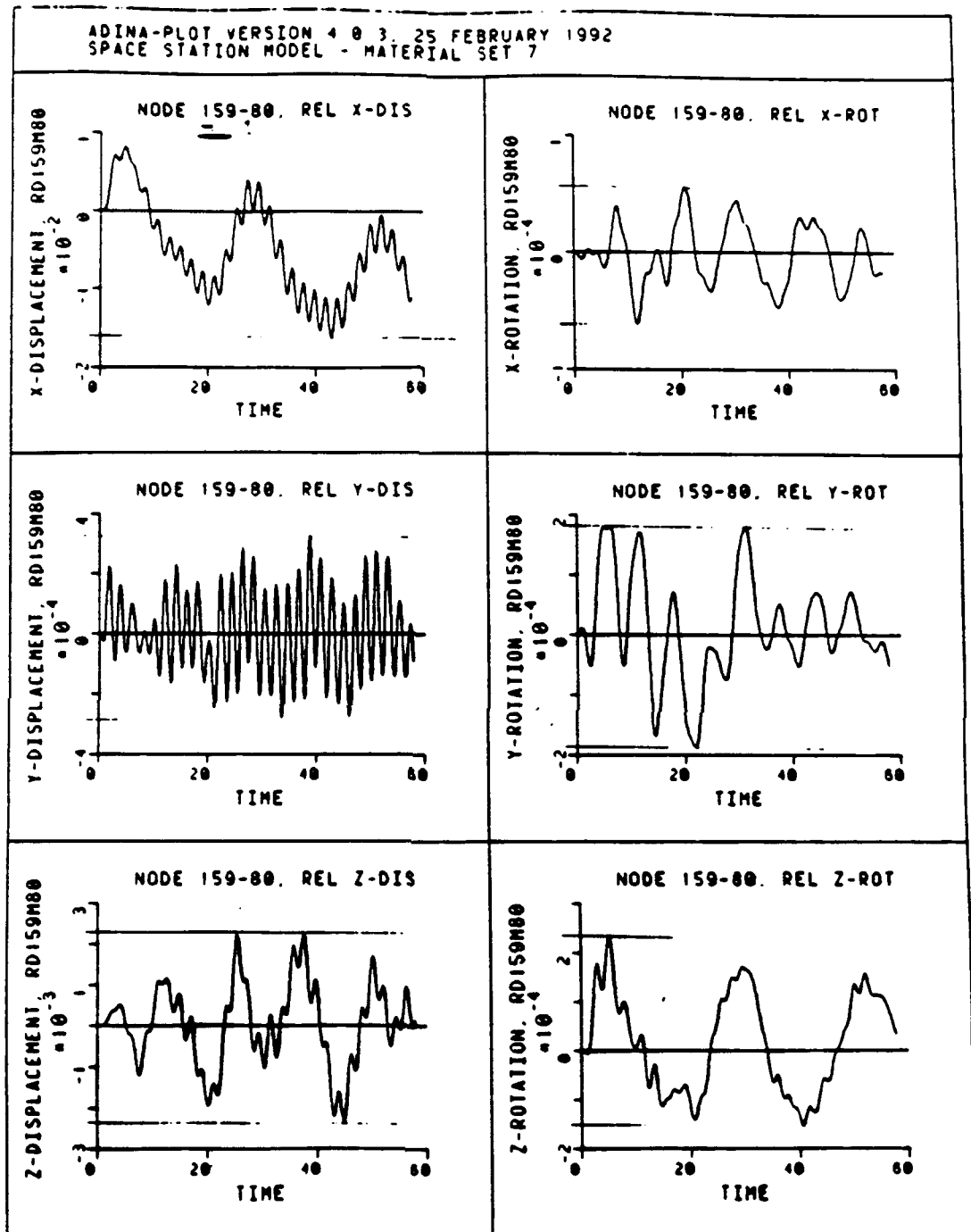


Figure 71 Node 159 vs. 80 Response E=34% X,Y,Z Displ./Rot.

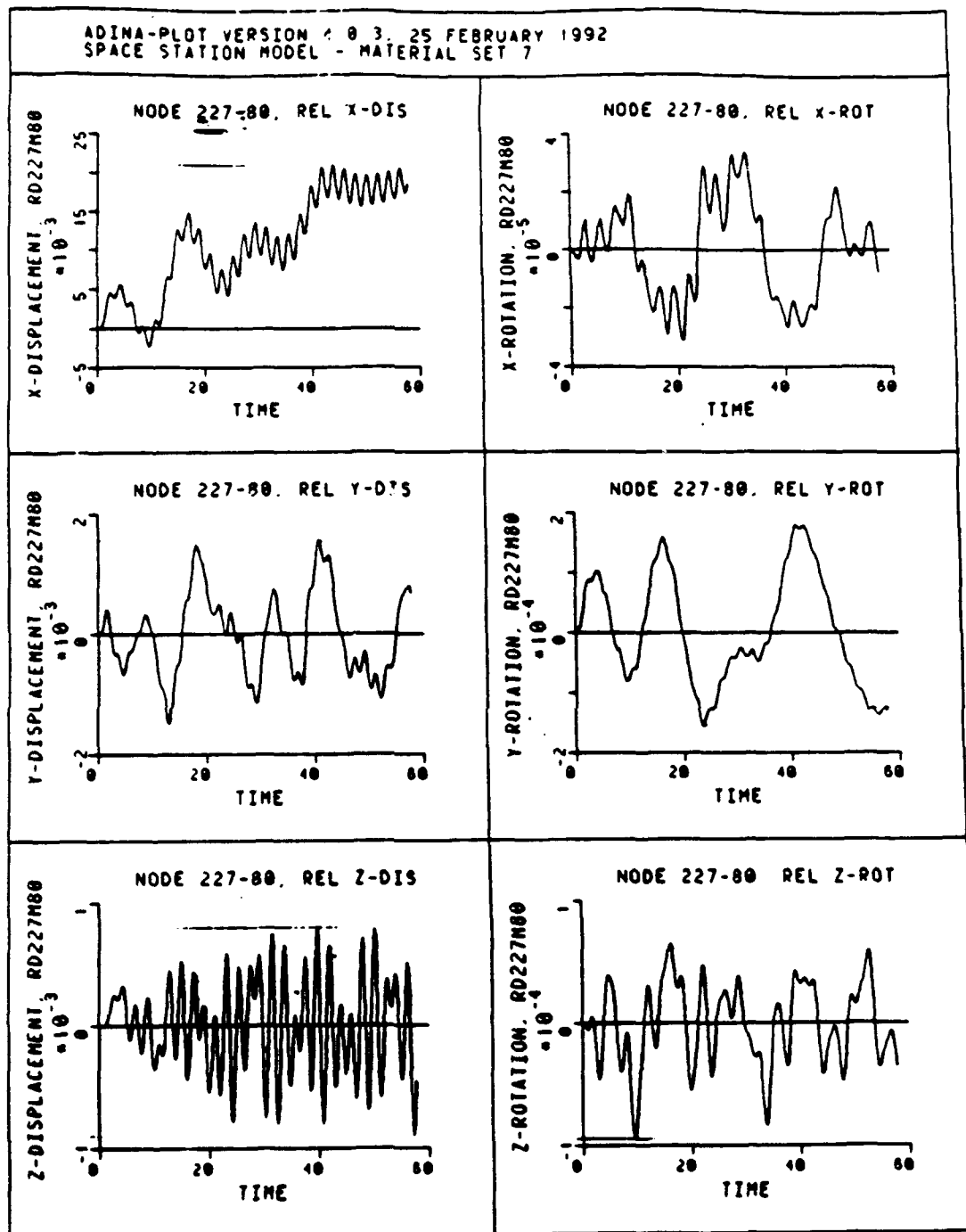


Figure 72 Node 227 vs. 80 Response E=34% X,Y,Z Displ./Rot.

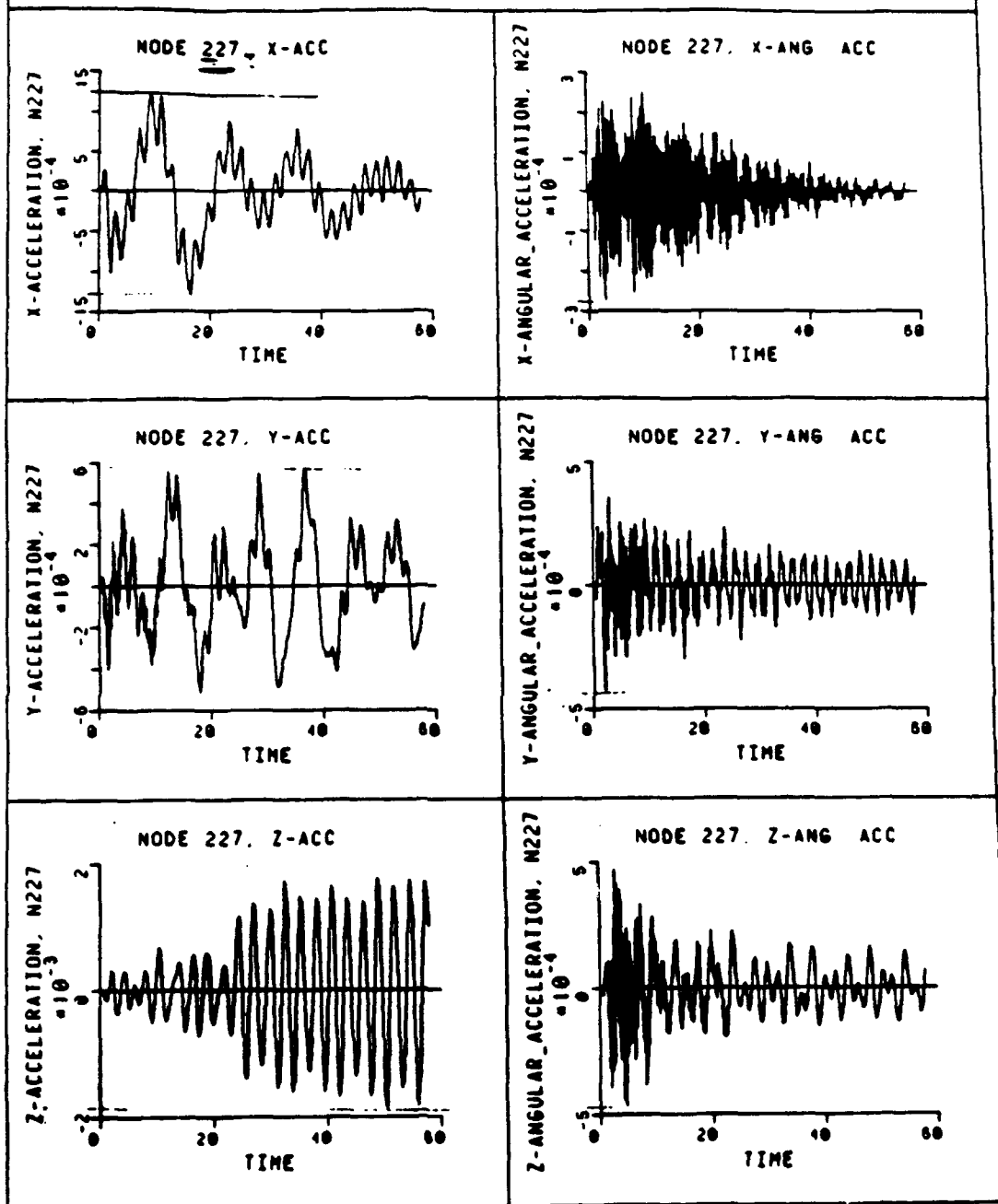


Figure 73 Node 227 Response E=34% X,Y,Z Lin./Rot. Accel.

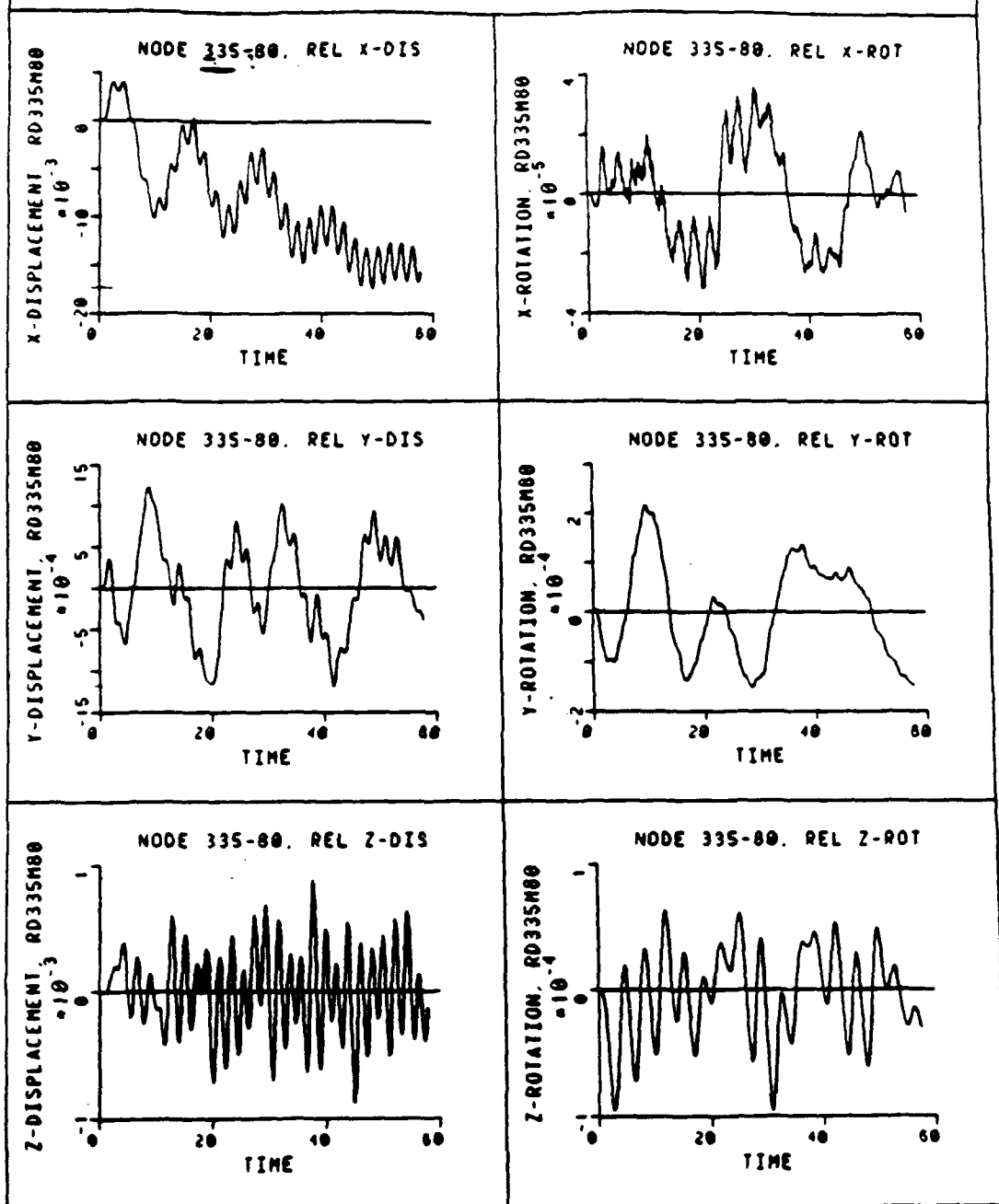


Figure 74 Node 335 vs. 80 Response E=34% X,Y,Z Displ./Rot.

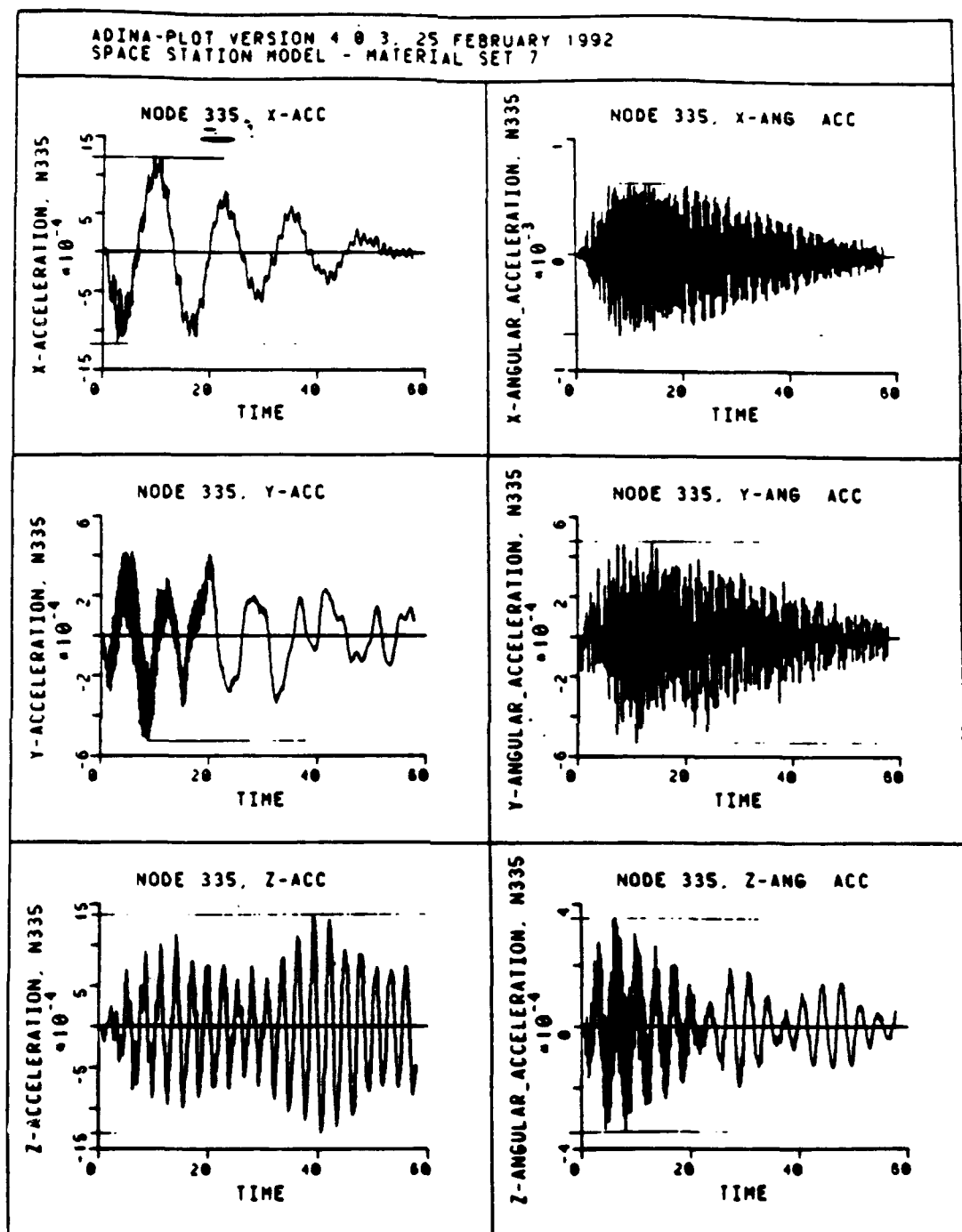


Figure 75 Node 335 Response E=34% X,Y,Z Lin./Rot. Accel.

ADINA-PLOT VERSION 4.0.3, 25 FEBRUARY 1992
SPACE STATION MODEL - MATERIAL SET 7

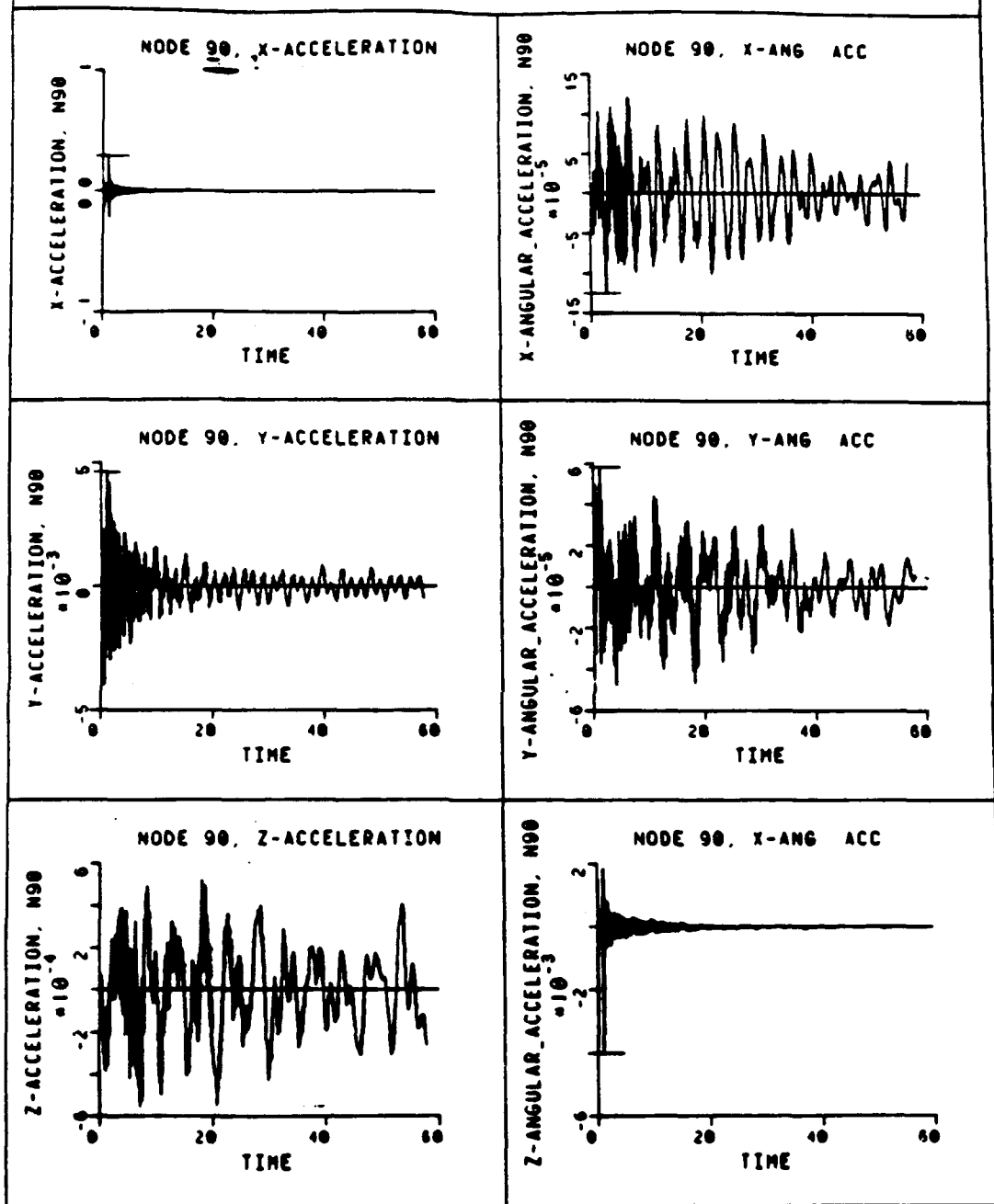


Figure 76 Node 90 Response E=34% X,Y,Z Lin./Rot. Accel.

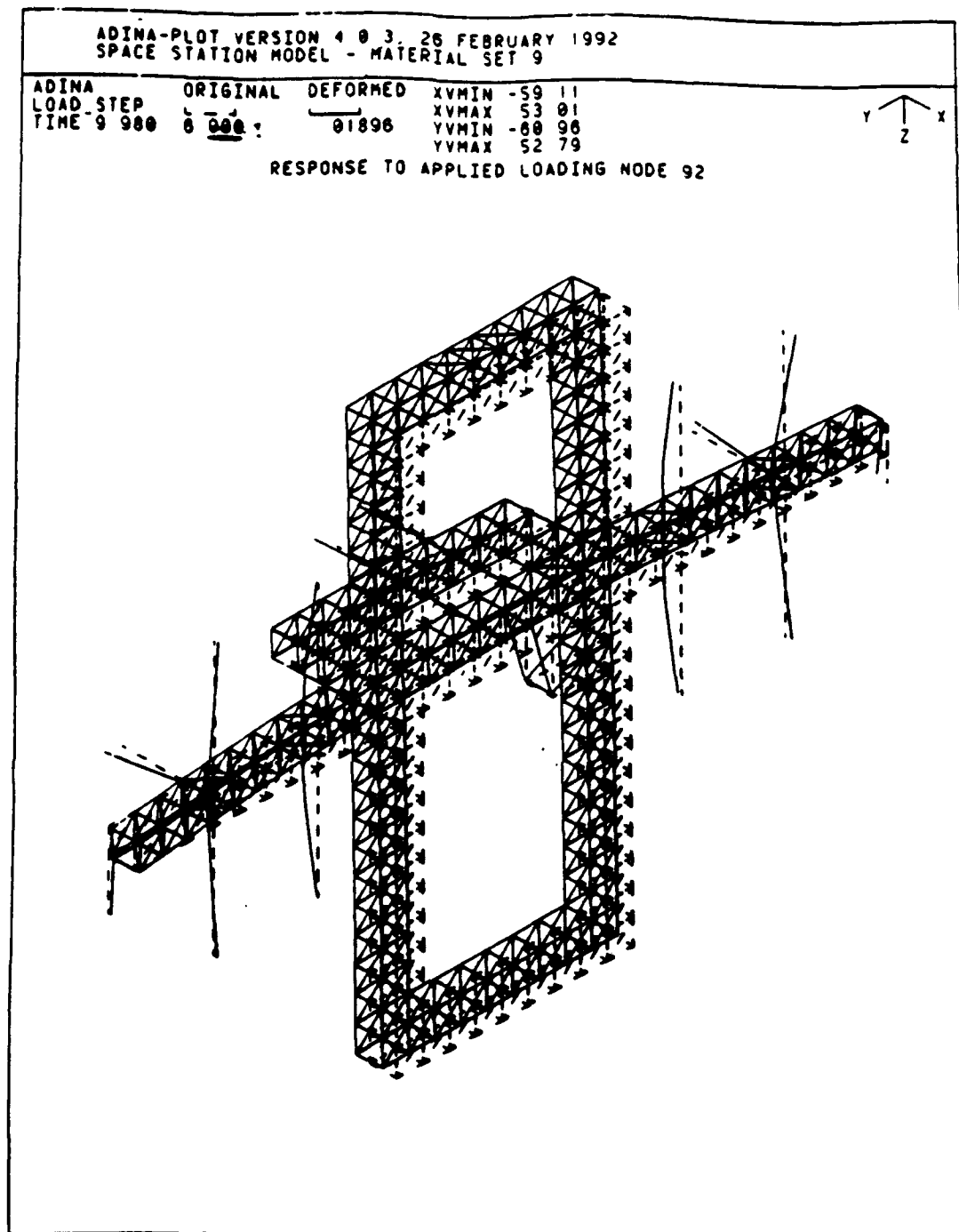


Figure 77 Global Structural Response $E=12\%$ at $t = 10$ sec.

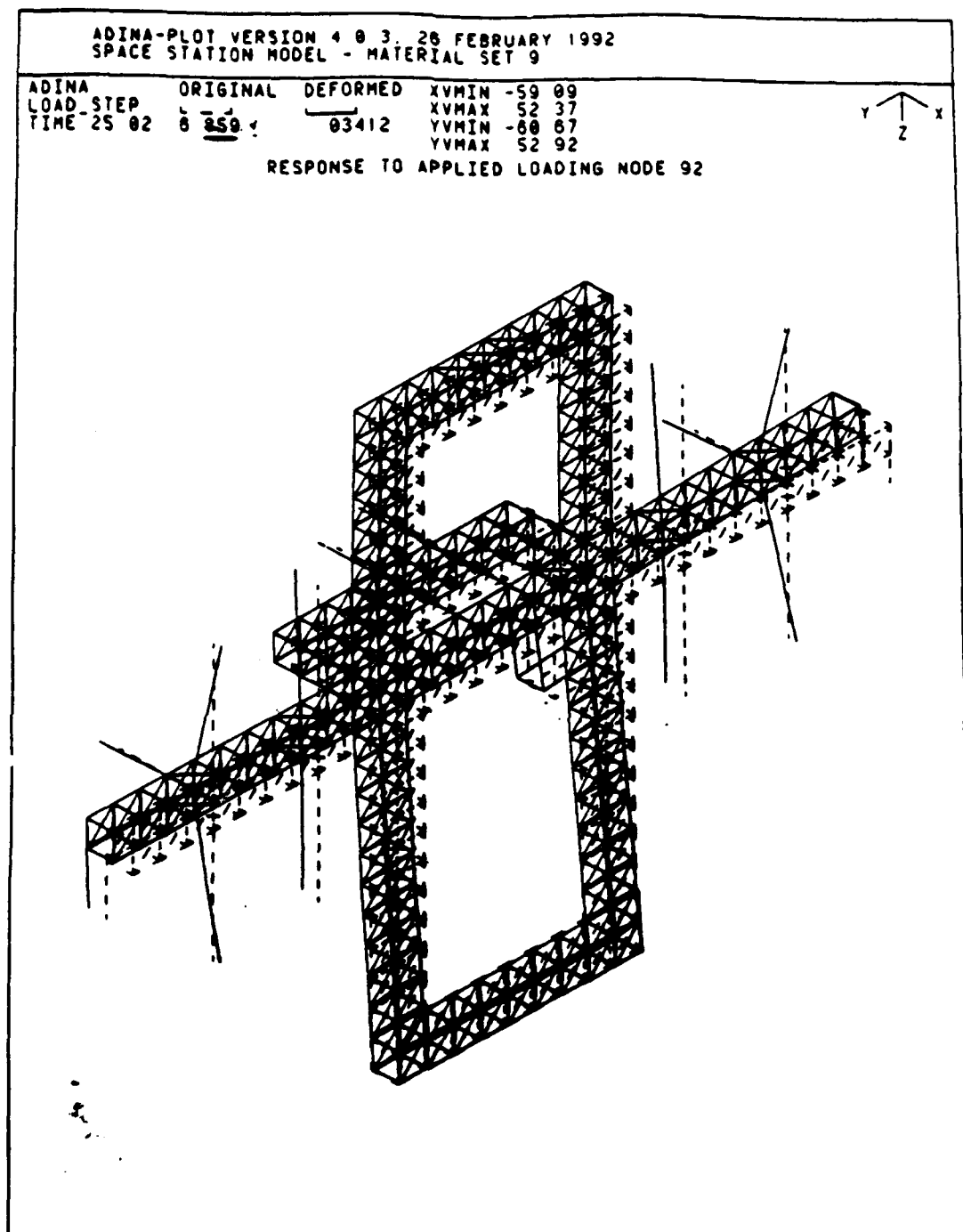


Figure 78 Global Structural Response E=12% at t = 25 sec.

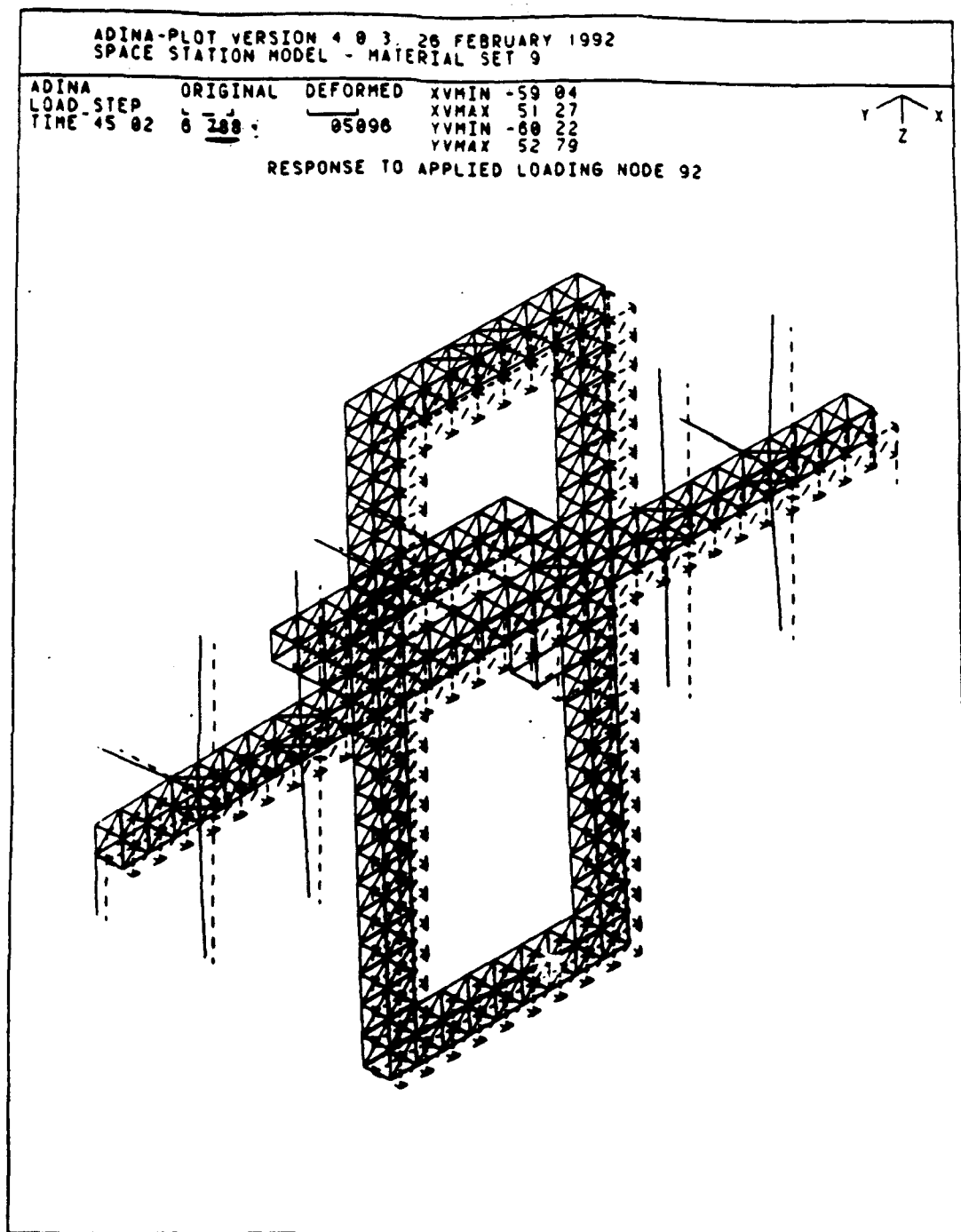


Figure 79 Global Structural Response $E=12\%$ at $t = 45$ sec.

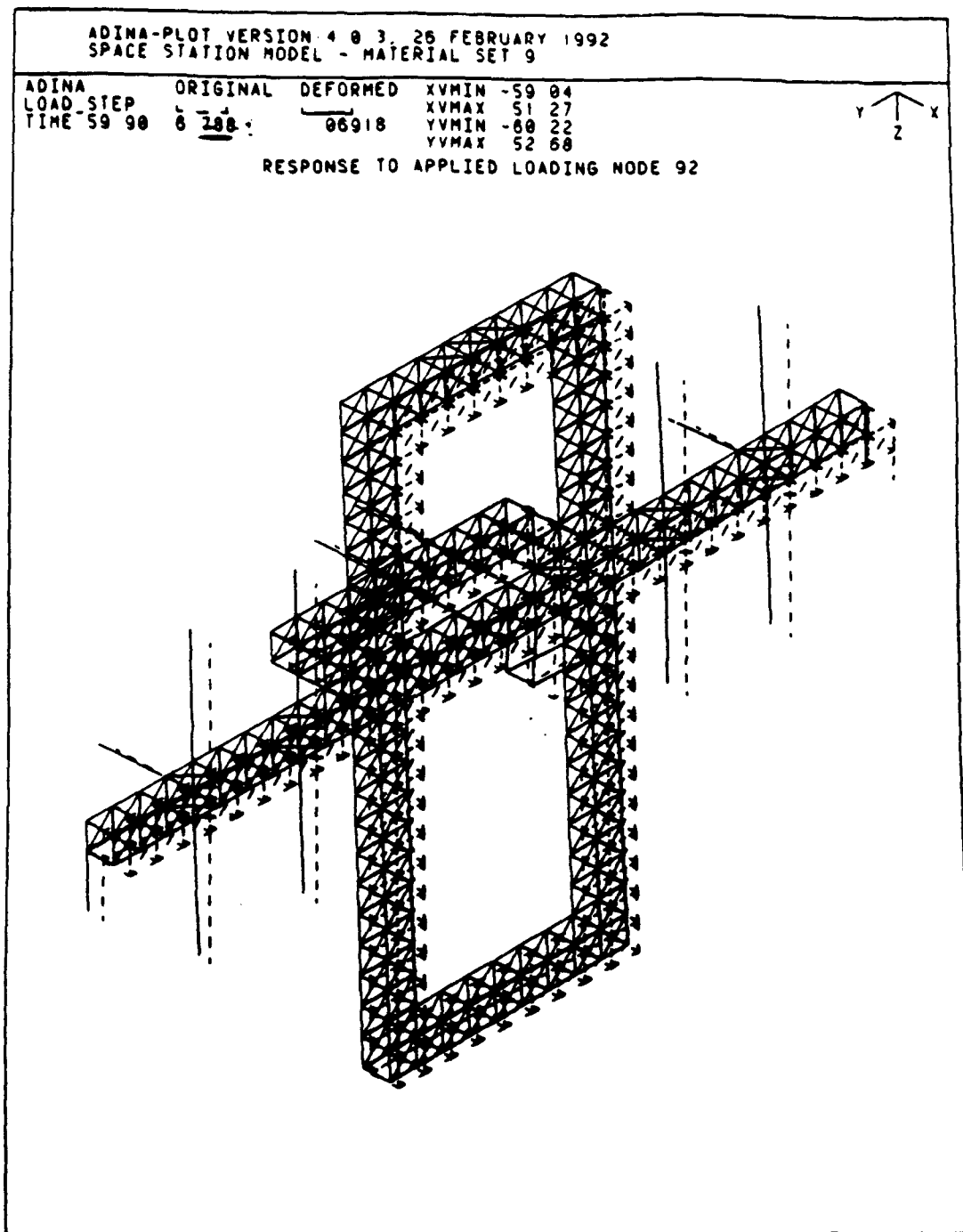


Figure 80 Global Structural Response $E=12\%$ at $t = 60$ sec.

ADINA-PLOT VERSION 4.0.3, 19 FEBRUARY 1992
SPACE STATION MODEL - MATERIAL SET 9

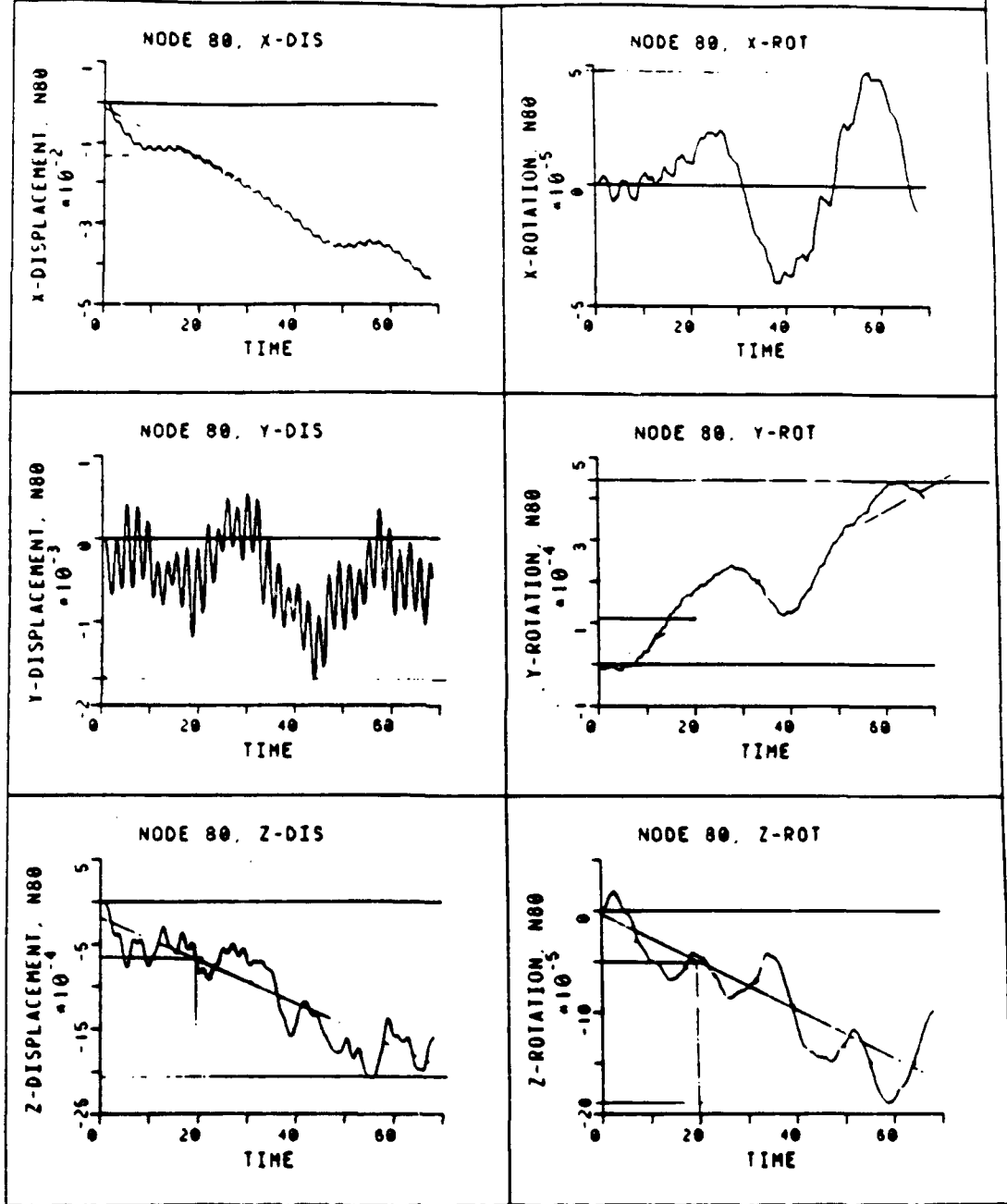


Figure 81 Node 80 Response E=12% X,Y,Z Displ./Rot.

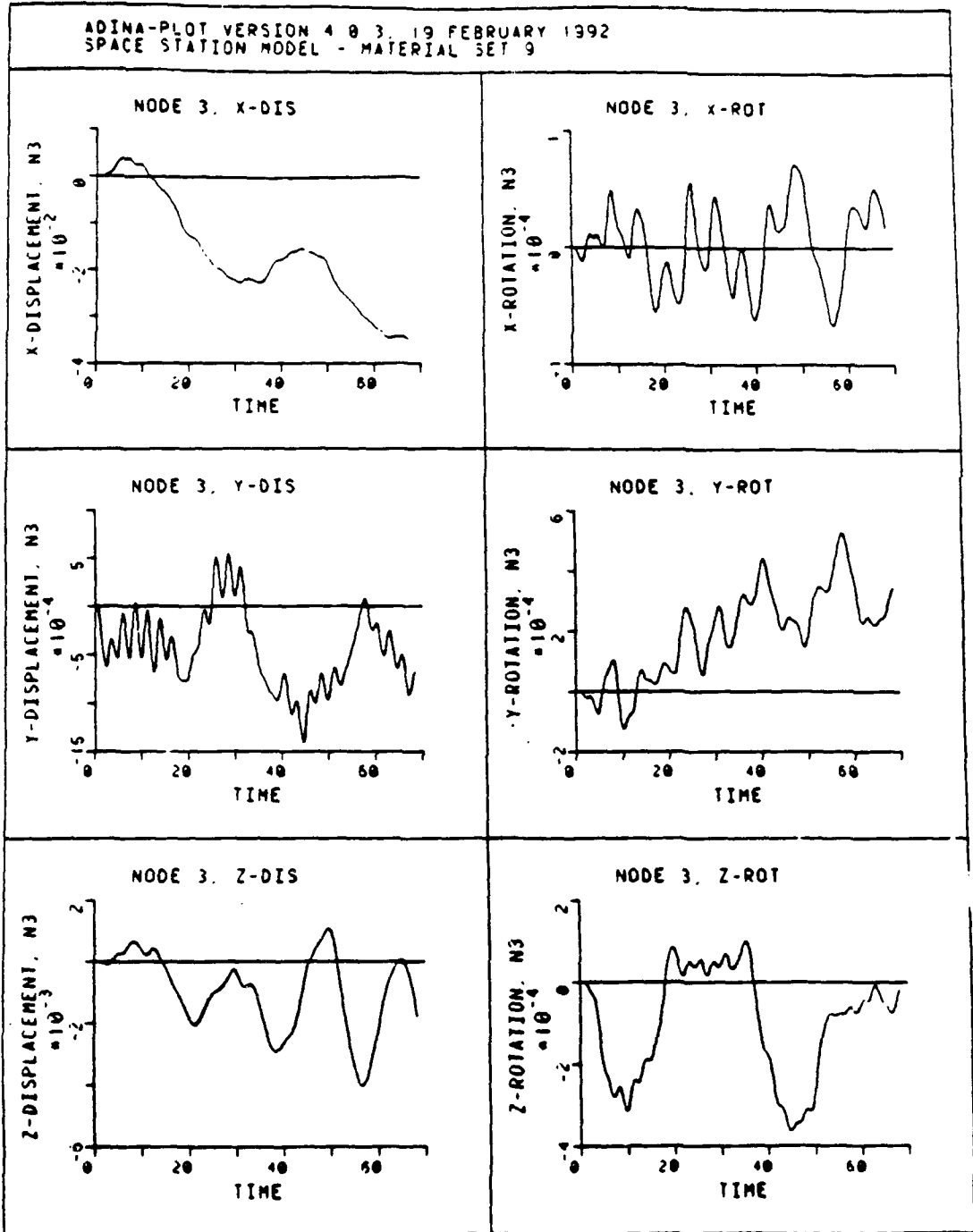


Figure 82 Node 3 Response E=12% X,Y,Z Displ./Rot.

ADINA-PLOT VERSION 4.0.3, 19 FEBRUARY 1992
SPACE STATION MODEL - MATERIAL SET 9

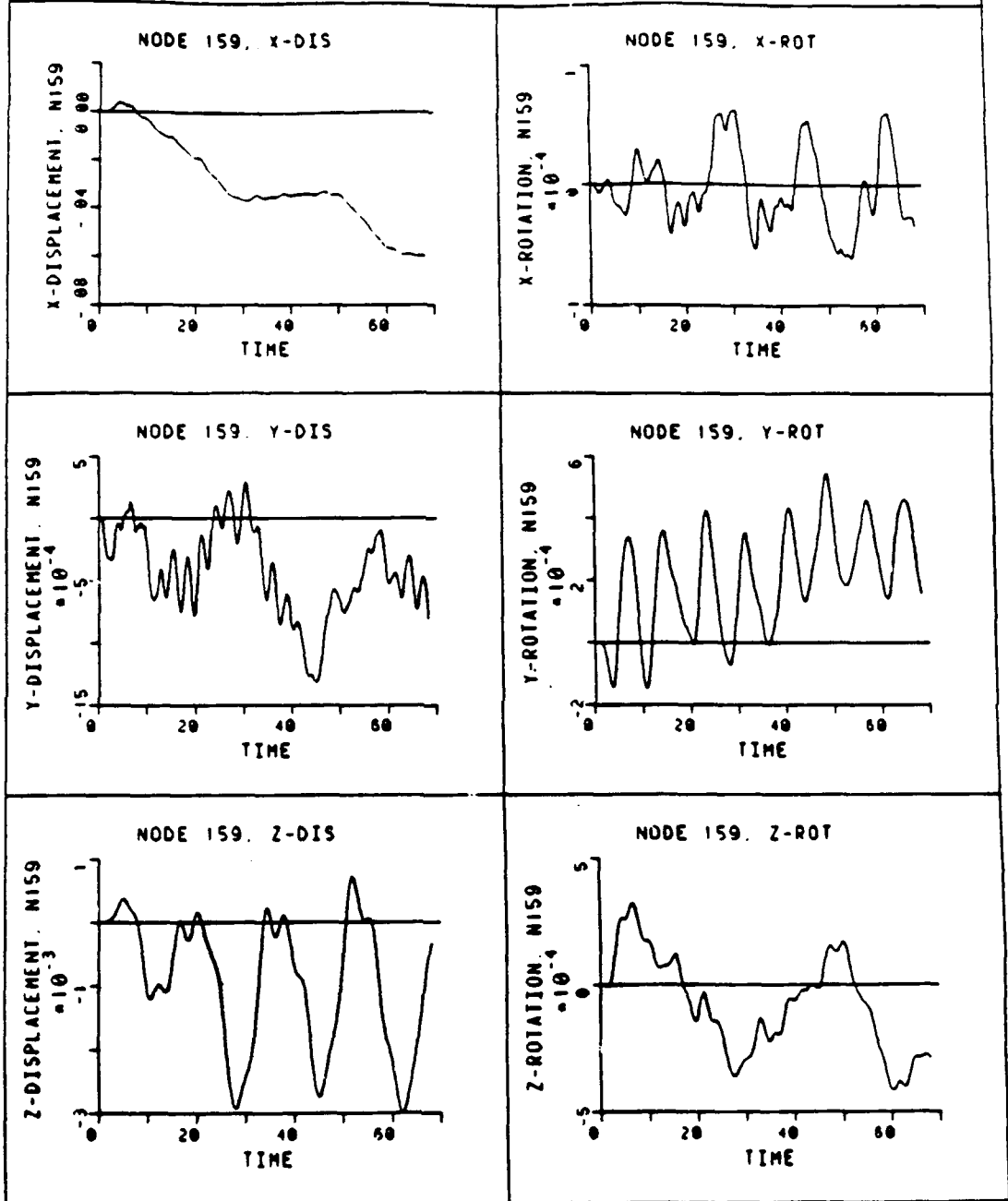


Figure 83 Node 159 Response E=12% X,Y,Z Displ./Rot.

ADINA-PLOT VERSION 4.0.3, 19 FEBRUARY 1992
 SPAC. STATION MODEL - MATERIAL SET 9

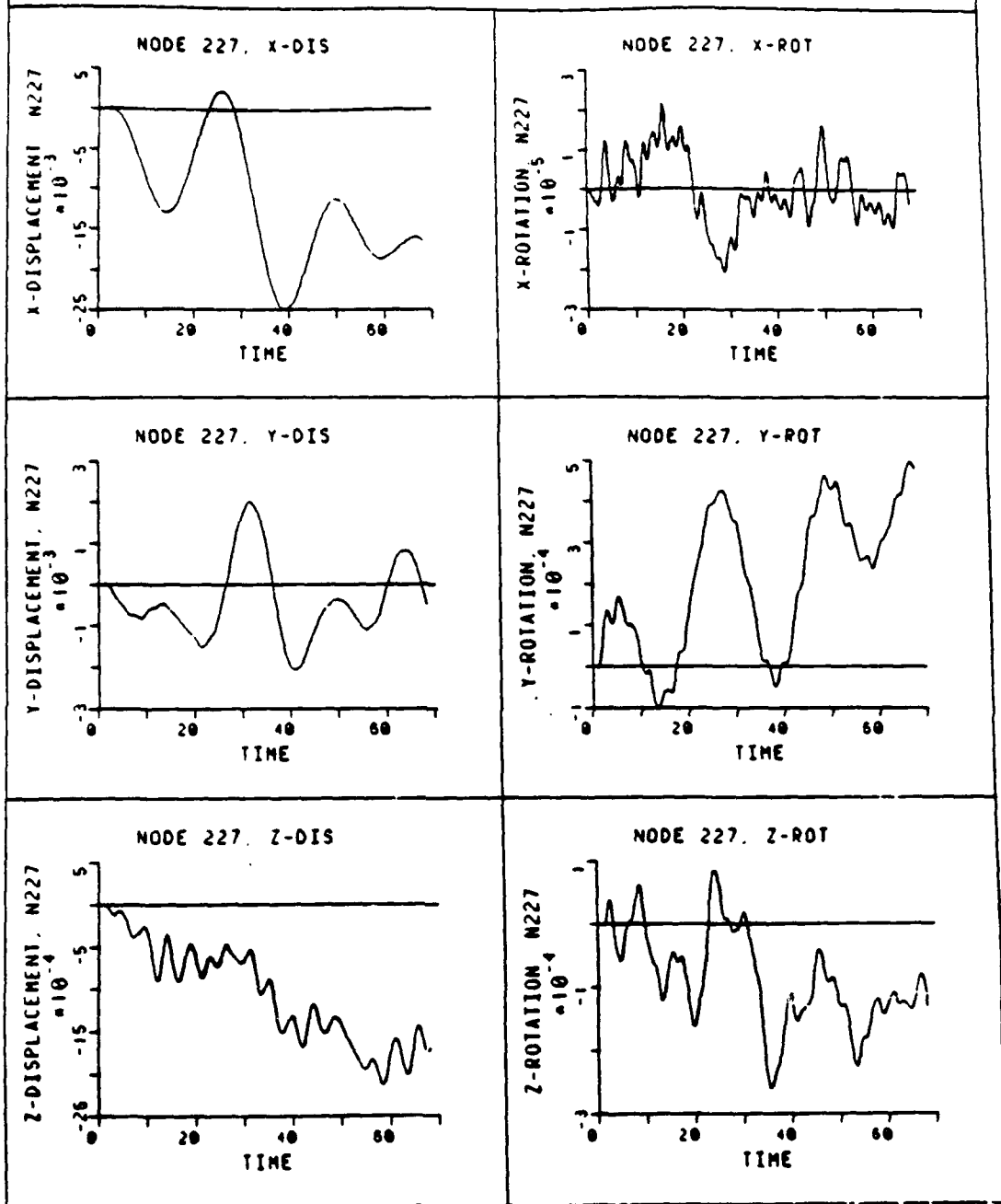


Figure 84 Node 227 Response E=12% X,Y,Z Displ./Rot.

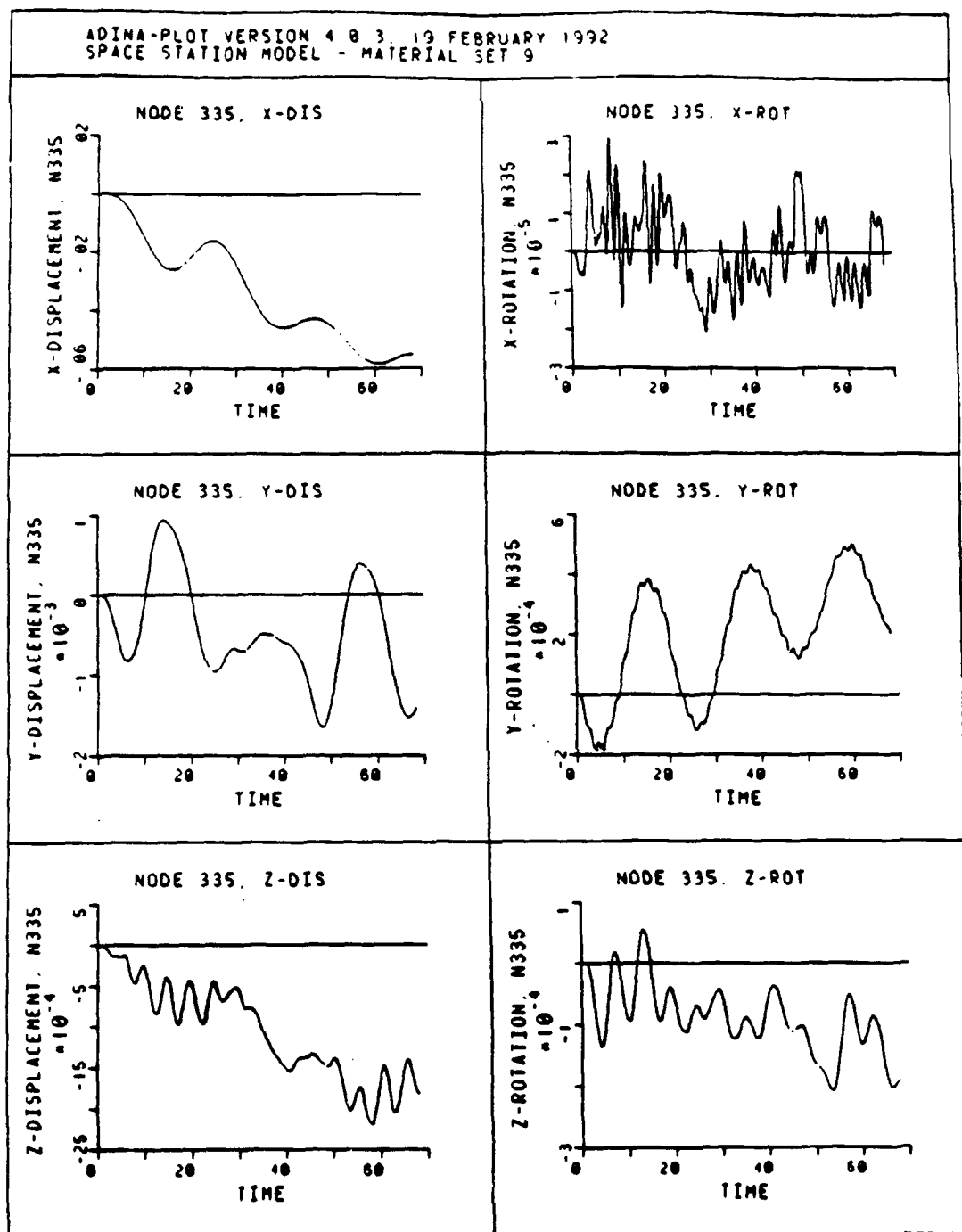


Figure 85 Node 335 Response E=12% X,Y,Z Displ./Rot.

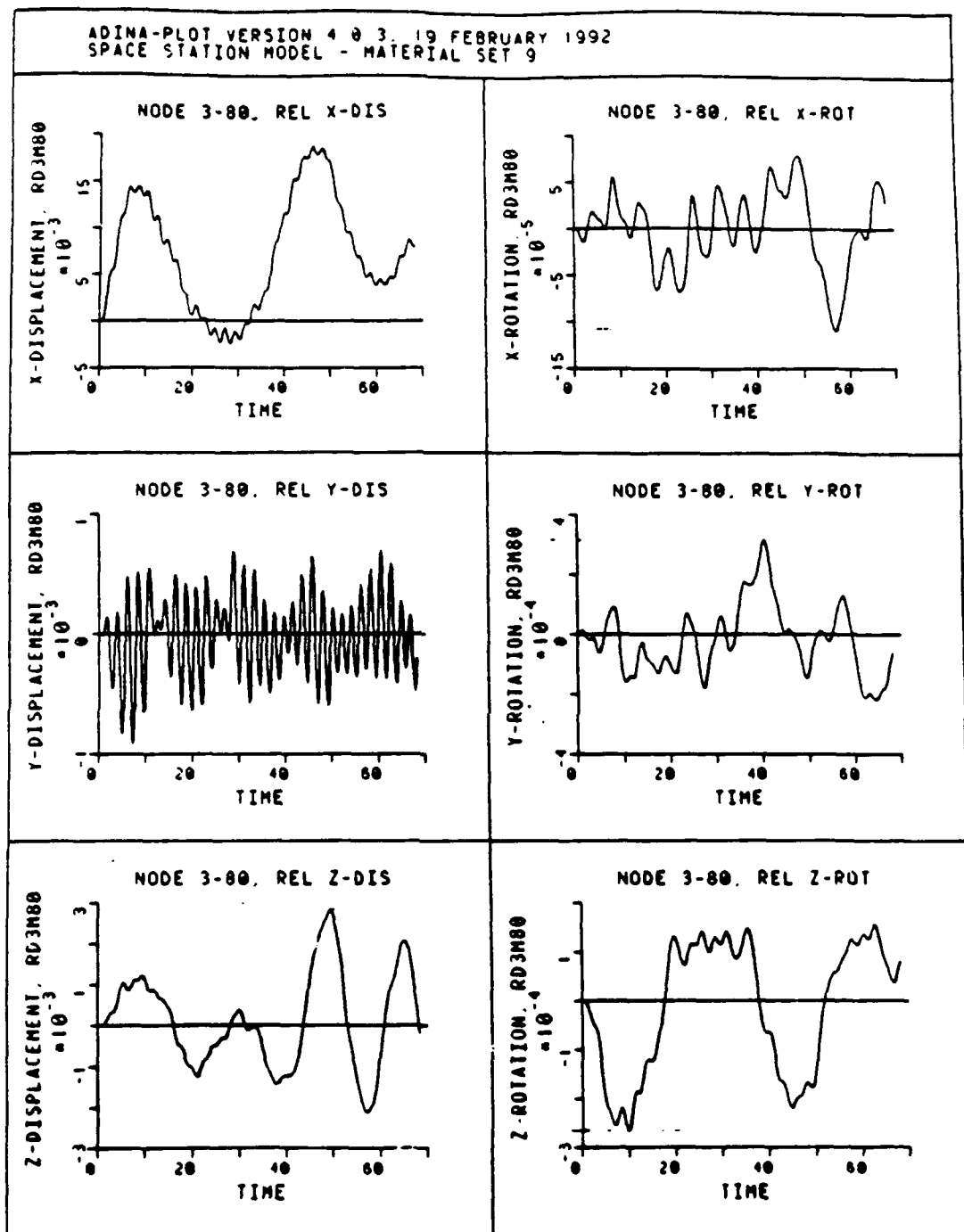


Figure 86 Node 3 vs. 80 Response E=12% X,Y,Z Displ./Rot.

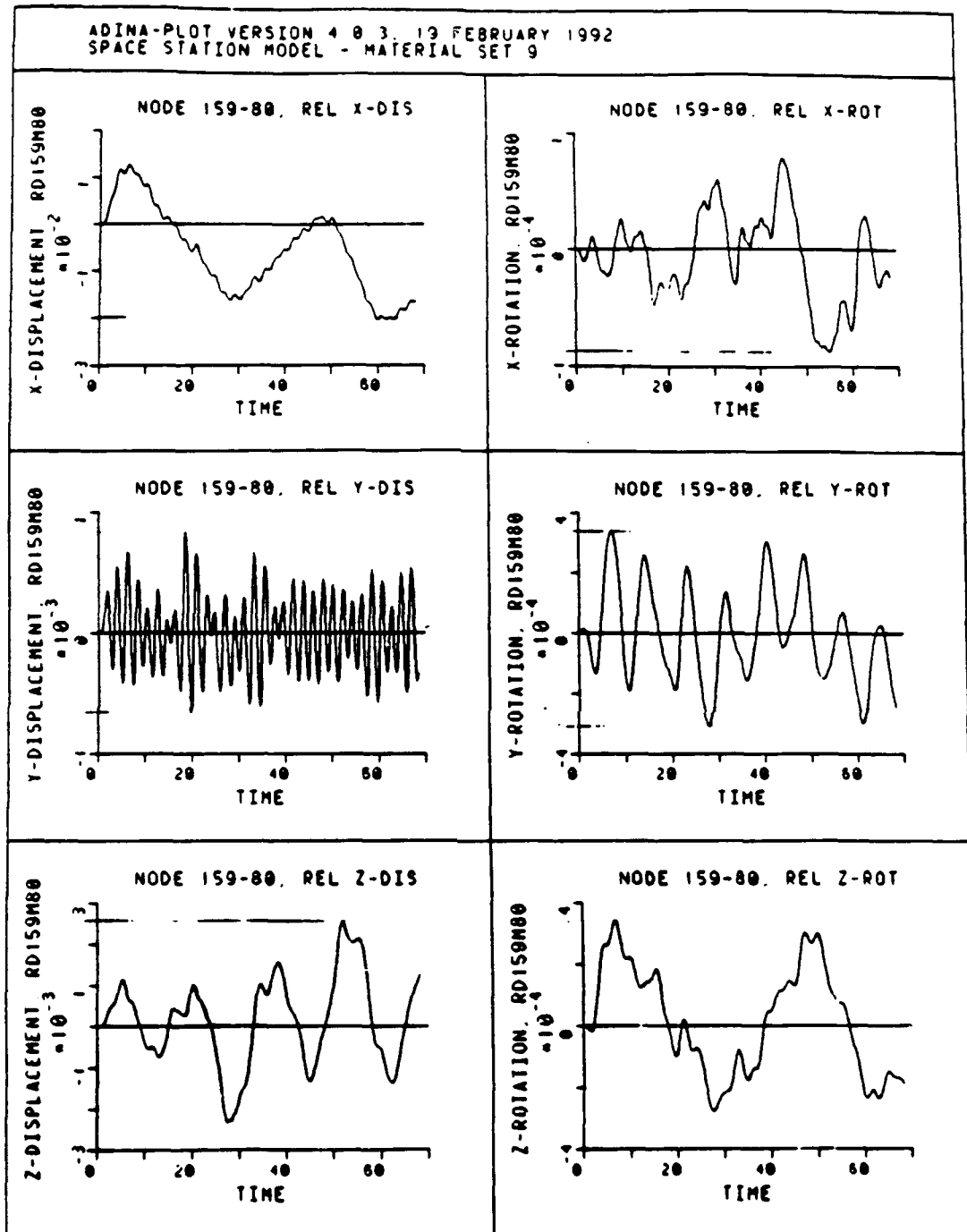


Figure 87 Node 159 vs. 80 Response E=12% X,Y,Z Displ./Rot.

ADINA-PLOT VERSION 4.0.3, 19 FEBRUARY 1992
SPACE STATION MODEL - MATERIAL SET 9

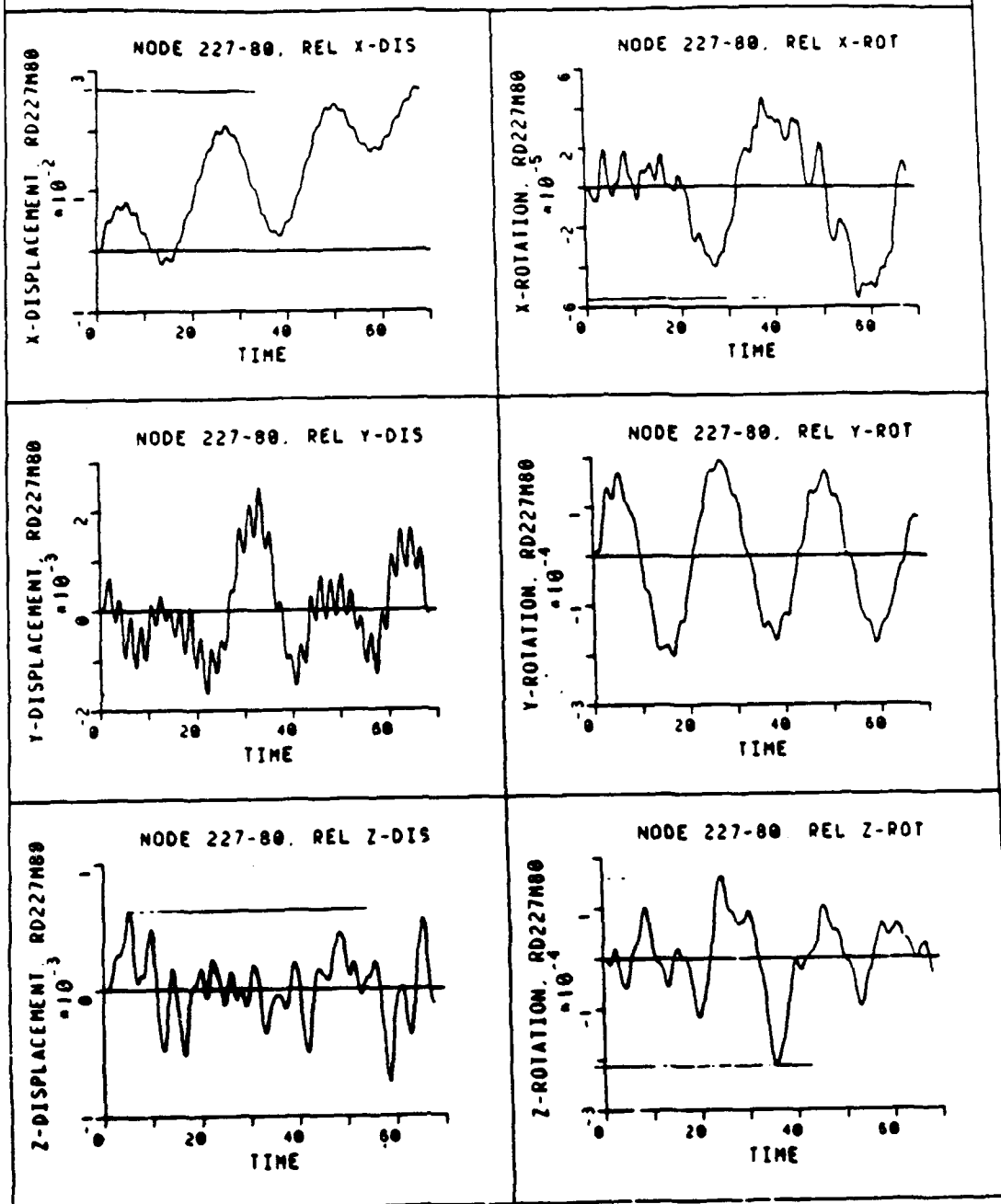


Figure 88 Node 227 vs. 80 Response E=12% X,Y,Z Displ./Rot.

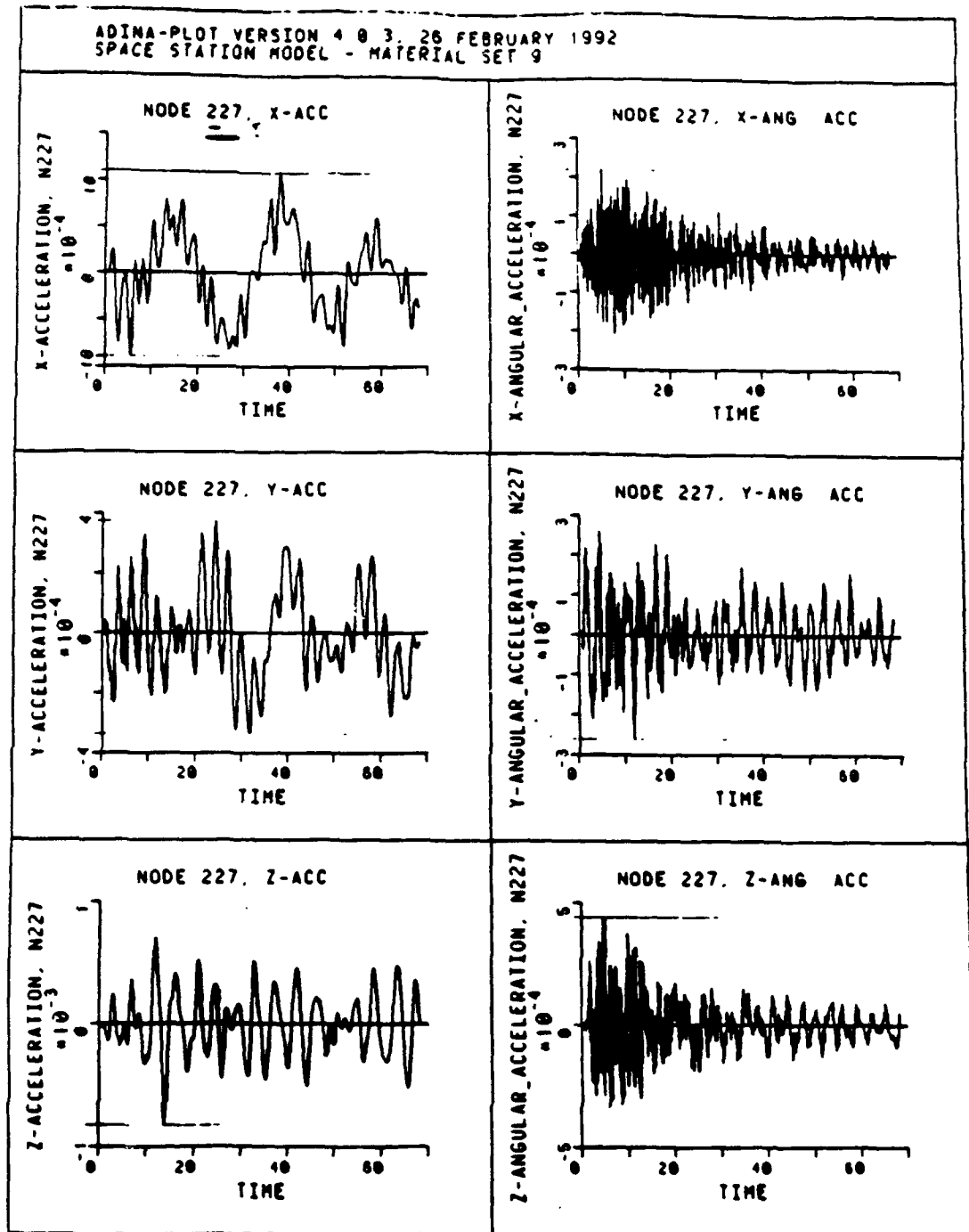


Figure 89 Node 227 Response E=12% X,Y,Z Lin./Rot. Accel.

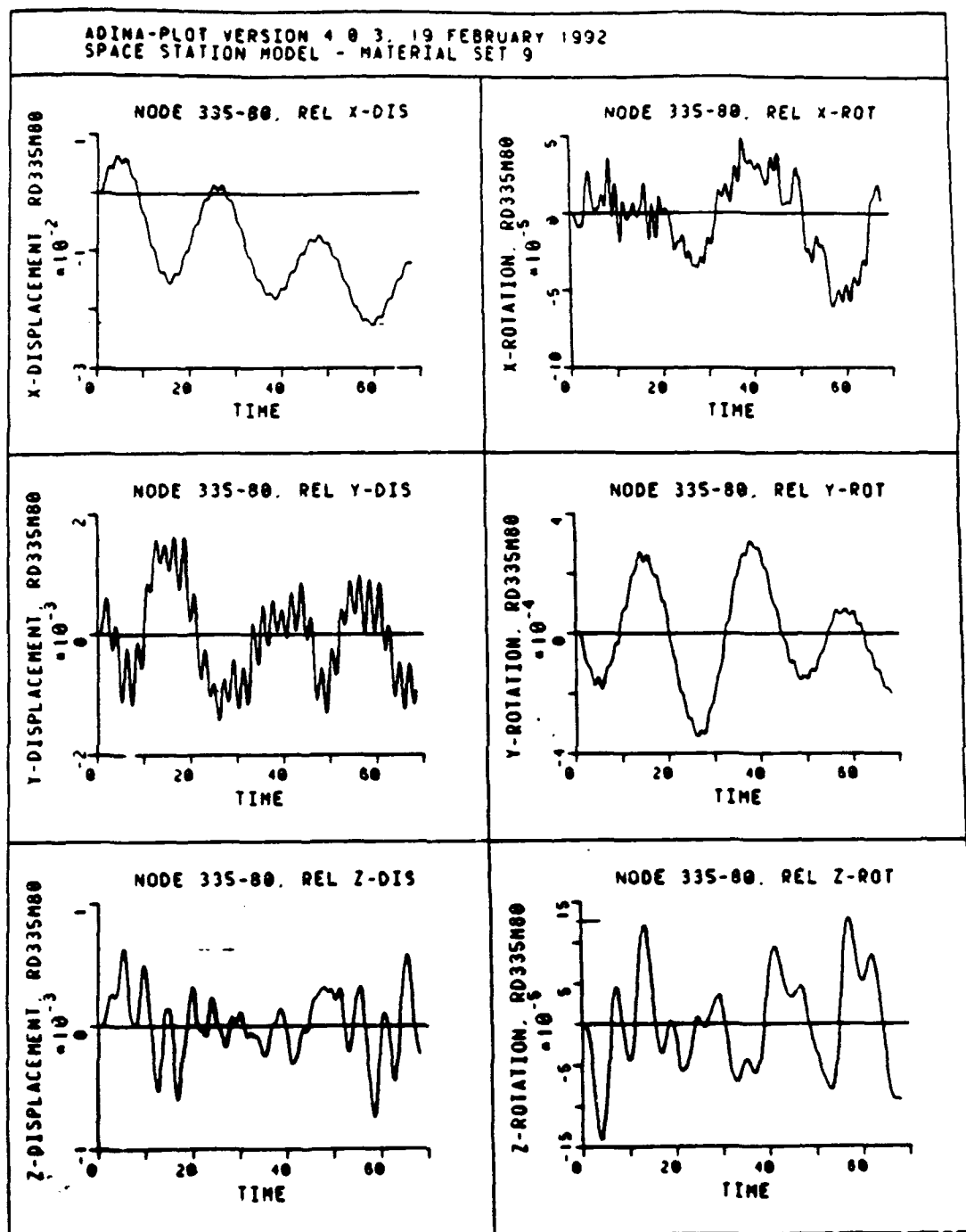


Figure 90 Node 335 vs. 80 Response E=12% X,Y,Z Displ./Rot.

ADINA-PLOT VERSION 4.0.3, 26 FEBRUARY 1992
SPACE STATION MODEL - MATERIAL SET 9

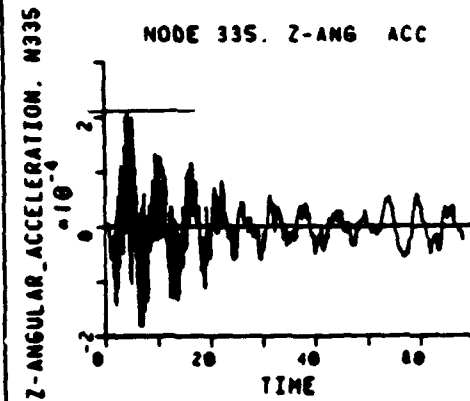
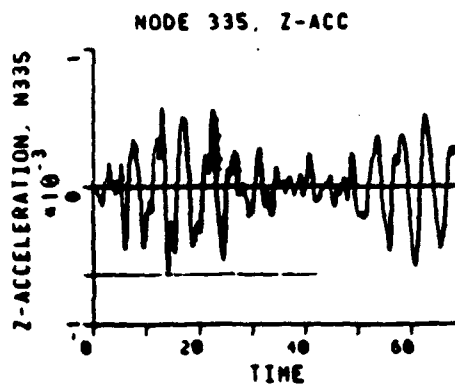
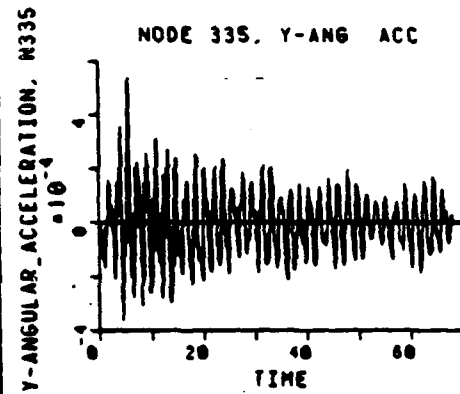
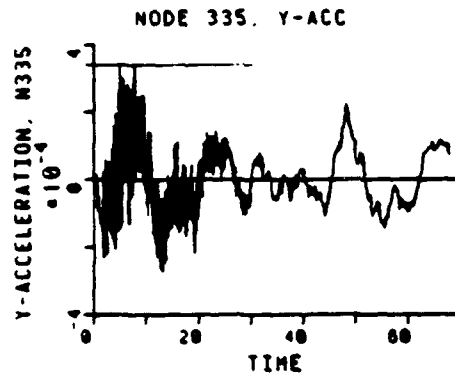
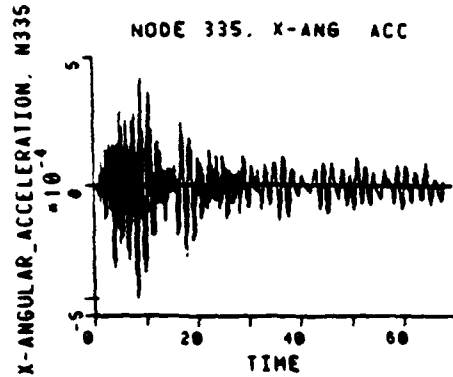
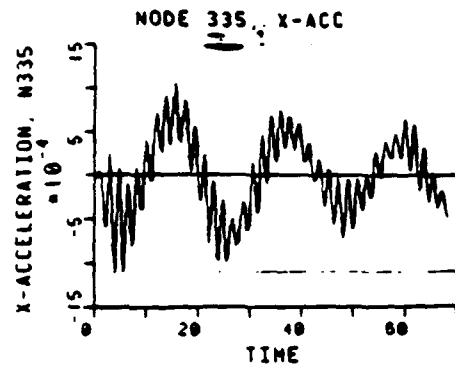


Figure 91 Node 335 Response E=12% X,Y,Z Lin./Rot. Accel.

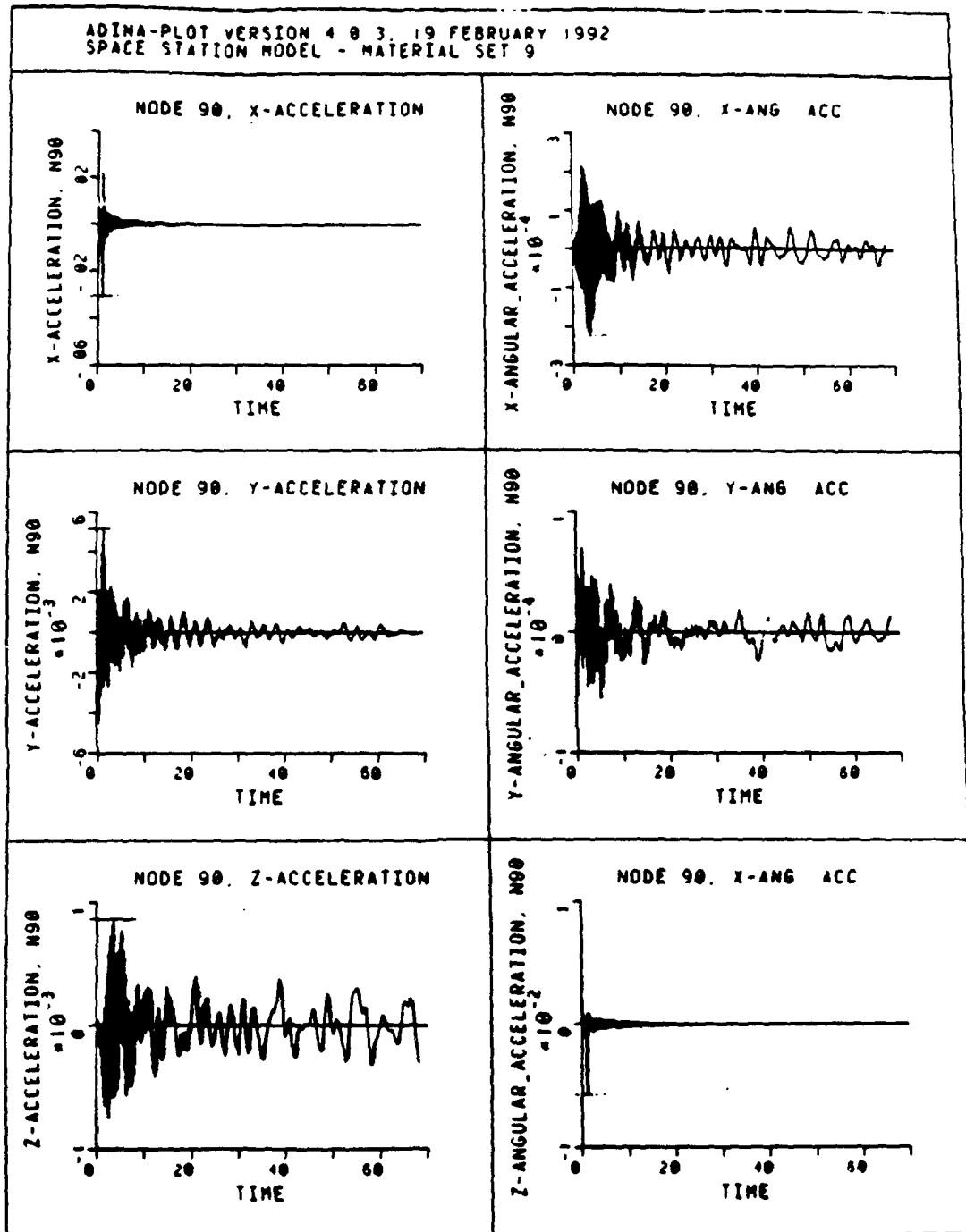


Figure 92 Node 90 Response E=12% X,Y,Z Lin./Rot. Accel.

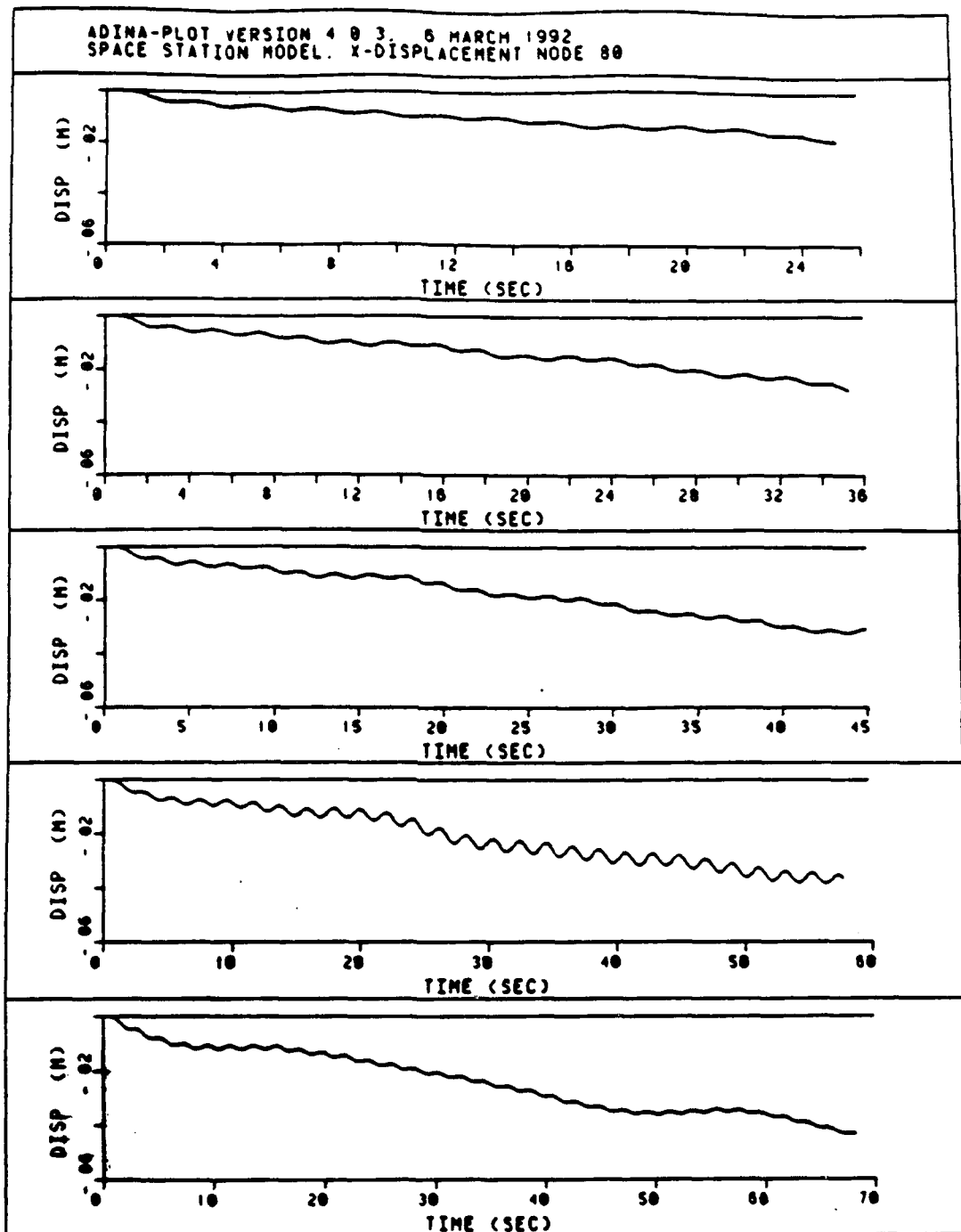


Figure 93 Comparative Plots Cases 1-5 Node 80 X-Displacement

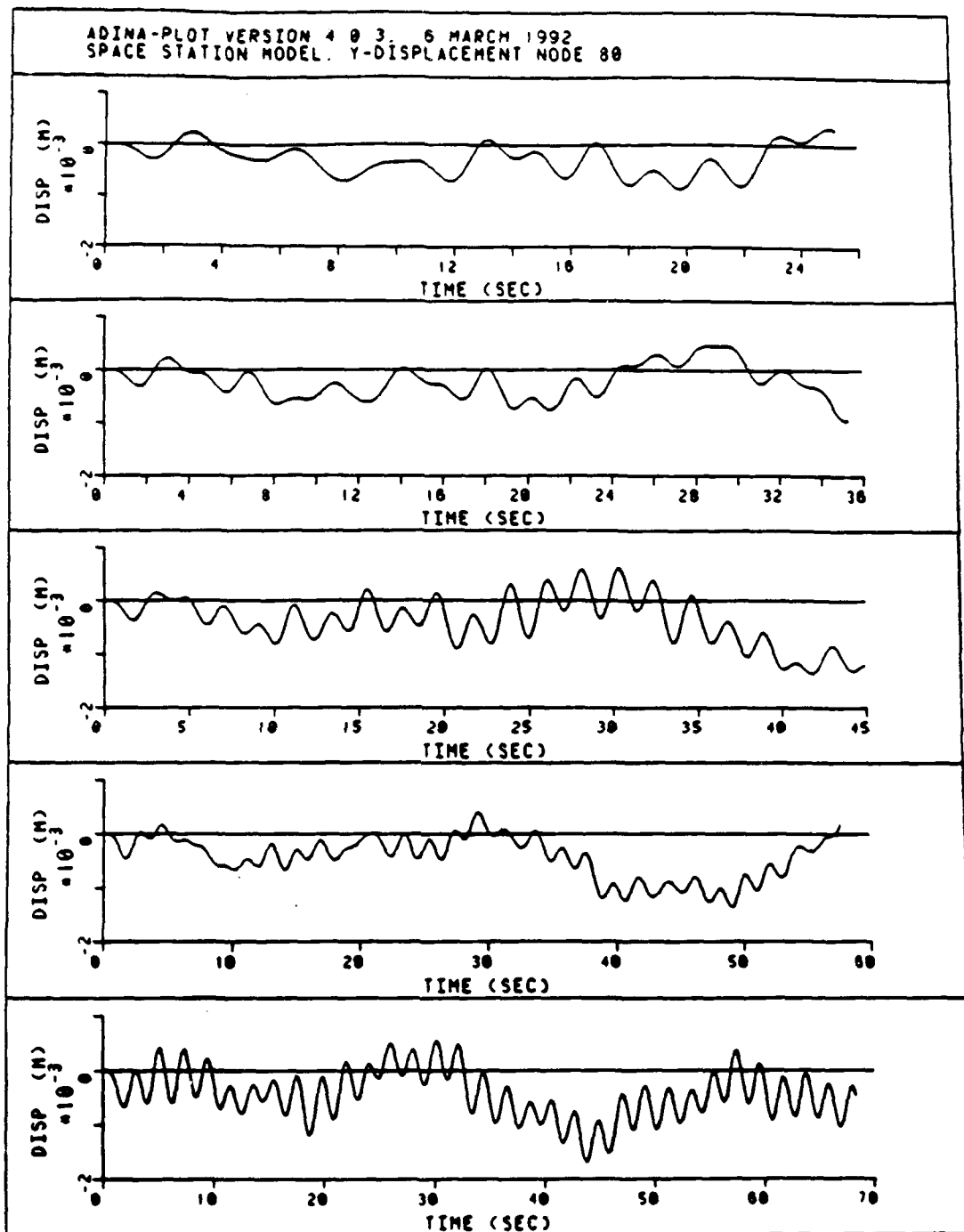


Figure 94 Comparative Plots Cases 1-5 Node 80 Y-Displacement

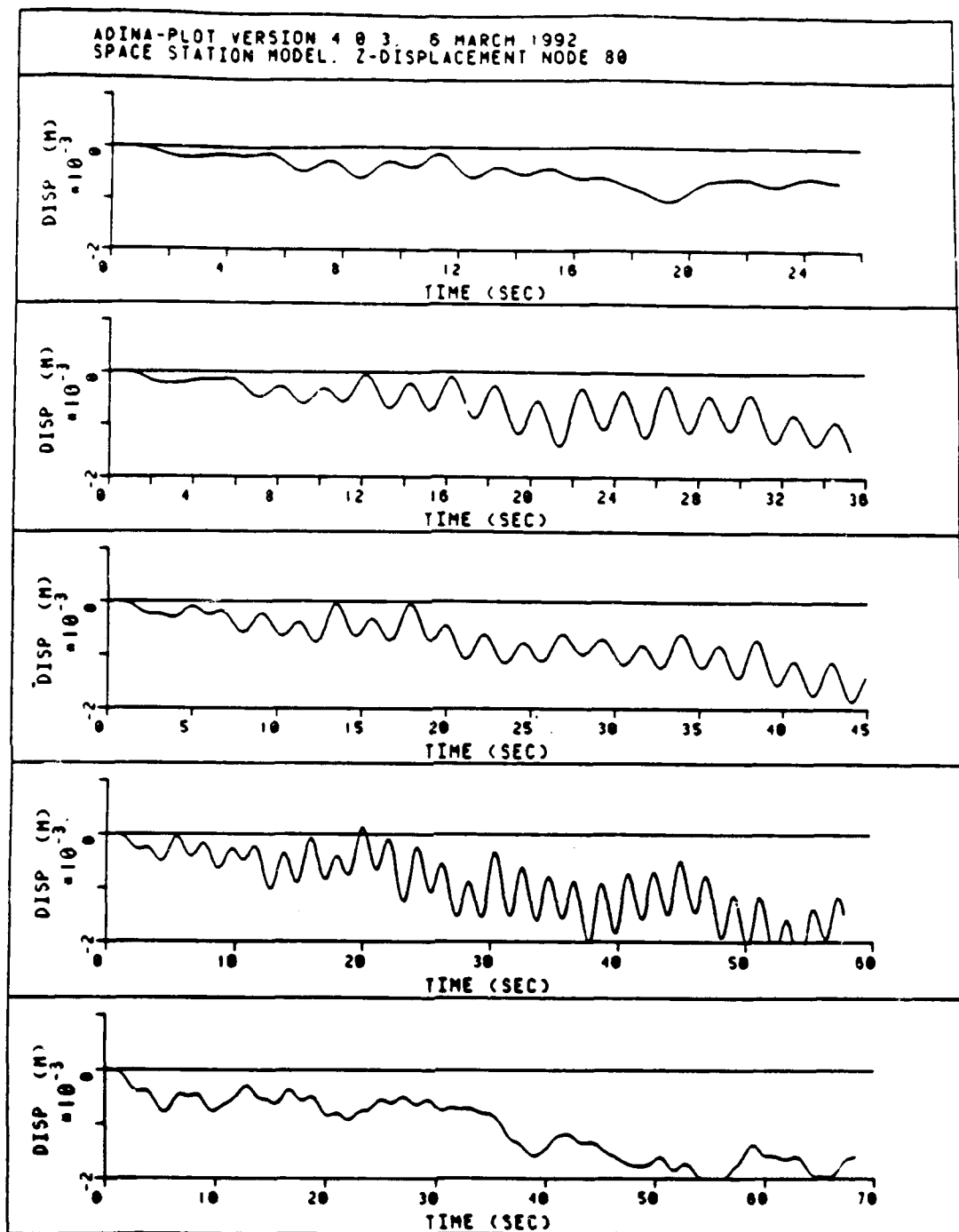


Figure 95 Comparative Plots Cases 1-5 Node 80 Z-Displacement

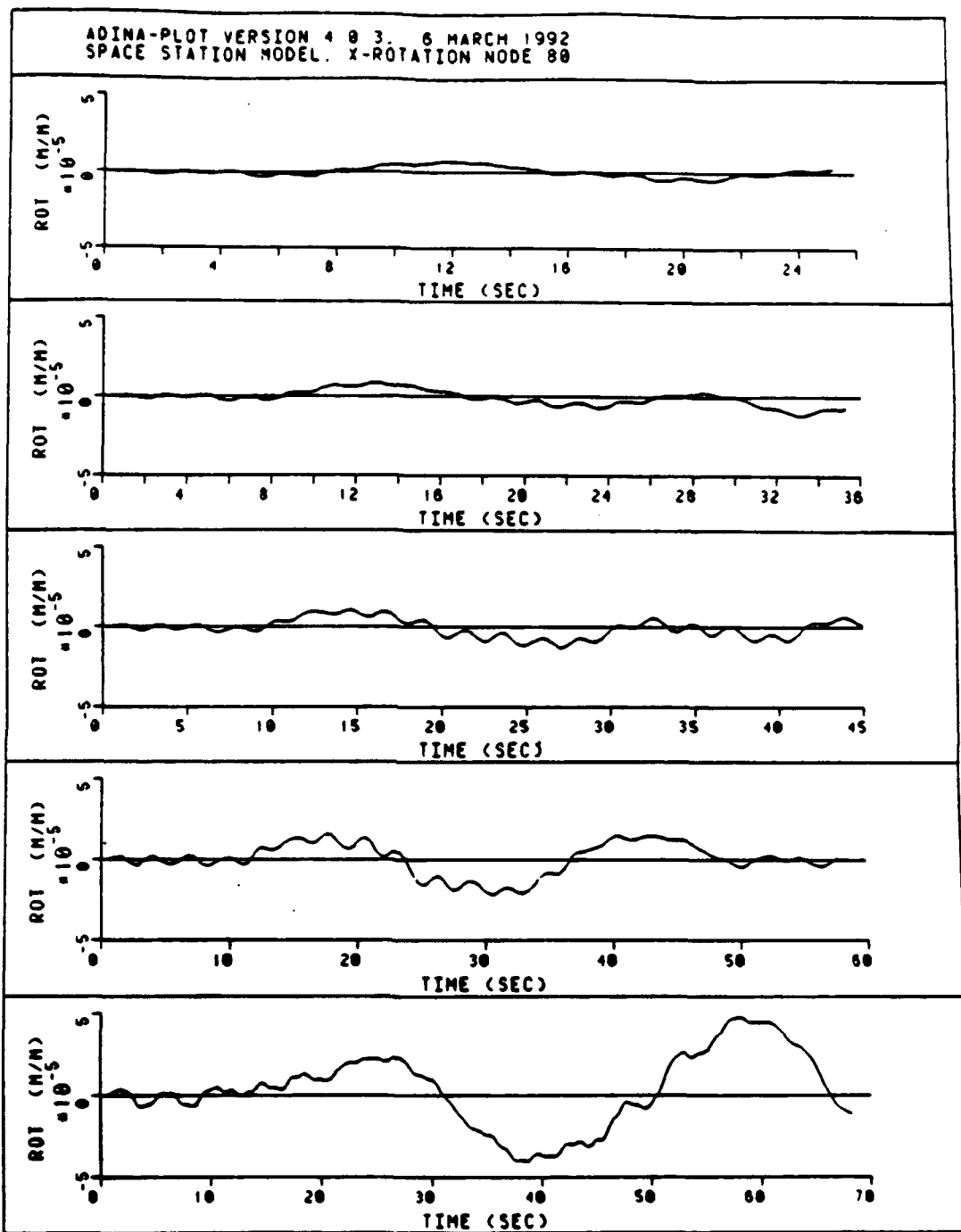


Figure 96 Comparative Plots Cases 1-5 Node 80 X-Rotation

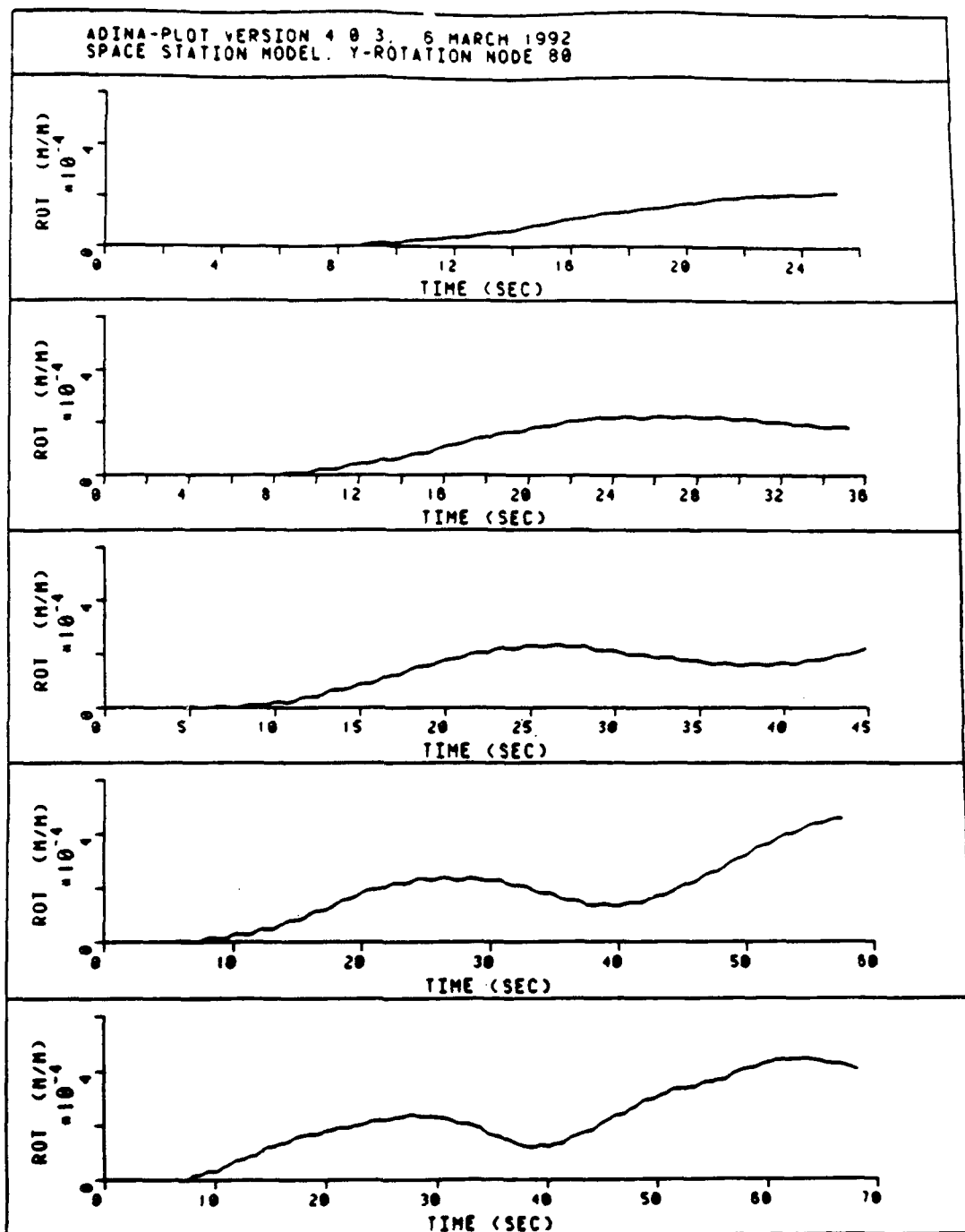


Figure 97 Comparative Plots Cases 1-5 Node 80 Y-Rotation

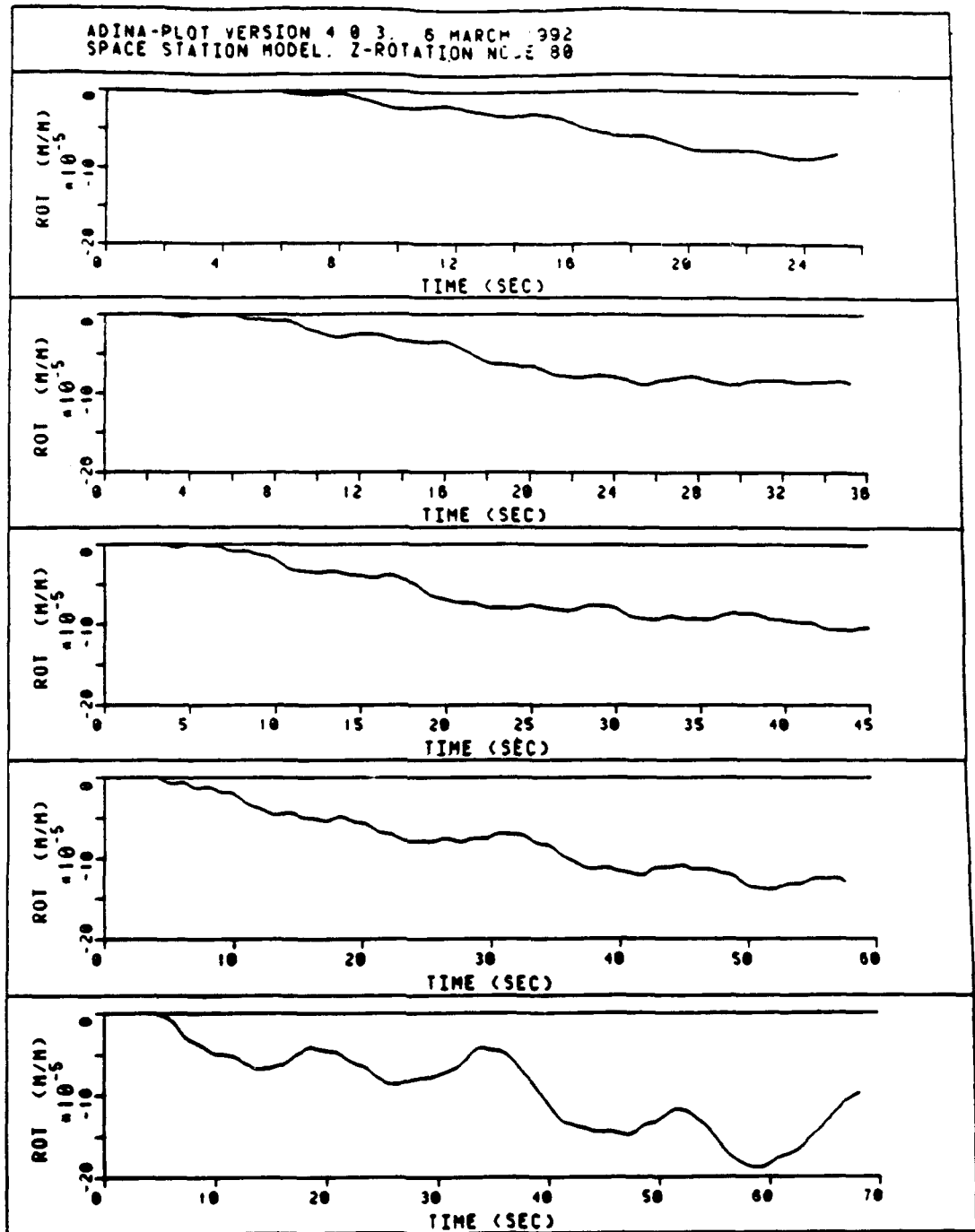


Figure 98 Comparative Plots Cases 1-5 Node 80 Z-Rotation

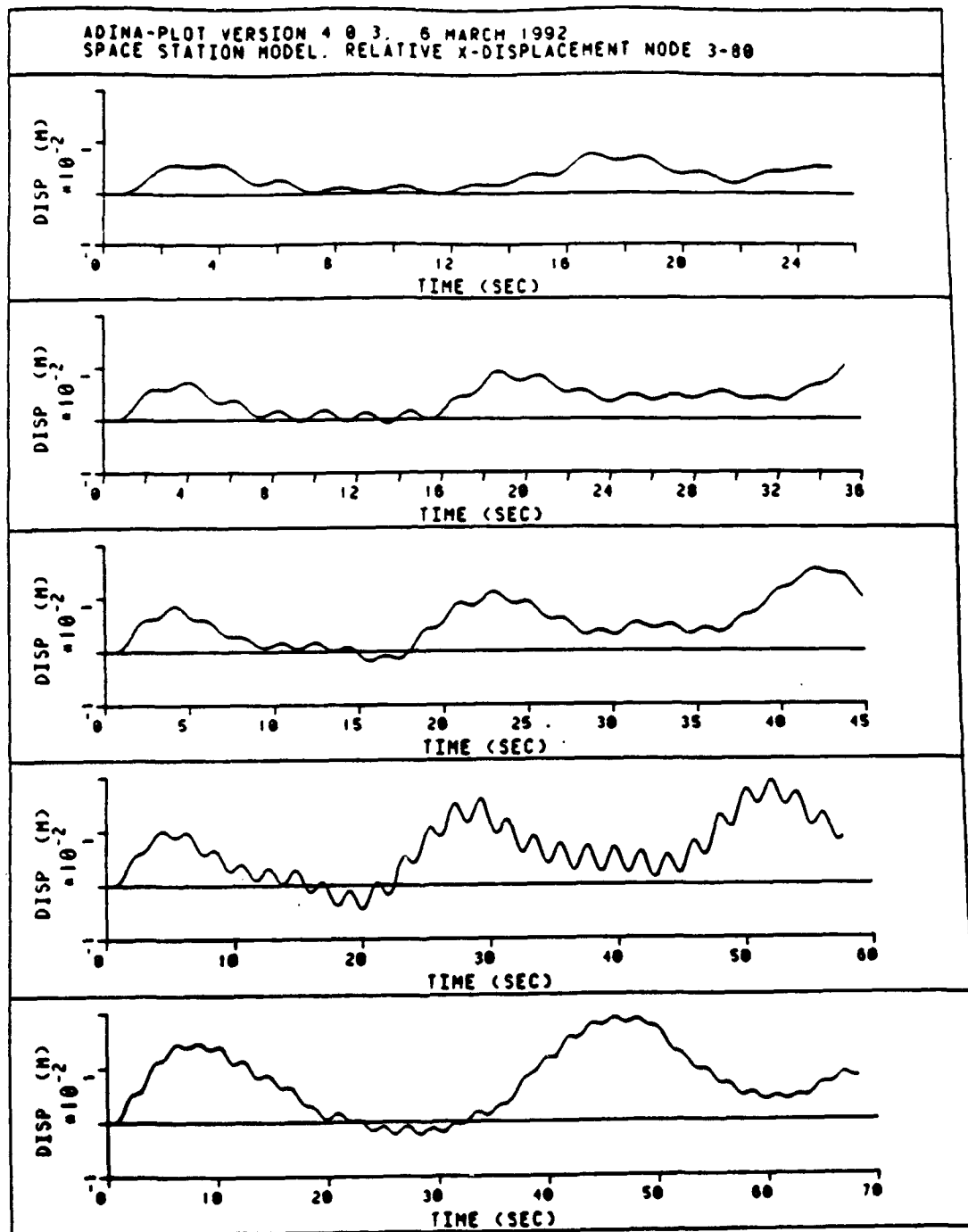


Figure 99 Comparative Plots Cases 1-5 Node 3 vs. 80 X-Displ.

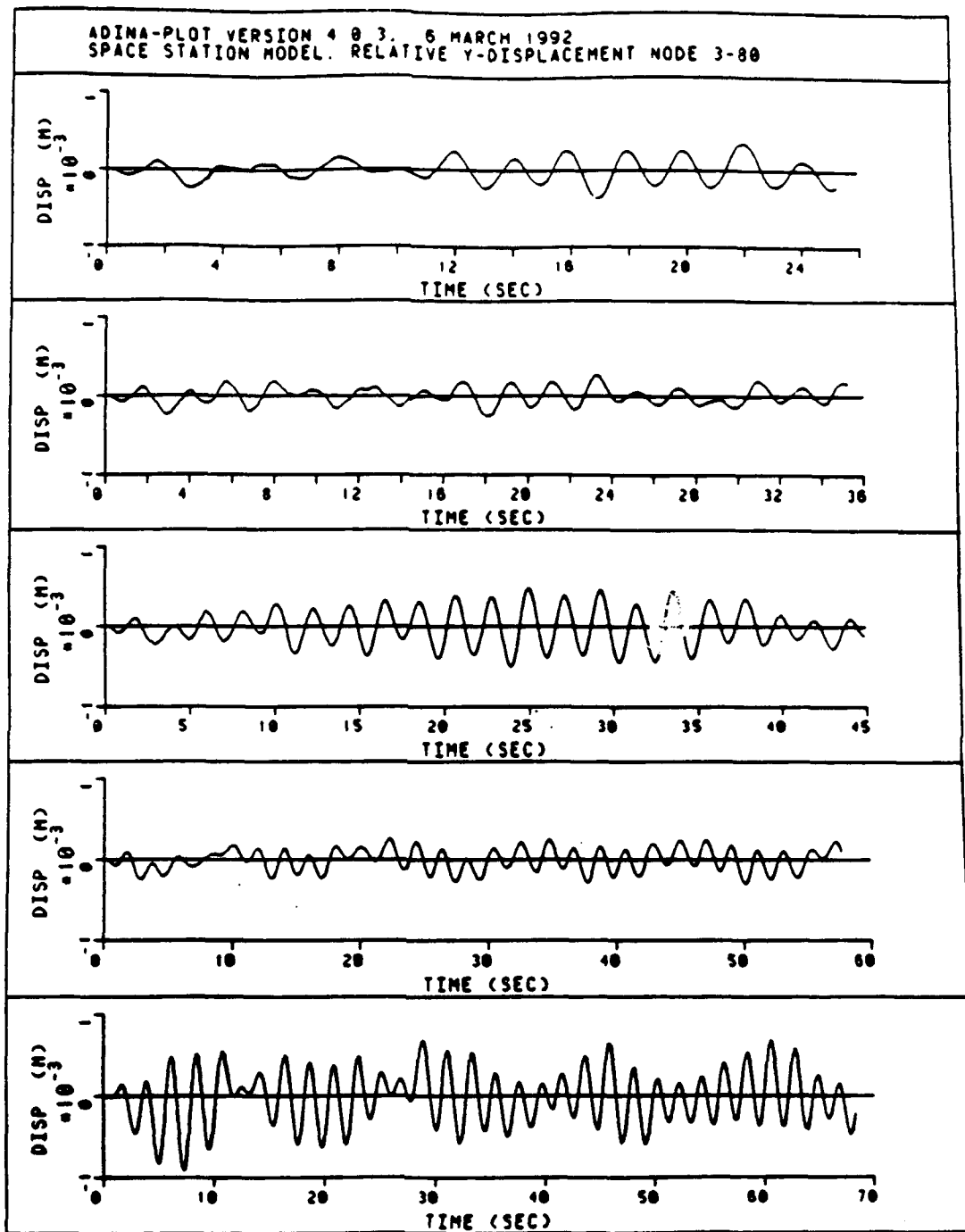


Figure 100 Comparative Plots Cases 1-5 Node 3 vs. 80 Y-Disp.

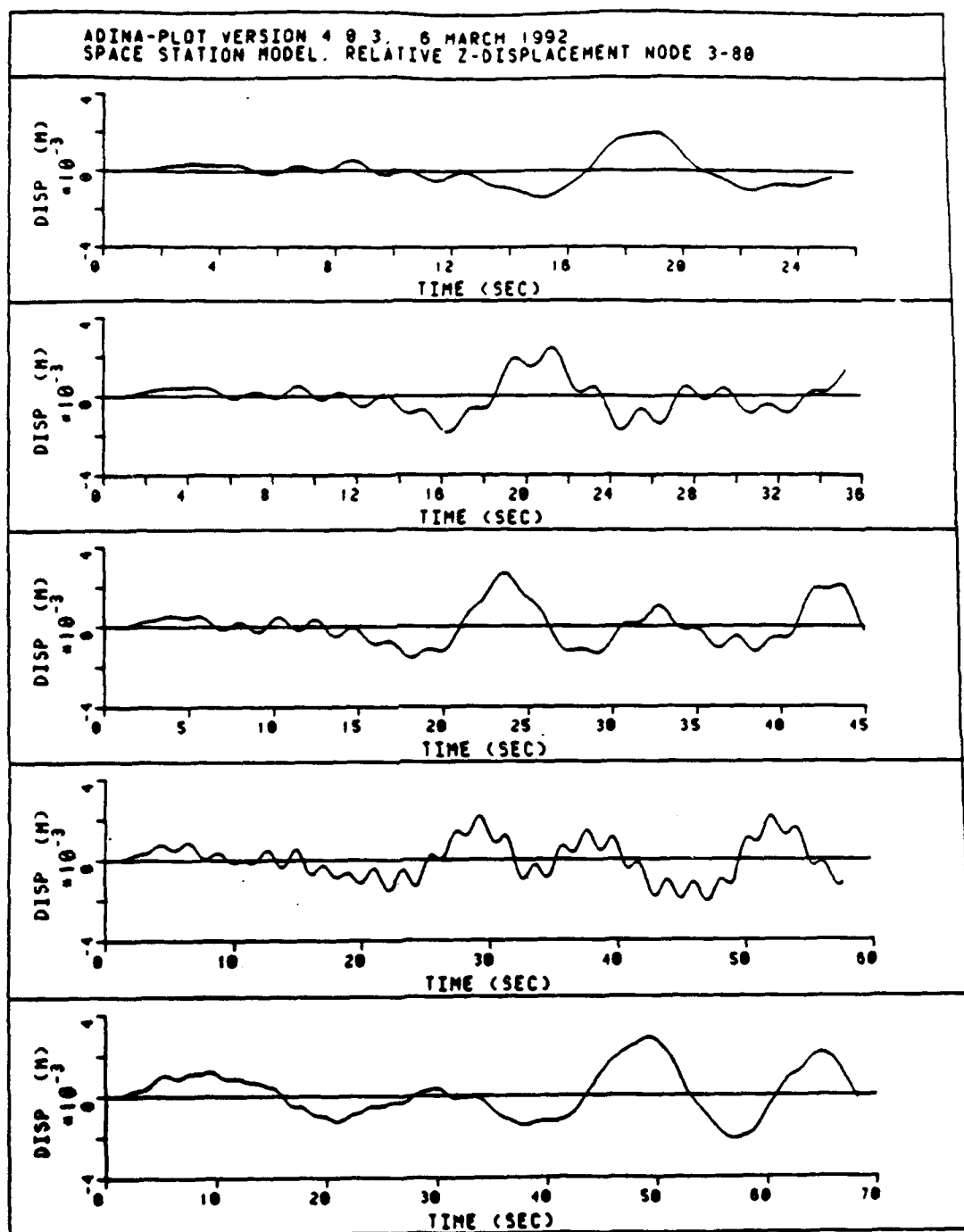


Figure 101 Comparative Plots Cases 1-5 Node 3 vs. 80 Z-Disp.

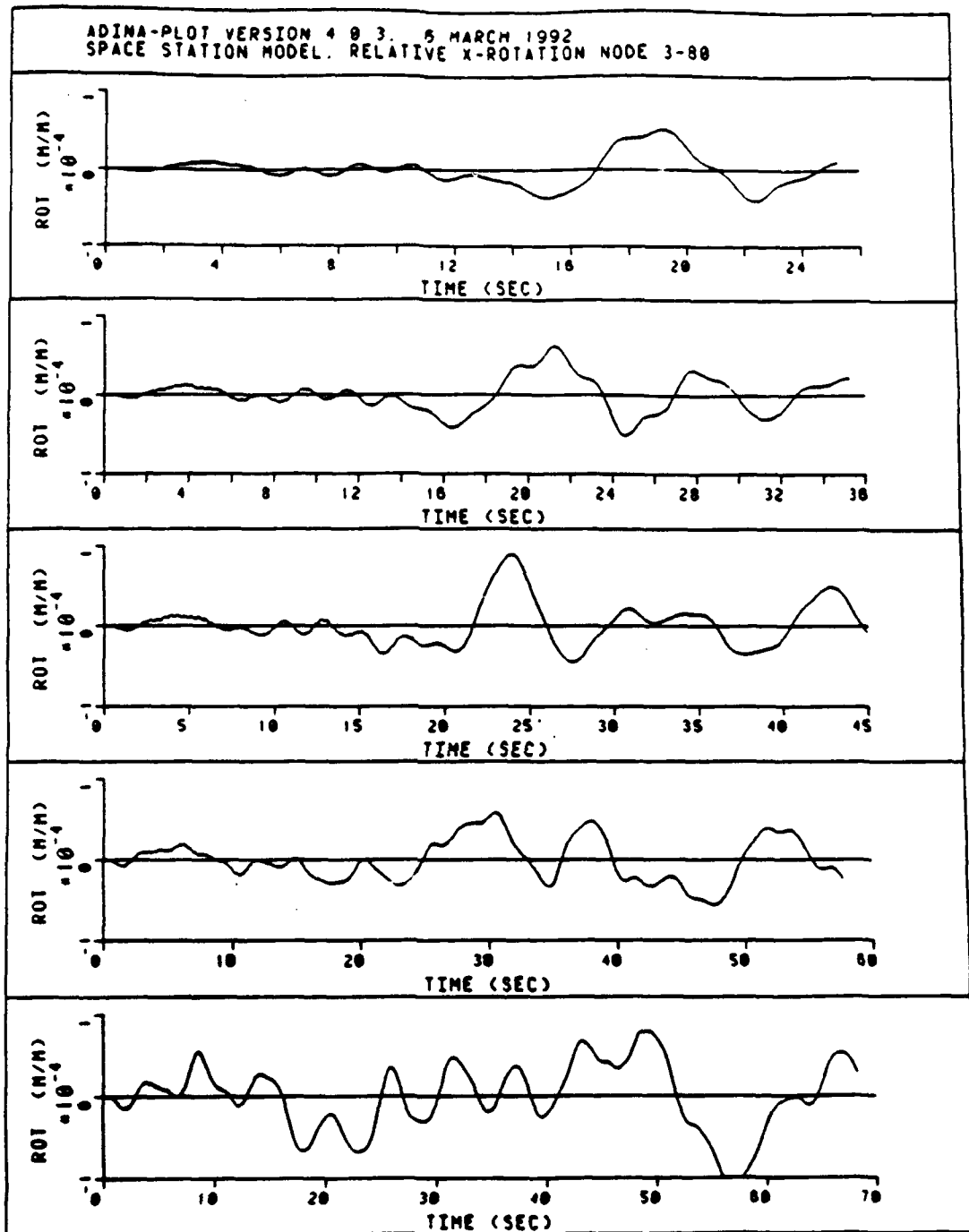


Figure 102 Comparative Plots Cases 1-5 Node 3 vs. 80 X-Rot.

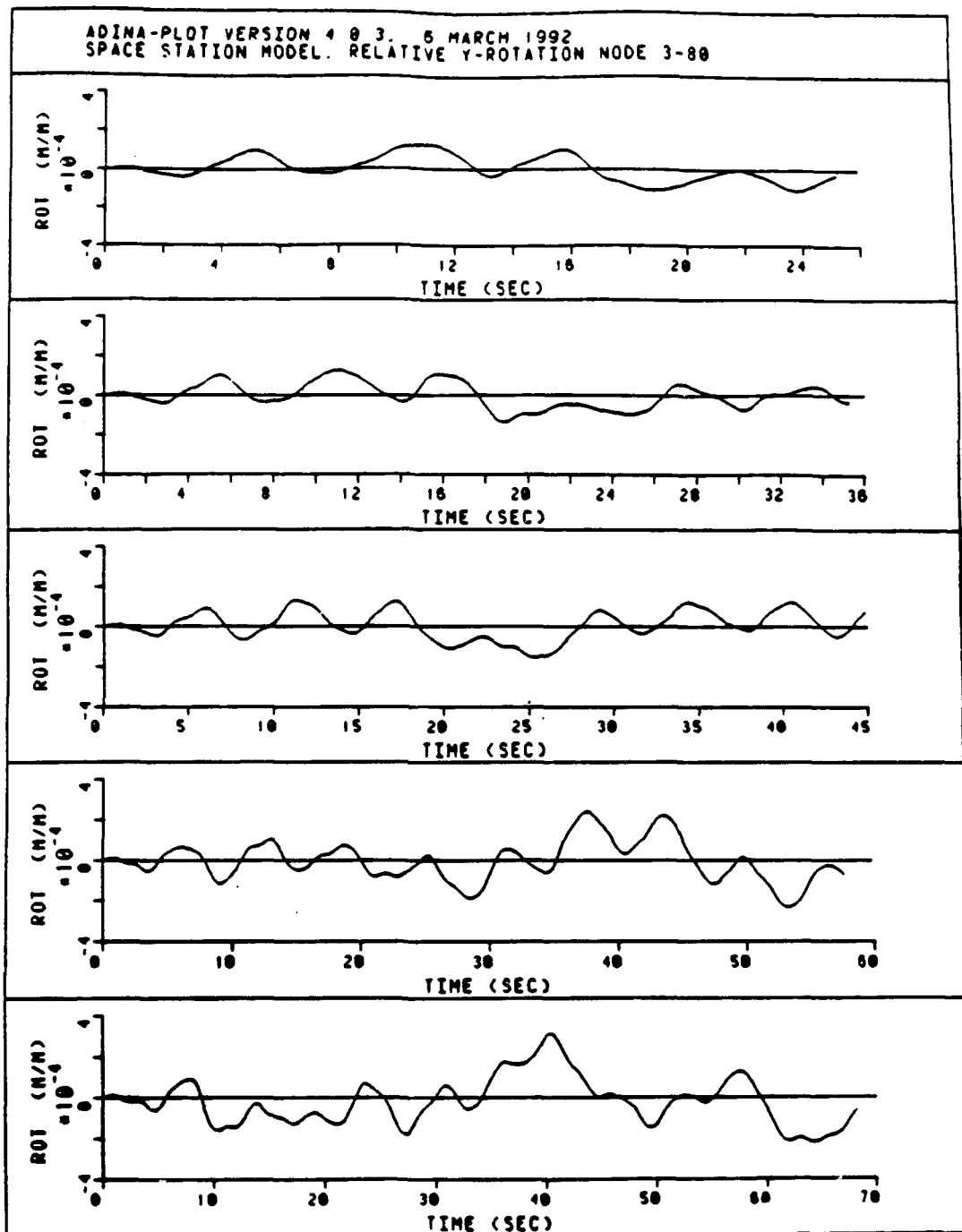


Figure 103 Comparative Plots Cases 1-5 Node 3 vs. 80 Y-Rot.

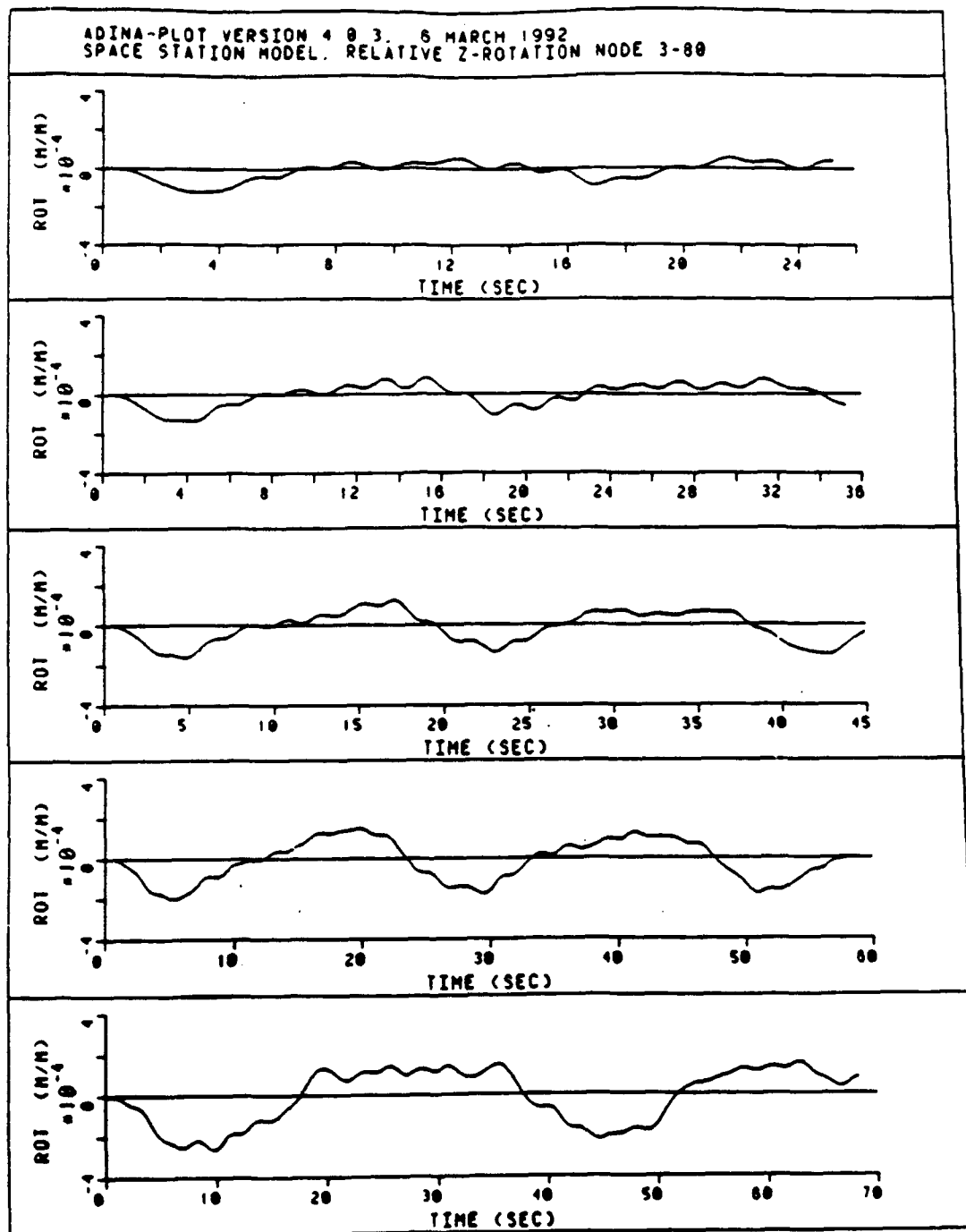


Figure 104 Comparative Plots Case 1-5 Node 3 vs. 80 Z-Rot.

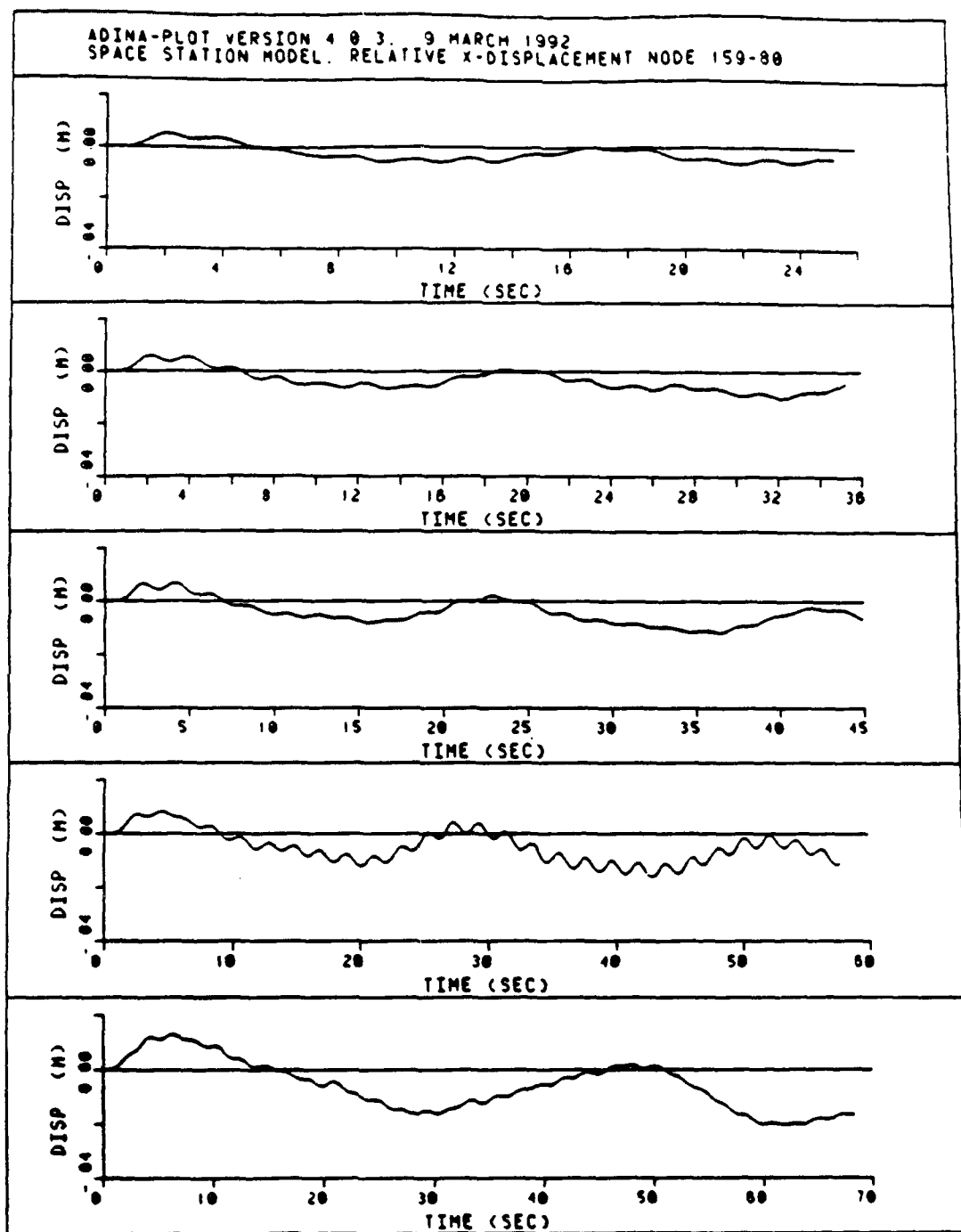


Figure 105 Comparative Plots Case 1-5 Node 159 vs. 80 X-Dis.

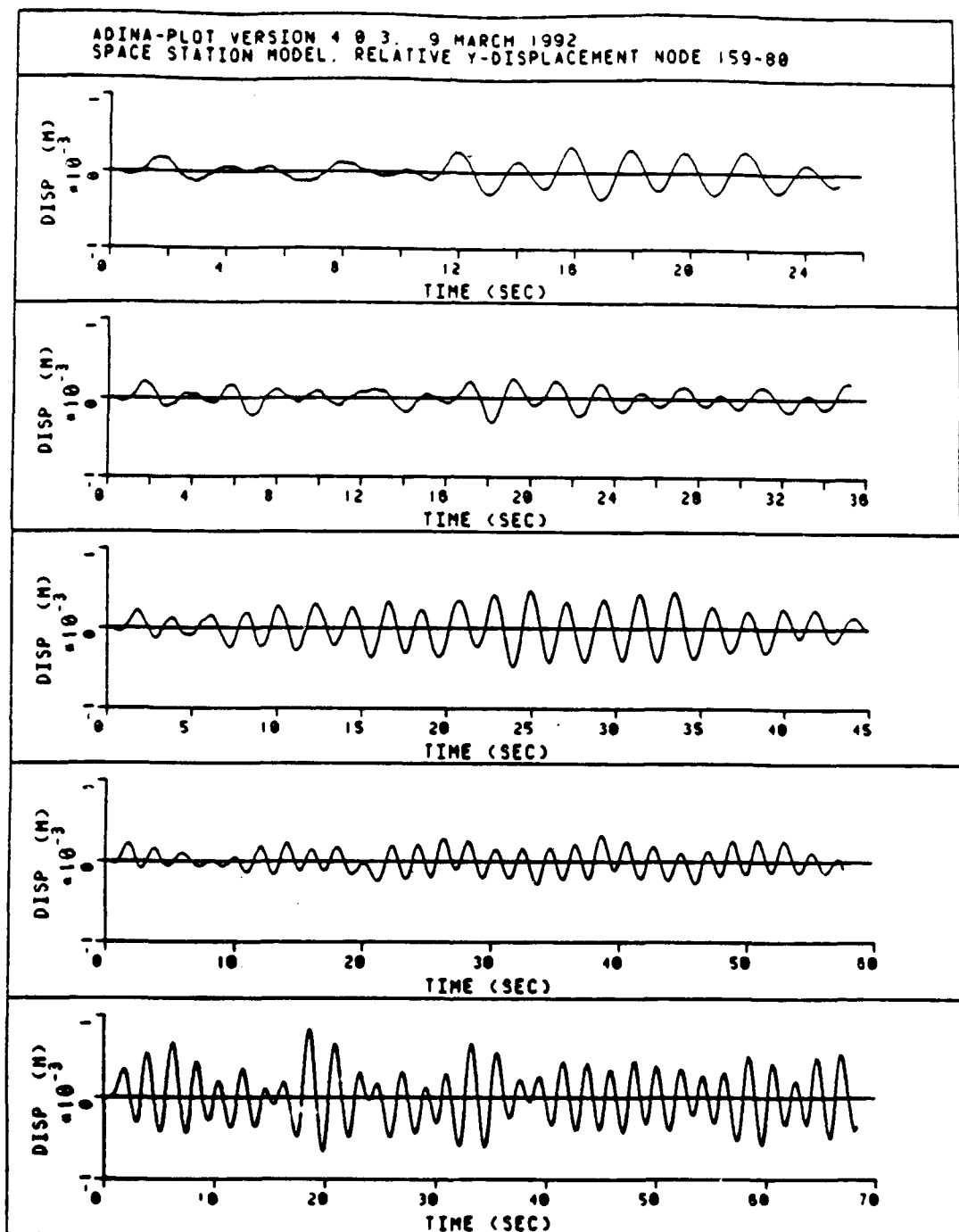


Figure 106 Comparative Plots Case 1-5 Node 159 vs. 80 Y-Dis.

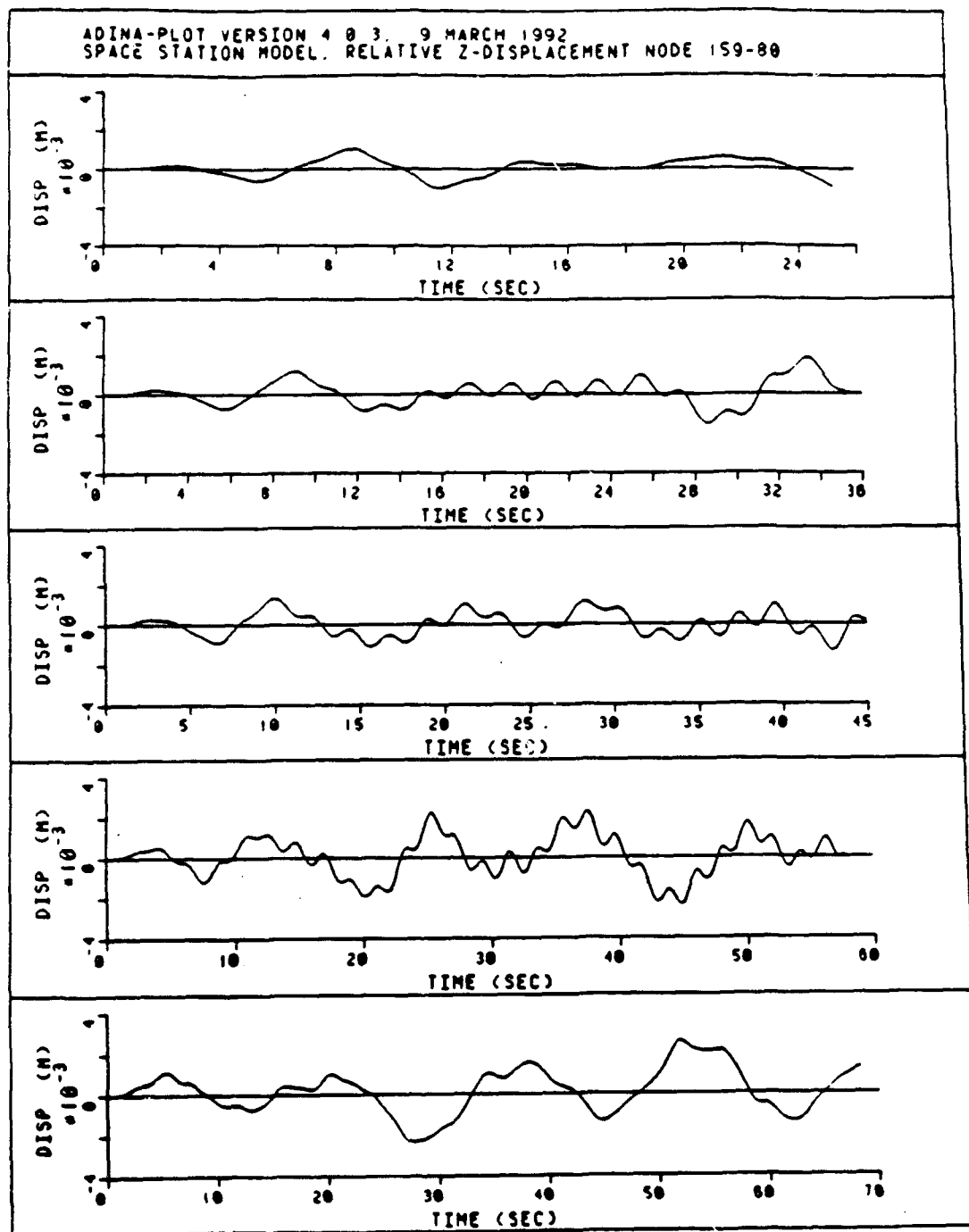


Figure 107 Comparative Plots Case 1-5 Node 159 vs. 80 Z-Dis.

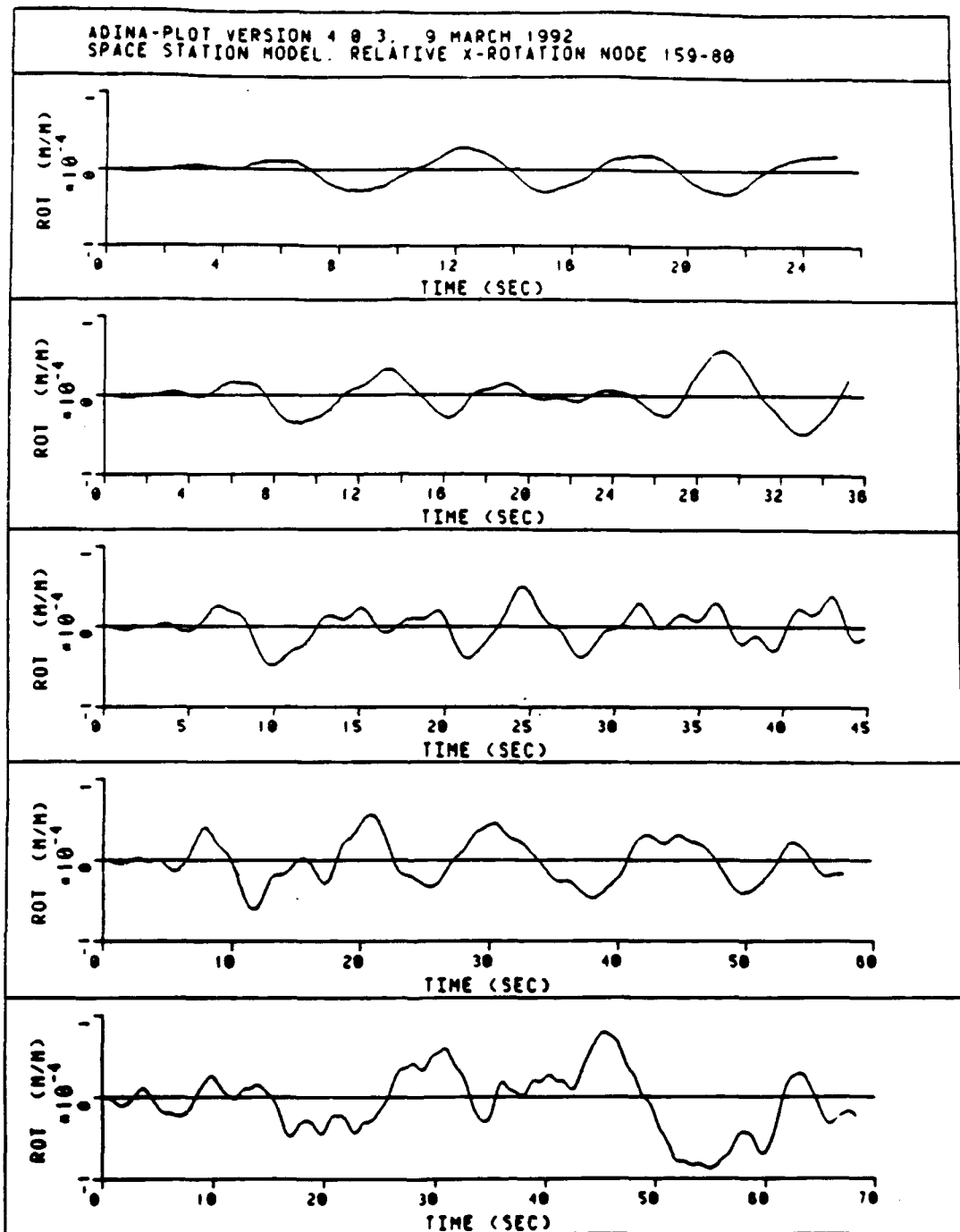


Figure 108 Comparative Plots Case 1-5 Node 159 vs. 80 X-Rot.

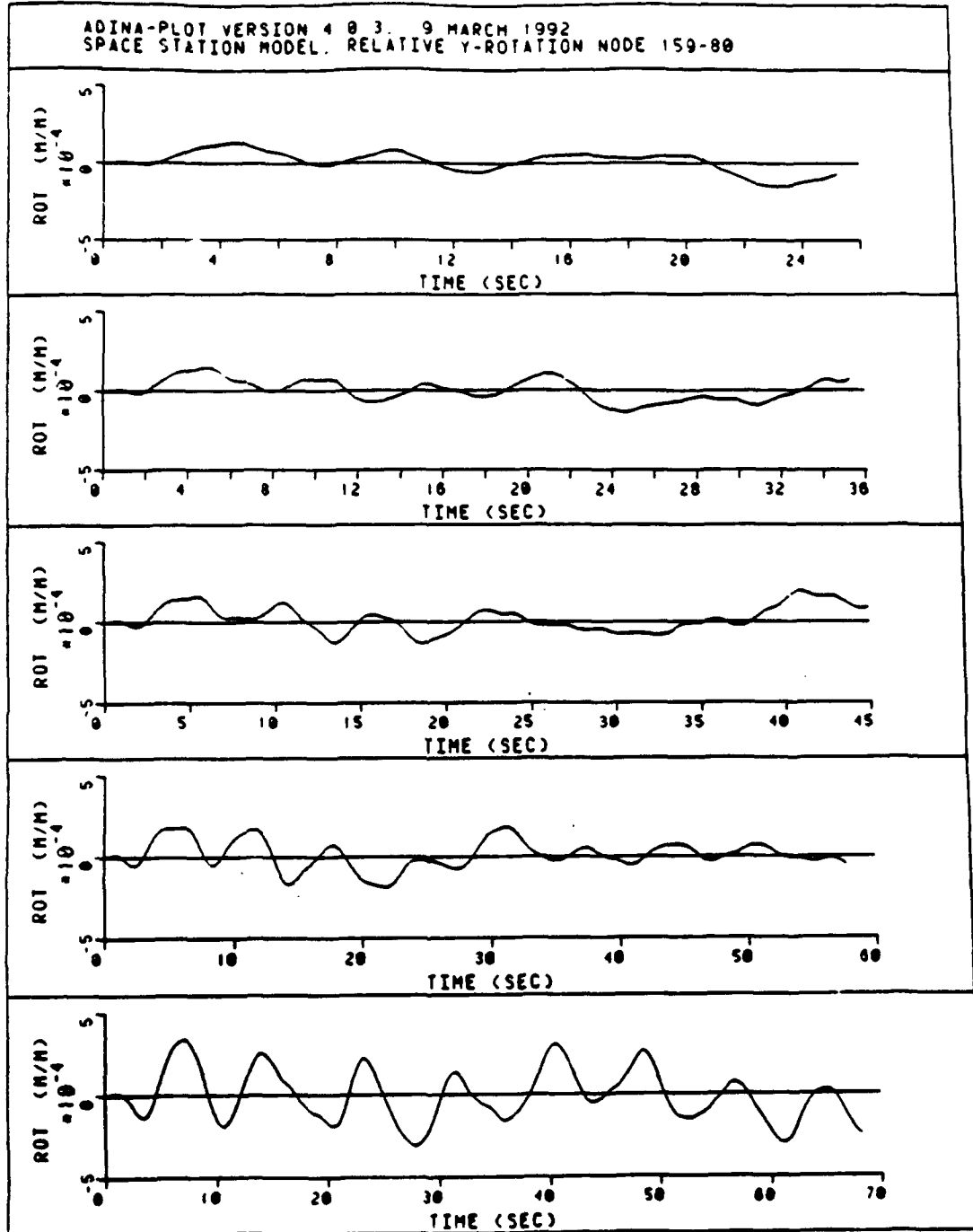


Figure 109 Comparative Plot Case 1-5 Node 159 vs. 80 Y-Rot.

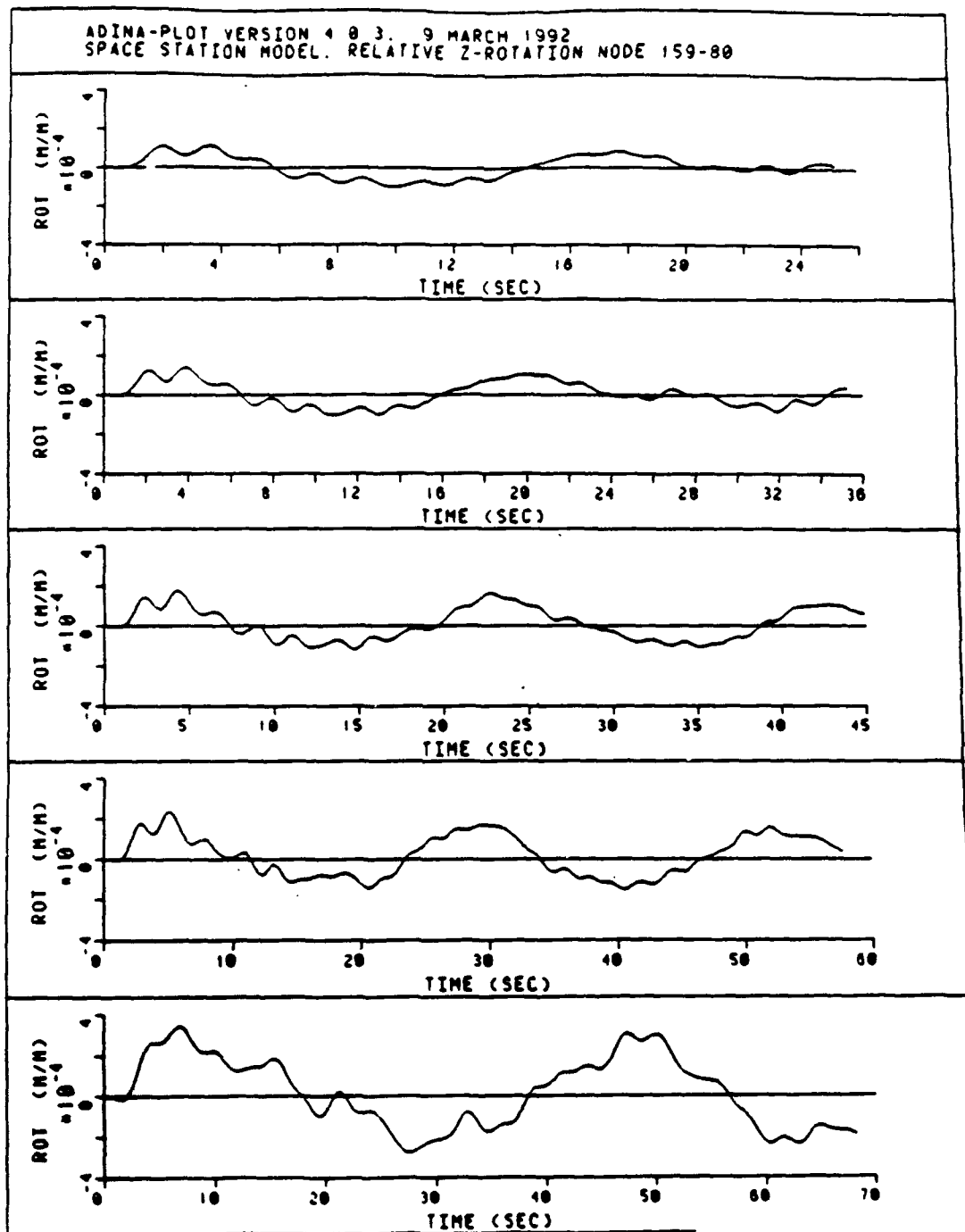


Figure 110 Comparative Plot Case 1-5 Node 159-80 Z-Rot.

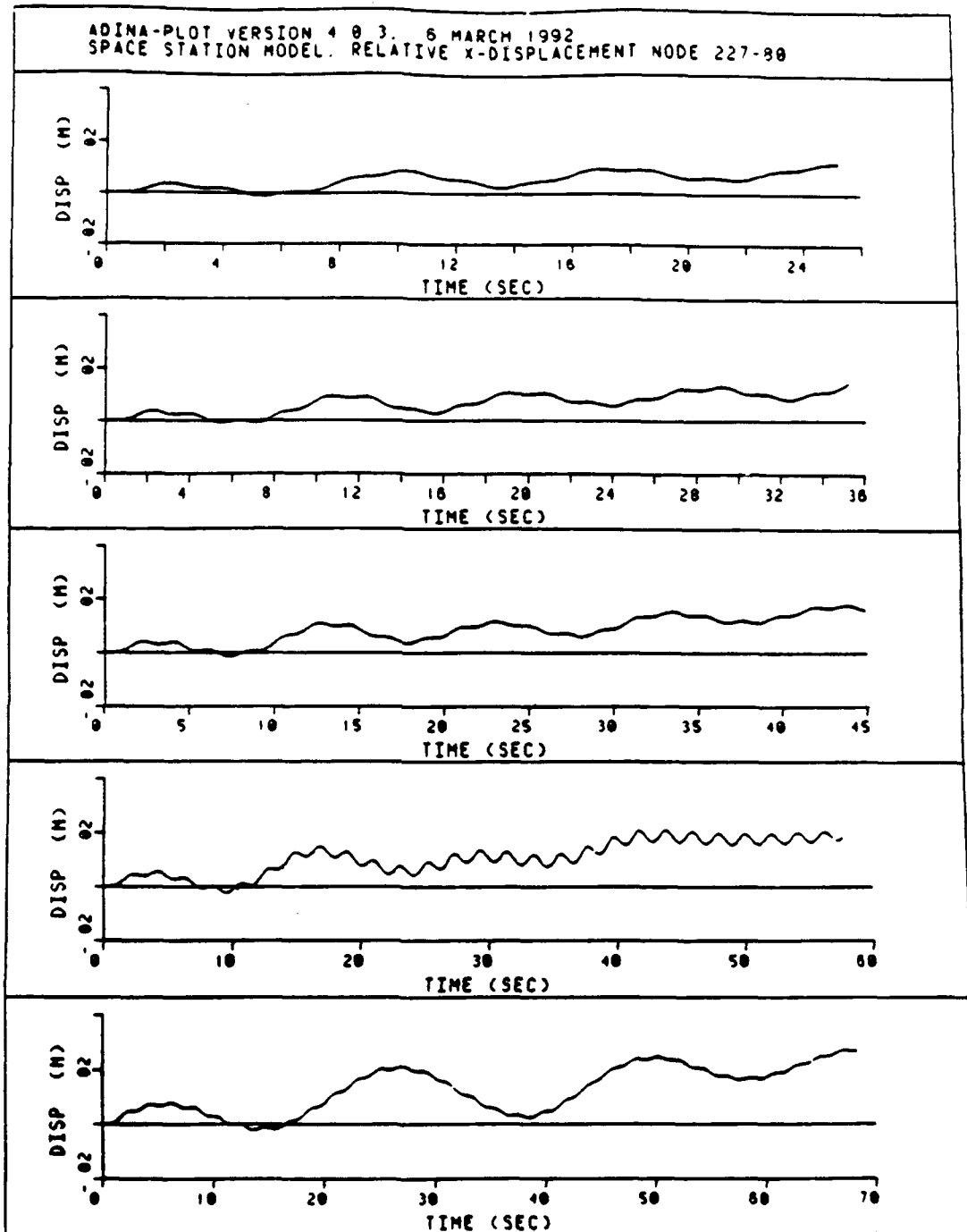


Figure 111 Comparative Plot Case 1-5 Node 227 vs. 80 X-Disp.

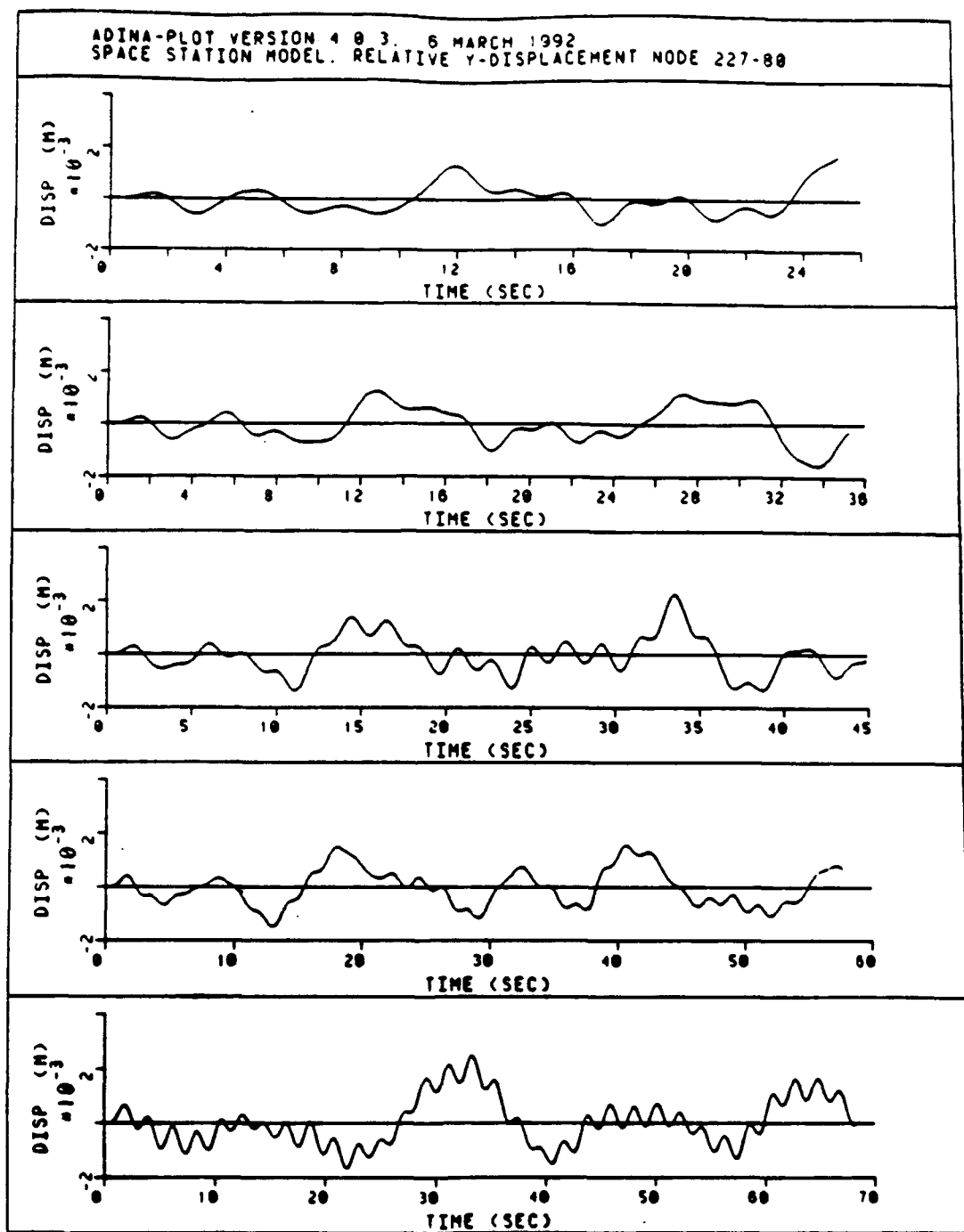


Figure 112 Comparative Plot Case 1-5 Node 227 vs. 80 Y-Disp.

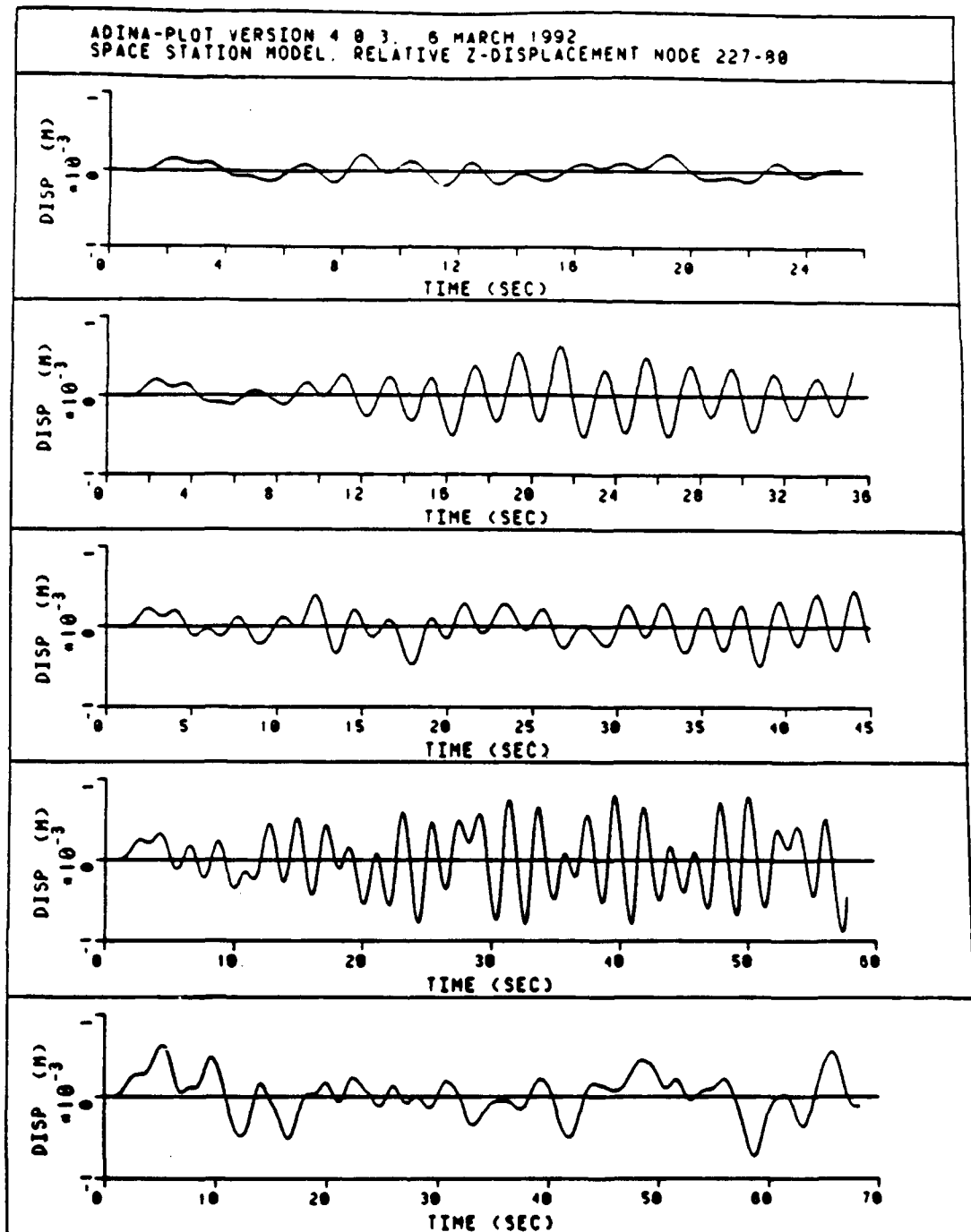


Figure 113 Comparative Plot Case 1-5 Node 227 vs. 80 Z-Disp.

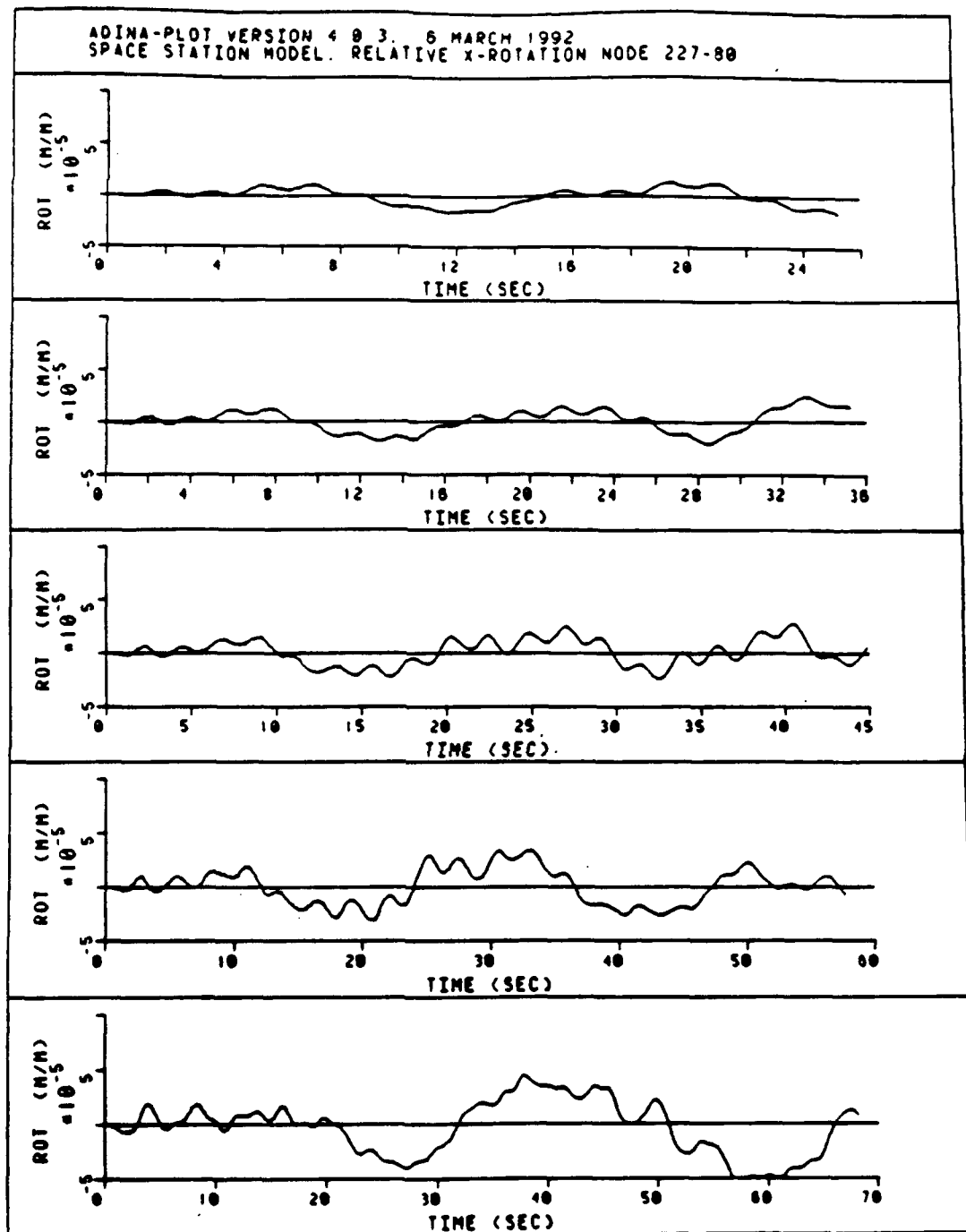


Figure 114 Comparative Plot Case 1-5 Node 227 vs. 80 X-Rot.

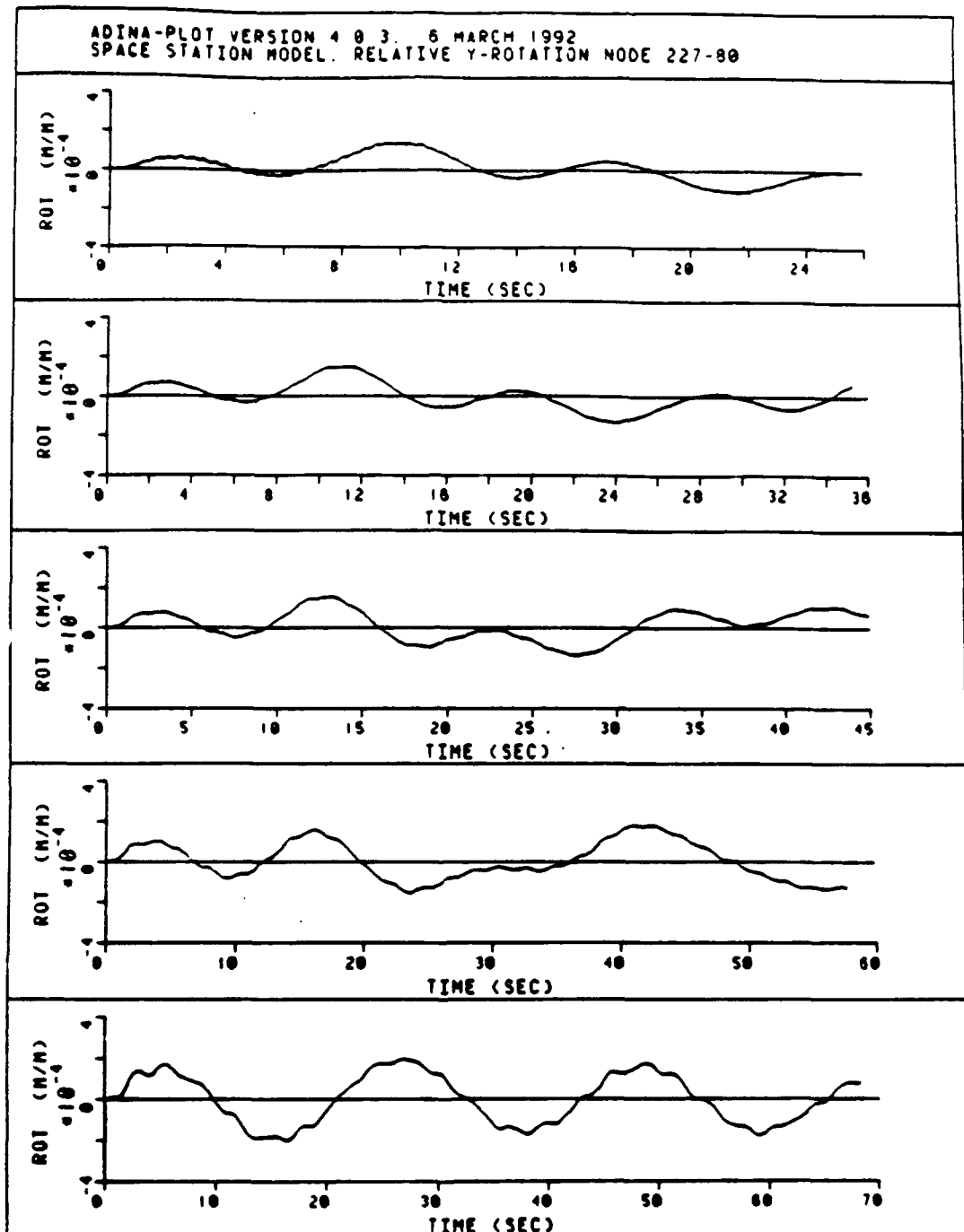


Figure 115 Comparative Plot Case 1-5 Node 227 vs. 80 Y-Rot.

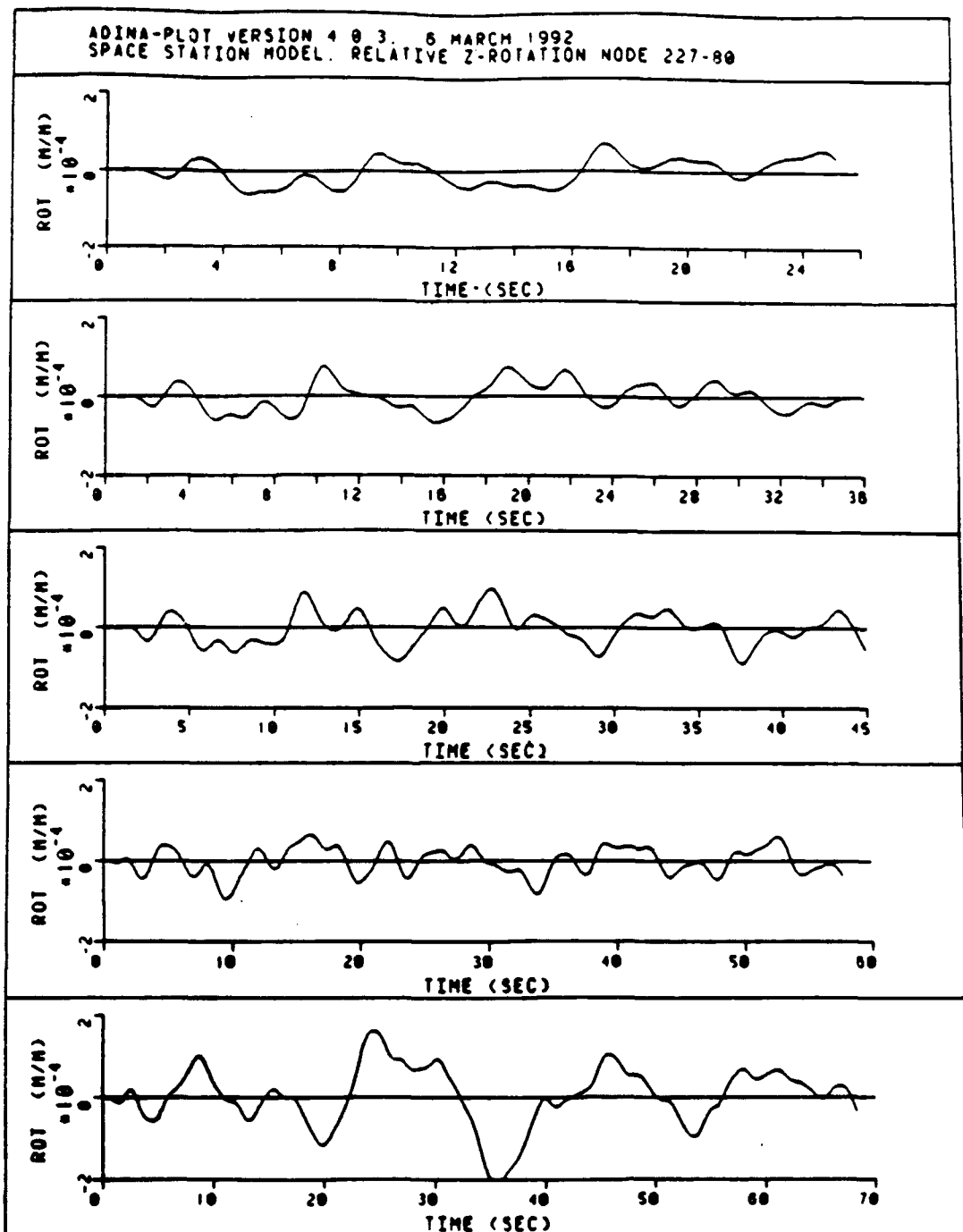


Figure 116 Comparative Plot Cases 1-5 Node 227 vs. 80 Z-Rot.

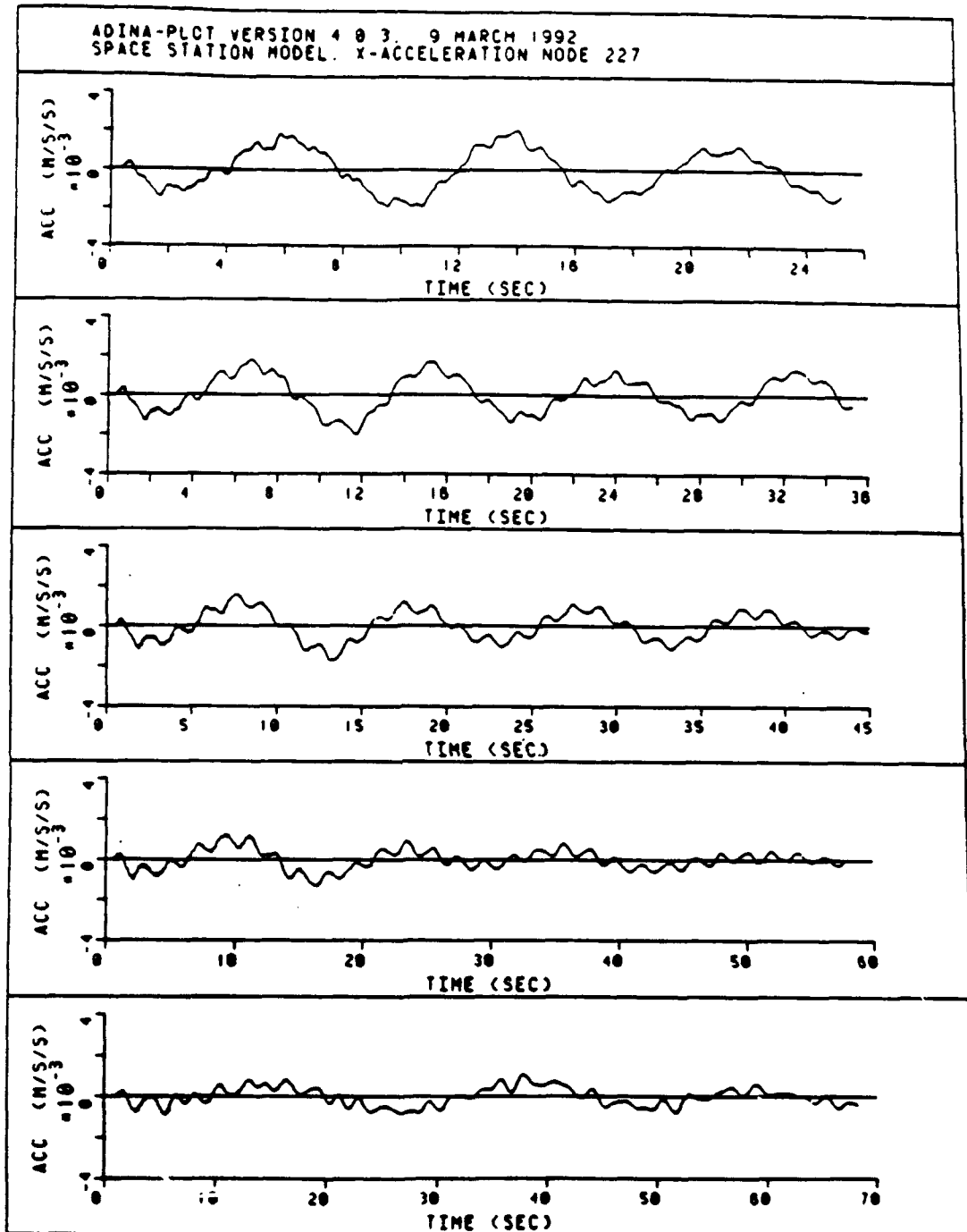


Figure 117 Comparison Plot Cases 1-5 Node 227 X-Accel.

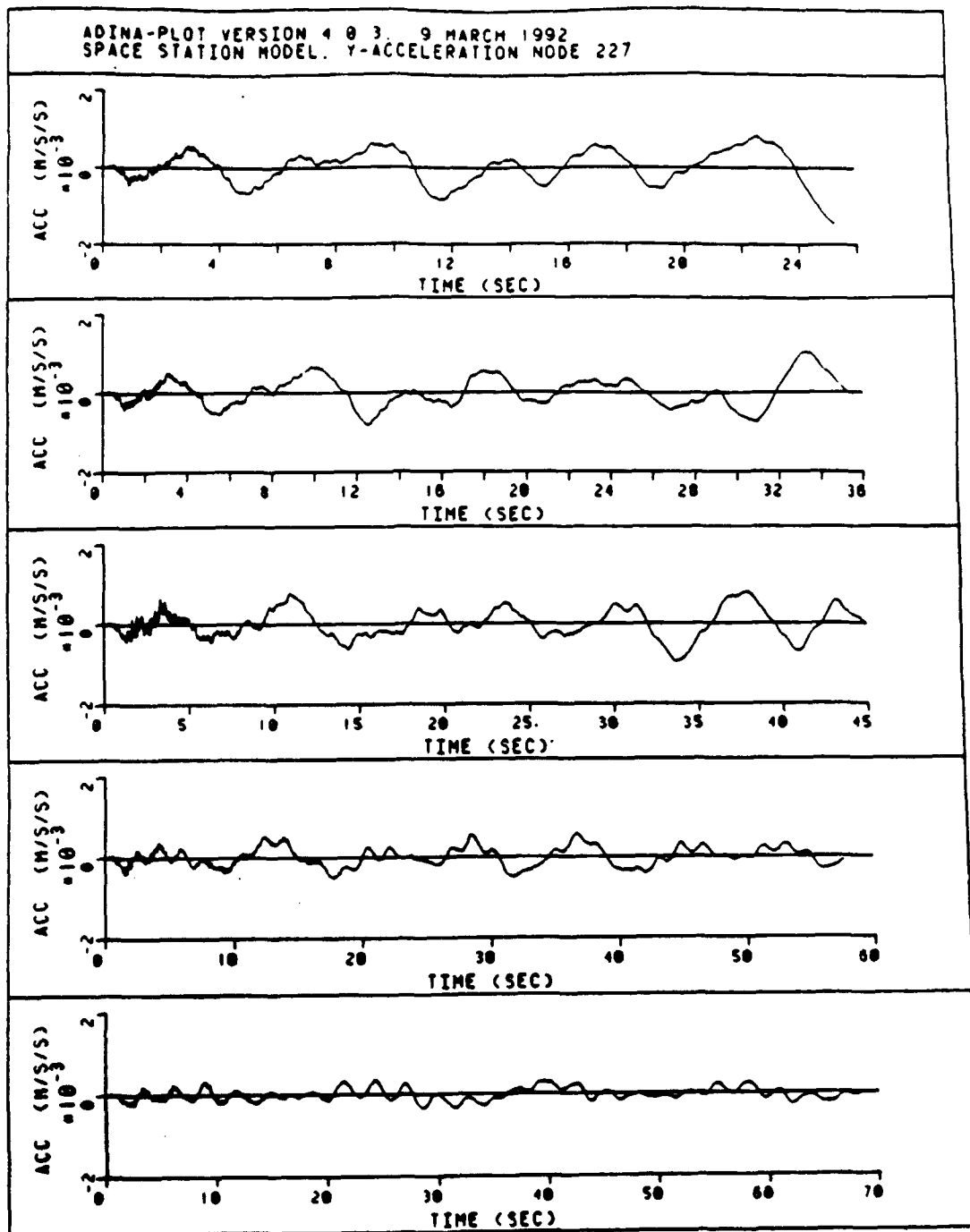


Figure 118 Comparative Plot Cases 1-5 Node 227 Y-Accel.

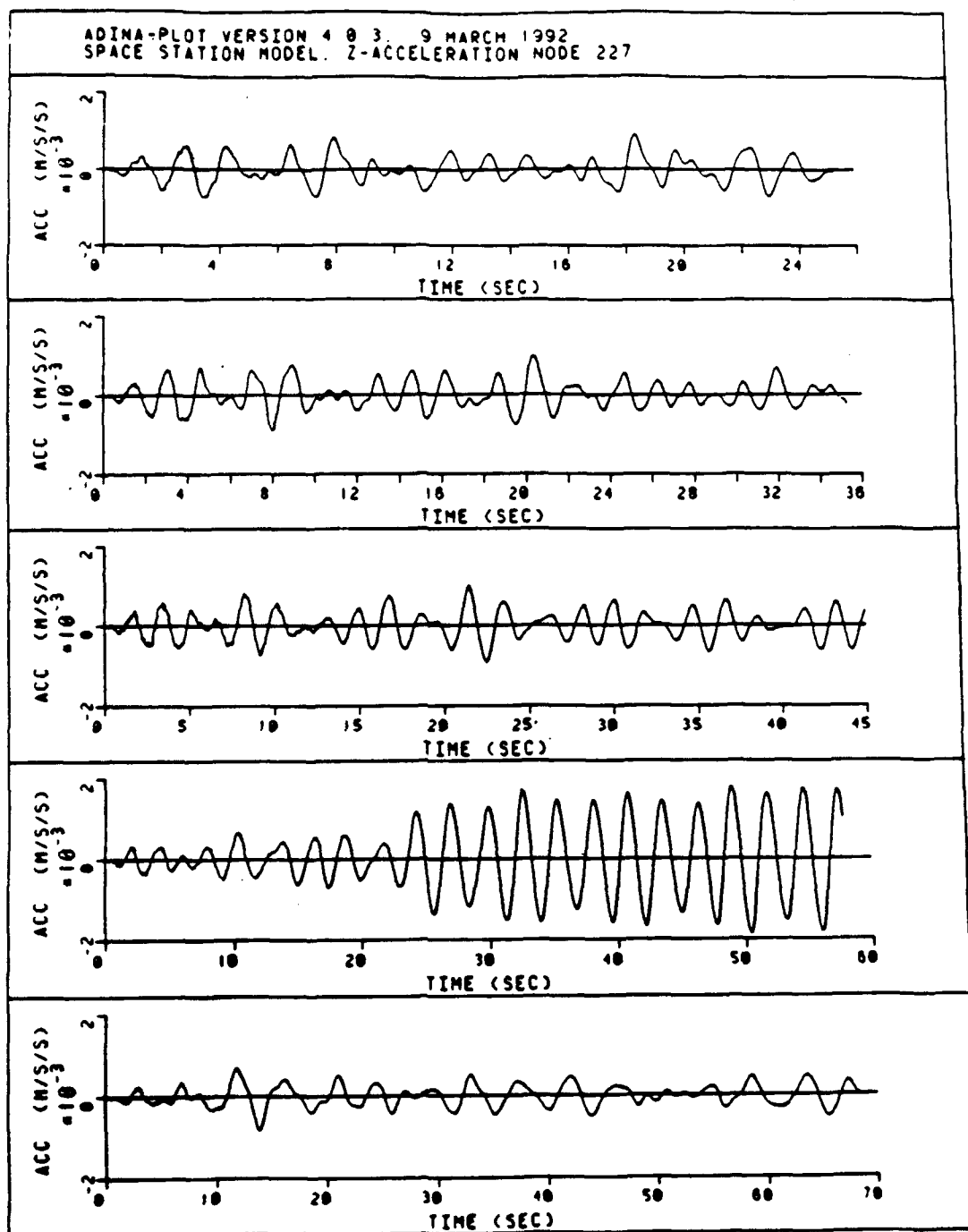


Figure 119 Comparative Plot Case 1-5 Node 227 Z-Accel.

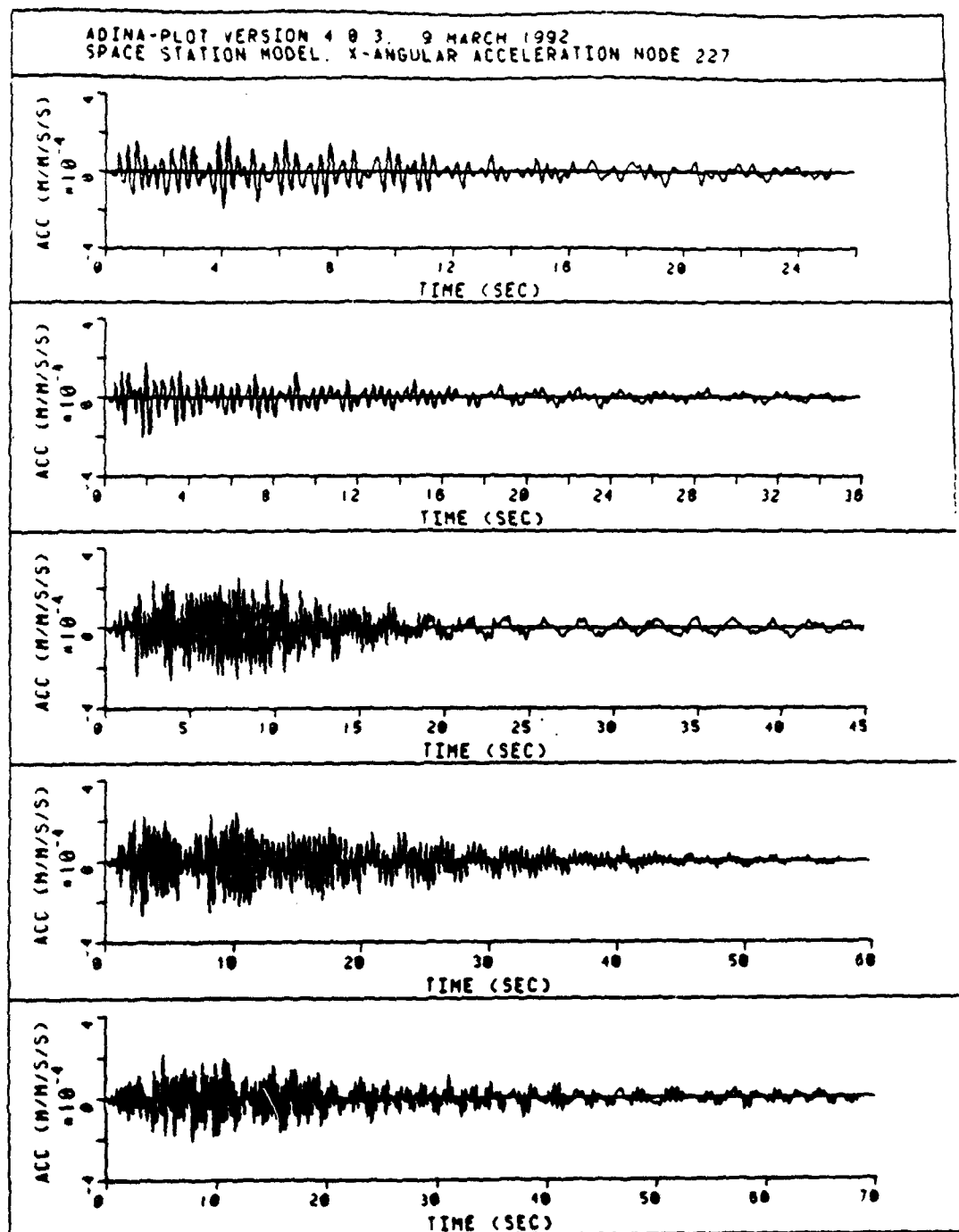


Figure 120 Comparative Plot Case 1-5 Node 227 X-Ang.Accel.

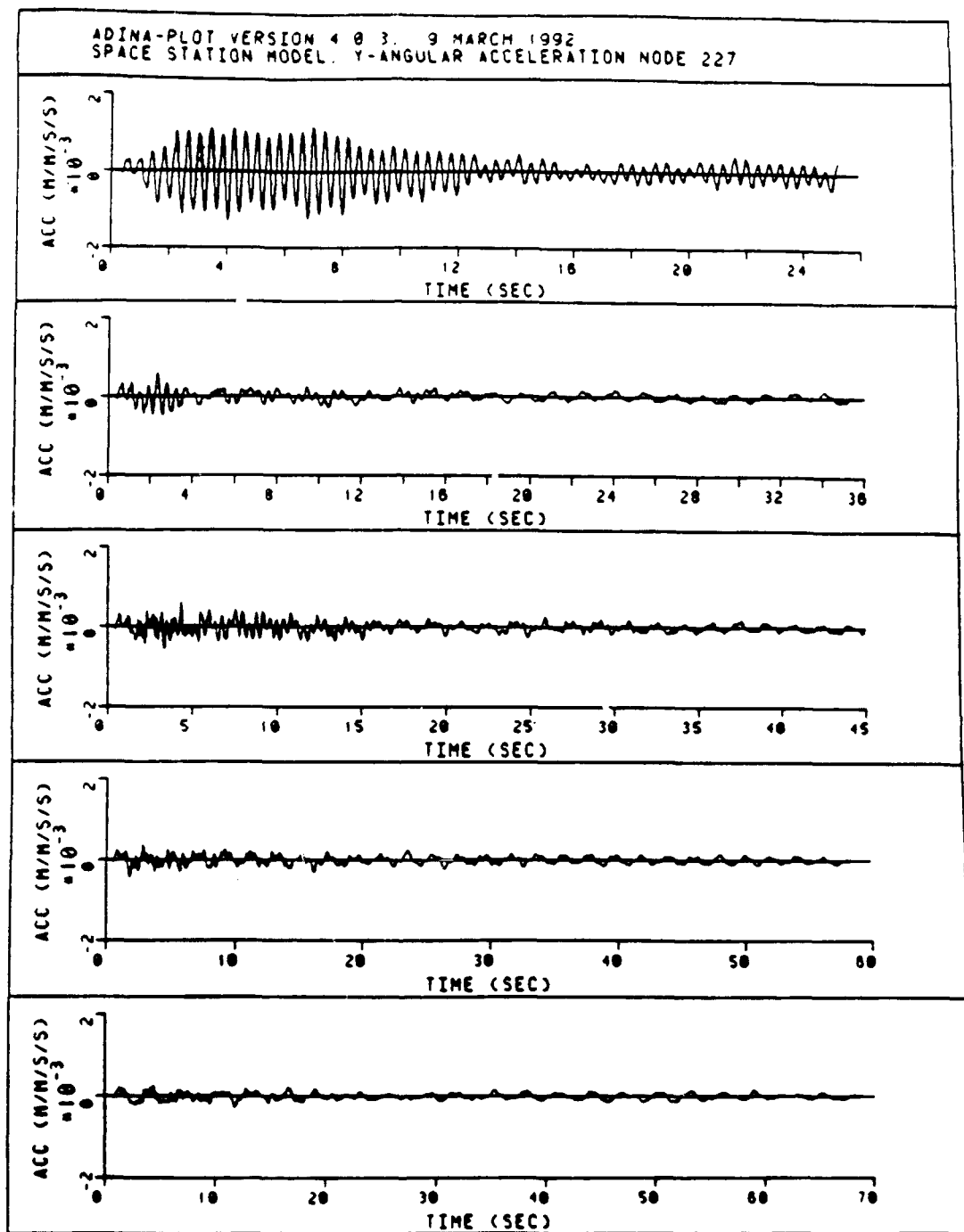


Figure 121 Comparative Plot Case 1-5 Node 227 Y-Ang.Accel.

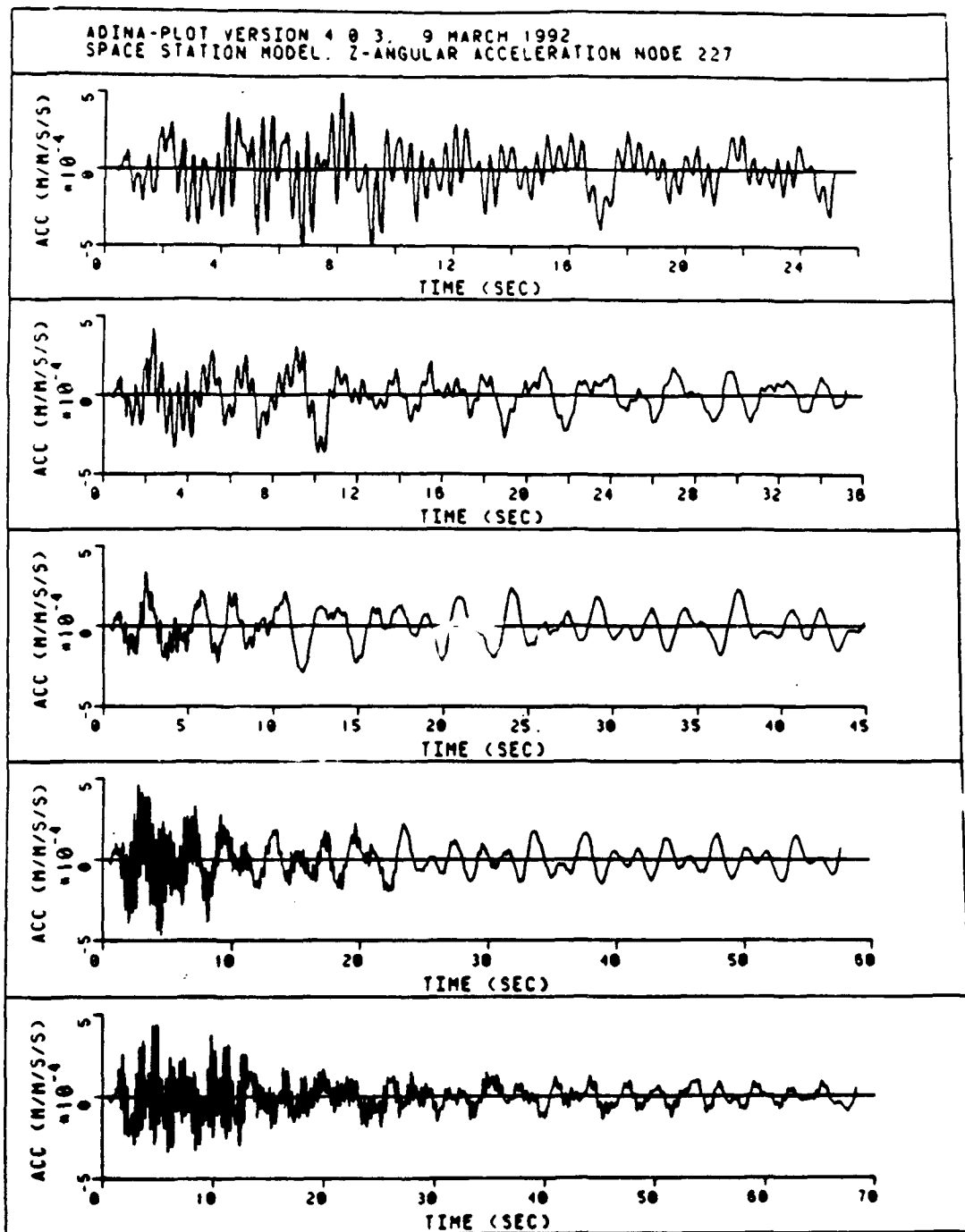


Figure 122 Comparative Plot Case 1-5 Node 227 Z-Ang. Accel.

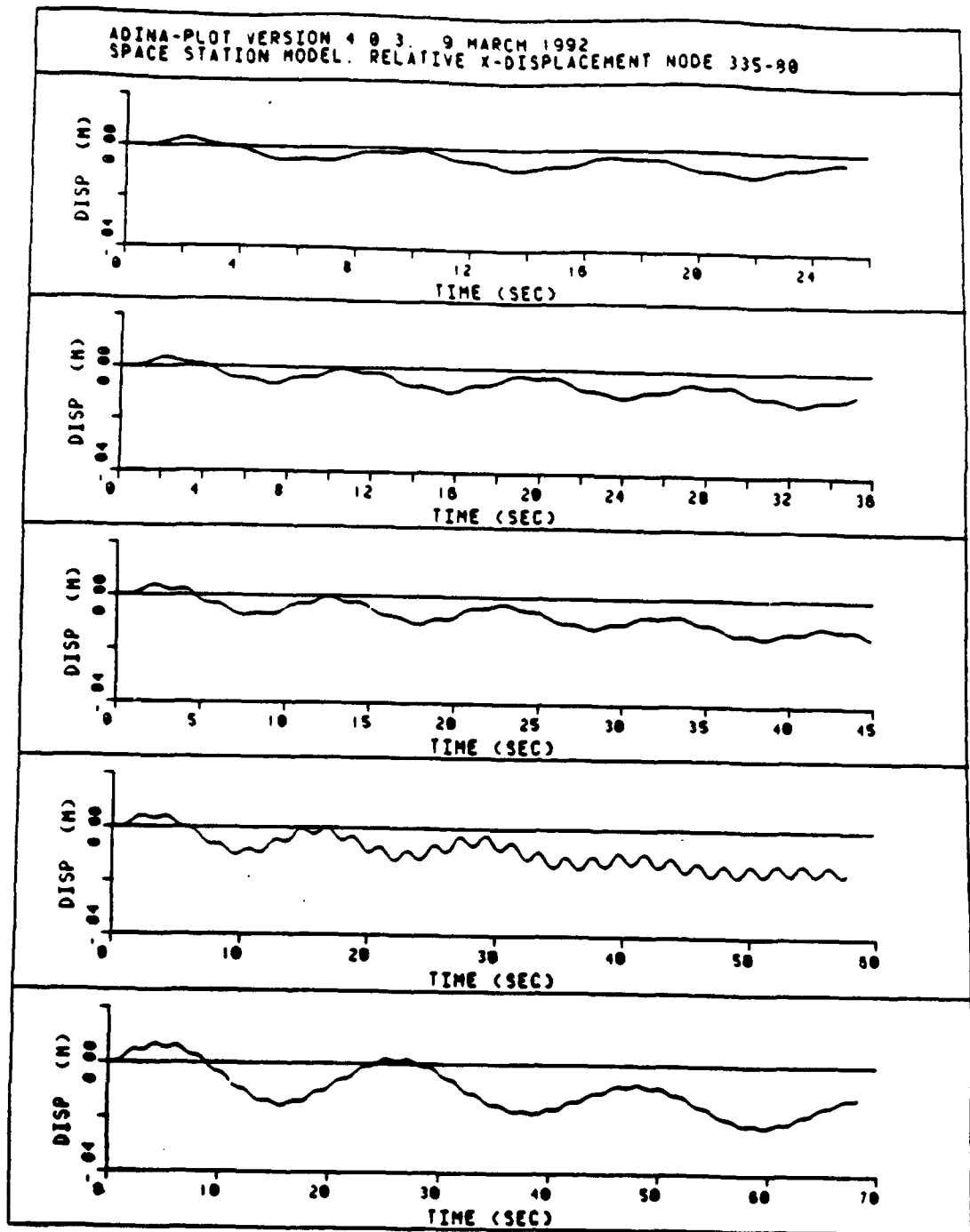


Figure 123 Comparative Plot Case 1-5 Node 335 vs. 80 X-Dis.

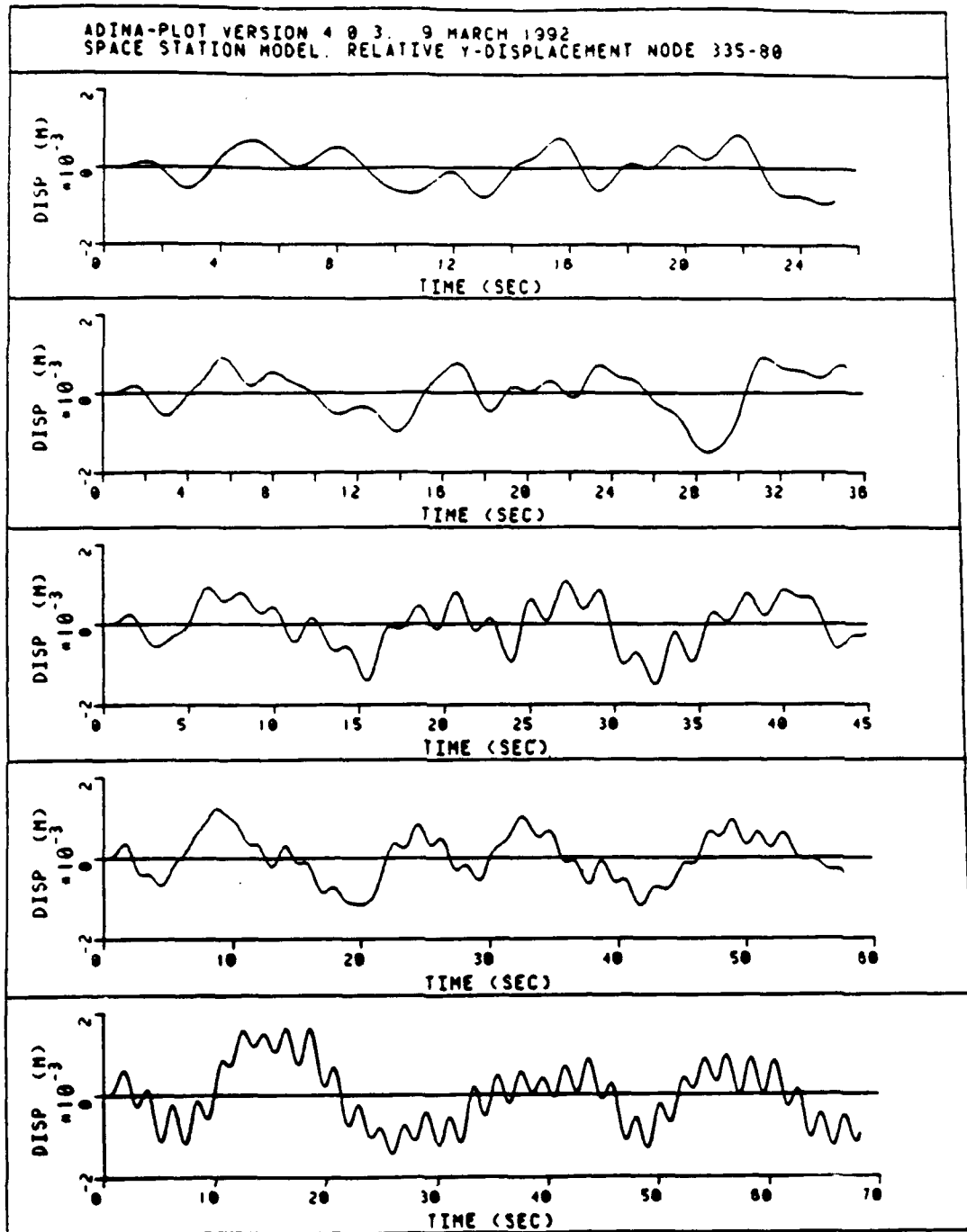


Figure 124 Comparative Plot Case 1-5 Node 335 vs. 80 Y-Dis.

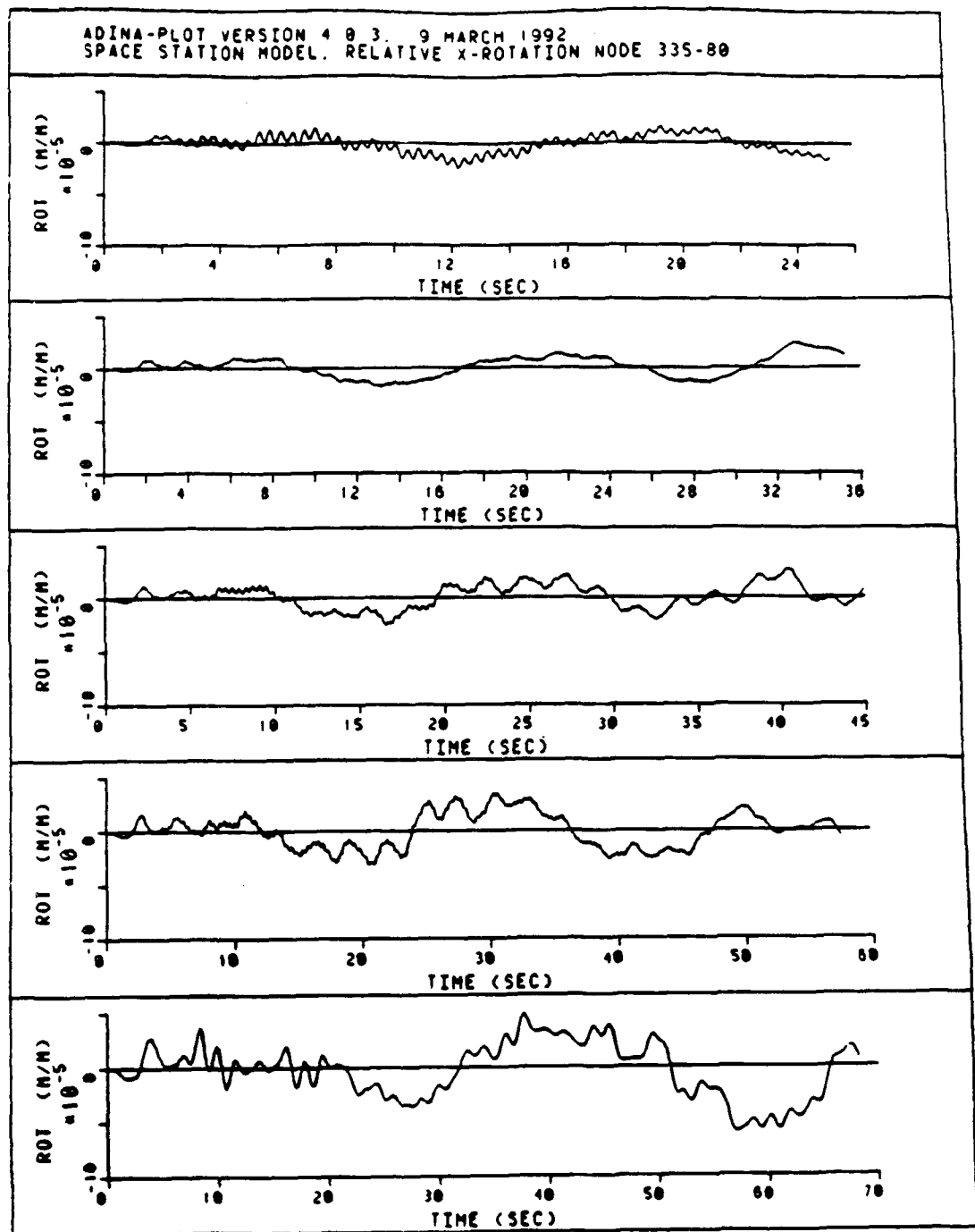


Figure 125 Comparative Plot Case 1-5 Node 335 vs. 80 Z-Dis.

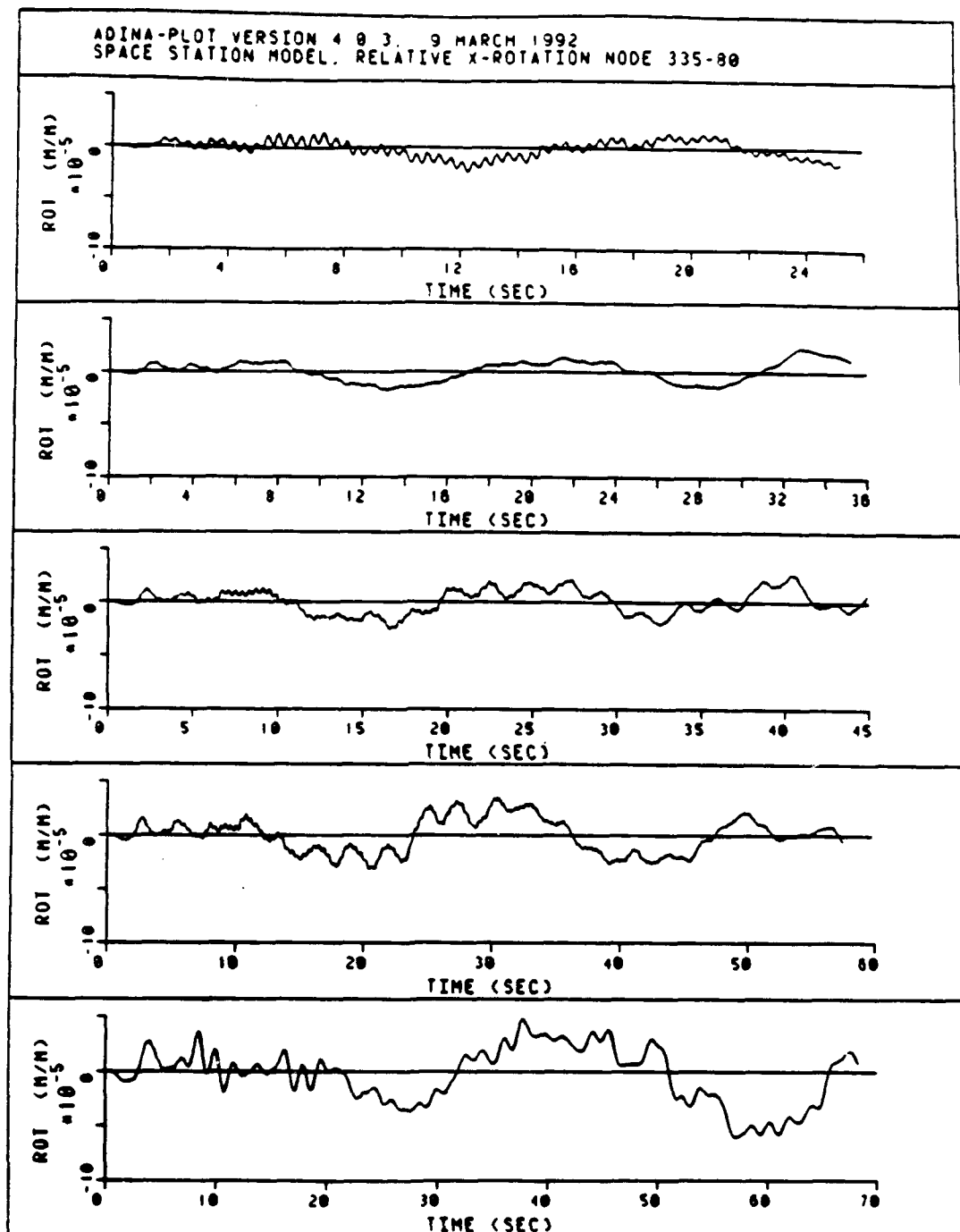


Figure 126 Comparative Plot Case 1-5 Node 335 vs. 80 X-Rot.

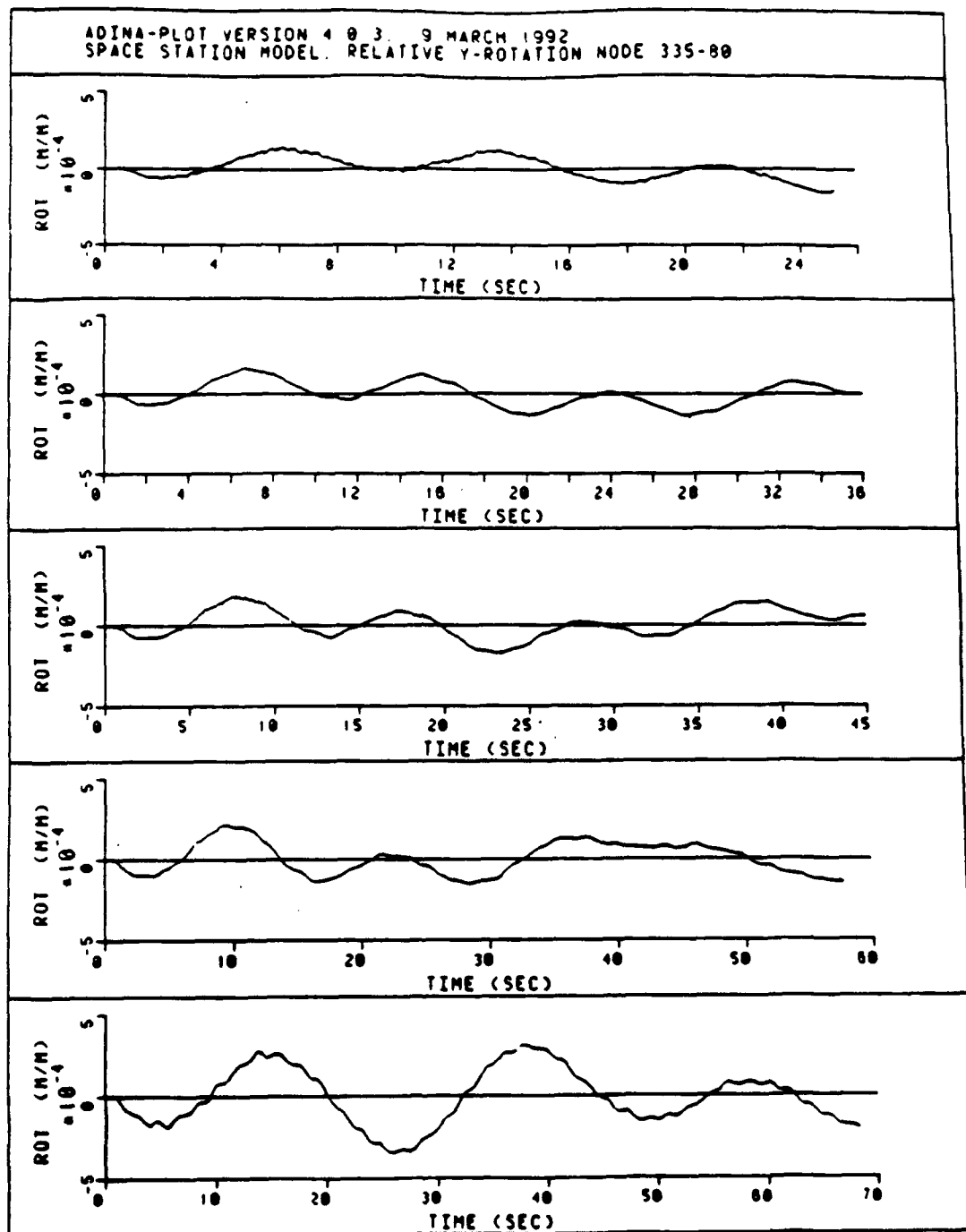


Figure 127 Comparative Plot Case 1-5 Node 335 vs. 80 Y-Rot.

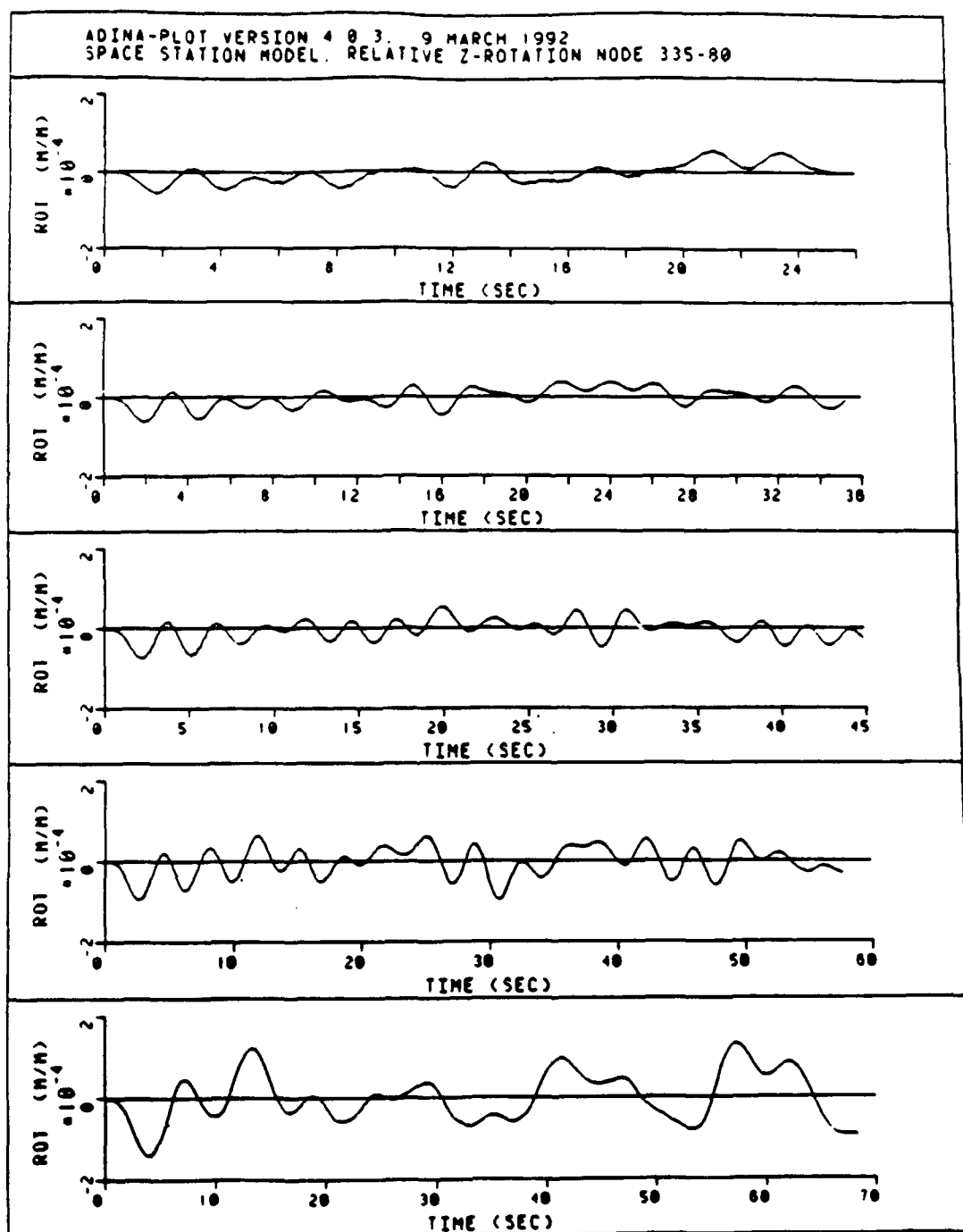


Figure 128 Comparative Plot Case 1-5 Node 335 vs. 80 Z-Rot.

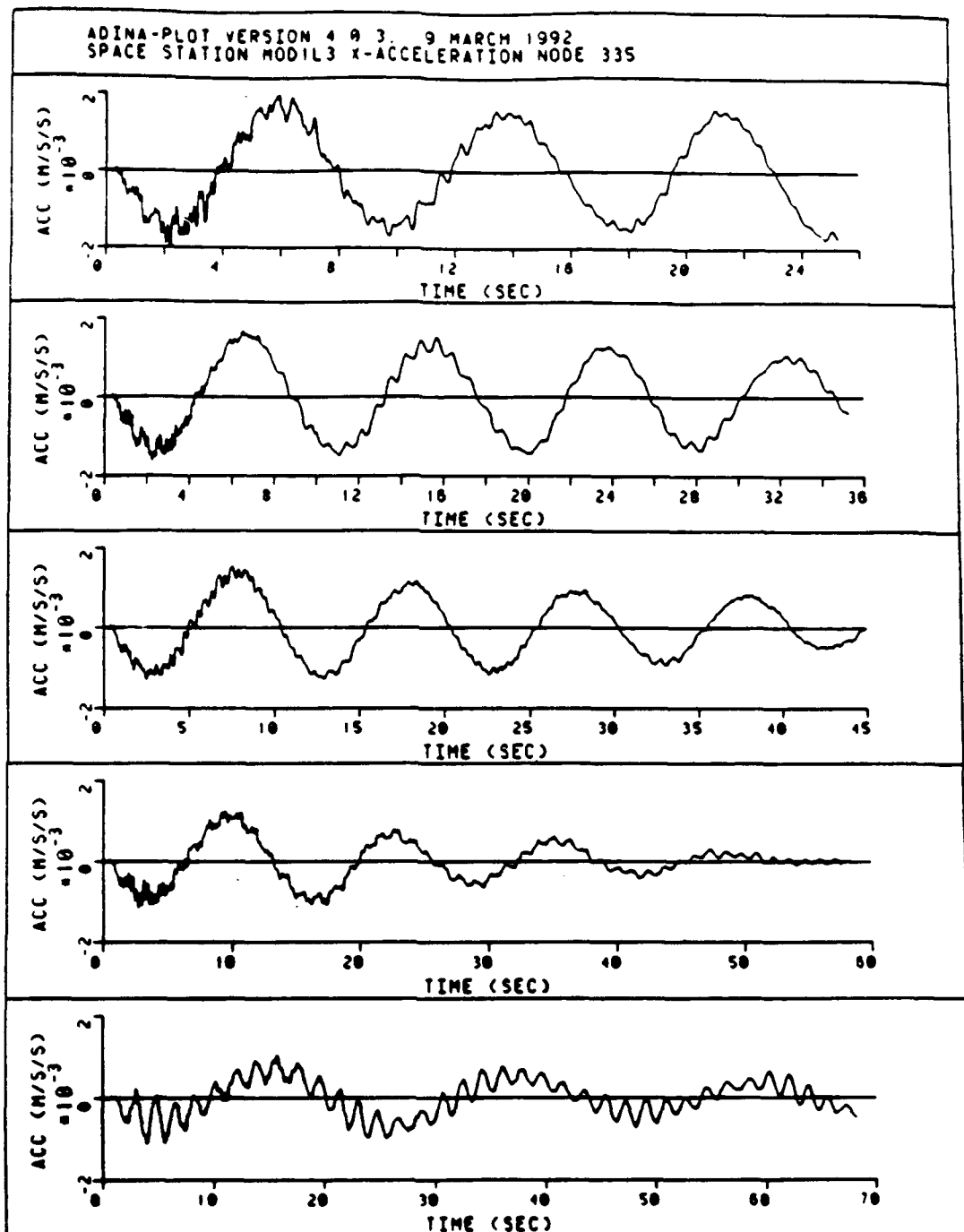


Figure 129 Comparative Plot Case 1-5 Node 335 X-Accel.

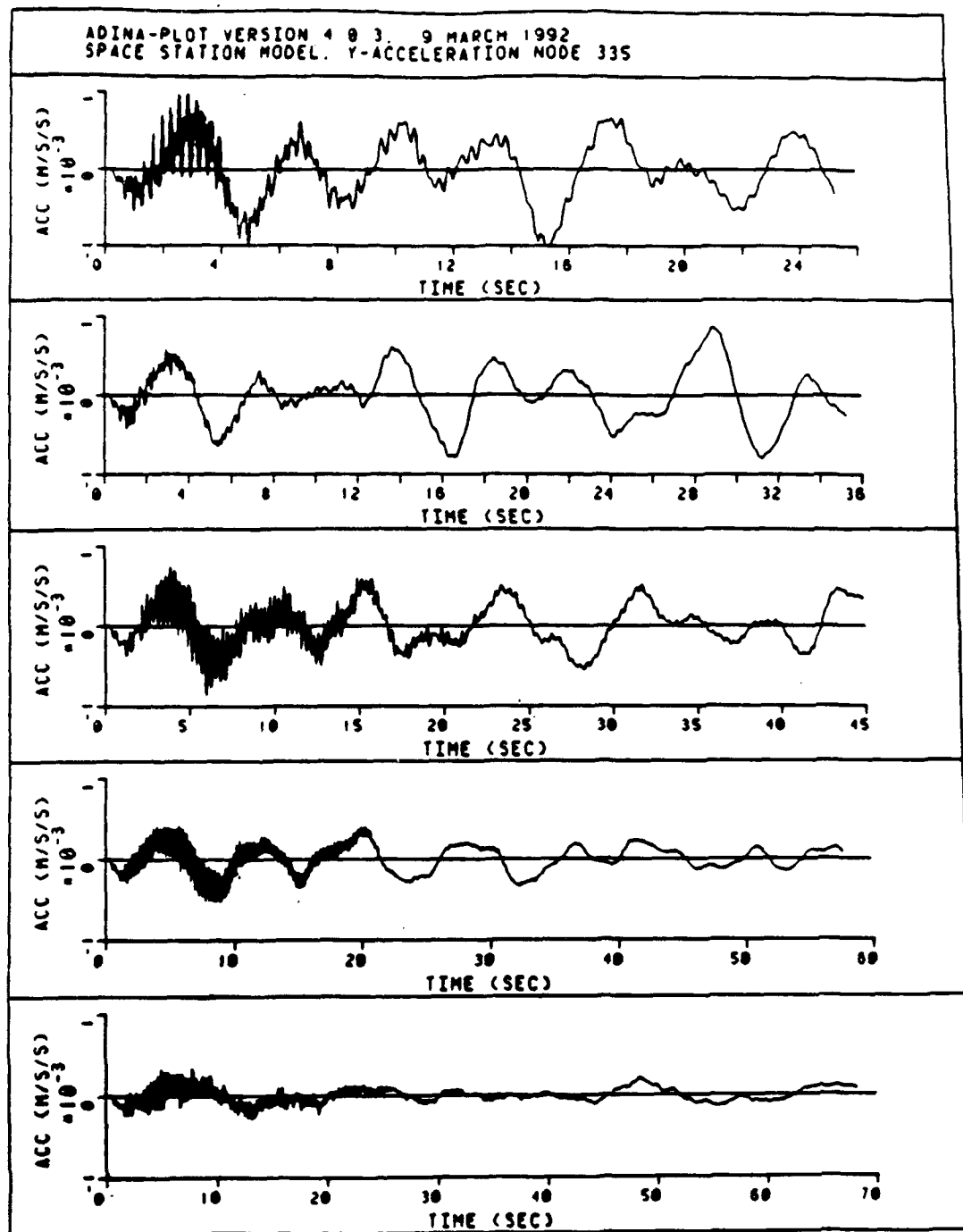


Figure 130 Comparative Plot Case 1-5 Node 335 Y-Accel.

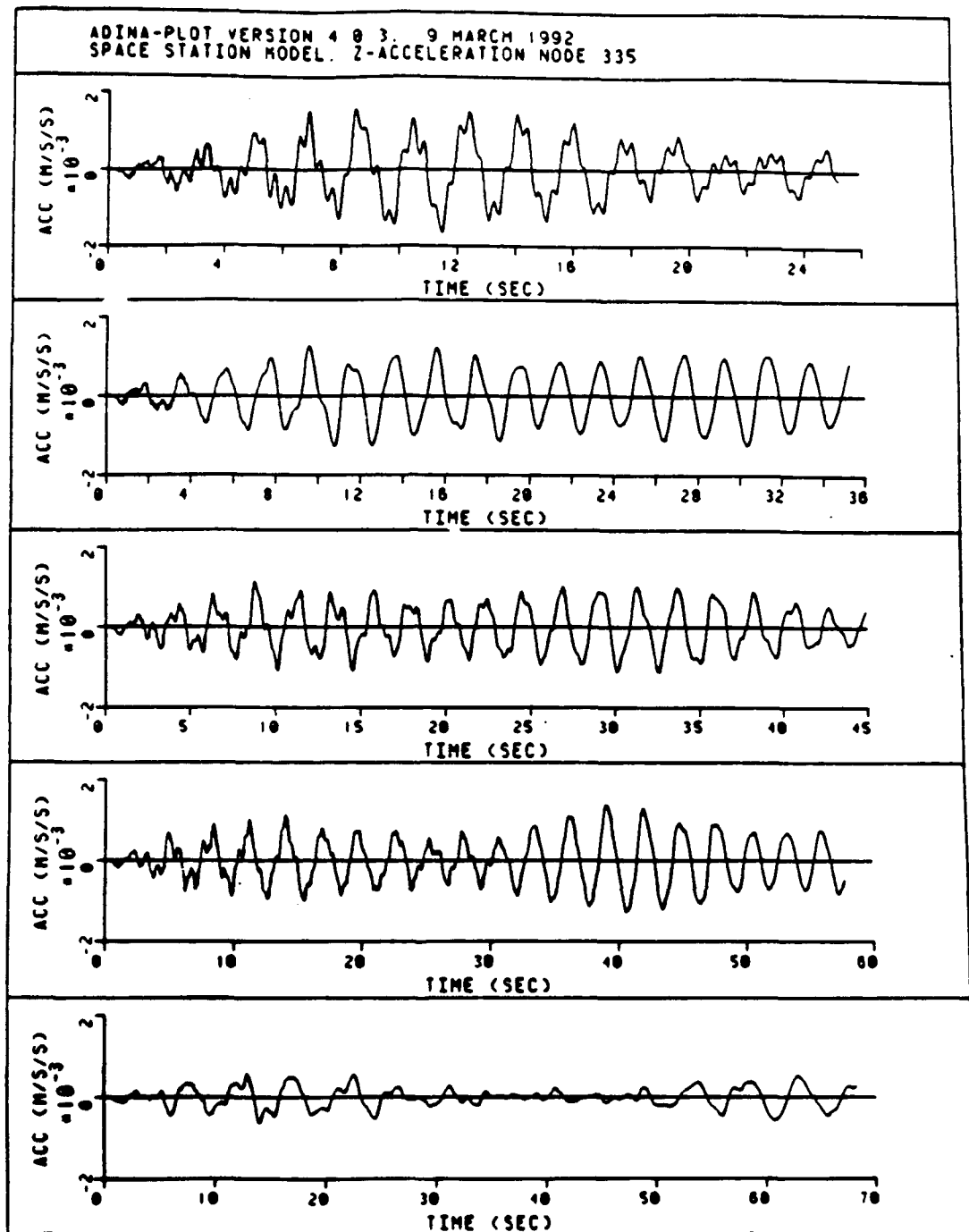


Figure 131 Comparative Plot Case 1-5 Node 335 Z-Accel.

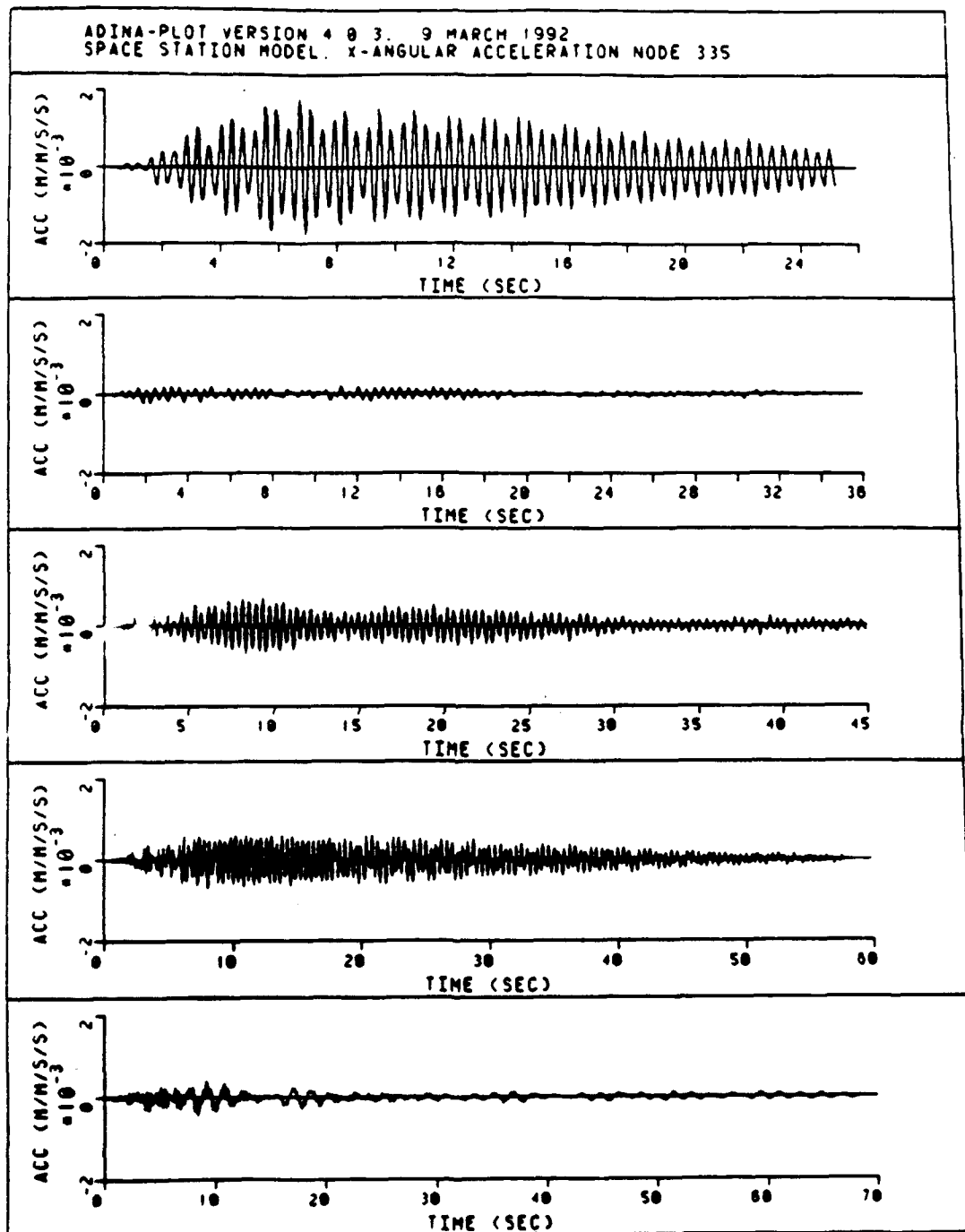


Figure 132 Comparative Plot Case 1-5 Node 335 X-Ang. Accel.

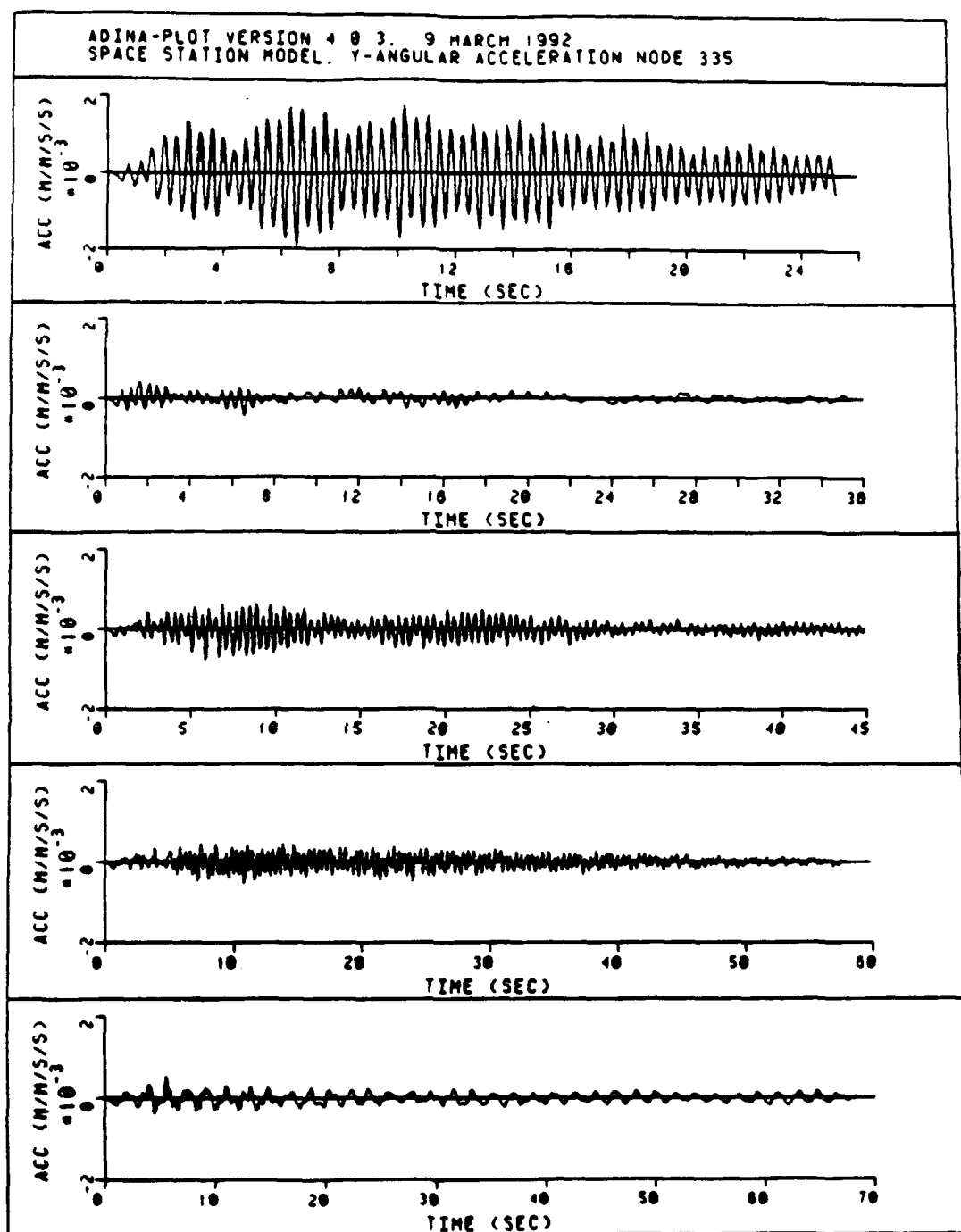


Figure 133 Comparative Plot Case 1-5 Node 335 Y-Ang. Accel.

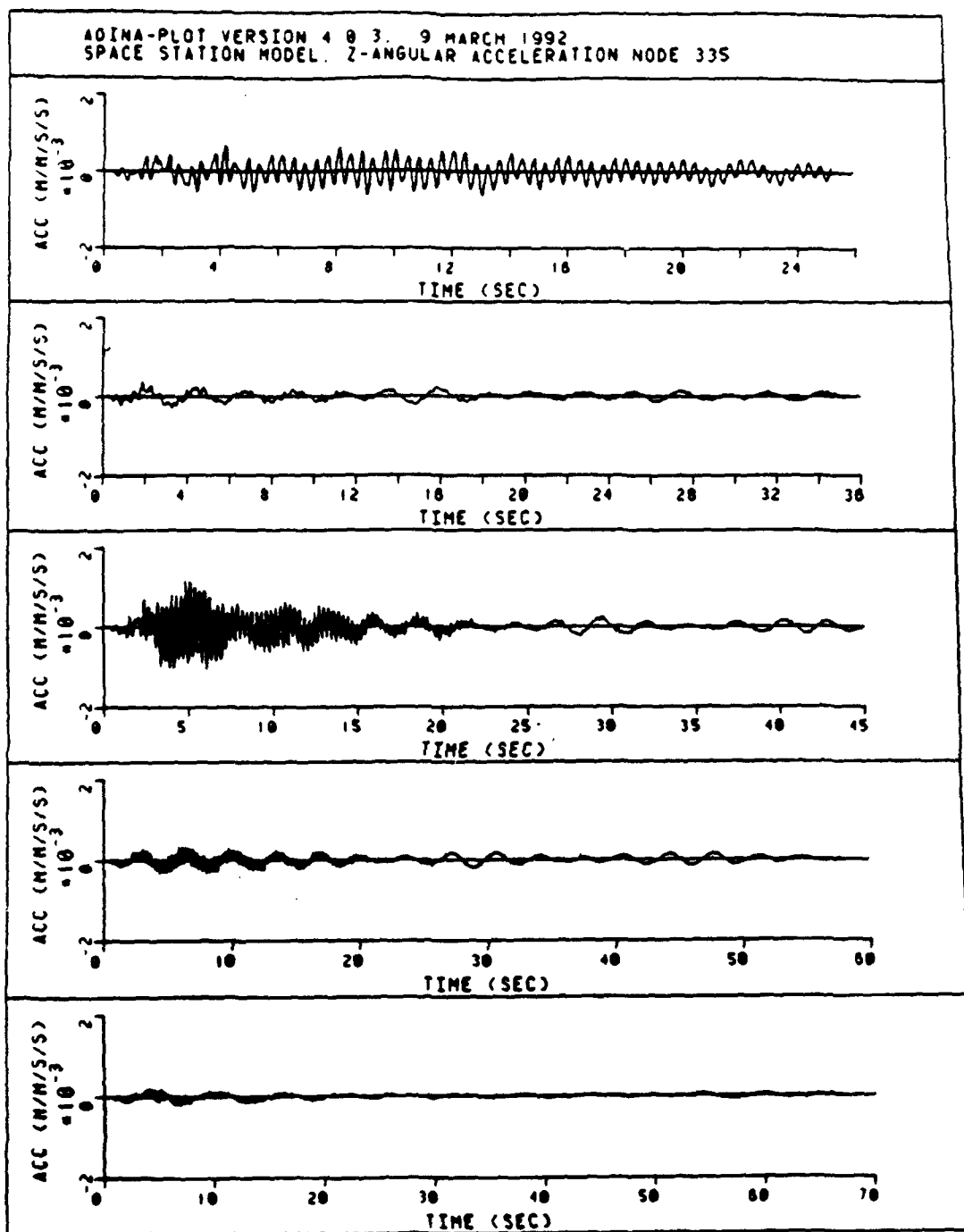


Figure 134 Comparative Plot Case 1-5 Node 335 Z-Ang. Accel.

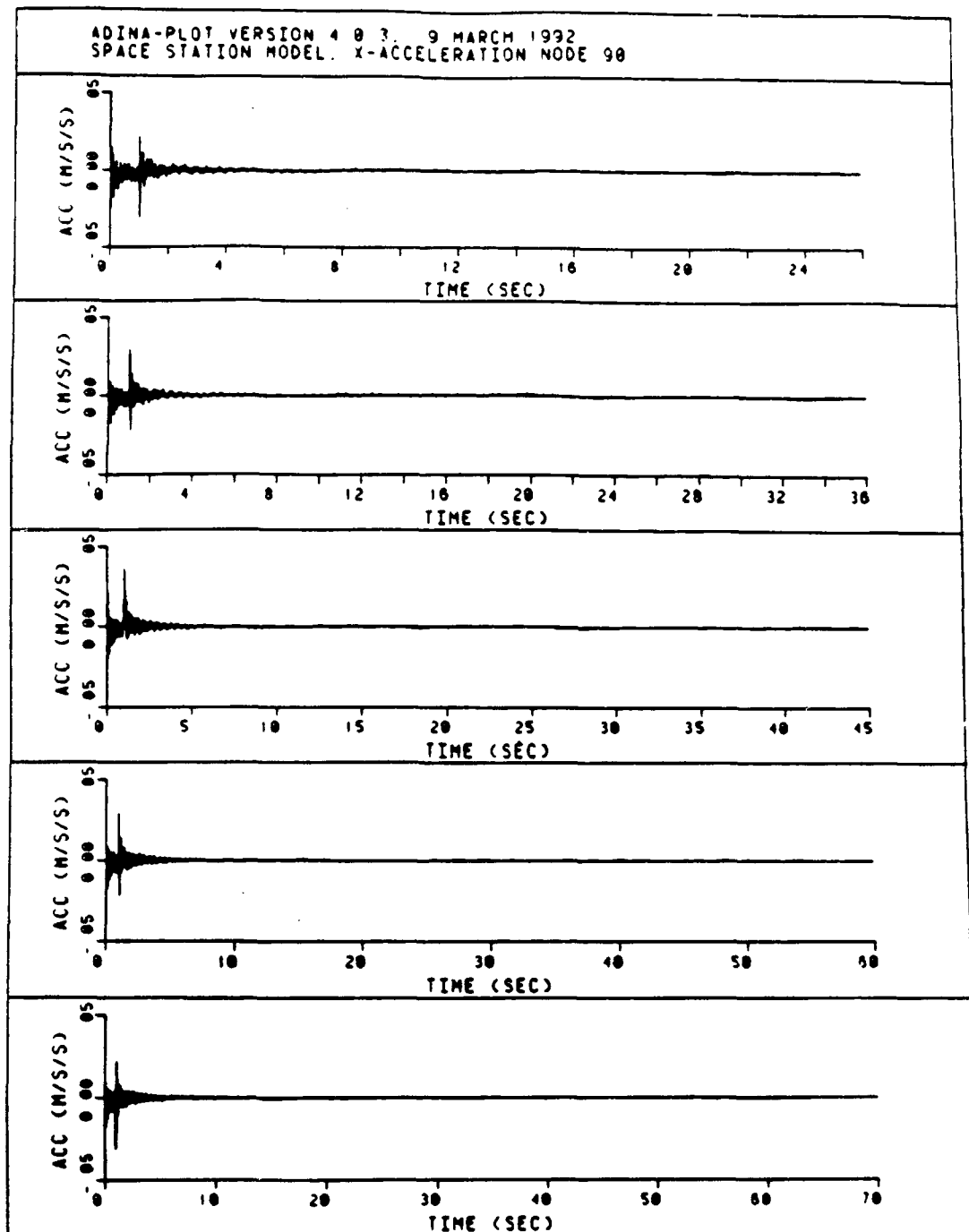


Figure 135 Comparative Plot Case 1-5 Node 90 X-Accel.

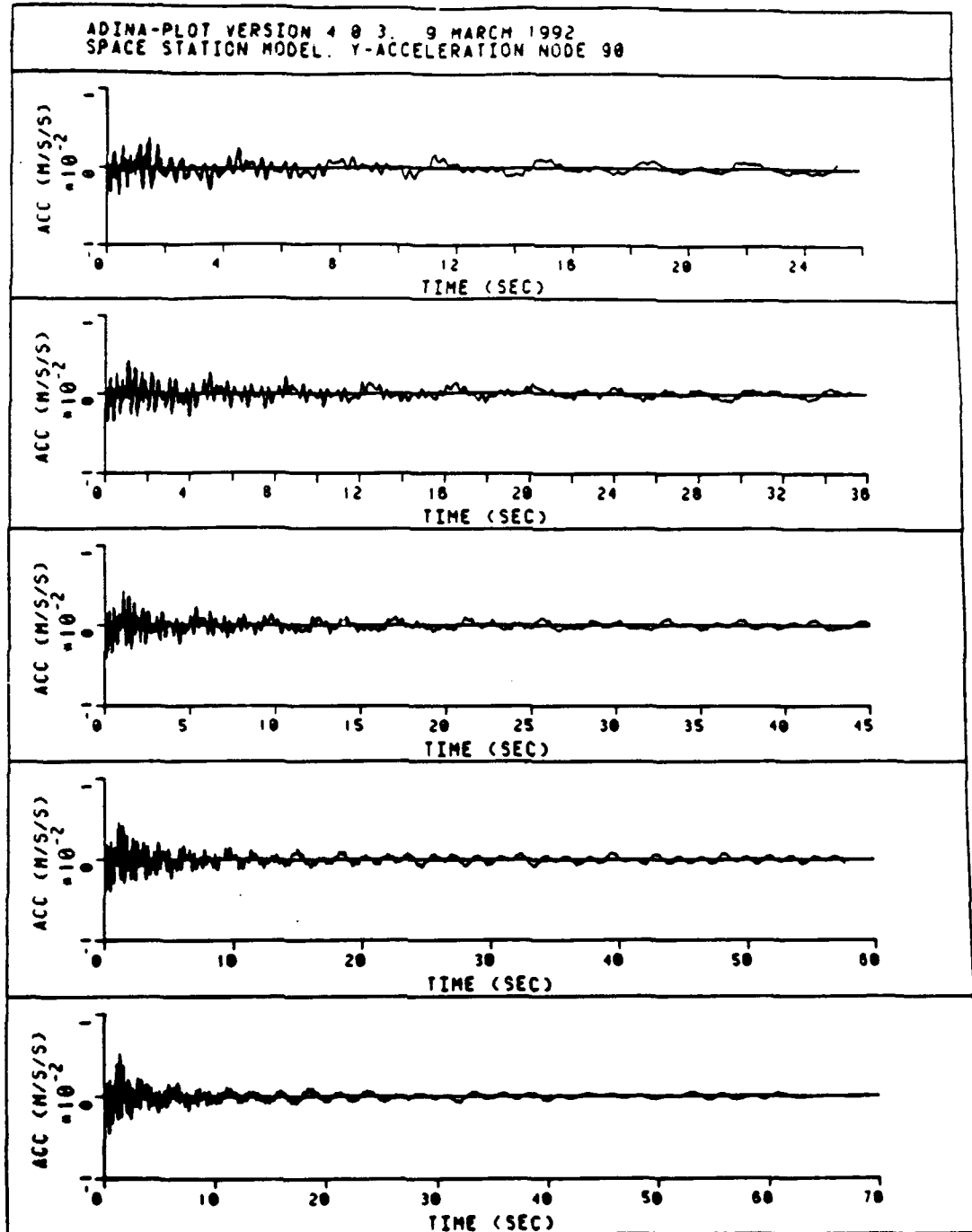


Figure 136 Comparative Plot Case 1-5 Node 90 Y-Accel.

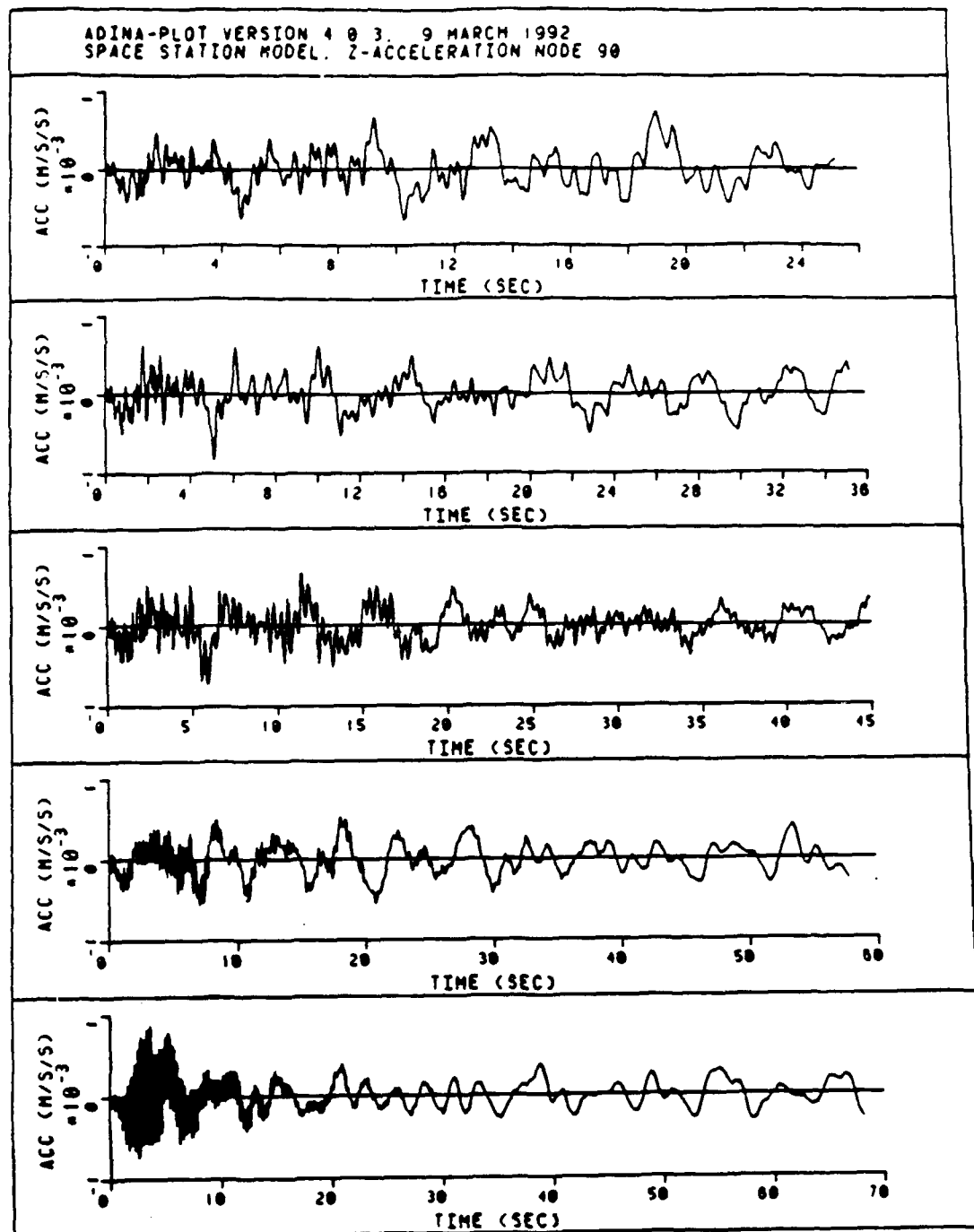


Figure 137 Comparative Plot Case 1-5 Node 90 Z-Accel.

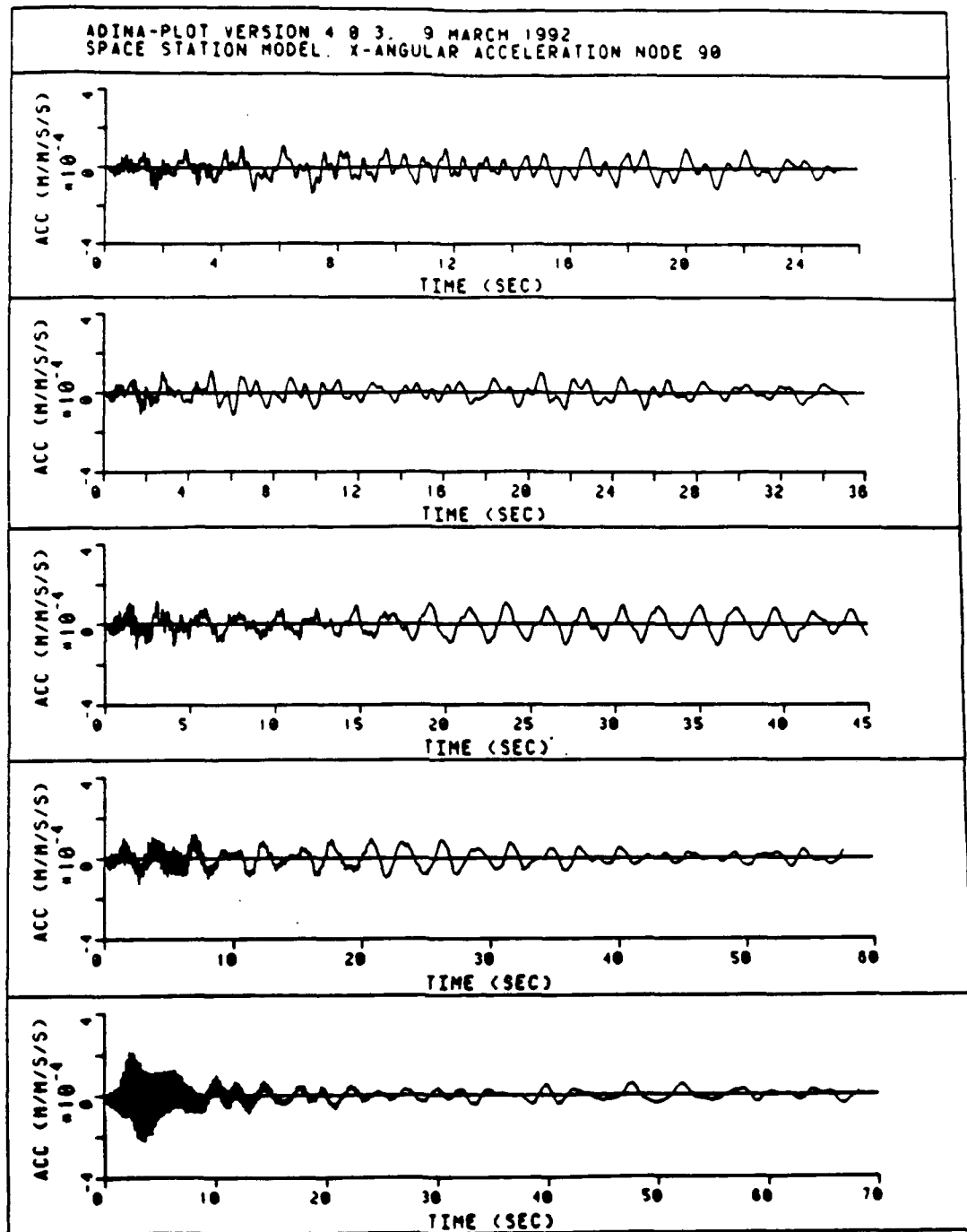


Figure 138 Comparative Plots Case 1-5 Node 90 X-Ang. Accel.

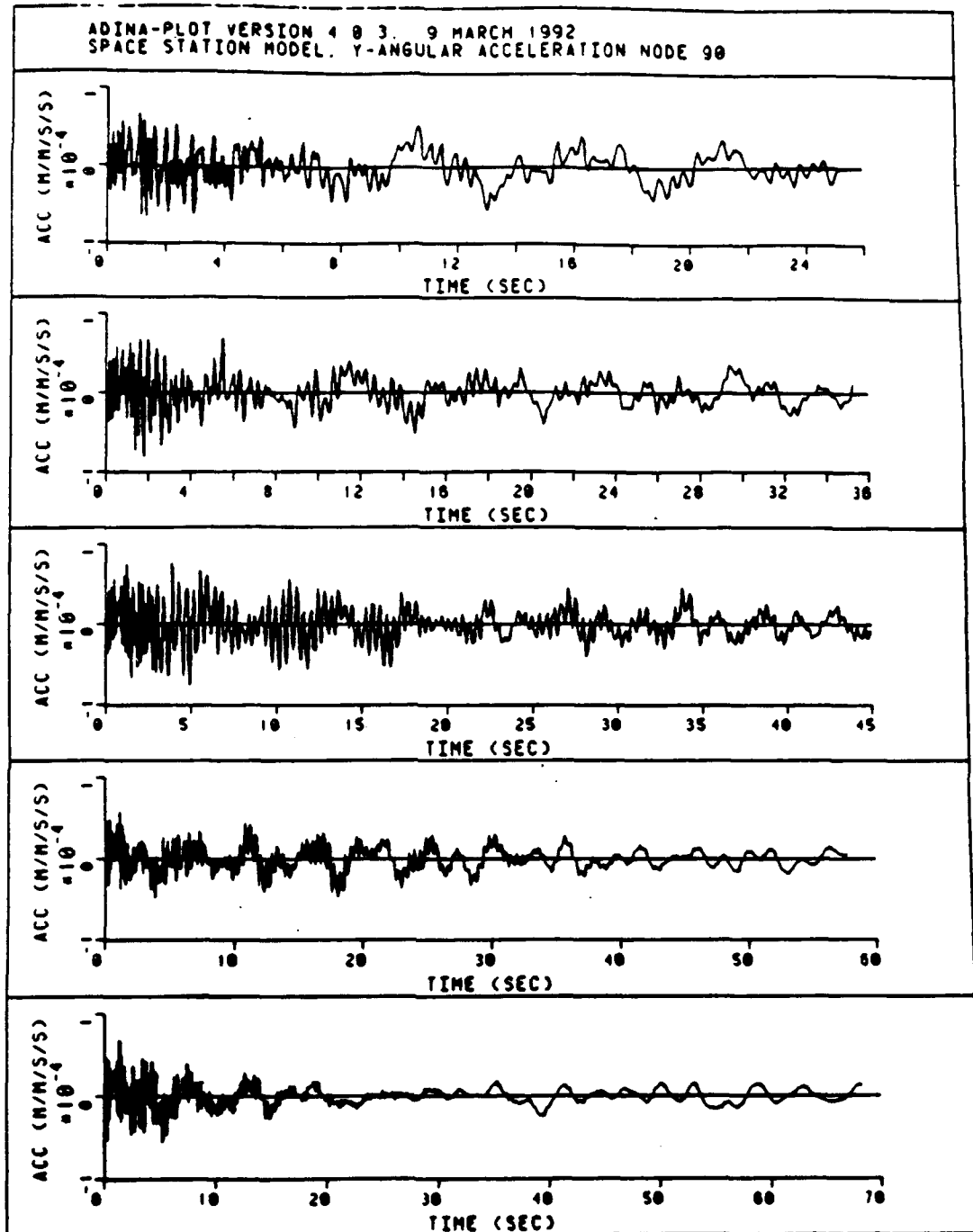


Figure 139 Comparative Plot Case 1-5 Node 90 Y-Ang. Accel.

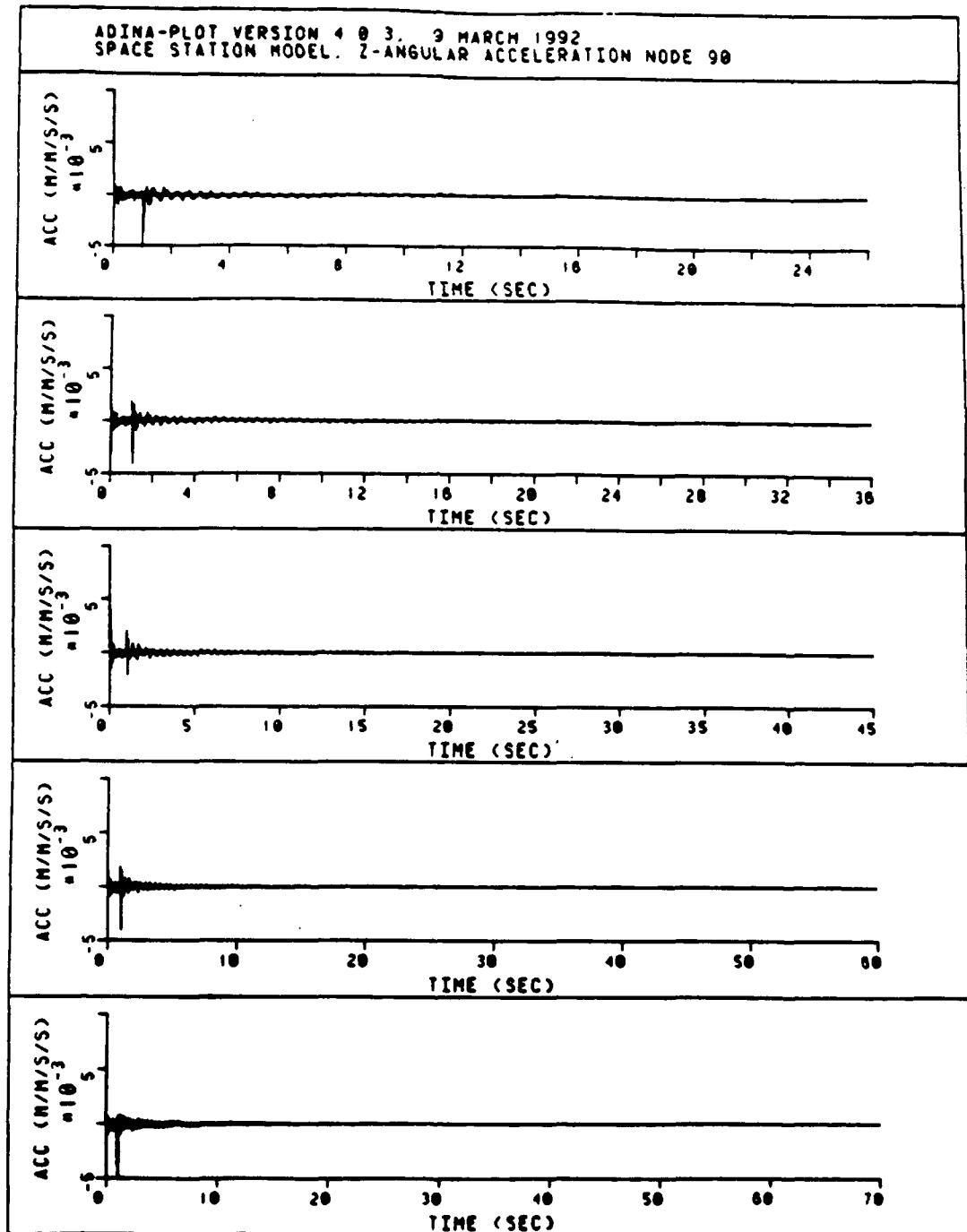


Figure 140 Comparative Plot Case 1-5 Node 90 Z-Ang. Accel.

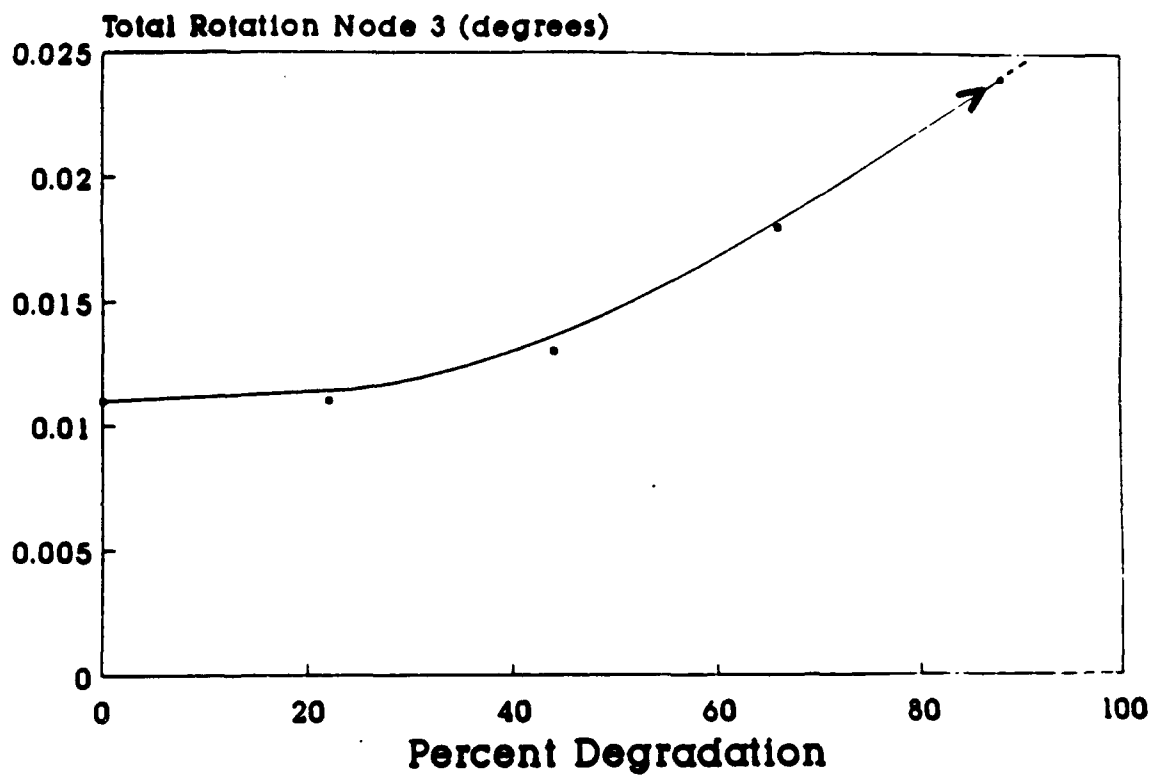


Figure 141 Total Rotation - Node 3 (degrees)

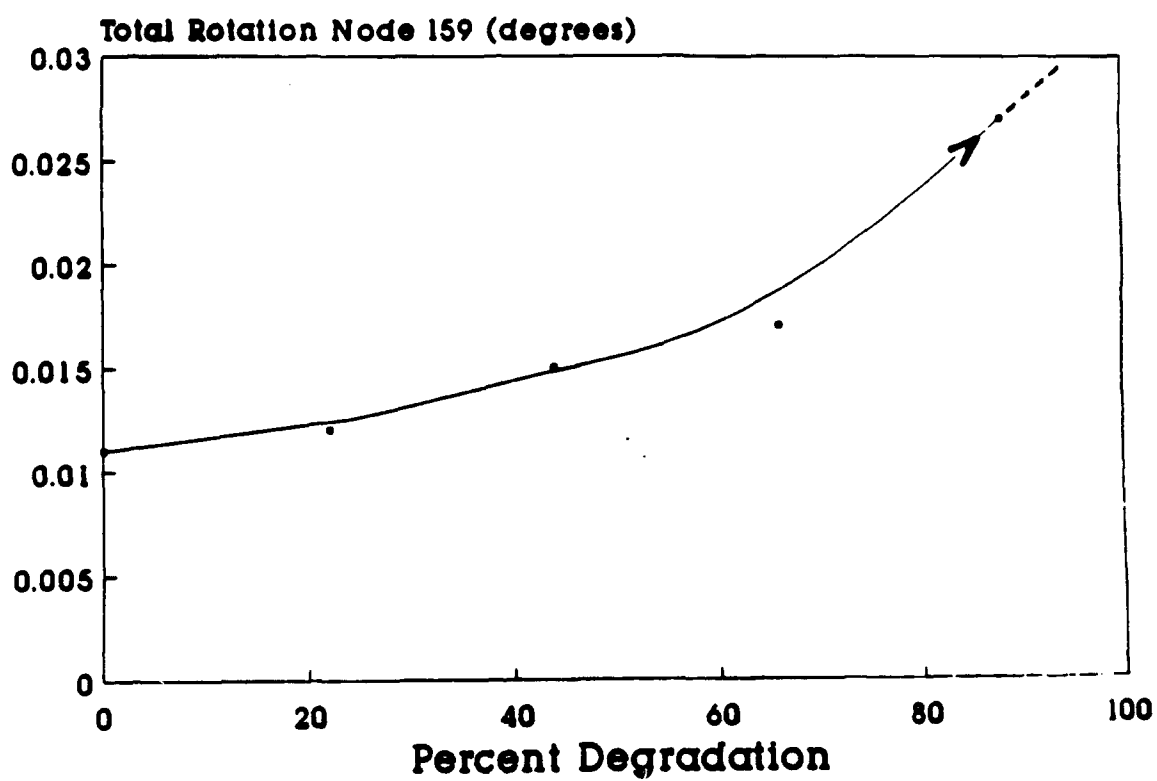


Figure 142 Total Rotation - Node 159 (degrees)

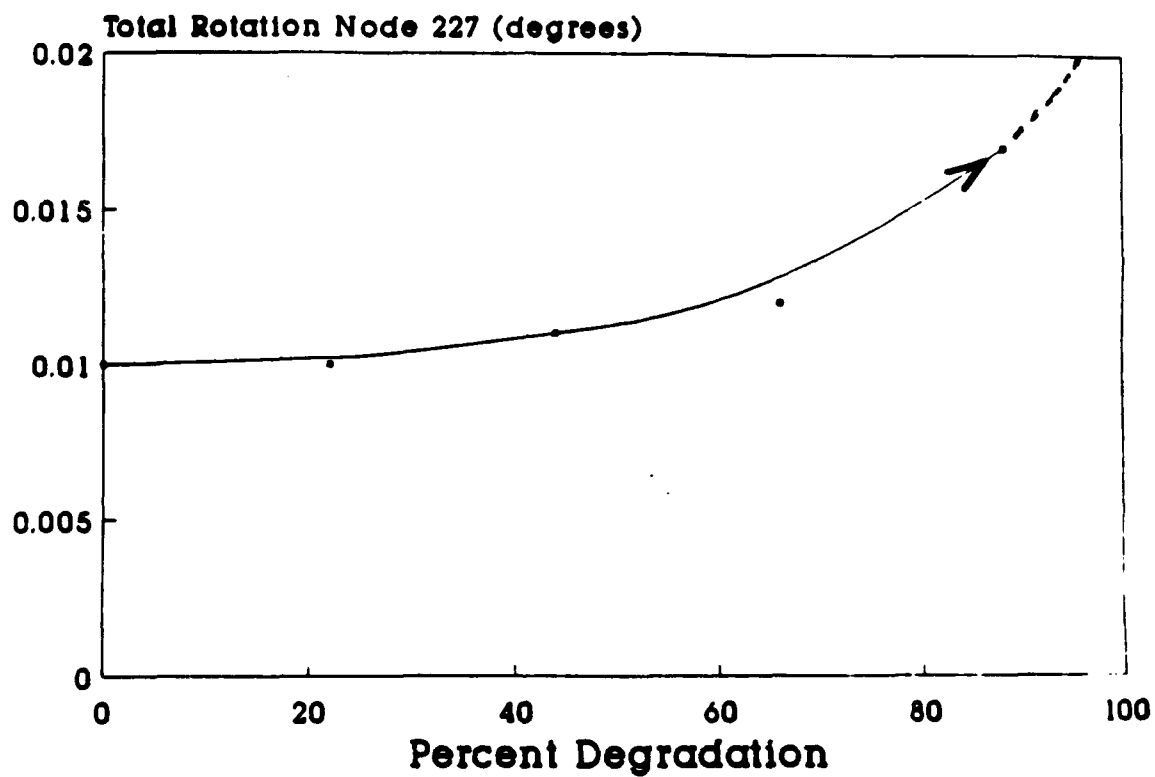


Figure 143 Total Rotation - Node 227 (degrees)

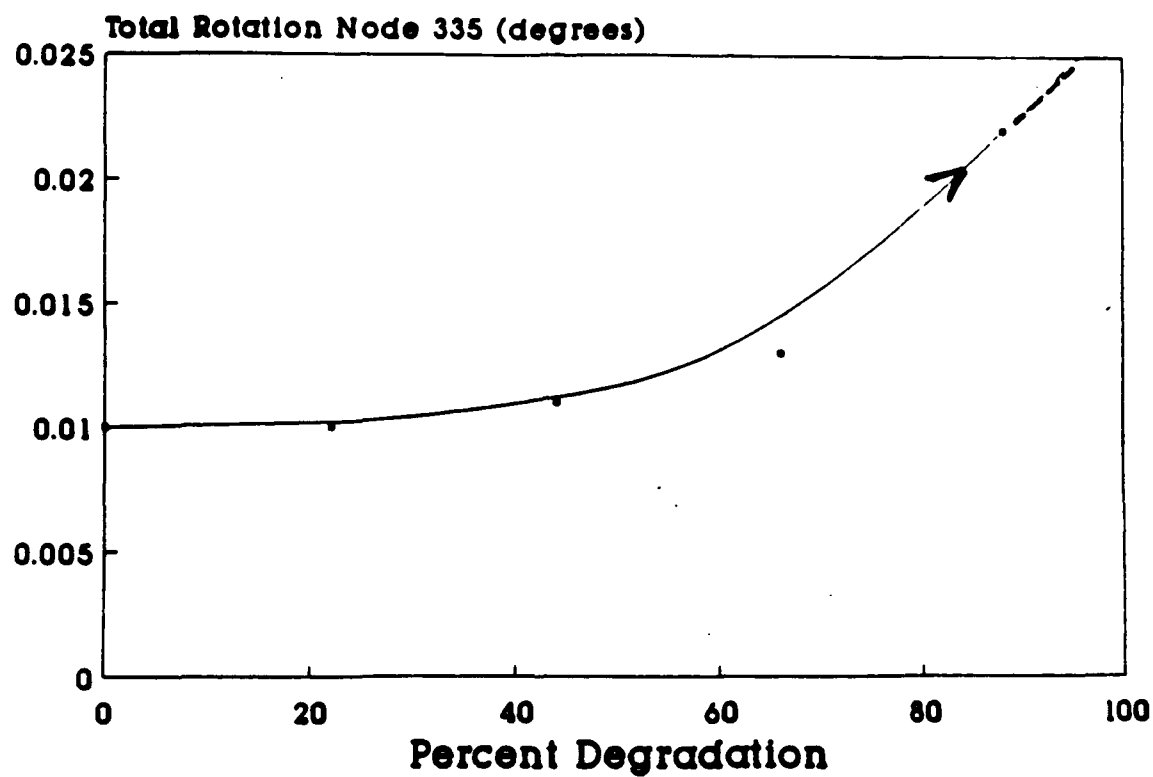


Figure 144 Total Rotation - Node 335 (degrees)

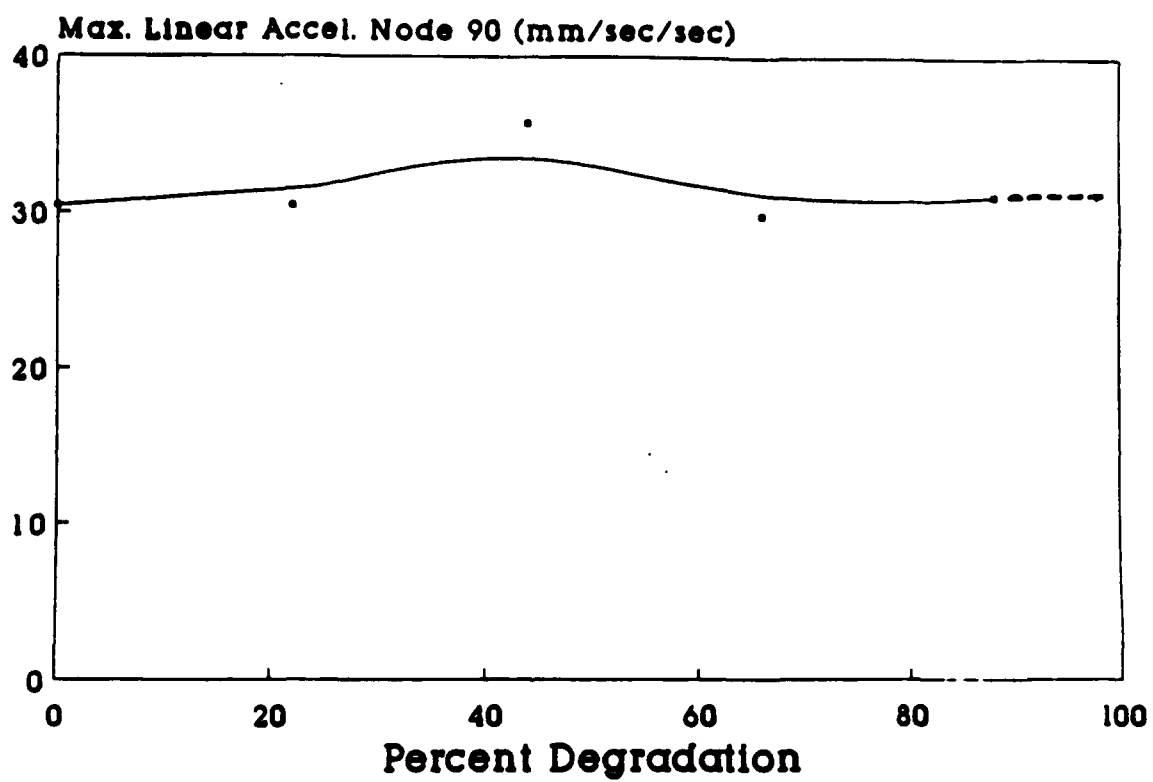


Figure 145 Max. Linear Acceleration - Node 90 (mm/sec/sec)

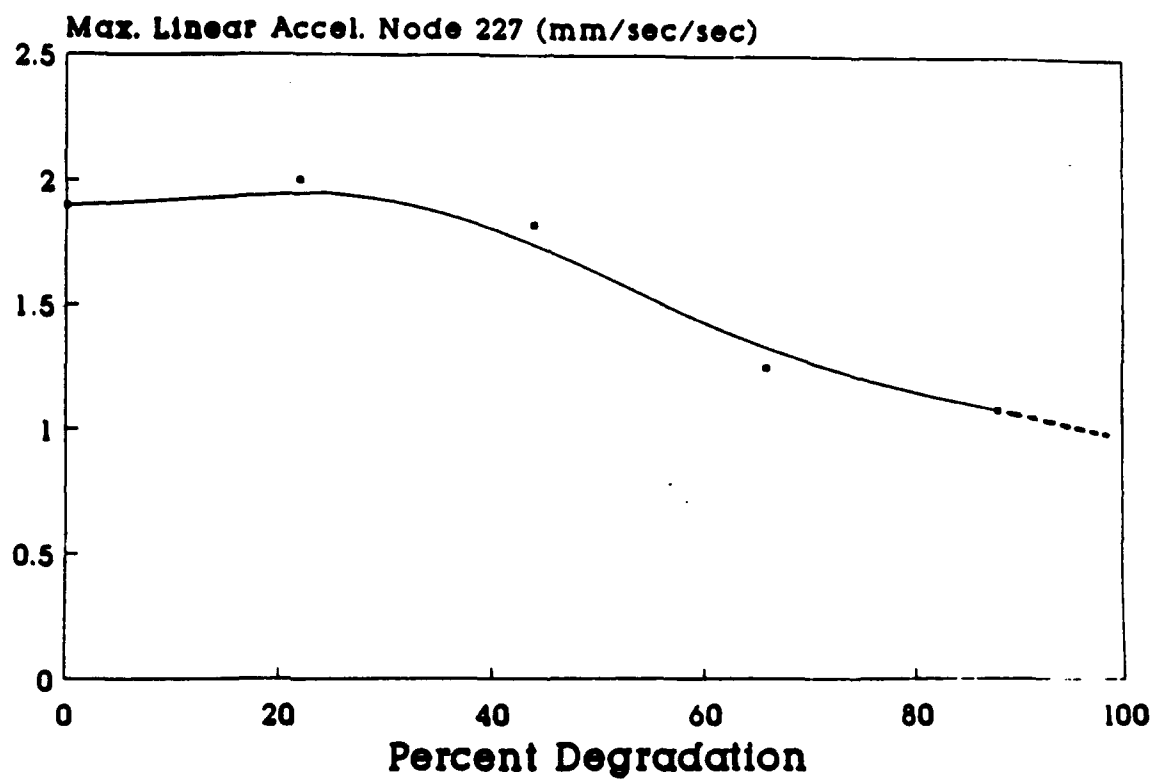


Figure 146 Max. Linear Acceleration - Node 227 (mm/sec/sec)

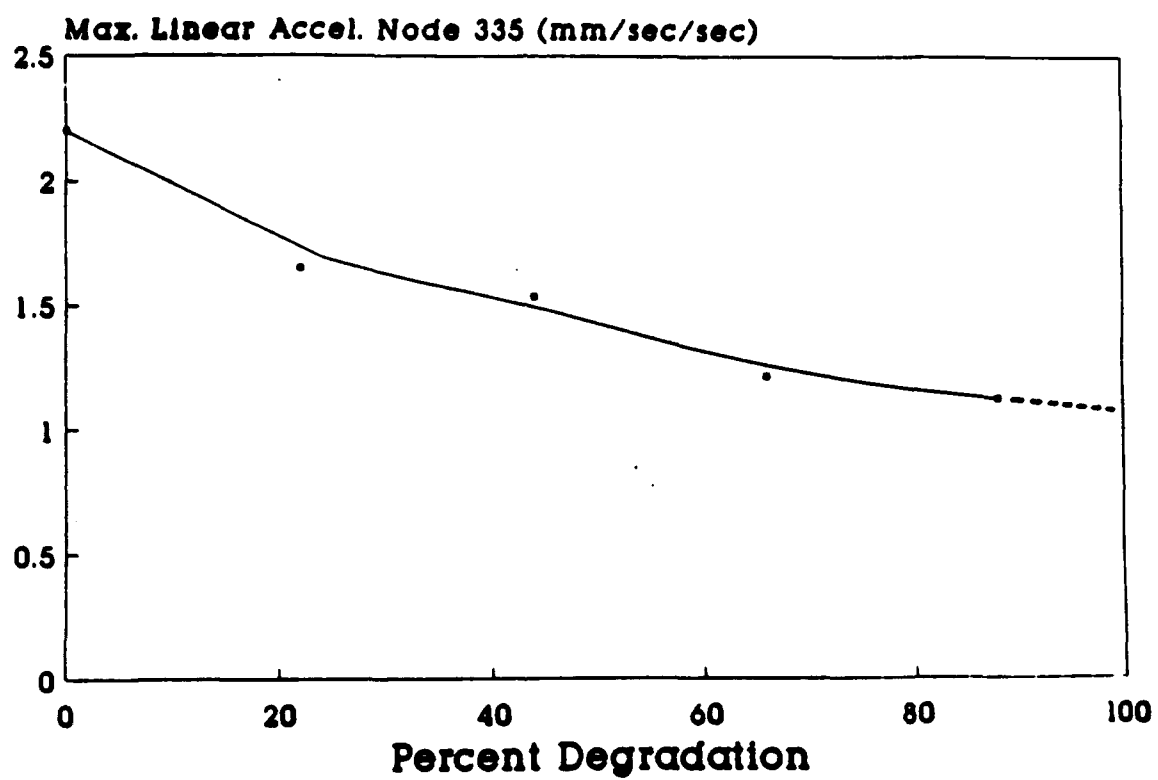


Figure 147 Max. Linear Acceleration - Node 335 (mm/sec/sec)

